Synthesis and Characterisation of BN-Isosteres of Polyaromatic Hydrocarbons

Limberti, Simone

Award date:
2019

Awarding institution:
University of Bath

University of Bath

Synthesis and Characterisation of BN-Isosteres of Polyaromatic Hydrocarbons

Simone Limberti

March 2019

Department of Chemistry

A thesis submitted to the University of Bath for the degree of Doctor of Philosophy

ABSTRACT

In the last few decades graphene-based materials have attracted a great amount of interest in the scientific and academic world because of their fascinating properties. Recently, graphene, because of the extraordinary electronic, optoelectronic and physical feature, has been proposed as innovative material for future electronic devices. However, one of the key challenges in advancing the graphene-based technologies in this area is the lack of an energy gap between the conduction and valence bands, limiting its application to replace silicon-based semiconductors in electronics. Therefore, the ability to impose a band gap in graphene and tailor the size of the band gap is of great significance to materials chemists. One of the most promising strategy that is currently emerging to overcome these limitations is the replacement of C=C bonds by isostructural and isoelectronic bonds such as polar B-N bond. Hybridised atomic sheets containing bonds between elements boron, nitrogen and carbon over wide compositional ranges could results in new materials with properties complimentary to those of graphene and the insulating *h*-BN, enabling a rich variety of electronic structures, properties and applications. While various materials-processing technologies to produce these materials in sizable quantities are improving in their synthetic methodologies, the organic electronic research is moving towards the synthesis of new BN doped polycyclic aromatic hydrocarbons (PAHs), which have showed interesting electronic properties. In this regard borazine based materials have the right requirements in terms of chemical and electronic properties, therefore they can provide new opportunities in the efforts to develop BN-PAHs materials.

Chapter 1 surveys the history of graphene, hexagonal boron-nitride and their corresponding boron, nitrogen and carbon hybrid materials, detailing the range of synthetic methods and analytical techniques used to analyse these materials. This section is followed by an introduction to polycyclic aromatic hydrocarbons (PAHs) exploring the most important synthetic methods and the physical and chemical properties of these materials. A particular attention is focused on a polyaromatic hydrocarbon known as truxene, who C_3 symmetric structure is the basis of our single organic molecules described. We then introduce the effects of boron and nitrogen incorporated into polyaromatic systems and how they alter optoelectronic properties in relation to their extent of doping. The chapter is concluded with a review of borazine, aminoborane and amine-borane synthesis and characterisation. Isoelectronic to benzene, the borazine core has been used as motif to construct our CBN-hybrid molecules.

Chapters 2 and 3 describes the total synthesis of novel single organic molecules known as borazatruxenes and benzo(c)naphtho(2,1-p)borazachrysenes. These molecules are well characterized by NMR and Mass Spectroscopy analysis. The electronic properties are studied by UV-Visible spectroscopic analysis. Finally, the self-assembly process characterizing the supramolecular aggregation of such systems is explored by variable temperature ^{1}H NMR studies.

Chapters 4 and 5 explores the possibility of synthesising hybrid boron, nitrogen and carbon extended 2D materials. In particular Chapter 4 is focused on the development of a synthetic method for the synthesis of BN-doped hemifullerene by either dehydrogenation or flash vacuum pyrolysis (FVP) of engineered borazatruxenes and benzo(c)naphtho(2,1-p)borazachrysenes. Chapter 5 details the attempted synthesis of 2D-CBN hybrid oligomers and polymer networks combining benzene and borazine regions. Synthesis of such materials is achieved using a protocol outlined for borazatruxenes utilising microwave-dielectric heating. Oligomer materials are characterised using the common analytical techniques while polymers are characterized by solid-state analytical techniques.

ACKNOWLEDGMENTS

These four years of doctorate at the University of Bath have been the greatest experience that I had in my life. It has been very emotional, and it made me to grow as a scientist but overall as a person. I learned many many things and met many new people that it would not have been possible without this experience! For this great opportunity that I had in my life I would like to express all my greatest gratitude to Dan, how gave me the possibility to join in his research group in 2014. He is the best supervisor that a person can meet in the growth of the own career. He transmitted me all the passion in the chemistry field and the strength to carry on every time, especially in the dark moments that research generate and make you feel lost. I will be endless grateful for all the support and the help that Dan gave me in these years. Despite occasionally scaring moments, he made the working environment enjoyable constricting us to hear the same anecdotes on his PhD experience in Austin for four years. He perfectly knew that we knew those stories, but he liked to refresh our mind starting with "Did guys I tell you when I was with..."

In a begrudging second place, I want to give a tight hug to my colleagues Giles and Afi who have had the great patience to teach me english among many coffee breaks at Tiki. Giles has been my first buddy drinking in England pushing m me every Friday to leave everything under the fume and run for a frozen beer to the Parade. With Afi I passed great times to talk about everything above all about food and cooking techniques since we are both cuisine gourmet. Also, do not forget the extraordinary help that Dora and Tibi gave me during my last period of doctorate. I would like to warmly thanks both and I wish them the best. I must acknowledge Dr Steven Flower, Dr Fabienne Pradeaux-Caggiano, Dr John Lowe for his assistance and expert knowledge of the NMR machines that kept my research going and Dr. Gabriele Kociok-Köhn not only for her help to solve crystal structure of my compounds but also for the time spent to talk about travels and food.

I feel to warmly thanks Giorgia, who has been an important person in the path of my life. We decided, after our master's degree, to venture into this experience together. Although we knew that it would not be easy at the beginning, we always supported each other, giving us the desire and the strength to go forward until the end. She is one of the best girls I have never met, and I never forget all the time passed together. I wish all the best for her because she deserves all the happiness of this world.

Another person that I wish to thank is Pecchio, who is not only a great friend for me but also a great person and one of the best scientists I know. We know each other since the beginning of high school and our passion for chemistry, and science in general, led us to take the same decision to choose a PhD abroad. Although we have been in two different parts of the Europe (England-Germany), we never stopped to be in contact, updating us about all our adventures/misadventures, supporting us morally. Alongside Pecchio, I take the opportunity to thank the rest of my closest friends that have been with me throughout high school and university; Bisso, Betta, Biagio, Bulli, Iozzo and Nanni. Thank you all for the friendship, and for all the time passed together and the crazy things we did most of the night we were outside.

Another important group of closest friends that I must to mention in this section is that of my water polo team, which includes Bene, Biaso, Foffo, Homo, Marchino, Zirpo and Rabbo. I consider these guys as brothers, because we know each other since we have started our sport career, more than 20 years ago. We grew up together among so many different stories and exciting adventures that only few groups of friends, like us, have the privilege and also the honour to enjoy. We are so different one from one another, but we know that for any problem or difficulty, we can rely on each other. Thanks for being my friends for all this time and for the time will come. I thank you for all over your help, support, encouragement, debauchery and friendship and just to mention one of our favourite groups, 883, I am feeling to say you all with a smile:

"Noi abbiam capito tutto è un po' come nel calcio"
È la dura legge del gol
gli altri segneranno però
che spettacolo quando giochiamo noi
non molliamo mai
Loro stanno chiusi ma
cosa importa chi vincerà
perché in fondo lo squadrone siamo noi
lo squadrone siamo noi.

This PhD would not have been the same without the special support of the crazy spanish group composed by Andrea (a very nice and sensible person), Eva (my lovely flatmate), Lucia, Maya, and Sara, headed by Marina. About the latter, the ration between size and destructive power of this girl is unimaginable: she can easily destroy 5 pubs in only one night without any problem. But we love her like this, she gave us so many enjoyable moments all together and she is one of my closest friends met in Bath with Fernando and Sofia. I must thank Sofia for all the time spent together exploring Bath and Bristol by bike, and going around for live music gigs, while Fernando for the strong friendship developed during my final year.

At this point, nearly the end of the acknowledgments, I must thank two more guys who have been very very close to me during all these years: Vincenzo e Federico. Despite I find difficult to express myself in defining our friendship, because there are no real words to describe it, I can only say neither time nor distance will be able to dull it. I thank you guys for all the time spent (which is huge), and things done together. Also, the great passion for both, finest spirits and the same kind of music, have been two of the main topics of our endless chats until late in the night. Many many thanks for all the help, support, motivation, and advices you gave me and thanks for being my friends.

Finally, an endless thank to my mum and dad, that without them help, support and understanding I would have never achieved all these good results. They have been and always will be the core of my success because they believe in me and always they encourage me in everything I do, or I decide to do. A great thank to two special people like them an also to my little brother, that despite so many fights (as usual among brothers), we enjoy playing video games together and going out for drinks.

Thanks, also, to the University of Bath and EPSRC association for funding me during all the period of my doctorate, the Chemical Characterisation and Analysis Facility (CCAF) and the EPSRC National Mass Spectrometry Facility at Swansea University.

ABBREVIATIONS

1D	one-dimensional
2D	two- dimensional
3D	three-dimensional
Å	amstrong
AB	amine-borane
AFM	Atomic force microscopy
AO	atomic orbitals
BN	boron nitride
°C	celsius degrees
***c*-BN**	cubic- boron nitride
CD_3OD	deuterated methanol
$CDCl_3$	deuterated chloroform
CH_3COOH	acetic acid
CH_3COOEt	ethyl acetate
CNT	carbon nanotubes
COOH	carboxilic group
COSY	correlation spectroscopy
CVD	chemical vapour deposition
Δ*G*	change in Gibbs free energy
Δ*H*	change in enthalpy
Δ*S*	change in entropy
DCM	dichlorometane
DFT	density functional theory
DMF	dimethylformamide
DMS	dimethylsulfide
DMSO	dimethylsulfoxide
ECL	electrochemical luminescence
EDG	electron donating group
equiv.	equivalents
ES-MS	electrospray mass spectroscopy
Et	ethyl
eV	electronvolts
EWG	electronwithdrawing group
FET	field effect transistor
FVP	flash vacuum pyrolysis
GHz	gigaHertz
GNRs	graphene nanoribbons
hr	hour
HBC	hexa-peri-hexabenzocoronene
***h*-BN**	hexagonal-boron nitride
HMBC	*heteronuclear Multiple Bond Correlation*
HPLC	*high-performance liquid chromatography*
HRMS	high resolution mass spectroscopy
HRTEM	high resolution transmission electron microscopy
HOMO	highest occupied molecular orbital
HSQC	h*eteronuclear Single Quantum Coherence*
Hz	hertz
IR	infra-red
J	coupling constant
J	Joule
K	kelvin
Ka	association constant
LEC	light-emitting electrochemical cells
$LiAlH_4$	lithium aluminium hydride
Ln	general ligand
LTMP	lithium 2,2,6,6-tetramethylpiperidine
LUMO	lowest unoccupied molecular orbital
m	*meta*-position
M	molarity
Me	methyl group
mg	milligrams
MHz	mega Hertz
min	minutes
µL	microliters
mL	milliliters
mmol	millimoles
m/z	mass to charge ratio
***n*-BuLi**	*n*-butyl lithium
NEt_3	triethylamine
NMR	nuclear magnetic resonance
o	*ortho*-position
OFET	field-effect transistors
OLED	organic light emitting diode
OPV	organic photovoltaics
p	*para*-position
PAH	policyclic aromatic hydrocarbon
Ph	phenyl group
PLQY	photoluminescence quantum yield
ppm	parts per million
R – R^x	general substituen groups
R_f	retention factor
RT	room temperature
SEM	scanning electron microscopy
STEM	scanning tunnelling electron microscopy
STM	scanning tunnelling microscopy
TCE	1,1,2,2-tetrachloroethane
TEM	transmission electron microscopy
THF	tetrahydrofuran
TLC	chromatography on a thin slab
TMP	2,2,6,6-tetramethylpiperidine
TMS	trimethylsilyl group
u.m.a	atomic mass unit
UV	ultraviolet
V	volts
W	watt
***w*-BN**	wurtzite- boron nitride
XPS	X-ray photoelectron spectroscopy
XRD	X-ray diffraction
δ	chemical shift
Δ	reflux heating
v	frequency

Table of Contents

CHAPTER 3

Synthesis and Characterization of Benzo(c)naphtho(2,1-p)borazachrysene and derivatives

CHAPTER 4

Attempted synthesis of Hybrid Boron, Nitrogen and Carbon C_3-Hemifullerene

CHAPTER 5

Synthesis and Characterization of Hybrid Boron, Nitrogen and Carbon Oligomers and 2D Polymeric Materials

CHAPTER 6

CHAPTER 7

CHAPTER 1

Introduction to Carbon, Boron and Nitrogen Hybrid Materials: An Overview to the Synthesis, Characterization and Advances of their Applications

1.1 From Polycyclic Aromatic Hydrocarbons (PAHs) to more complexed nanocarbon materials

The discovery of C_{60}-fullerene in 1985,[1] subsequently carbon nanotubes in 1991[2] and finally the isolation of single-layer graphene in 2004[3] led, in the following years, the modern nanocarbon science to expand rapidly. Indeed, all these distinct families of all-carbon molecules exhibit a wide range of remarkable properties, which paved the way for the development of new functional materials with large applications in many different areas included the organic electronic.[4] In this area the necessity to fine tune the electronic properties of these materials led chemists to set the sights on developing new laboratory methods to provide structurally well-defined carbon materials. In this regard, structurally confined nanoscale graphene segments called nanographenes or graphene quantum dots (GQDs) are characterized by a non-zero bandgaps[5,6] differently from the infinite 2D graphene. The ability to tune the band-gap opening by manipulation of the degree of π-extension, shape, width and edge topology, clearly suggested these materials to be very promising new n-type organic semiconductors.[7] For the precisely controlled synthesis of structurally uniform nanocarbon materials a novel bottom-up methodology was strategically developed starting form polycyclic aromatic hydrocarbons (PAHs).[7]

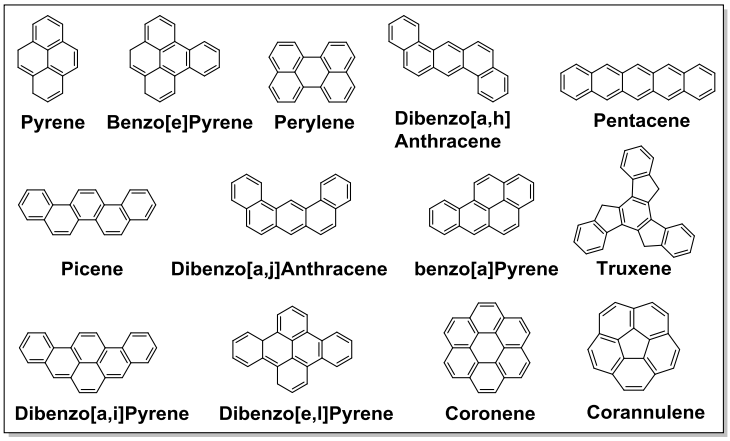

Figure 1.1 Examples of polycyclic aromatic hydrocarbons (PAHs)

Polycyclic aromatic hydrocarbons can be considered substructures of the graphene consisting of sp^2 carbon frameworks extending over 1 nm with well-defined geometric confinement and a finite energy gap.[4,8] A great contribution to the synthesis and characterization of PAHs was made by R. Scholl[9–11] and E. Clar,[12–14] who in the first half of the 20th century prepared the D_{6h} symmetric hexa-peri-hexabenzocoronene (HBC) which is one of the most representative PAHs.

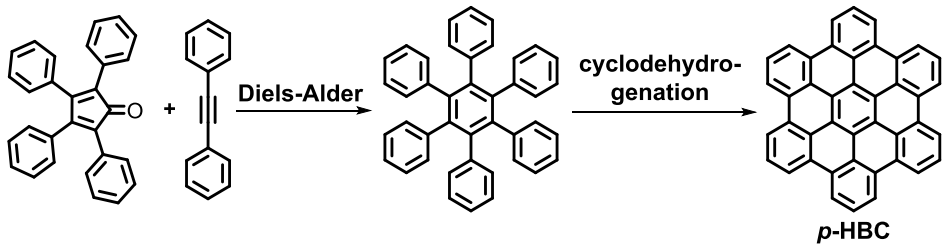

Scheme 1.1 Synthesis of hexa-peri-hexabenzocoronene (p-HBC 2) through intramolecular oxidative cyclodehydrogenation.

This molecule, as well as its derivatives have gained a particular interest due to their high stability, facile self-assembly, and promising applications.[15] Over the last two decades, with the progress of modern synthetic methods and the development of more efficient reactions yielding PAHs under milder conditions, a wide variety of π-extended PAHs have been prepared.[16–19] A solution-synthesis protocol has been successfully applied to synthesise structurally well-defined PAHs used for the fabrication of nanographene structures with atom-by-atom precision.[20,21] The first attempt at the synthesis of extended PAHs date back to 1970, when Stille *et al.* reported the synthesize a fully conjugated ladder-type polymer consisting of hexagonal and pentagonal aromatic rings.[22] However, the poor solubility of this material due to strong π–π stacking interactions made the structural characterization inconclusive. A more soluble fully conjugated ladder-type polymer, called ‘‘angular polyacene,’’ was achieved in 1993 by Scherf *et al*.[23,24] Although this polymer consisted only of six-membered rings it can be considered one of the narrowest possible GNRs with a defined structure. The synthesis followed a solution-mediated procedure where the final product was obtained by carbonyl olefination of functionalized poly(para-phenylene).

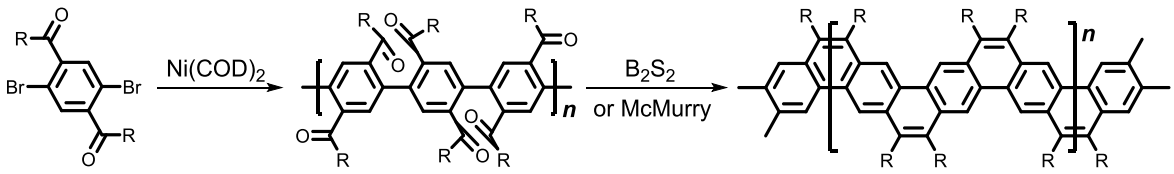

Scheme 1.2 Synthesis of a fully aromatic ladder-type polymers.

Over the time several considerable improvements in the synthetic methodology allowed to have access to a large variety of π-extended PAHs and nanographenes by a rapid and controlled bottom-up organic synthesis.[15] Highly functionalized and solution-processable PAHs derivatives have been prepared starting from small π-molecules. Usually Diels-Alder reactions,[25–27] Suzuki-Miyaura cross-couplings[28,29] and C–H activation[30] reactions have been proved to be very effective synthetic tools to extend smaller molecular platforms to larger graphene subunits. Specifically, metal catalysed cross-coupling reactions have been extensively used in modern PAH chemistry for the elaboration of more complex oligoaryl precursors,[31–33] which in turn can be cyclized to PAH targets using, for example, oxidative coupling reactions[34] or by annulation reactions.[20]

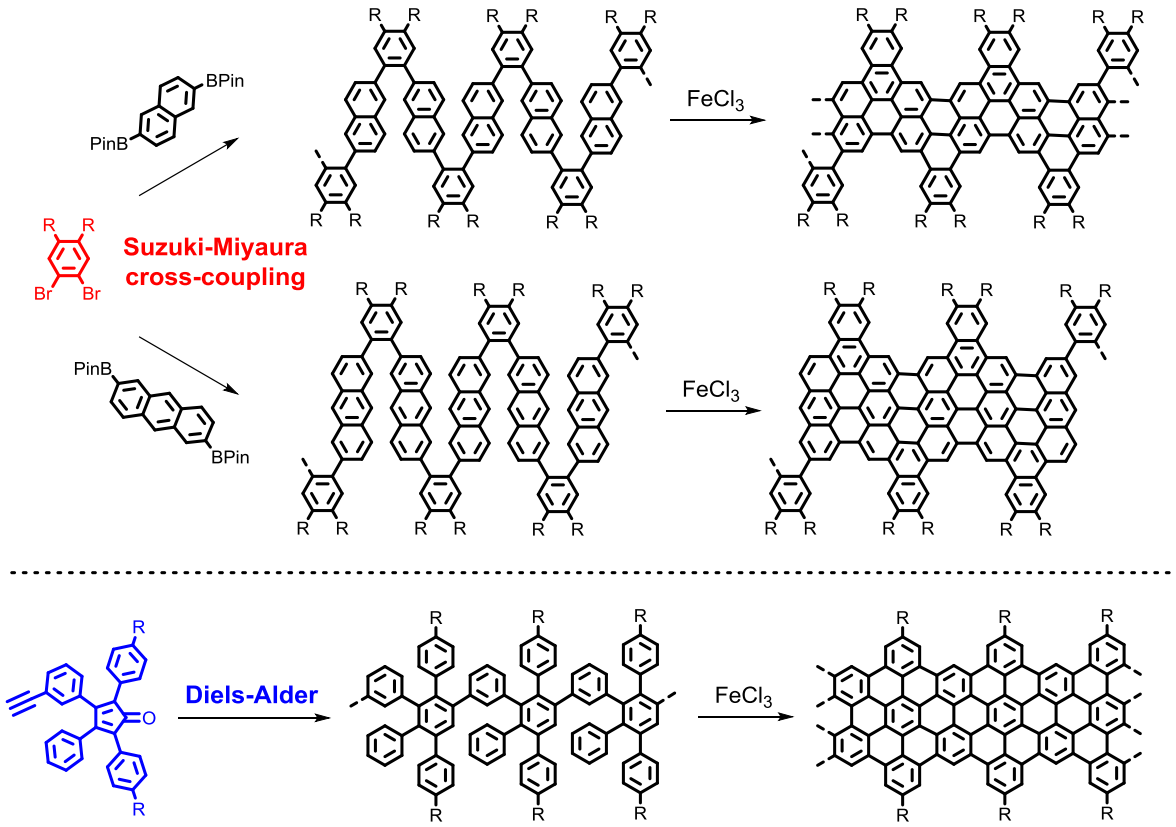

Scheme 1.3 Examples of synthesis of nanographene structures by Suzuki or Diels-Alder polymerization followed by oxidative cyclodehydrogenation.

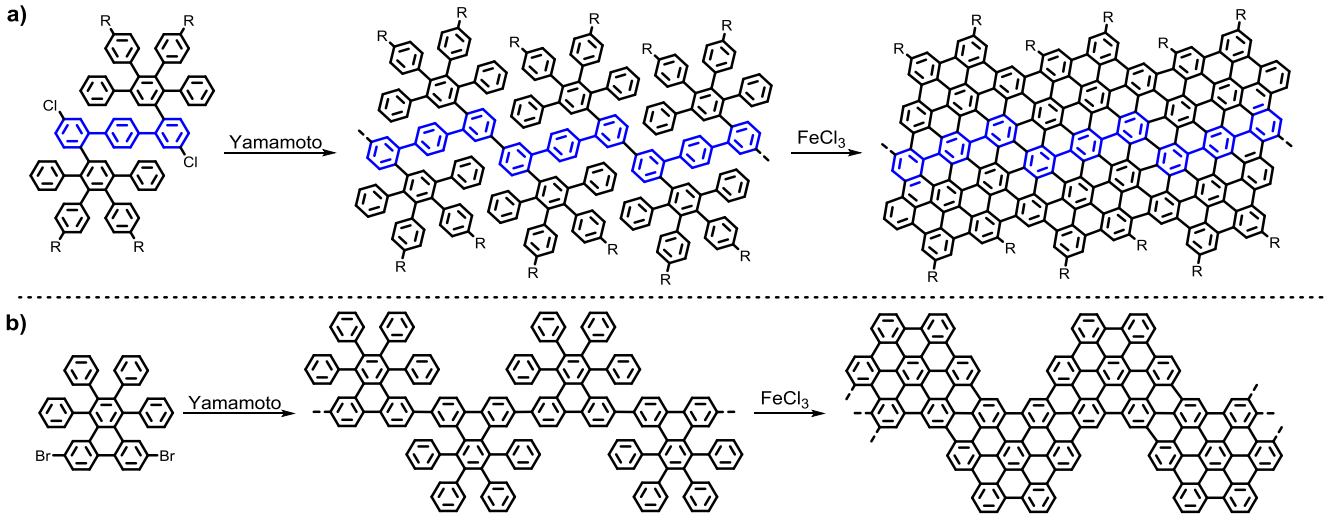

Scheme 1.4 Examples of synthesis of a) laterally extended and b) chevron-type GNRs through AA-type Yamamoto polymerizations.

Polycyclic aromatic hydrocarbons (PAHs) have also been used as intermediate for the preparation of circular nanotube sections,[35–37] bowl-shaped fullerene fragments[38–40] and disc-shaped graphene substructures[4,41]. Extended disc-shaped PAHs have conventionally been prepared by a combination of substitution and metal-catalysed coupling reactions, Diels-Alder cycloaddition of alkyne and tetraphenylcyclopentadienone derivatives[15,25,27] followed by intramolecular oxidative

cyclodehydrogenation performed with a variety of oxidants and Lewis acids[34]. This general synthetic protocol has been widely used employing different aryl derivatives providing potential access to previously unavailable graphene molecules. For example, Wei and co-workers reported in 2014 an elegant two-step synthetic procedure for the preparation of C_3 symmetrically substituted hexa-cata-hexabenzocoronenes (c-HBCs).[42] Polyphenylene 1,3,5-tribenzylbenzene precursors (TBBs) were prepared via three-fold Suzuki coupling and then exposed to the intramolecular oxidative cyclodehydrogenation with different aryl aldehyde to give graphene fragments with different size.

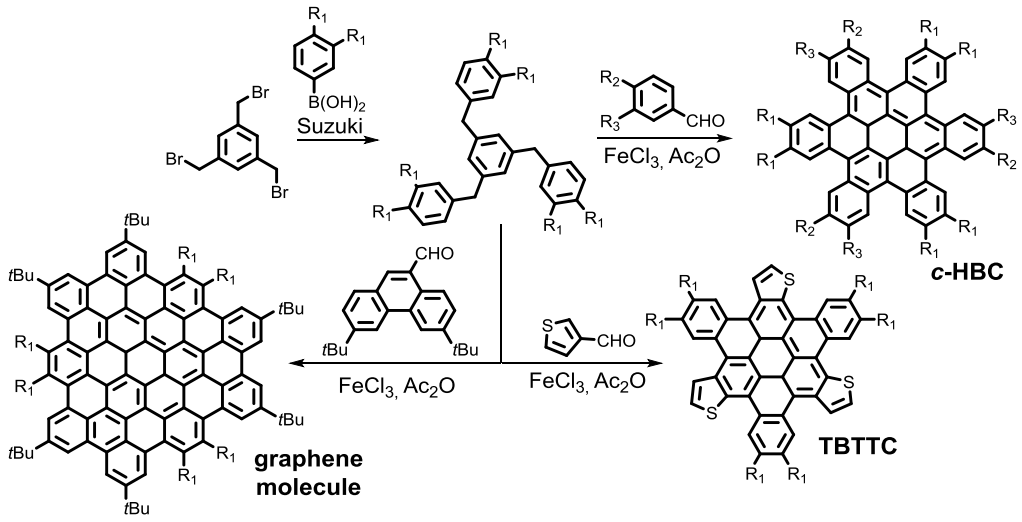

Scheme 1.5 Representation of two-step synthetic route for obtaining *C_3* symmetrical *c*-HBC, TBTTC and graphene molecule.

More recently extended PAHs containing rings of other sizes (including five-, seven- and eight-membered rings) as defects, have been explored[43–45] with the aim of studying, by simplified models, defects identified at the grain boundaries of graphene sheets. A pioneering work on developing new strategies for the synthesis of curved graphene molecules is addressed to Itami and co-workers, who in 2013 reported the two-step synthesis of grossly warped graphene molecule PAH (C80)[21] with one five-membered ring at the centre and five lateral embedded seven-membered rings. The synthesis started from corannulene following a palladium-catalysed C-H arylation procedure to prepare polyphenylene precursors which in turn, by intramolecular cyclisation, provided PAH (C80) in good yields. The distorted molecular structure of the products conferred a good solubility in common organic solvents, moreover the tert-butyl derivative could be dissolved even in hexane.

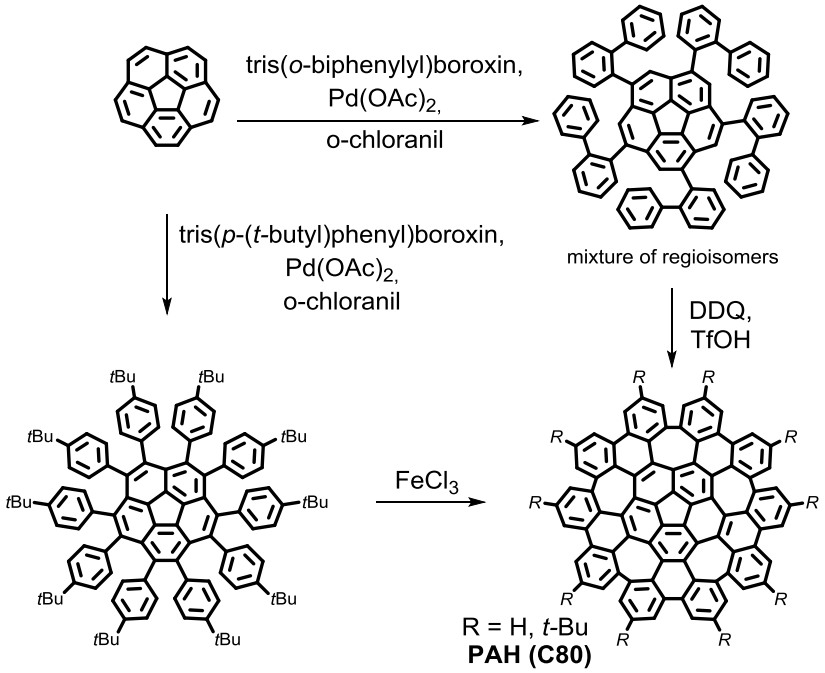

Scheme 1.6 Synthesis of grossly warped graphene molecules PAH (C80) through C-H arylation and cyclodehydrogenation of corannulene.

In the same years Scott's group reported the synthesis of the C_3-symmetric "hemifullerene" (Triindenotriphenylene) by the unconventional application of Flash Vacuum Pyrolysis (FVP) starting from different PAHs. Specifically, starting from two brominated benzo(c)naphtho(2,1-p) chrysene regioisomers A and B precursors,[46,47] the desired hemifullerene could be prepared by FVP heating up to 1000 °C. This temperature promotes the formation of the intermediate aryl radicals[48] by losing a radical bromine followed by 1,2-shifts of hydrogen atoms resulting into the C-C bond formation.

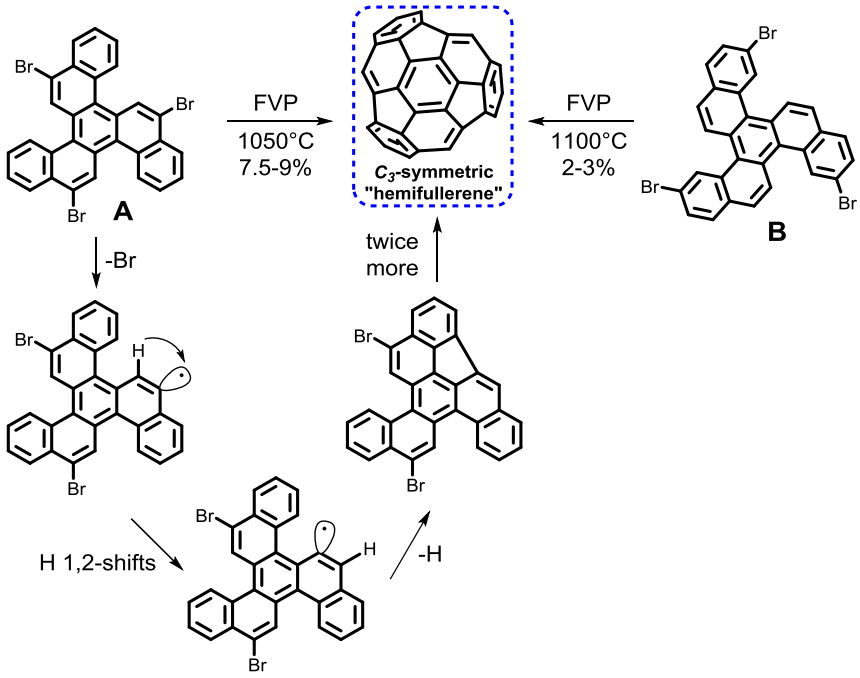

Scheme 1.7 Synthesis of C_3-symmetric "hemifullerene" starting from two brominated benzo(c)naphtho(2,1-p) chrysene regioisomers **A** and **B**.

1.2 Band structure engineering of Polycyclic Aromatic Hydrocarbons (PAHs) by boron and nitrogen doping

Recent studies have demonstrated that another feasible method to finely tune the energy levels of carbon-based materials is the replacement of the CC units with a pair of different atoms.[49,50] This chemical doping, intentionally used to tailor the electrical properties of intrinsic semiconductors, can also be used to modify the electronic band structure of PAHs, opening further the energy gap between the valence and conduction bands.[51] Specifically, theoretical modelling and simulations alongside experimental studies have shown the possibility of making p-type and n-type semiconducting materials combining carbon atoms, with electron rich elements of group 15 or electron deficient elements of group 13.[52,53] Currently, among the available elements, substitution of CC units specifically with boron and nitrogen atoms is one of the most attractive strategy for the PAHs bandgap engineering.[54] Considering the isoelectronic (having the same number of electrons) and the quasi-isosteric (being very similar in size) relationship between C=C and B-N bonds,[55] replacement of the CC units with the corresponding BN units would not alter parameters like bond length[56] and crystal packing[57] compared with the all carbon counterparts. However, this replacement, due to the differences in the electronegativity between B (2.05) and N (3.04) atoms, would create polarization in the carbon network, thereby altering the electronic, optical, and electrochemical properties of these materials[58–60], allowing also the formation of self-assembled architectures.[61] The isoelectronic nature between the B-N and C=C bonding is due to the same valence electron count (eight valence electrons) that characterize both units.

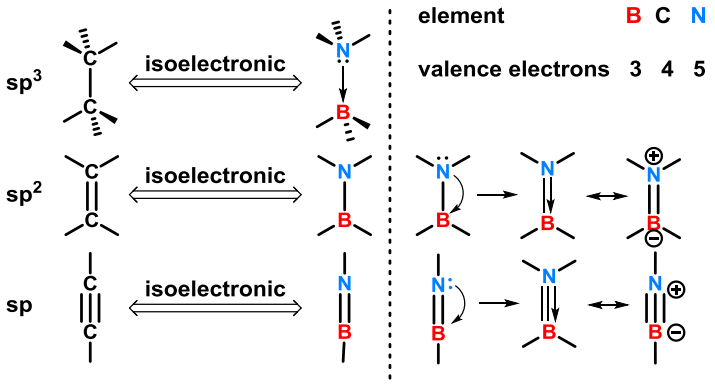

Figure 1.2 Isoelectronic relationship between CC and BN.

As direct neighbours of carbon in the Periodic Table of Elements, the combination of boron and nitrogen atoms result in the same number of electrons as the carbon-carbon double bond. The electron configuration of boron atom (Z = 5) at the ground state is $1s^2\ 2s^2\ 2p^1$, while that of nitrogen (Z = 7) is $1s^2\ 2s^2\ 2p^3$. The formation of trivalent borane compounds implies the hybridization of the valence 2s and 2p atomic orbitals (AO) of boron, changing the electronic structure in the more energetically stable

configuration $1s^2\ 2s^1\ 2p^2$. The four valence atomic orbitals 2s, $2p_x$, $2p_y$, $2p_z$, and only three valence electrons enable boron to form three σ bonds with the participation of AO having the sp^2 configuration leaving an empty $2p_z$ orbital available. Nitrogen atom, instead with the same number of AO of boron and five valence electrons results in the formation of three σ bonds with a lone pare of electrons in an $2sp^3$ hybridized orbitals. Combination between boron and nitrogen atoms can lead to different derivatives that Wiberg classified into the three major groups: i) amine-boranes (Borazane), ii) aminoboranes (Borazene), iii) borazines (Borazole) according to the nature of the B-N bond in the molecules.

1.3 The nature of the BN dative bond in Amine-Boranes

Amine-borane is classic examples of compounds to describe the chemical interaction between a Lewis base and a Lewis acid species. The dative bond characterizing the formal molecular structure of these material is a consequence of the donation of the lone pair of a trivalent nitrogen into the empty p_z orbital of a trivalent boron atom. This structure can be associated to that of alkanes counterparts, in the sense that in the latter two sp^3 hybridized carbon atoms are linked by a σ bond. The adduct resulting from the combination of the two fragments, is formally uncharged, however the difference in electronegativity between boron and nitrogen suggest a partial negative charge at the nitrogen and a partial positive charge at the boron atom (structure **A**).

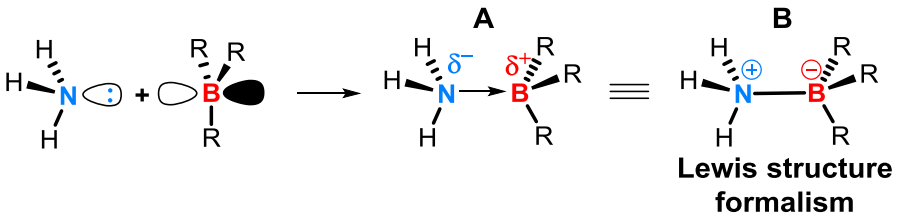

Scheme 1.8 Orbital overlapping to form the amine-borane adduct characterized by B-N bond polarization towards nitrogen atom. The Lewis structure formalism, however suggest a positive charged nitrogen atom and negative charged boron atom.

This interpretation was confirmed by experimental measurements of the dipole moment of simple adducts determined by gas phase microwave analysis.[62] The bonding pair resulted to be more closely associated with the donor atom also, the dative bond leads to pyramidalization of the borane moiety inducing a change in hybridization at boron from approximately sp^2 to sp^3 (Scheme 1.8).[63] However, the electron-transfer process from the donor to the acceptor atom represented by an arrow, can be also represented with the Lewis structure formalism for valance electrons implying the use of charges (structure **B**).[64] The simplest example of amine-borane adduct is ammonia borane (H_3N-BH_3, **AB**), which all carbon counterparts can be attributed to ethene. Direct comparison between ethane vs. **AB** shows differences in

terms of chemical and physical properties, which reflect the diverse binding nature characterizing the two species. Indeed, ethane is a volatile gas under standard conditions (bp -89 °C), with no effective dipole moment and a C-C bond dissociation energy (BDE) of 90.1 kcal mol^{-1}. In contrast, **AB** is a solid (bp 104 °C) characterized by a strong dipole moment of 5.2 D and a B-N bond dissociation energy of 27.2 kcal mol^{-1}, significantly smaller than that of ethane. One of the main peculiarities of **AB** and amine-borane in general is that these compounds contain both hydridic (B-H) and protic (N-H) hydrogens due to a difference in polarity between hydrogen, boron and nitrogen atoms. This opposite polarity can easily engage in so-called *dihydrogen bonding* (DHB): $N\text{-}H^{\delta+}\cdots H^{\delta-}\text{-}B$, which facilitates hydrogen release under mild conditions by thermal treatment,[65–67] acid- [68] -or base catalysis,[69,70] or metal-based catalysis.[71] Thermodynamic calculations demonstrated that thermal dehydrogenation of **AB** is enthalpically more favourable compare with that of ethane. Dehydrogenation of ethane to ethylene, is endothermic with a calculate ΔH of 32.6 kcal mol^{-1}, while in contrast, dehydrogenation of ammonia borane to aminoborane ($H_2N\text{-}BH_2$) is exothermic with a ΔH of -5.09 kcal mol^{-1}. These divergent data can be rationalized considering that in ethane the cleavage of two strong C–H bonds is not totally compensated from the formation of the C=C π-bond and the release of H_2, while the opposite is true for the conversion of the dative B–N bond into the stronger covalent one. For this reason, **AB** has been identified as a promising candidate for hydrogen storage purpose due to the high gravimetric hydrogen densities of 19.6 wt %, and potential regenerability.[72] Detailed studies on the thermolysis of **AB** revealed that hydrogen is released in three distinct steps at precise temperature ranges (Scheme 1.9).

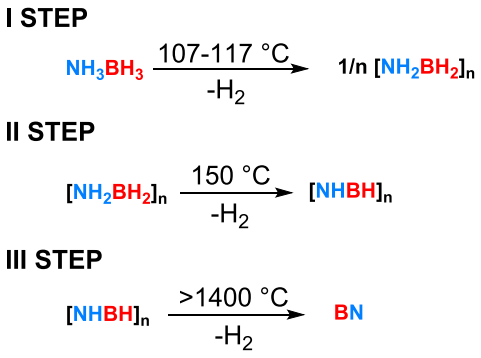

Scheme 1.9 Thermolysis of ammonia borane.

The initial weight loss of ≈1.1 eq. of dihydrogen (≈7.2 wt%) occurs between 107 and 117 °C leading to the formation of the corresponding aminoborane intermediates. The second equivalent of H_2 is lost over a much broader temperature range, with a maximum rate at ≈150 °C, and the rest released at much higher temperatures. Analysis (IR and MS) of the volatile thermolysis products for the first dehydrogenation step revealed traces of diborane (B_2H_6), aminoborane ($H_2N\text{-}BH_2$) and borazine accompanying the evolved hydrogen. Since all steps are exothermic, the high temperature requirement is mainly due to the significant

kinetic barriers. Dehydrogenation of **AB** and amine boranes in general, typically yields a variety of oligomeric products depending on starting materials, conditions and methods used. Pioneering studies by Manners and co-workers demonstrated that this process can be directed towards the selective formation of specific products rather than others using metal-based catalysts.[73] To date a number of **AB** dehydrocoupling mechanisms have been elucidated and mechanistic studies demonstrated that products formed by metal-based catalysis dehydrogenation are strongly dependent on the choice of catalyst and starting materials used.[71]

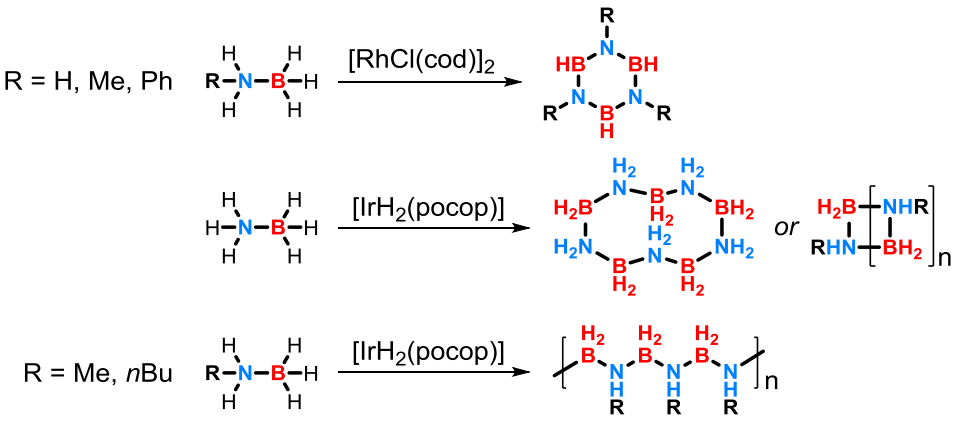

Scheme 1.10 Diverse products derived from metal-catalysed amine-borane dehydrogenation.

Reactivity studies on the catalytic dehydrogenation of ammonia-borane suggested that the very active catalysts complex with aminoborane intermediate in the first or second coordination sphere resulting in the linear or branched oligomers and polymers formation following a classic polymerization-type mechanism.[74,75] On the contrary selective catalysts which bind weakly with aminoborane expel the latter in solution undergoing to cyclization.

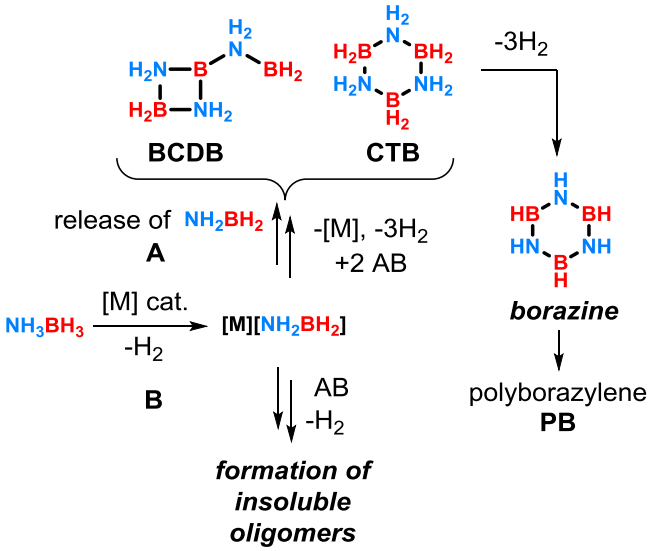

Scheme 1.11 Proposed mechanisms for the metal catalysed dehydrogenation of ammonia-borane.

Particularly interesting is the study reported by Baker in 2015 on the dehydrocoupling of ammonia-borane in different reaction conditions with and without catalysts.[71] They observed that one of the recurrent products obtained by dehydrogenation of ammonia borane using different reaction conditions was the formation of borazine. To gain insight the mechanism of this reaction and explain the formation of this product, they carried out a systematic analytic study of intermediates discovering that a branched, cyclic aminoborane tetramer, B-(cyclotriborazanyl)amine-borane (BCTB) was formed. Isolation of this product and further reactivity studies in different reaction conditions demonstrated that thermolysis of BCTB yields borazine as main product.

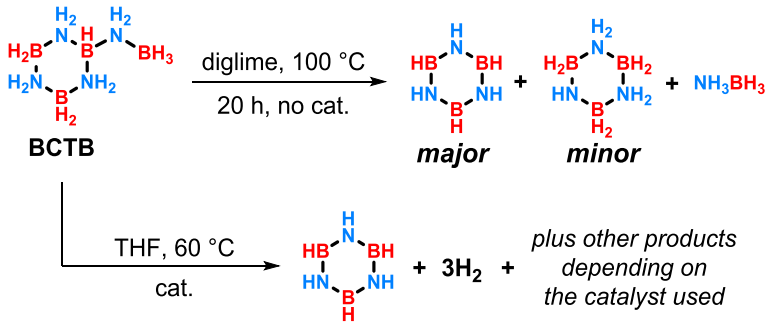

Scheme 1.12 Reactivity of BCTB in different reaction conditions, with and without metal-based catalysts.

Although the detailed mechanisms of these reactions require additional elucidation, previous computational studies[74,76,77] suggested that this selective oligomerization could proceed *via* B-H-B bridged intermediates followed by intramolecular attack of NH_2 on the three-coordinate boron (Scheme 1.13). Intermediate **I** bearing both BH and BH_3 groups reacts in the same manner with a third aminoborane monomer to generate intermediate **II**. Initially It was proposed intermediate **II** to react intramolecularly with an NH_2 group on three-coordinate boron to give BCDB selectively. Instead they later discovered that intermediate **II** undergoes to intermolecular reaction with a fourth equivalent of aminoborane, which led to the branched cyclic aminoborane tetramer, BCTB selectively.

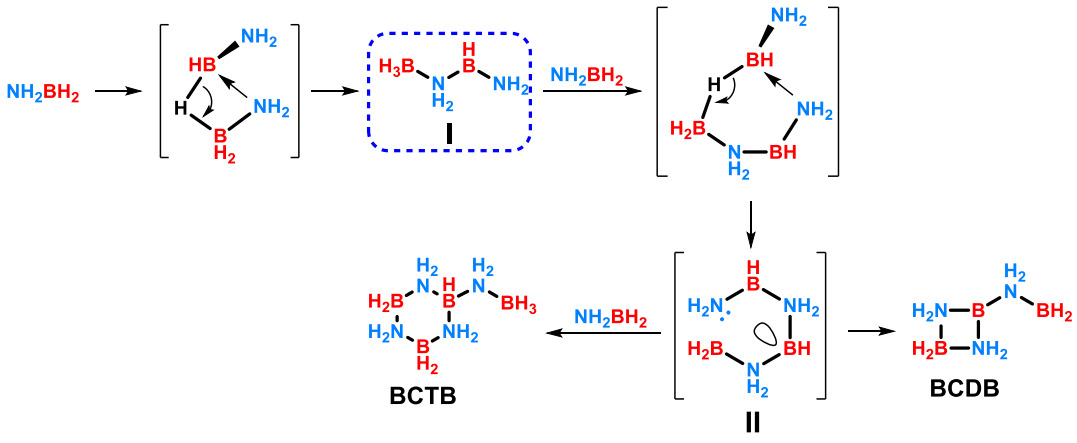

Scheme 1.13 Oligomerization of aminoborane through B–H–B bridged intermediates.

The formation of borazine takes place in the last step of the thermolysis process attributed to hydrogen transfer processes as studied recently by Manners and co-workers.

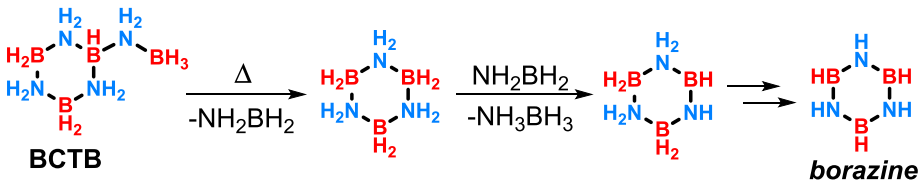

Scheme 1.14 Formation of borazine by hydrogen transfer processes.

This proposal was confirmed by experimental observations of thermolysis of BCTB in presence of cyclohexene. In these reaction conditions neither **AB** nor borazine was formed since cyclohexene effectively trapped the aminoborane monomer, which did not take part to the cyclocondensation.

1.4 Synthesis and reactivity of Amine-Boranes

The first amine-borane coordination adduct was prepared in 1809 by Gay-Lussac upon direct reaction between ammonia and boron trifluoride to give the corresponding ammonia-trifluoroborane $H_3N{\cdot}BF_3$.[78] Subsequently, chemical syntheses of analogues to ammonia-trifluoroborane was pioneered by Wiberg and,[79] however the first amine-borane containing only hydride substituents on boron was reported only in 1937 by Burg and Schlesinger with the synthesis of N,N,N-trimethylamine-borane, $Me_3N{\cdot}BH_3$.[80]

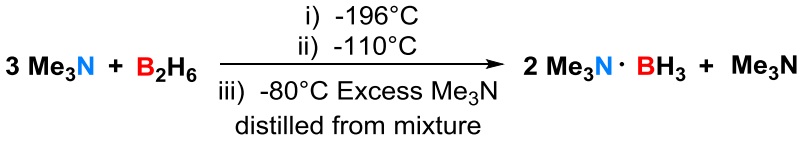

Scheme 1.15 Synthesis of N-substituted amine-boranes by using diborane.

This compound was obtained by direct reaction of trimethylamine and diborane, however due to particular reaction conditions adopted plus the highly reactive nature of diborane,[81] this method was soon abandoned. As detailed before difficulties in handling boron hydride species were overcome replacing these reactants with different in solution boron sources complexed with the solvent such as boron halides BX_3 in benzene or hexane or borane-tetrahydrofuran ($BH_3{\cdot}THF$) and borane-dimethylsulfide ($BH_3{\cdot}SMe_2$). These species are easier to handle and they react directly with free amines, commonly in THF or DCM solution to give the desired amine-borane complex (Scheme 1.16).[73]

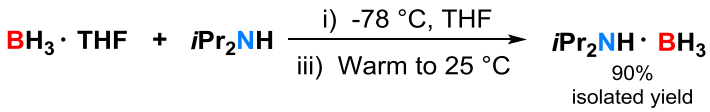

Scheme 1.16 Synthesis of N-substituted amine-boranes by using borane-tetrahydrofuran complex.

However, problems associated with the low long-term stability of these species,[82] which easily decompose, plus the large quantities of flammable, toxic, highly malodorous and mutagenic solvents such as dimethyl sulphide [83] limit their applications to the lab-scale production. With the progress of modern synthetic methods and the development of more efficient reactions substituted amine-borane could be prepared using more handleably starting materials such as alkali metal borohydrides and the hydrochloride salt of the required amine (Scheme 1.17).[84–86]

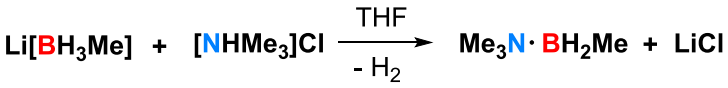

Scheme 1.17 Synthesis of BN-substituted amine-boranes.

In turn a convenient method to prepare substituted alkali metal borohydrides is threating borate esters with alkyl lithium bases to introduce the alkyl groups. The number of alkyl groups introduced is dependent on the stochiometric ratio. The desired hydridic substituents are subsequently introduced upon reduction with $LiAlH_4$ followed by the amine-borane adduct formation by direct exposure to the desired amine hydrochloride.[73]

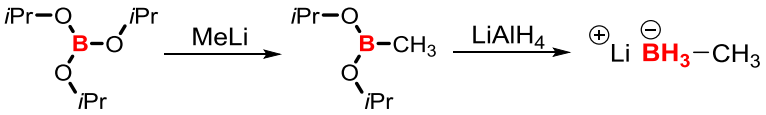

Scheme 1.18 Synthesis of lithium methyl borohydride starting from triisopropyl borate.

This procedure is also used to prepare cyanoboranes, isocyanoboranes, and subsequently, amine- or phosphine-(iso)cyanoborane adducts *via* a similar methodology. Recently one of more versatile approach to synthesis stable amine-borane adducts is the intramolecular cyclization of molecules containing both amine and borane functional groups. In this regards Snyder and co-workers pioneered new synthetic methods to produce stable, aromatic functionalized cyclic amine-borane under mild reaction conditions.[87] These species can be easily prepared by $LiAlH_4$ reduction of appropriate aryl boronic acids or esters containing an amine or a masked (oxidized) amine group (Scheme 1.19).

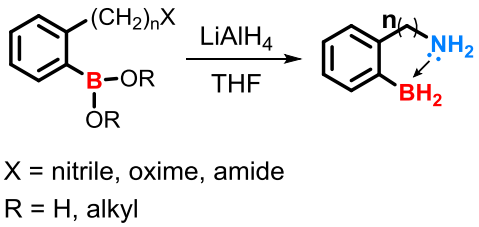

Scheme 1.19 Synthesis of cyclic amine-boranes by reduction of boronic ester group and a potential masked amine function.

The advantages of using this protocol is that a wide range of functional groups are tolerated, and no toxic reactants are employed.[87] Moreover, the easy access to differently aromatic *ortho* substituted boronic acids and boronic esters to use in the synthesis make this an elegant procedure that provide access to previously unavailable amine-borane molecules. Boronic acid and ester species can be also easily synthesised using reliable cross coupling reactions such as the Miyaura borylation,[88] or either by lithium-bromine exchange or lithiation-borylation of halogenated aromatic species containing coordinating groups like amine, amide, carboxylic acid ester, cyano etc (Scheme 1.20).[89–91]

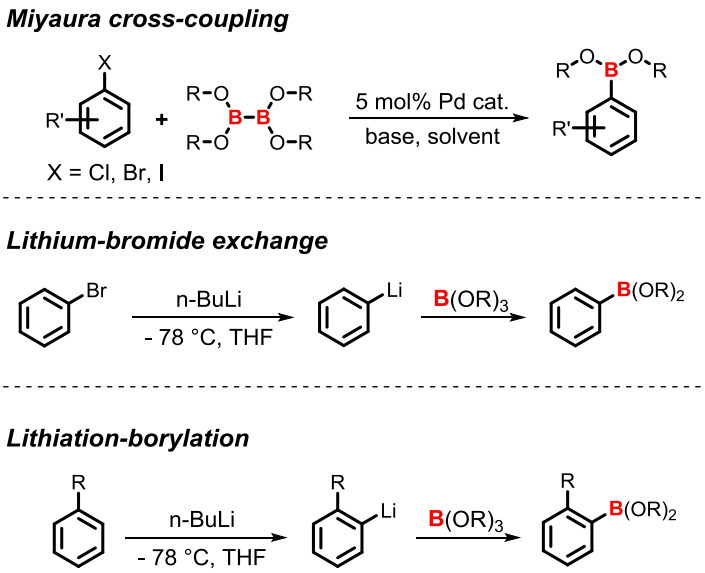

Scheme 1.20 Different synthetic pathways to prepare boronic acid/esters derivatives.

Recent advances in developing new synthetic strategies to prepare cyclic amine-boranes have been made by Vedejs and co-workers.[92] They reported a metal-free, non-dissociative hydroboration method employing unsaturated linear amine-borane complexes.

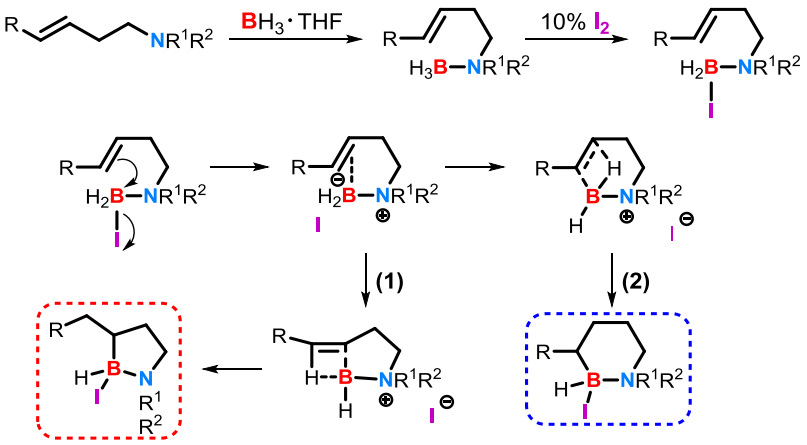

Scheme 1.21 Synthesis of cyclic amine-boranes by reduction. Proposed mechanisms for the Intramolecular hydroboration in homoallylic amine-iodoboranes.

The key step of this synthesis is the formation of the amine-iodoborane complex by iodine activation of the homoallylic amine-borane. In the following step of the intramolecular hydroboration a tethered olefin π-complex is formed, the leaving of iodine is the driving force which allows this reaction to proceed towards the products by two possible nucleophilic substitution pathways: by a dissociative S_N1-like mechanism via an ion pair (1), or by an S_N2-like internal nucleophilic substitution process via the bonding interactions showed for (2).

1.5 The nature of the BN covalent bond in Aminoboranes

The general structure of the aminoborane system is characterized by a covalent bond between a trivalent boron atom linked with a trivalent nitrogen atom where, the unshared electron pair of the nitrogen can participate in this linkage thereby introducing a degree of double bond character. A great contribution to the synthesis and characterization of aminoborane compounds was made by Wiberg,[93] who first postulated the existence of a B-N double bond due to participation of the free electron pair from the nitrogen atom in to the empty p_z orbital of the boron atom (Scheme 1.22). Aminoboranes, therefore, are isoelectric to the all carbon counterpart alkene species, hence they often exhibit similar physical characteristics.

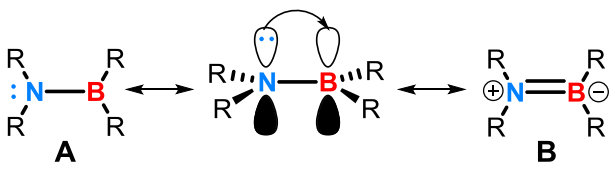

Scheme 1.22 Resonance structure of aminoborane species.

In the ground state boron atom has an external electron configuration of $2s^2$ $2p^1$ with three valence electrons allowing the formation of three σ-bonds. However, in this configuration the shell of valence electrons is incomplete therefore boron tends to stabilize itself by back-coordination of the unshared electrons of the nitrogen to the boron (B). The planarity of aminoboranes was later demonstrated by Goubeau and Becher[94,95] by calculation of the binding constants which resulted to be of 1.8 for the B-N bond confirming the sp^2 hybridization of both boron and nitrogen atoms. Theoretical calculations of the energy barrier to internal rotation in the aminoborane system resulted to be about 10 kcal/mol. This value was later confirmed by experimental observations made by Niedenzu and Dawson.[96] They determined, by NMR analysis, the exact temperature at which two magnetically non-equivalent methyl groups of an unsymmetrically substituted aminoborane (Scheme 1.23) become equivalent by free rotation along the B-N bond.

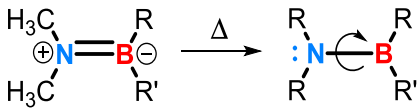

Scheme 1.23 Energy of activation of rotation alongside the boron nitrogen bond.

The energy of activation of rotation calculated resulted to be around 10-15 kcal/mol in good agreement with the theoretical value. The relatively low values found for the rotational barrier of aminoboranes compared with the alkene counterpart species is mainly due to the electronegativity difference between boron and nitrogen atoms. Apparently, the dipole moment expected from formula **B** is considerably reduced by an asymmetrical electron sharing between boron and nitrogen confirmed also by molecular orbital calculations, which clearly suggested that in this system, nitrogen bears a larger negative net charge than the boron. This fact decreases the probability of isolating *cis* and *trans* isomers of BN substituted aminoboranes, although the B-N bond order of these species is greatly influenced by substituents on both boron and nitrogen atoms. Direct evidence of the inter convertible cis-trans isomerism in the aminoborane system has been verified by proton NMR and near infrared spectroscopy (NIR) analysis of a series of asymmetric aminoborane species.

1.6 Synthesis and reactivity of Aminoboranes

The simplest aminoborane system NH_2-BH_2 is not known in monomeric form and due to the high reactivity tends to react with its-self leading to the formation of linear and branched polymeric species.[97] To by-pass this limitation and create more stable aminoborane compounds new synthetic methods were developed to introduce substituents at both boron and nitrogen atoms. One of the earliest preparation of substituted aminoborane was reported by Buchheit in 1949, obtained by a thermolysis process. Thermal dehydrogenation of dimethylamine-borane at 200 °C resulted in the dimethylaminoborane formation with loss of hydrogen (Scheme 1.24).[98,99] Similarly, ammonia-trimethylborane eliminates methane at 280 °C under high pressures yielding aminodimethylborane, H_2N-$B(CH_3)_2$.[100]

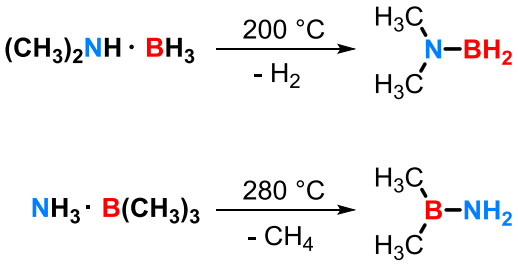

Scheme 1.24 Synthesis of dimethylaminoborane by loss of hydrogen and aminodimethylborane by loss of methane.

Although this synthetic procedure was abandoned for years due to problems linked to lab operating systems requiring high vacuum and inert atmosphere, recently this method has been attracting renewed interest. Schaeffer and Anderson pioneered new synthetic methods to produce amminoboranes in milder reaction conditions.[101] As a valid alternative to the amine-borane, they used functionalised secondary amine salts and metal hydroborates to synthesise substituted aminoboranes (Scheme 1.25).

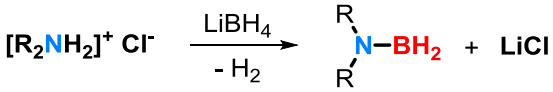

Scheme 1.25 Synthesis of N-substituted aminoborane by reaction between lithium borohydride and an amine salt.

Another important class of aminoboranes are aminodihalogenoboranes of general formula R_2N-BX_2. These compounds were prepared by Michaelis more than sixty years ago by direct exposure of secondary amines to boron halides such as BCl_3 or BBr_3 followed by dehydrohalogenation.[102] As previously described for the synthesis of B-trichloroborazines, a stoichiometric amount of a tertiary amine as additive is used to promote the elimination of HX and to avoid side reactions with both, starting materials and the aminodihalogenoborane formed.[103]

Scheme 1.26 Synthesis of N-substituted amino B-halogenated boranes.

Aminodihalogenoboranes are important intermediates, which can be further functionalized at the boron atom for example by reacting a properly substituted aminomonohalogenoboranes with the appropriate Grignard reagent.[104,105]

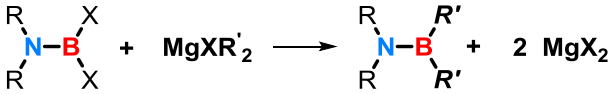

Scheme 1.27 Synthesis of BN-substituted aminoboranes by functionalization at the boron atom with Grignard reagents.

Usually functionalization with Grignard reagents is carried out under mild reaction conditions with ordinary laboratory equipment. Therefore, this method has been widely used to have easy access to a large variety of differently substituted aminoboranes. Another important method to functionalise boron atom of substituted aminoboranes is by Friedel-Crafts reaction in presence of $AlCl_3$ and aromatic compounds.

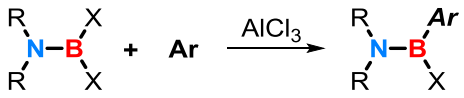

Scheme 1.28 Functionalization of aminoboranes by Friedel-Crafts reaction.

Chemical syntheses of BN isosteres of simple PAH was pioneered by Dewar and co-workers in the 1950s and 60s, triggering significant research interest in azaborine chemistry.[106] The first BN-substituted aromatic heterocycle synthesised by Dewar's group was 9-aza-10-boraphenanthrene reported in 1958.[107] This compound was obtained upon treatment of 2-phenylaniline in presence of the Lewis acidic species BCl_3 and $AlCl_3$ followed by Friedel-Crafts cyclization. The highly reactive B-Cl intermediate species in presence of various Grignard nucleophiles reagents produced a family of BN-substituted phenanthrene derivatives also, the reduction with $LiAlH_4$ gave the parent 9,10-azaboraphenanthrene.

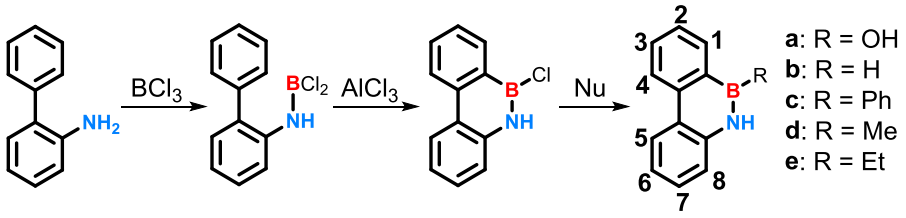

Scheme 1.29 Preparation of boron-substituted 9,10-azaboraphenanthrene derivatives.

A year later the same group reported the synthesis of the first BN-naphthalene[108] obtained by the reaction between 2-aminostyrene with phenylboron dichloride leading to the direct formation of 2-phenyl-1,2-azaboranaphthalene. Also, BN-naphthalene derivatives differently functionalized at the boron atoms were prepared from the reaction between *p*-amminostyrene and BCl_3 followed by a nucleophilic substitution in presence of Grignard reagents.[109,110]

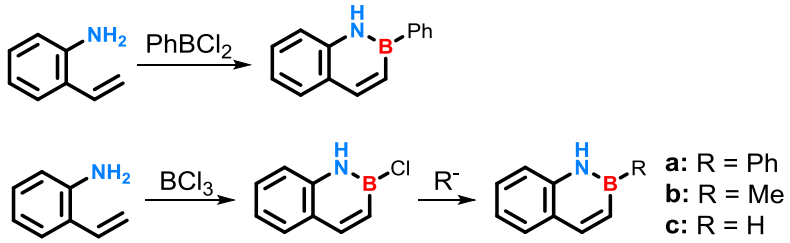

Scheme 1.30 Synthesis of B-substituted 1,2-azaboranaphthalenes.

Based on similar strategies, Dewar and co-workers synthesised and characterise several other BN-substituted PAHs determining the chemical and physical properties as well as the reactivity of these new species towards different nucleophile and electrophile. With this pioneering work Dewar and co-workers greatly enriched the heterocyclic chemistry with the synthesis of BN incorporated aromatic molecules, contributing to understand the chemistry of these new materials. However, all these studies were developed from the synthetic viewpoint driven by the fundamental interest of organic chemists, and no applications were reported for these numerous materials. These new compounds were not fully characterized due to the limited instrumentation availability and characterization capability, therefore their properties were not well studied.[106] After decades of hibernation, this topic is now attracting again a great deal of interest due to the rapid development of organic π-conjugated materials for applications in electronic and optoelectronic devices. In 2000 the Ashe group reported an innovative synthetic protocol for the synthesis of aromatic BN-heterocycles renewing scientific interest in this field.[111] Specifically, they reported the synthesis of 1,2-azaborines following a ring-closing metathesis/oxidation procedure under milder reaction conditions compared with the previous reported.

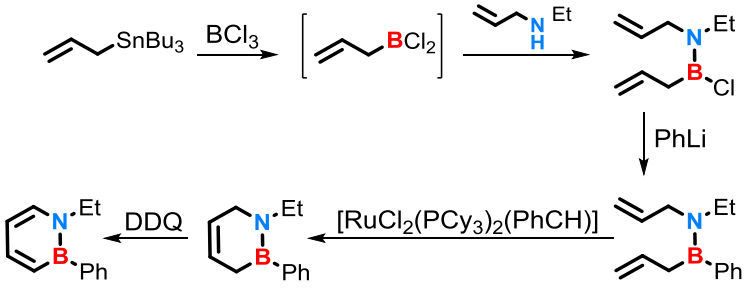

Scheme 1.31 Mild synthesis of 1,2-azaborine by ring-closing metathesis.

Transmetalation of allyltributyltin with BCl_3 generated allylboron dichloride, which in turn reacted in presence of the Lewis base allylethylamine producing bis(allyl) aminoborane. The reaction with PhLi led to the displacement of chloride atom to give the corresponding B-Ph aminoborane in good yield. Ring-closing metathesis was performed with Grubbs' first-generation catalyst and the intermediate produced was oxidized to 1,2-azaborines using 2,3-dichloro-5,6-dicyano-1,4-benzoquinone (DDQ) at 35 °C. Following this protocol, the Ashe group explored the synthesis of a wide variety of 1,2-azaborines differently substituted at both boron and nitrogen atoms. Also, to expand the scope of their studies they reported the synthesis of a five membered 1,2-azaborolide heterocycle, which is formally isoelectronic with the ubiquitous cyclopentadienide (Cp) ion.[112] Furthermore, the Ashe group made considerable advances in developing new synthetic strategies to prepare BN-azaborines complexed with transition-metals. For example, they reported the synthesis of η^6 piano-stool type chromium and molybdenum complexes,[112] ruthenium sandwich compounds,[113] as well as η^1 zirconium complexes bound at the deprotonated azaborine nitrogen.[114] In one of the most recent work reported, Ashe and co-workers investigated the ligand properties of deprotonated BN-styrene in presence of ruthenium complex [{Cp*RuCl}$_4$].[115] They observed that one equivalent of [{Cp*RuCl}$_4$] was used the η^6-binding complex occurs between BN-styrene and ruthenium, while with two equivalents the second ruthenium atom binds η^1 to the 1,2-azaborine nitrogen and η^2 to the B-vinyl group.

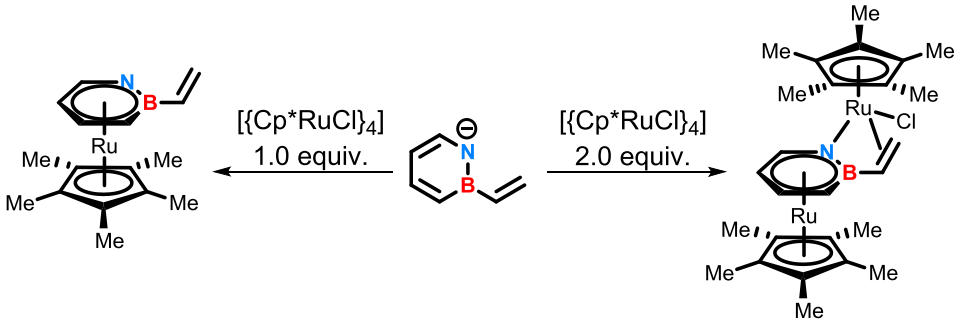

Scheme 1.32 Synthesis of ruthenium complexes from BN-styrene.

Since Dewar's initial work, however, investigation on the spectroscopic properties of BN heteroaromatics revealed that they resembled those of their carbon analogues. Basically, when compared with the all-carbon counterparts, they showed similar absorption and emission band with the only exception of the intensity of the α-band, which was enhanced due to removal of the orbital degeneracy in the BN heteroaromatics.[106,116] The synthesis of BN-embedded polycyclic aromatics reported by Piers and co-workers in 2003 marked a breakthrough point in the potential use of these materials for electronic and optoelectronic applications.[117] In 2006 they reported the synthesis of BN-substituted triphenylene **I** and dibenzo[g,p]chrysene **II** structures describing in detail the spectroscopic and the redox properties of these materials as well as a careful evaluation of the aromaticity was done.[118]

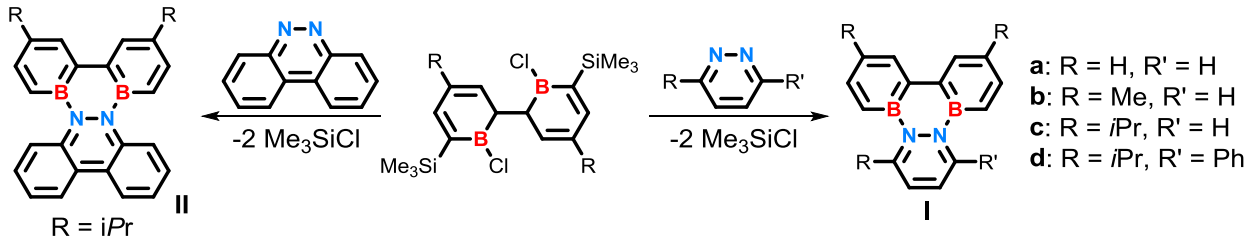

Scheme 1.33 Synthesis of BN-substituted triphenylene derivatives.

The spectroscopic results obtained comparing the Uv-Visible spectra of BN-substituted triphenylene with the all-carbon triphenylene analogue revealed a striking difference in absorption band. The fluorescence maximum of the BN-derivative was red-shifted of 203 nm (from 335 to 558 nm) respect to triphenylene. Presumably the lower energy charge-transfer absorptions of the BN-derivative resulted in fluorescence being in the visible region.

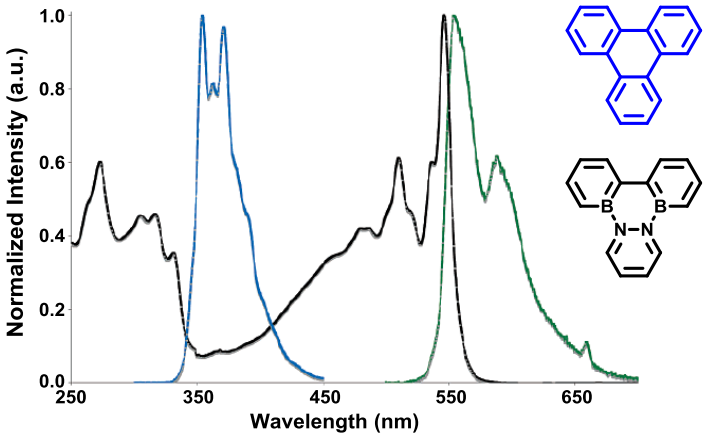

Figure 1.3 UV-Visible (black) and fluorescence (green) spectra of BN-substituted triphenylene and fluorescence (blue) spectrum of triphenylene.[118]

Moreover nucleus-independent chemical shift (NICS) calculations (B3LYP/6-31G(d) level) on BN-substituted triphenylene indicated the central $B_2N_2C_2$ ring with a stronger aromatic character compared to the outer borabenzene rings. The opposite trend, instead, was observed for triphenylene confirming that BN-substituted polycyclic aromatics possess different properties compared to their carbon analogues. In addition, Piers and co-workers observed that the location of polar BN units within the same aromatic framework can dramatically alter the photophysical properties of the resulting materials.[61] They studied this phenomenon by direct comparison of the UV-Visible spectra of two different BN-substituted phenanthrenes with their carbon analogue.

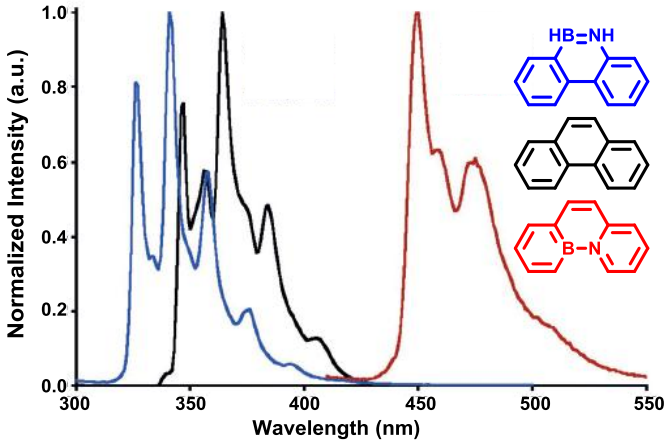

Figure 1.4 Fluorescence emission spectra of phenanthrene (black), external BN-phenanthrene (blue) and internal BN-phenanthrene (red).[61]

Phenanthrene, in cyclohexane, exhibited an emission maximum in the UV region at 347 nm with a low quantum yield, φ_F = 0.09. Internal BN-substituted phenanthrene (red) showed a remarkable red shift in emission spectrum of 103 nm with a great increase in quantum efficiency to φ_F = 0.58, when compared with phenanthrene. External BN-substituted phenanthrene (blue), instead, showed a blue-shift in emission spectrum of 123 nm, with band structure closer to phenanthrene. These results clearly suggested that the energy levels can be also finely tuned by the BN units location. More extended BN-PAHs have also been explored by Nakamura and co-workers who reported in 2011 the synthesis of BN-Fused Polycyclic Aromatics.[119] They adapted the Dewar's original protocol for the construction of extended π-conjugated frameworks with BN ring fusion developing a tandem intramolecular electrophilic arene borylation method promoted by a combination of a Lewis acid and a Brønsted base in the appropriate ratio.

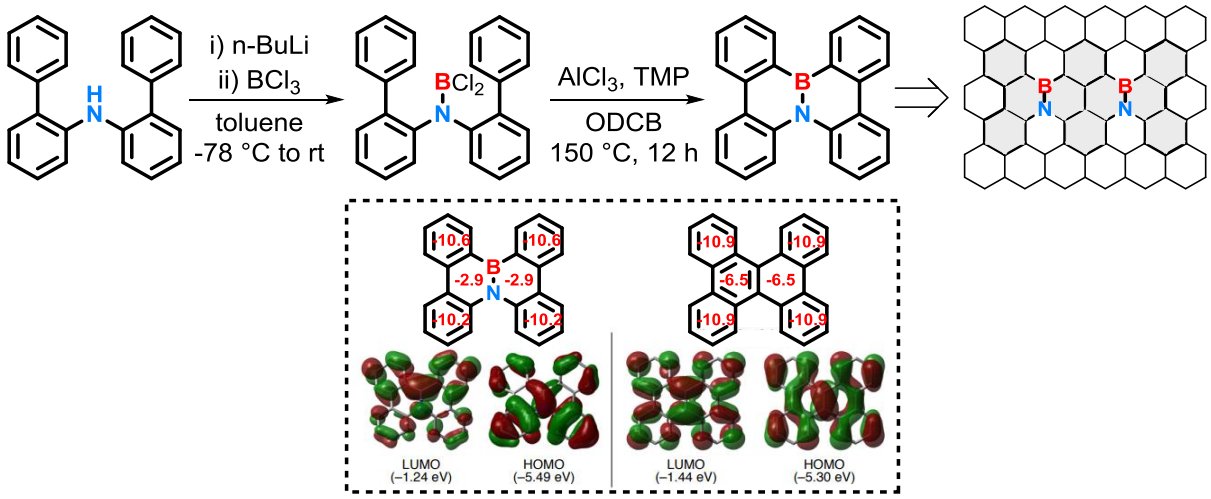

Scheme 1.34 Tandem Intramolecular Electrophilic Arene Borylation To Synthesize BN-Fused PAHs. NICS(1) values of BN- dibenzo[g,p]chrysene and dibenzo[g,p]chrysene with comparison of the LUMO and HOMO level.[119]

Time-resolved microwave conductivity (TRMC) experiment revealed BN-dibenzo[g,p]chrysene to be a semiconducting materials with potential applications in electronics since the intrinsic hole mobility

measured of 0.07 $cm^2 V^{-1} s^{-1}$ was comparable of that of rubene (0.05 $cm^2 V^{-1} s^{-1}$), which is one of the most popular organic semiconductors.[120] The aromaticity evaluated by NICS calculations, indicated a lower aromatic character of the central BNC_4 compared with the central rings of the carbon analogue, while the external rings seem not to be affected from the BN substitution. Other important contributions to the synthesis of extended BN-PAHs came from the Yamaguchi Group from Nagoya University[121] and the Kawashima Group from University of Tokyo.[122] More recently Liu and co-workers reported the synthesise of BN-anthracene isosters, similar to that previously obtained in Dewar's group. Notably, Liu detailed a four-step procedure for the synthesis of mono 1,2-BN anthracene and di 1,2-8,9-bis BN anthracene as reported in Scheme 1.35.[123]

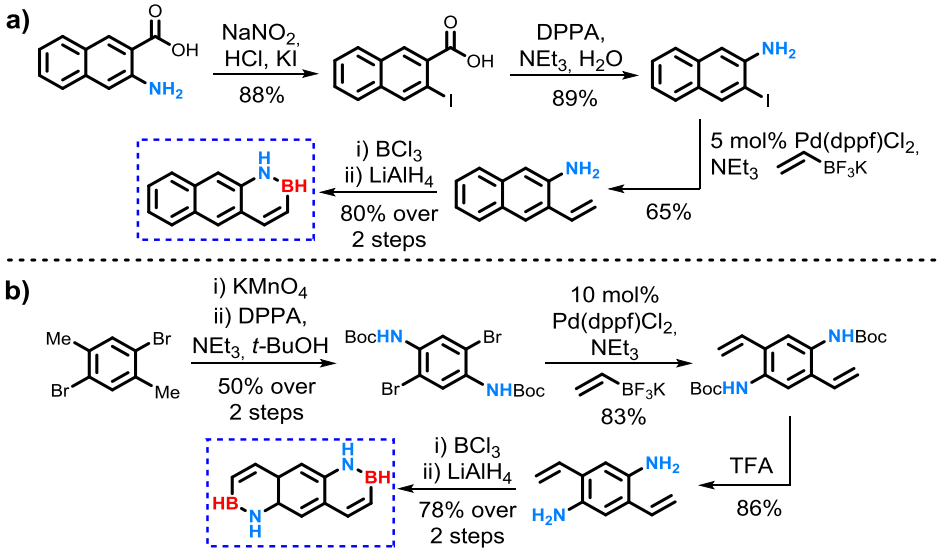

Scheme 1.35 a) Synthesis of 1,2-BN anthracene; b) synthesis of 1,2-8,9-BN anthracene.

The electronic structures of mono 1,2-BN anthracene and di 1,2-8,9-bis BN anthracene were investigated combining the UV-PES/computational and experimental data to determine the energies of occupied molecular orbitals (HOMOs). They found that, introduction of BN units altered, in both cases, the HOMO energy levels destabilising the molecules.

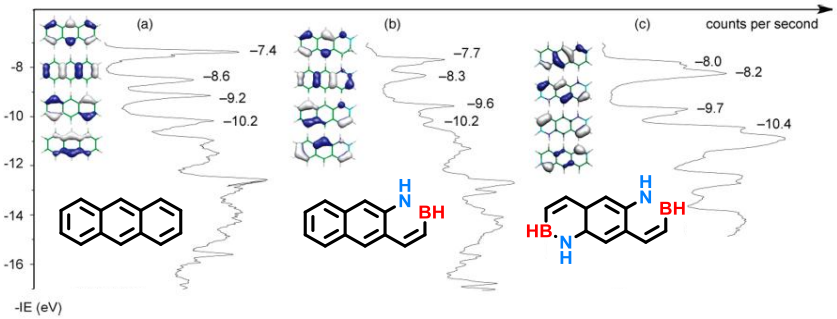

Figure 1.5 UV-PE spectra of (a) anthracene, (b) BN anthracene, and (c) bis-BN anthracene. The vertical axis is defined as the negative value of the experimentally determined ionization energy (−IE).[123]

Absorption spectra of the BN-anthracenes shows identical low energy absorption and comparable fine band structure centred around 377 nm, similar to anthracene. In contrast to the carbonaceous anthracene, there is a second electronic transition observed for BN-1,2-anthracene (λ_{max} = 327 nm) and BN-1,2-8,9-anthracene (λ_{max} = 311 nm) which showed a bathochromic shift from their lower energy absorption.

1.7 Synthesis and reactivity of Borazine and its derivatives

Borazine, known as "inorganic benzene", was synthesised and isolated for the first time in 1926 by Stock and Pohland upon thermolysis of the adduct of ammonia with borane at 200 °C in a bomb tube (Scheme 1.36).[124] In spite of the successful in the synthesis of this new material the overall yield after purification was very low. Subsequently Wiberg and Bolz further investigated on the reactivity of ammonia-borane in different reaction conditions demonstrating a direct correlation between yield and temperature.[125] Indeed, following the same procedure, they obtained borazine in higher yield by increasing the temperature to 280-300 °C.

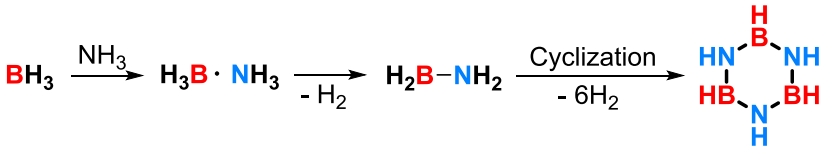

Scheme 1.36 First synthesis of borazine by thermolysis of amine-borane complex.

Over the years the best conditions to synthesise borazine were obtained by rapidly heating to 250 °C of diborane B_2H_6 and NH_3 in molar ratio of 1:2, at one atmosphere for 45 minutes. However, one of the difficulties surrounding the development of this protocol to synthesise borazine materials was essentially due to the handling of the boron hydrides and ammonia.[81] To overcome these limitations scientists developed new synthetic procedures using more handleably starting materials such as metal hydroborates and ammonium chloride as readily available source of boron hydride and ammonia, performing the reaction in anhydrous ethereal solvents under milder reaction conditions.[85,126,127] Later, great improvements in the preparative technique were achieved by Brown and Laubergayer,[128] who synthesised B-trichloroborazine reacting ammonium chloride in presence of boron trichloride in chlorobenzene (Scheme 1.37).

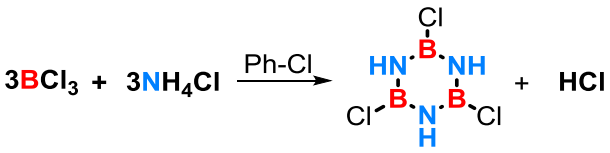

Scheme 1.37 Synthesis of B-trichloroborazine.

1.7.1 Chemical and physical properties

Borazine is a six-membered boron-nitrogen heterocycle, where three nitrogen and three boron atoms are alternate each other along the cycle satisfying the symmetry of D_{3h}. Electron diffraction and X-ray data [129,130] are consistent with a planar hexagonal molecule. The B-N bond length is 1.44 Å, which is in between with that expected for a single bond (1.54 Å) and a double bond (1.36 Å) (Figure 1.6).[131]

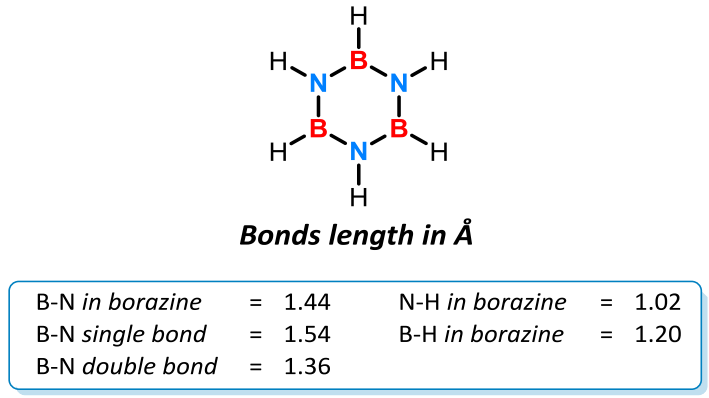

Figure 1.6 Bonds length in the borazine system.

In the borazine system both boron and nitrogen atoms are sp^2 hybridized with four valence atomic orbitals (AO) 2s, $2p_x$, $2p_y$, $2p_z$ and three valence electrons for boron atom and five valence electrons for nitrogen atom.[132–134] Both form three σ-bonds, one with the terminal hydrogen atom and two with the neighbouring boron or nitrogen atoms respectively. This results in boron with an empty p_z orbital and nitrogen with a lone pair, both being perpendicular to the planar ring.[135] Electron donation of the nitrogen lone pair to the boron electrophilic centre empty p_z orbital, gives a weak aromatic character to the borazine ring [136,137] satisfying the Hückel's Rule ($6e^-$ in 6π orbitals) (Figure 1.7).

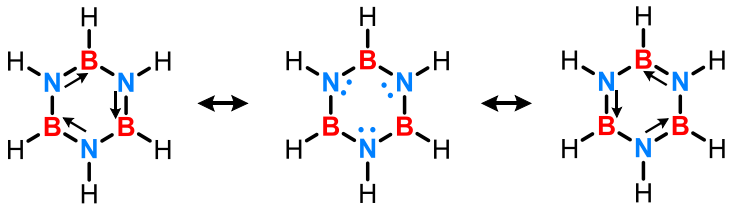

Figure 1.7 Representation of the borazine limit forms by the electronic delocalization along the ring.

However, the electrons of the π-system are not equally shared between boron and nitrogen atoms because of the difference in electronegativity, therefore the strong local dipole moment results in a different reactivity from benzene.

Table 1.1 Comparison of Fundamental Properties of boron, carbon, and nitrogen atoms.

	Boron	***Carbon***	***Nitrogen***
Valence electrons	3	4	5
Covalent radius (pm)	88	77	70
Pauling electronegativity	2.0	2.5	3.0

A classic example is the different reactivity of these two species in presence of HCl. In fact, borazine, being more reactive than benzene, led to the addition product $B_3N_3Cl_3H_9$ while benzene is unreactive under the same reaction conditions (Scheme 1.38).

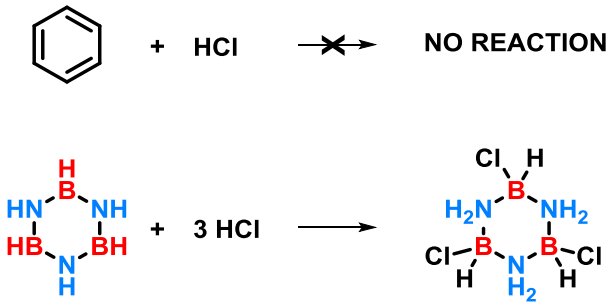

Scheme 1.38 Difference in reactivity of benzene and borazine with HCl.

The strong local dipole moment also widens the HOMO-LUMO gap to 6.2 eV when compared to that of benzene which is 6.0 eV, essentially due to a decrease in the HOMO energy level. The borazine structure was fully characterised by electron diffraction and X-ray data,[129,138] which proved the planar hexagonal geometry of alternating B-H and N-H groups. Uv-Visible,[139] IR and Raman spectra [140,141] have been also well investigated in the past assigning the fundamental frequencies on the basis of benzene-like symmetry D_{3h}. Also, molecular modelling calculations were used to predict the electronic density and define molecular orbitals of borazine.[142–144]

1.7.2 Functionalization of the borazine ring

Chemical and physical properties of borazine were intensively investigated between the 1960's and 1970's, however all these studies were developed from the synthetic viewpoint and no applications were reported for this material.[64] Also, difficulties surrounding the synthetic and purification procedures as well as the ability to be processed made this material less appealing to be further studied. One of the main problems was related to the instability of borazine, since it was observed that a prolonged storage of liquid borazine at room temperature resulted in a violent explosion without any apparent cause.[145] To overcome these problems scientists developed new synthetic methods to create stable borazine compounds substituted at boron and nitrogen atoms with different aliphatic and aromatic functional groups. Therefore, at the

beginning of the 1990's borazines started again to gather certain interest from the scientific community mainly as precursors for the synthesis of hexagonal boron nitride (h-BN), the insulating analogue of graphene, but in general to synthesise boron nitride (BN) ceramics.[146,147] Borazine derivatives have been investigated for the first time in 2005 as potential active materials in optoelectronic devices.[148] Later on, in parallel with the synthetic developments of polyaromatic hydrocarbons (PAHs), a wide range of functionalized borazines at both boron and nitrogen atoms have been synthesised.

1.7.3 Functionalization at the nitrogen atoms

Borazine functionalization at the nitrogen atom was investigated for the first time in 1938 by Ritter and Burg.[149] They prepared N-trimethylborazine (-BH-NCH_3-)$_3$, by condensation of diborane and methylamine. This synthetic method was later developed for the preparation of a wide range of differently substituted borazines at the nitrogen atom by cyclotrimerization of alkylammonium salts in presence of lithium/sodium hydro borate (Scheme 1.39).

Scheme 1.39 Synthesis of N-substituted borazine derivatives.

Other valid precursors alternative to amines used for the synthesis of borazines were nitrile compounds as reported by Emelus and Wade[150] with the preparation of N-ethyl borazine (-BH-NC_2H_5-)$_3$ using diborane B_2H_6 and acetonitrile. In an extension of this concept N-alkylhalogenated borazines were prepared using for example CCl_3CN or CF_3CN in the same reaction conditions. Curiously, the nitrile-borane adducts revealed to be unstable at room temperature decomposing in a few days to give N-alkylborazines in 50-60% yields. In the following years the synthetic procedures to prepare borazine derivatives were further optimized replacing diborane with boron halides such as BCl_3 or BBr_3, which could be used in solution complexed with the solvent.[81] Notably, B-trichloroborazine (-BCl-NH-)$_3$ is one of the most convenient starting materials in borazine chemistry, because it can be used as intermediate to be further functionalize to the boron atoms. N-Alkylated-B-trichloroborazines can be readily prepared following the Brown-Laubengayer procedure exposing primary alkyl/aryl ammines to the highly reactive boron halides forming the borazine ring upon mineral acids elimination.[64] Usually a stoichiometric amount of a tertiary amine is used to promote the elimination of HX leading to the formation of an insoluble ammonium salt.

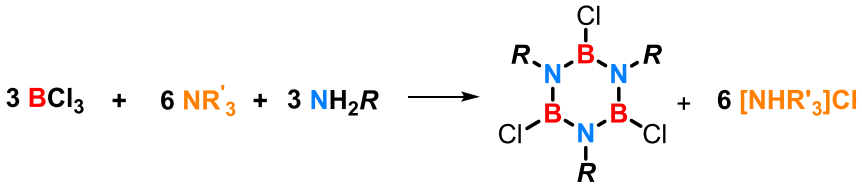

Scheme 1.40 Synthesis of N-substituted B-trichloroborazine derivatives.

Boron trichloride BCl_3 and boron tribromide BBr_3 are preferentially used in the borazine synthesis than boron trifluoride BF_3 since B-F bond is stronger than B-Cl and B-Br bonds, and this makes more difficult the elimination of HF during the cyclocondensation.[64]

1.7.4 Functionalization at the boron atoms

As highlighted previously N-alkyl/aryl functionalization of borazines is performed by a careful choice of primary amine or nitrile precursors, while functionalization of the boron atom is achieved by direct nucleophilic substitution of B-trichloroborazine intermediates in presence of organo-lithium, or Grignard reagents.[151]

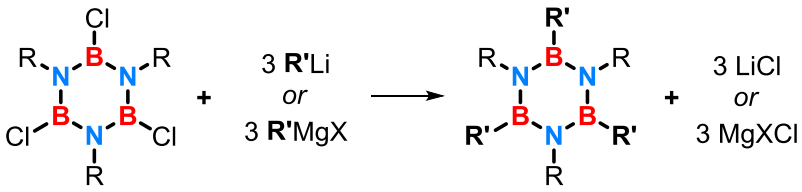

Scheme 1.41 Functionalization at the boron atoms by organo-lithium or Grignard reagents.

This procedure introduced by Groszos and Stafiej in1958,[152] has become one of the most versatile approach to introduce substituents at the boron atom. Due to the high reactivity of the latter, alkyl/ aryl functionalization is usually carried out under mild reaction conditions at room temperature in anhydrous ethereal solvents such as THF giving satisfactory yields of the desired products.[153] Alternatively, hydroborazines can also be used as effective substrates to give B-alkyl derivatives following the same method previously described, however starting from B-trihalogeno borazine is preferred because of the substitution at the boron atom occurs faster in the latter case. B-trichloroborazine intermediates can also be used in the Friedel-Crafts reaction in presence of $AlCl_3$ and aromatic compounds or reduced to the corresponding hydroborazines when threated with reducing agents [64] such as lithium aluminium hydride $LiAlH_4$ or sodium borohydride $NaBH_4$.[154]

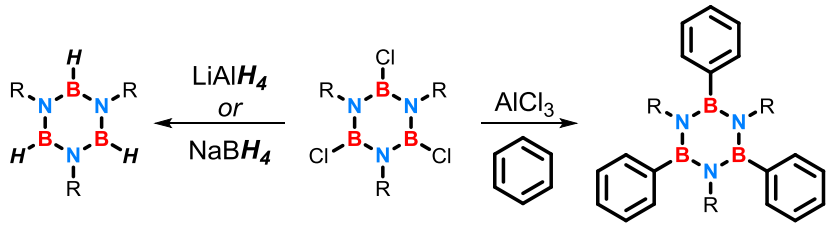

Scheme 1.42 Functionalization at the boron atoms by Friedel-Crafts reaction and reduction of B-Cl bond to B-H bond of N-substituted B-trichloroborazine derivatives.

Another important functionalization is the transhalogenation of B-trichloroborazines with another halogen atom. This reaction plays a decisive role for the synthesis of B-trifluoroborazines since, as previously reported, these intermediates are not accessible *via* Brown-Laubengayer protocol.[155] Therefore this is one of the most feasible methods to achieve these materials. Niedenzu reported for the first time fluorination of substituted B-trichloroborazines using a variety of metal fluorides (MF).[156]

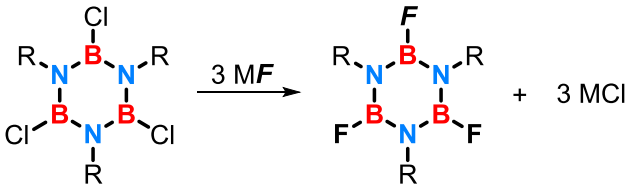

Scheme 1.43 Transhalogenation of N-substituted B-trichloroborazine derivatives.

In particular titanium tetrafluoride TiF_4 and antimony trifluoride SbF_3 have been successfully employed to prepare B-trifluoroborazine,[157] however, in the following years, several different fluorinating agents have been investigated.[158] Interestingly, SbF_3 in combination with antimony chlorides has been used to prepare mono 2-fluoro-4,6-dichloro and 2,4-difluoro-6-chloro substituted borazines as shown in Figure 1.8.[159]

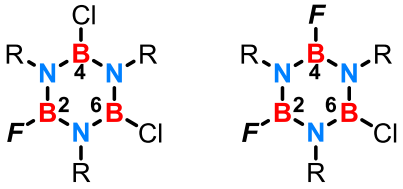

Figure 1.8 Example of controlled mono and di transhalogenation using different fluorinating agents.

1.8 BN-doped Polycyclic Aromatic Hydrocarbons (BN-PAHs) applications

As highlighted, BN-substituted PAHs and BN-heterocyclic compounds in general, have gained a significant attention in materials science as they can be attractive tools for organic electronic applications. These materials are playing an important role as precursors for preparing bulk and thin-layer BN-based ceramics, ultrathin insulators, hydrogen storage and biomimetic materials.

1.8.1 Electronic applications

One of the earliest applications of BN-substituted PAHs in electronic devices was reported in 2013 by Pei and co-workers. They reported the synthesis[160] of a series of BN-substituted tetrathienonaphthalene derivatives substituted with lateral alkyl chains and used as active materials for the fabrication of organic field-effect transistors (OFETs).[161]

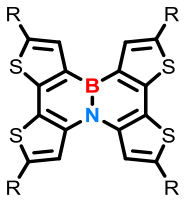

a: R = CH_3
b: R = C_2H_5
c: R = n-C_3H_7
d: R = n-C_4H_9
e: R = n-C_5H_{11}
f : R = n-C_6H_{13}

Figure 1.9 Synthesis of BN-substituted tetrathienonaphthalene derivatives.

The high thermal stability (340 to 400 °C), determined by thermogravimetric analysis (TGA), allowed these materials to be thermally evaporated onto the CYTOP-modified Si/SiO_2 substrates followed by the assembly of gold source/drain electrodes fabricated in a bottom-gate/top-contact (BG/TC) device configuration. They observed that the device performances were highly dependent from the alkyl chain length since they influenced the solid-state properties, including intermolecular packing, energy levels, and thin film morphology. Indeed, the increase in the alkyl chain length caused in turn an increase of the intermolecular B···N distance leading to a disruption of the intermolecular BN dipole-dipole interactions characterizing the molecular packing of these materials. This resulted in a disordered BN dipole orientation which made the films discontinuous, hence influencing the device performance. The highest hole mobility up to 0.15 $cm^2\ V^{-1}\ s^{-1}$ was measured for BN-substituted tetrathienonaphthalene with propyl side chains while the lowest of 0.03 $cm^2\ V^{-1}\ s^{-1}$ was observed for the hexyl side chains derivative.

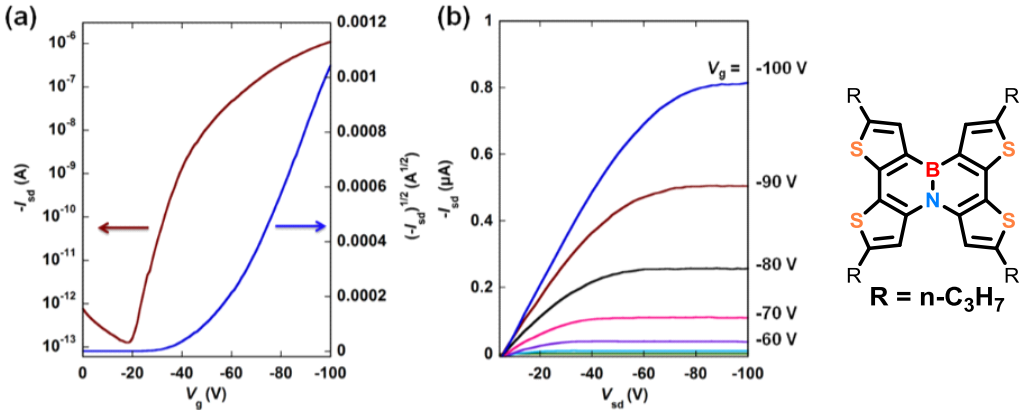

Figure 1.10 a) Transfer and b) output characteristics of the OFET of BN-substituted tetrathienonaphthalene with propyl alkyl chains with a hole mobility of 0.15 $cm^2\ V^{-1}\ s^{-1}$.[161]

Improvements in the hole mobility were achieved a year later from the same group with the synthesis and application of BN-substituted heterocoronene derivatives for the fabrication of micro-ribbon FET devices.[162] The devices, made with the hexyl chains derivative, exhibited the highest hole mobility of 0.23 $cm^2\ V^{-1}\ s^{-1}$, with a low threshold of -3 V and a current on/off ratio over 10^4. Also, a photoresponsive electrical conductivity from the micro-ribbons was observed in the same device configuration in a two-wire resistor mode. Remarkably, the electrical conductivity was greatly enhanced when the device was exposed to the light suggesting these materials powerful tools for organic photovoltaics.

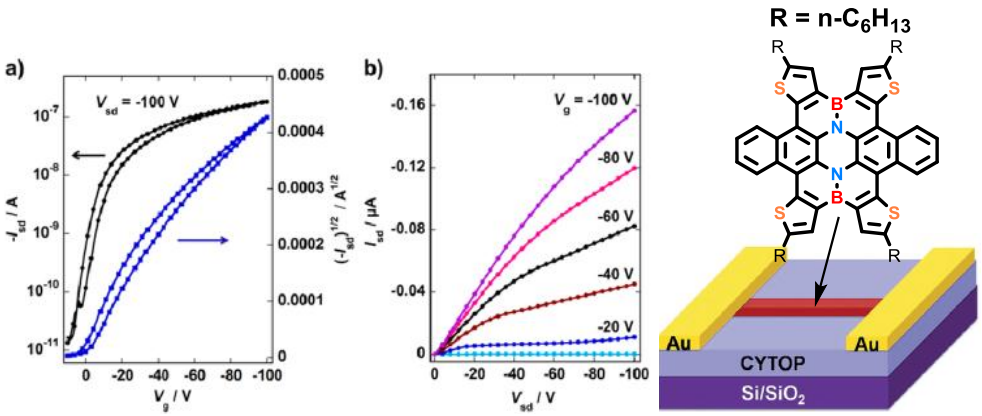

Figure 1.11 (a) Transfer and (b) output characteristics of the microribbon FET devices based on BN-substituted heterocoronene, and graphic illustration of the micro-ribbon FET device.[162]

Investigation of the optoelectronic properties of borazine-based materials by fabrication and characterization of light-emitting diodes (LEDs) and light-emitting electrochemical cells (LECs), was reported for the first time by Bonifazi and co-workers in 2013.[163] They synthesised hexaryl-substituted borazine derivatives in one-pot reaction by cyclotrimerization of aniline and BCl_3 followed by nucleophilic substitution in presence of aryl lithiated or Grignard reactants.

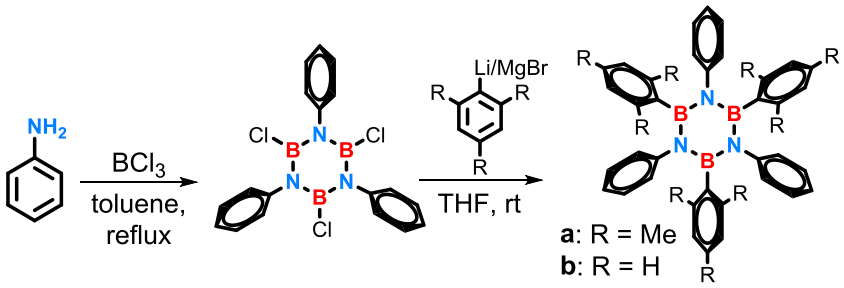

Scheme 1.44 Synthesis of hexaryl-substituted borazine derivatives.

The mesityl derivative was chosen as active material to investigate the emission properties under electrical injection conditions when incorporated in LEDs and LECs devices. The LEC device was assembled as reported in Figure 1.12: the active material was blended with polyethylene oxide (PEO), used as ion-transporting polymer, and a salt to reduce charge-injection barriers on the electrode interfaces. LEC device, instead, incorporated in the active layer only neat borazine and both devices were built on an indium-tin oxide (ITO) anode, with an 80 nm hole-injection layer of poly(3,4-ethylenedioxythiophene) (PEDOT)/polysodium styrene sulfonate (PSS) spin-cast from a 2.8% solution in water.

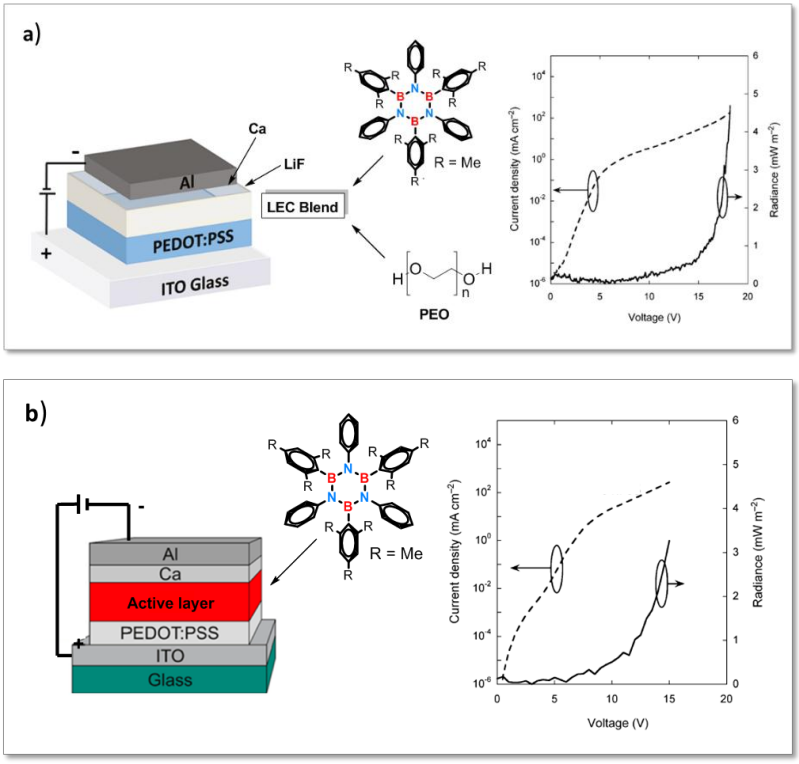

Figure 1.12 Examples of a) LEC, b) LED devices with incorporated B, B, B-trimesityl-N, N, N''-triphenylborazine as active material in the emissive layer.[163]

For the representative LEC a charge injection was observed and the current density J *vs*. the applied voltage V showed a nonlinear dependence. current densities of >100 mAcm^{-2} were achieved at ≈15 V indicating an intrinsically low charge mobility of the borazine used. However, luminescence was observed at ≈9.5 V with

an emission in the UV range, at wavelengths <400 nm. Similar results were observed for the representative LED device.

1.8.2 Hydrogen storage applications

One of the current hot topics that is attracting a great deal of attention in the scientific and technological world is the efficient and safe storage of hydrogen seen as the fuel of the near future to supply energy.[164,165] Of particular interest are boron-and nitrogen-containing chemical hydrides, which are emerging as potential candidates for hydrogen storage purpose due to their high gravimetric hydrogen densities and favourable kinetics of hydrogen release.[166] One of the remarkable examples is ammonia borane (H_3N-BH_3, **AB**), with a gravimetric density of 19.6 wt % H_2.[72] **AB** can release hydrogen *via* chemical reactions under mild conditions. However, one of the key challenges in advancing of this technology remains the regeneration of the spent fuel.[167] This problem has been extensively investigated in the recent past[68] however, most of the methods developed are feasible only on laboratory scale. Liu and co-worker proposed in 2011 a catalytic cycle with the charged fuel being a BN-heterocyclic analogue of cyclohexane.[168]

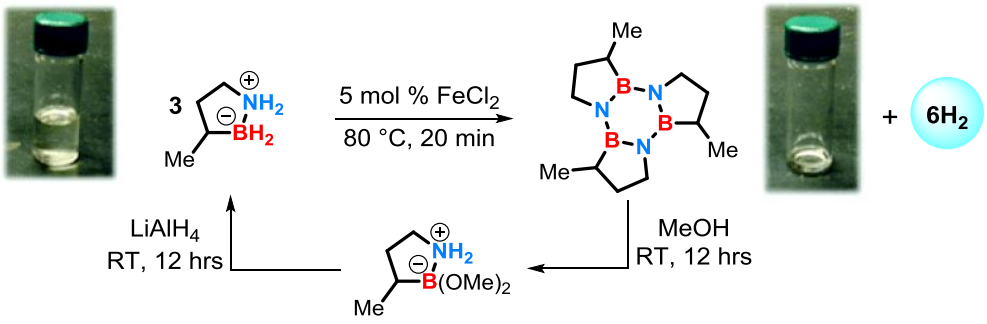

Scheme 1.45 Catalytic cycle where the spent fuel back to charged fuel after released of six molecules of hydrogen.[279]

Air and moisture stable 1,2-BN-5-methylcyclopentane, when used in a thermolysis process catalysed by Lewis acidic species (e.g. $FeCl_2$), release six molecules of hydrogen at 80°C. The corresponding borazine, representing the "spent fuel", is regenerated by a methanolysis process followed by reduction with $LiAlH_4$ to give the starting material ready for another cycle. In the same year El-Kaderi and co-workers proposed a new class of highly porous borazine-linked polymers (BLPs) as potential gas (H_2, CO_2, CH_4) storage materials.[169,170] They prepared porous covalent organic frameworks (COFs) containing doping B_3N_3 rings as functionalized polar building blocks units to improve hydrogen-framework interactions.

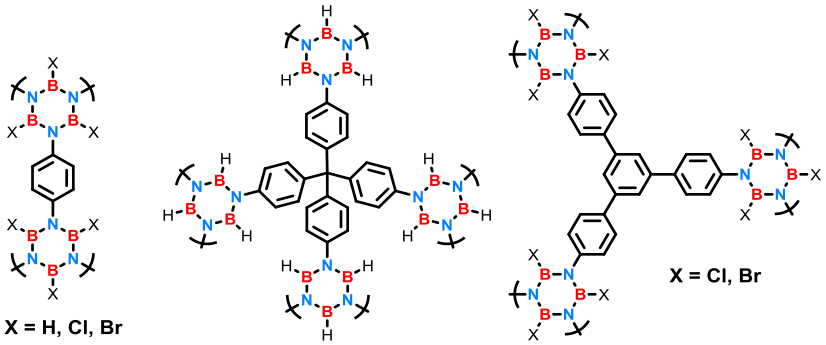

Figure 1.13 Examples of highly porous borazine-linked polymers for gas storage applications.

Preliminary tests on the performance of these materials in the storage of hydrogen indicated that BLPs can be competitive with other organic polymers of similar surface areas since percentages of hydrogen absorbed were comparable. Additionally, they investigated on the performance of BLPs in storing different gas such as syn-gas CH_4 and CO_2. Results obtained suggested that these materials have a high affinity for CO_2 probably due to the favourable interaction between the polarizable CO_2 molecules and borazine rings. Instead, the CH_4 storage capacity was in line with those of COFs and organic polymers under similar condition.[171,172]

1.8.3 Biological applications

Isosteric BN/CC replacement has become a powerful strategy in biomedical research to create new biochemically active compounds used as biomimetics. Liu and Heider have demonstrated that the BN isosteres of ethylbenzene possess biological activity and in particular they observed that N and B-ethyl-1,2-azaborine are strong ethylbenzene dehydrogenase (EbDH) inhibitors.[173]

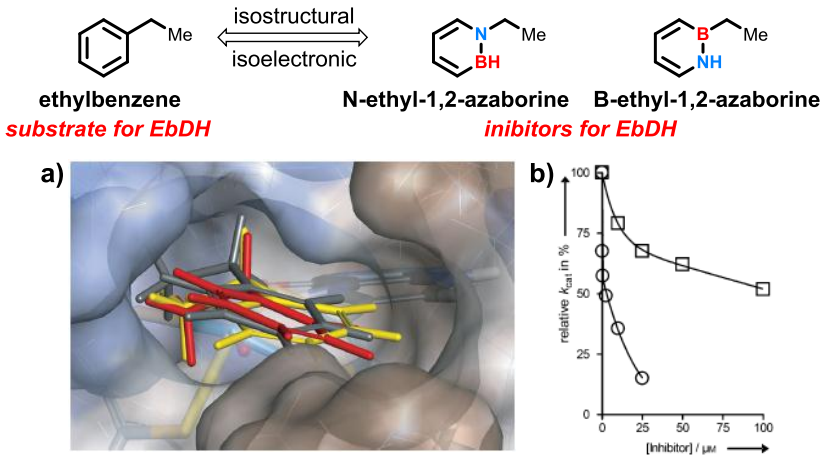

Figure 1.14 Effect of BN/CC isosterism on enzyme reactivity. a) Overlay of a) N-ethyl-1,2-azaborine (red), b) B-ethyl-1,2-azaborine (yellow) modelled into the EbDH active site. b) Biological activity of EbDH when preincubated with different concentrations of N-ethyl-1,2-azaborine (circles) and B-ethyl-1,2-azaborine (squares).[173]

This enzyme containing molybdenum in the binding pocket, hydroxylates a broad range of alkylated aromatic and heteroaromatic compounds in an enantioselective manner. For example, ethylbenzene is hydroxylated to (S)-1-phenylethanol while N and B-ethyl-1,2-azaborines, being isosteric to ethylbenzene, fit nicely inside the EbDH substrate binding pocket without to be hydroxylated. Also, the enhanced electronic interactions between azaborines and the pocket decrease the affinity of the enzyme towards other substrates inhibiting the catalytic activity.

1.9 Borazine ring as potential dopant for Polycyclic Aromatic Hydrocarbons (PAHs)

Recently one of the most versatile approaches to tune the electronic and optoelectronic properties of PAHs and the corresponding larger graphitic materials is the direct replacement of benzene rings with the inorganic "mimic" borazine ring.[174] Earlier investigation by theoretical analysis on the electronic effect due to the replacement of benzene ring by borazine (B_3N_3) units was pioneered by Bettinger and co-workers in 2012.[55] Bettinger's group investigated, by computational methods, the influence on the structural, energetic, vibrational, and optical properties of hexa-peri-hexabenzocoronene (HBC, $C_{42}H_{18}$), as a representative graphene molecule, when the central aromatic core was replaced by a borazine (B_3N_3HBC, $C_{36}B_3N_3H_{18}$).

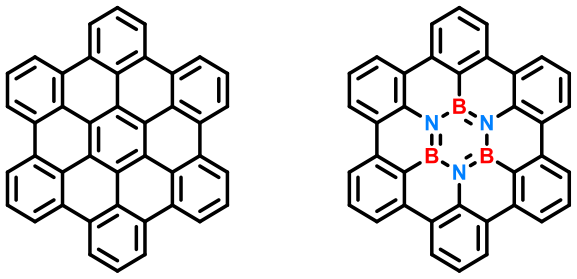

Figure 1.15 Representation of hexa-peri-hexabenzocoronene (HBC) and the central borazine substituted (B_3N_3HBC).

The results obtained indicated a significant change in the IR vibrational spectrum of B_3N_3HBC respect to HBC, due to the polarity of the borazine core. Also, the central borazine ring of B_3N_3HBC shifted to higher energies the optically allowed electronic transitions in the electronic spectra when compared with that of HBC. Chemical syntheses of B_3N_3HBC was then investigated[175] in order to compare the experimental analysis with the computed data. Precursor 1,2:3,4:5,6-tris(biphenylylene)borazine (B_3N_3HBT), the borazine analogue of hexabenzotriphenylene, was initially synthesised following the Kçster's original protocol[176] and subsequently obtained by an alternative procedure developed by the same group.[177] The synthetic approach initially followed for the synthesis of B_3N_3HBC was based on the stilbene

photocyclization reaction path.[178,179] Basically, a photochemical synthesis was carried out using a high-pressure mercury vapour lamp irradiating B_3N_3HBT in an overnight (15 h) reaction. The reaction was performed in toluene in presence of Iodine to restore the aromaticity after photocyclization promoting the loss of H_2. They found that irradiation with wavelength ranging from 240 and 255 nm almost excited the solvent without product formation, while at higher wavelengths (420–630 nm), in the absorption bands of iodine, low conversion was obtained. The best yield was achieved exciting between 280 and 400 nm, however under these conditions the photocyclization resulted in the closing of only one C-C-bond while the second and the third to afford the desired BN-HBC was unsuccessful.

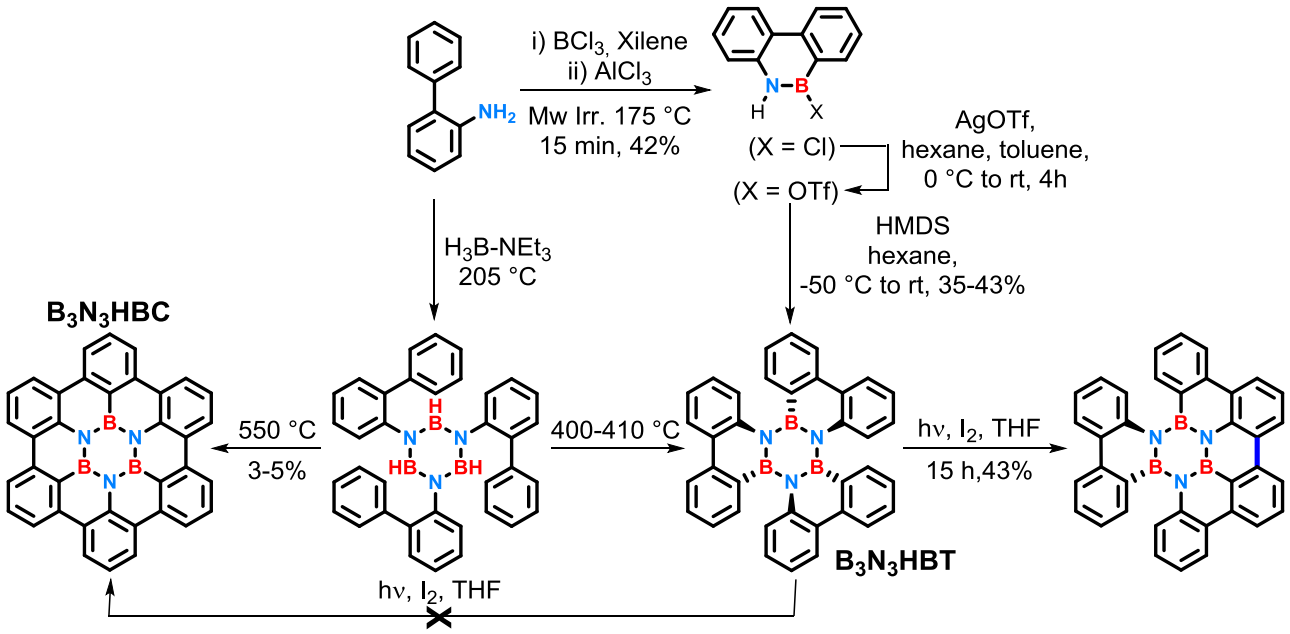

Scheme 1.46 Synthesis of B_3N_3HBTand B_3N_3HBC.

Borazine substituted hexa-peri-hexabenzocoronene B_3N_3HBC was obtained three years later by thermolysis of N,N',N''-tris(2-biphenylyl)borazine at 550 °C.[180] Despite B_3N_3HBC was obtained pure in very low yield (5%) after sublimation, it was fully characterized, and experimental data collected were overall in good agreements with values computed at the B3LYP/6-31G* theory level. In the same year Bettinger' group in collaboration with Ruffieux's group reported the bottom-up synthesis of BN-substituted heteroaromatic networks obtained by surface-assisted polymerization and subsequent cyclodehydrogenation of brominated B_3N_3HBT or hexaphenyl borazine HPB precursors.[181]

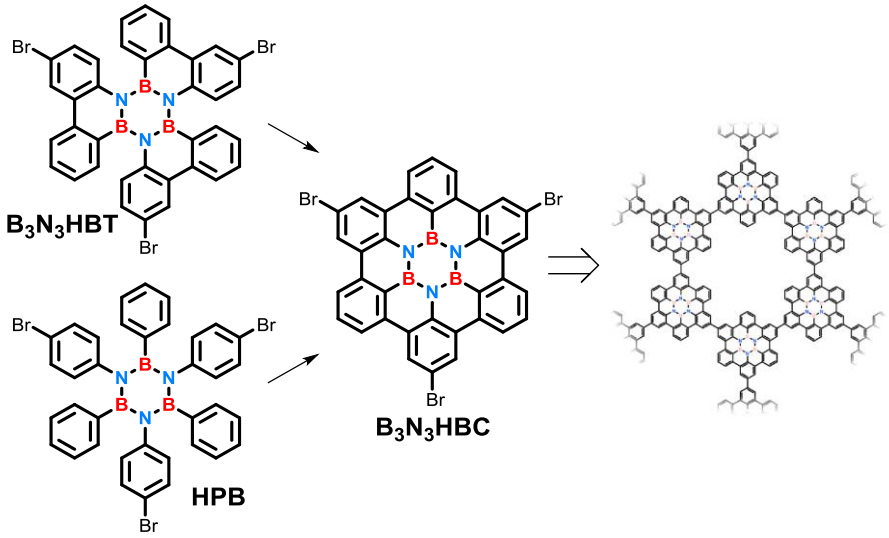

Scheme 1.47 Schematic representation of brominated monomers B_3N_3HBT and HPB used for the synthesis of intermediate B_3N_3HBC to achieve CBN-2D networks *via* aryl-aryl coupling.

The synthesis was performed under ultra-high vacuum (UHV) conditions depositing B_3N_3HBT on the clean Ag(111) surface monitoring the experiment by STM at different temperature to observe the proceeding of the reaction. At 425 K, STM image showed flower-like structures (Figure 1.16) suggesting the presence of monomers coexisting with more extended oligomers such as pentamers, hexamers, heptamers, and higher order rings. This observation was rationalized considering that at 425 K dehalogenation of organic molecules is favoured when deposited on Ag (111), due to the catalytic activity of the metallic surface[182] therefore intermolecular C-C covalent bond formation occurred. Post annealing at 475 K resulted in shorten intermolecular distances suggesting a transition from an organometallic self-assembled superstructure to a covalent network, with increased rigidity due to the formation of detriment. Annealing to 525 K induced a change in molecular appearance becoming flatter due to the intramolecular C-C bonding formation by cyclodehydrogenation, which was promoted by increasing the temperature to 575 K to give fully cyclodehydrogenated CBN-networks.

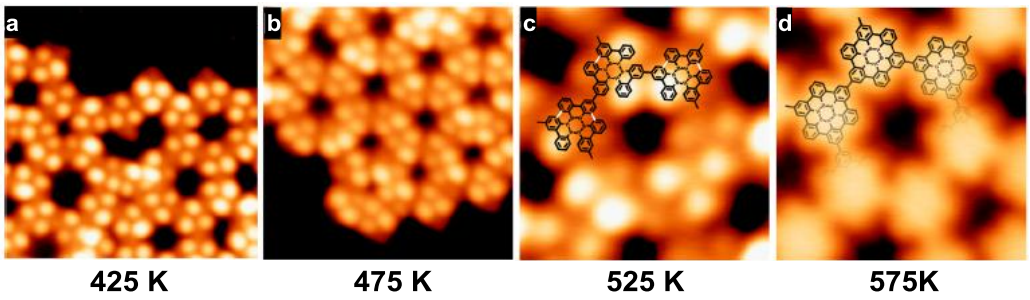

Figure 1.16 STM images of brominated monomer B_3N_3HBT deposited on the clean Ag(111) surface after annealing at 425 K (a), 475 K (b), 525 K (c), and 575 K (d).[181]

More recently advancing in the synthetic methodology to obtain B_3N_3-doped benzocoronene have been achieved by Bonifazi and co-workers. They reported in 2017 an elegant three-step synthetic procedure for the synthesis of substituted B_3N_3-doped benzocoronenes.[183] After a careful evaluation of all possible synthetic routes they considered that starting from a less strained non preorganized borazine precursors would have been beneficial in terms of stability under the ring-closure reactions conditions. Indeed, planarization of covalently preorganized aryl compounds into PAHs usually is achieved by Scholl-type oxidative reactions[25] and under these drastic reaction conditions borazine ring is highly susceptible to decomposition.[55] Therefore, they envisaged that a Friedel-Crafts-type substitution would have been more appropriate to achieve planarization of less strained non preorganized borazine precursors. Following a synthetic procedure developed in the group[163] they synthesised hexafluoro borazine precursor A after reaction of starting material 4-xylyl aniline with BCl_3 upon subsequent addition of difluoro-ArLi.

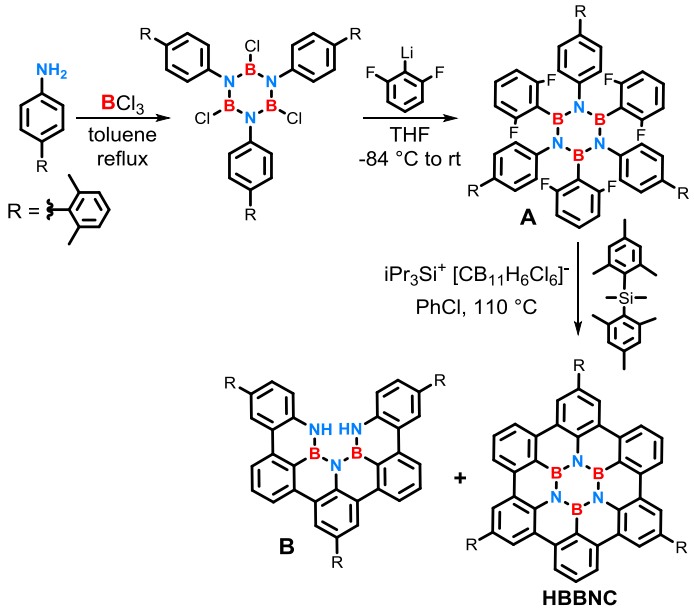

Scheme 1.48 Synthesis of xylyl-substituted HBBNC.

Finally, planarization of precursor A into HBBNC was achieved by Friedel-Crafts ring-closure reaction[184] in presence of $[iPr_3Si\cdots CB_{11}H_6Cl_6]$ and Me_2SiMes_2 at 110 °C in PhCl. HBBNC was isolated as minor product (5% yield) from the crude mixture while the major product (17% yield) was identified in the partially fused BN-derivative B, suggesting that the ring closure proceeds stepwise and the last C-C bond formation probably is rate-determining step. By UV-Visible spectroscopy data and cyclic voltammetry (CV) measurements the frontier orbital energies were estimated for HBBNC and compared with the all carbon congener HBC. HOMO and LUMO energies of HBBNC resulted to be -5.80 and -2.51 eV respectively while the calculated energies for HBC resulted to be -5.61 (HOMO) and -2.85 eV (LUMO), proving that introduction of BN doping induced a band gap opening.

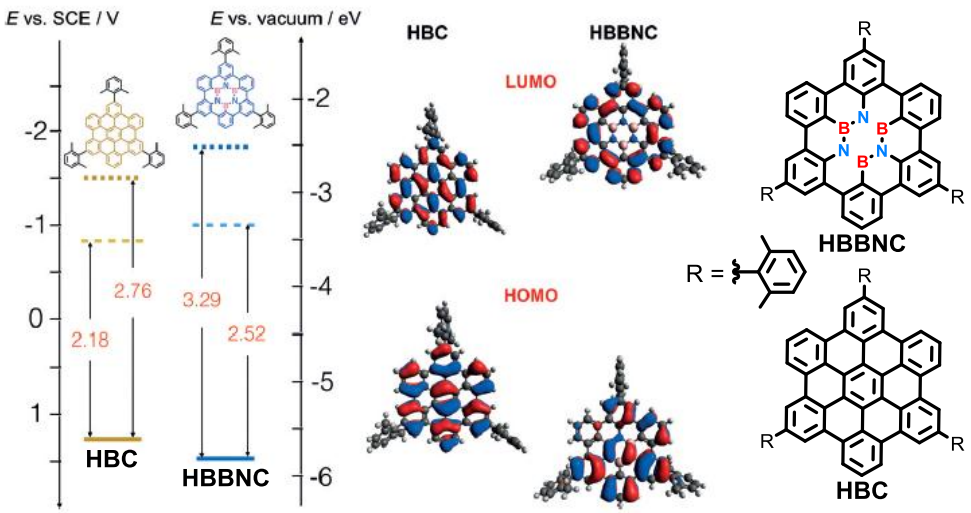

Figure 1.17 Frontier orbital energies estimated from the CV and photophysical data for HBBNC and HBC with comparison of HOMO and LUMO profiles at B3LYP/6-31G(d,p) level of theory (GAUSSIAN09).[183]

Also, in the same year Bonifazi and his group reported a pioneering work on the synthesis of branched hybrid BNC polyphenylenes with specified doping ratios, achieved by selected positions of borazine core dopants.[185] They demonstrated that by controlled orientations and dosages of the doping B_3N_3 rings as well as the extension of the BNC polyphenylenes, is possible to finely tune the electronic levels of these materials creating a multichromophoric derivatives with specific chemical-physical properties.

1.10 Aims of the Project

Functionalized borazine based materials are currently emerging as promising building block for the fabrication of 2D-CBN hybrid materials. However, the laborious synthetic procedures combined with the fact that often borazine precursors are extremely sensitive to the moisture, limit the preparation of these hybrid materials to lab-scale synthesis. Our ambition is to find defined molecular structures and functional groups capable to stabilize the borazine systems and to tune the electronic properties in view of their use in the organic electronic and optoelectronic field. In recent years, many polycyclic aromatic hydrocarbons (PAHs) have been synthesised to use as intermediate for the synthesis of more complex structures or to employ directedly as active materials for electronic applications.[186] However, one of the key challenging in applying PAHs and more extended polyarenes materials in organic electronics, remains the effective solubilization of these materials which is crucial in making these products industrially processable. One of the most fascinating, well-characterised and studied PAHs over the years due to its relatively high solubility, is truxene (10,15-dihydro-5H-diindeno[1,2-a;1',2'-c]fluorene). Well-designed truxene derivatives have been synthesised showing outstanding electronic and optical properties as well as

remarkable solubility in common organic solvents.[187] Truxene is a C_3-symmetric star-shaped polyarene existing as another possible isomer called isotruxene and they only differing in the way the fluorene moieties arrange.

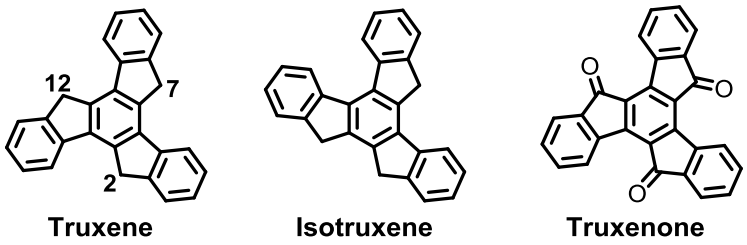

Figure 1.18 Structure of truxene, isotruxene and truxenone.

Truxene can be obtained in good yield following a method developed by Oded and Agranat[188], which includes a modified Huang-Minlon Wolff-Kischner protocol for the reduction of truxenone obtained in the first step. Functionalization of truxene can be achieved either on the peripheral aromatic rings or into the -CH_2- bridge. Specifically, introduction of functional groups at the 2,7,12-positions was reported, for the first time, in 1999 by Echavarren and co-workers introducing long alkyl chains upon treatment of truxene with strong bases such as KH or n-BuLi.[189] The following exposure of the trianion adduct formed to an alkyl halide, furnished a mixture of *anti* and *syn* trialkylated truxene in 3 : 1 to 1 : 1 ratios. With the use of a different base as sodium or NaH can be selectively obtained the *anti*-derivative,[190] which in turn can be easily isomerized to the more stable *syn* isomer by a base-catalysed reaction, using for example potassium tert-butoxide (t-BuOK).[191]

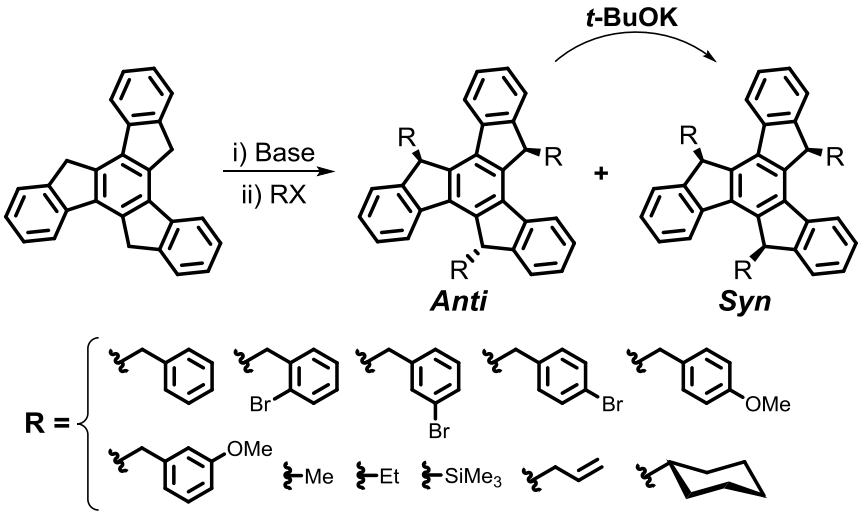

Scheme 1.49 Alkylation of truxene and conversion of the *anti*-derivative to the more stable *syn*-derivative.

Instead, functionalization of the peripheral aromatic rings is easily achieved using the standard synthetic protocols developed for aromatic compounds.[192–194] The easy handling of these materials has made them

ideal candidates for use as functional materials with potential applications in organic electronics. Over the time, well-designed truxene derivatives have been synthesised and utilized for their outstanding spectroscopic properties in organic photovoltaics (OPVs),[195,196] organic light-emitting diodes (OLEDs),[197] non-linear opticals (NLO),[198] two-photon absorption (TPA),[199] transistors,[200,201] etc. Also, other engineered analogues have found applications in dendrimers,[202–204] organogels,[205,206] self-assembly and liquid crystals[207,208]. Because of the outstanding properties of these materials, we decided to direct our work towards the synthesis of hybrid BN doped truxenes following an innovative bottom-up synthetic approach based on the use of microwave assisted conditions. The BN doping is achieved through the borazine ring synthesis starting from aromatic amine-boranes by a thermolysis process. Also, we considered this approach to be a scaffold for the synthesis of more extended BN-doped PAHs. One of the key challenges is the molecular engineering of the building blocks for: i) stabilizing the borazine systems, ii) tuning the electronic properties, iii) controlling the molecular assembly to engineer functional supramolecular materials. We envisioned that well-designed building blocks can provide to the synthesis of 0D or 2D unexplored heterostructures such as BN-doped hemifullerene or BN-doped nanographene (NGs) materials with controlled positions of individual BN units.

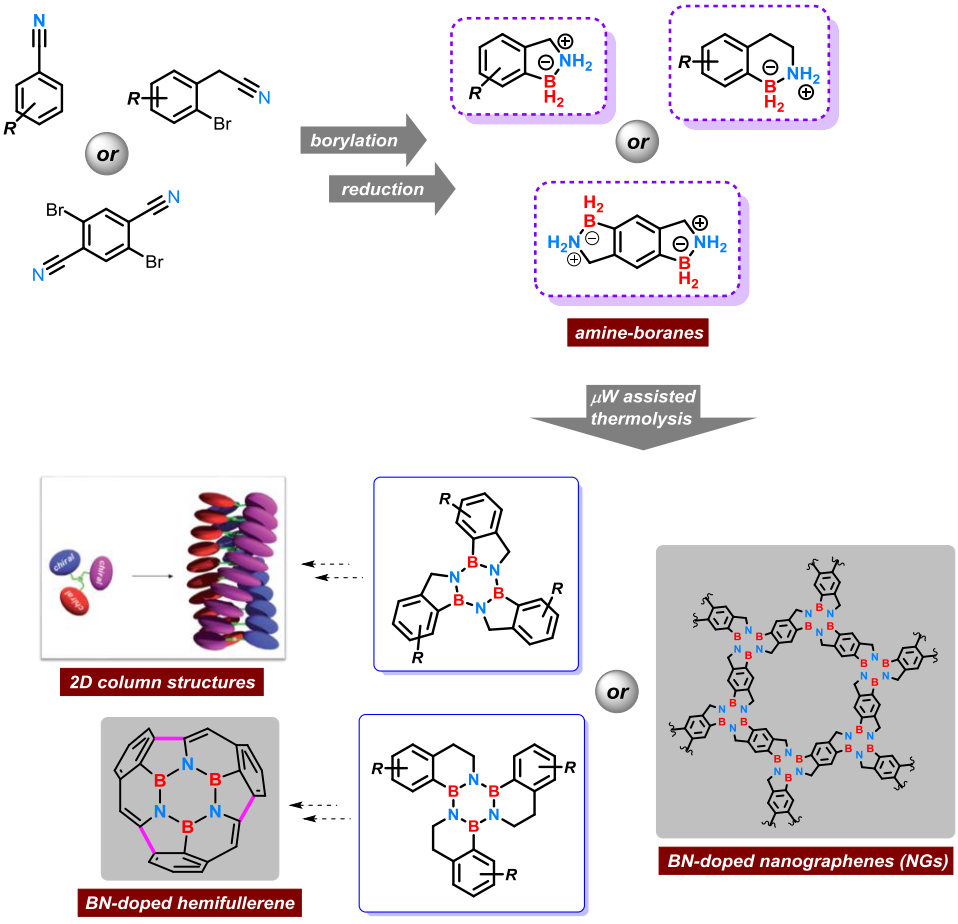

Figure 1.19 Envisaged synthetic strategy for the synthesis of 0D and 2D-CBN hybrid materials.

REFERENCES

1 H. W. Kroto, J. R. Heath, S. C. O'Brien, R. E. Smalley and R. F. Curl, *Nature*, 1985, **318**, 162.
2 S. Iijima, *Nature*, 1991, **354**, 56.
3 K. S. Novoselov, *Science*, 2004, **306**, 666.
4 L. Chen, Y. Hernandez, X. Feng and K. Müllen, *Angew. Chem. Int. Ed.*, 2012, **51**, 7640.
5 R. Rieger and K. Mullen, *J Phys Org Chem*, 2010, **23**, 315.
6 M. Bacon, S. J. Bradley and T. Nann, *Part. Part. Syst. Charact.*, 2014, **31**, 415.
7 M. Antonietti and K. Müllen, *Chemical Synthesis and Applications of Graphene and Carbon Materials*, John Wiley & Sons, 2017.
8 K. Müllen, *ACS Nano*, 2014, **8**, 6531.
9 R. Scholl, C. Seer and R. Weitzenbock, *Chem Ber*, 1910, **43**, 2202.
10 R. Scholl and C. Seer, *Chem Ber*, 1912, **55**, 330.
11 R. Scholl and C. Seer, *Liebigs Ann Chem*, 1912, **394**, 111.
12 E. Clar and D. G. Stewart, *J Am Chem Soc*, 1953, **75**, 2667.
13 E. Clar and J. F. Stephen, *Tetrahedron*, 1965, **21**, 467.
14 E. Clar and W. schmidt, *Tetrahedron*, 1979, **35**, 2673.
15 J. Wu, W. Pisula and K. Müllen, *Chem. Rev.*, 2007, **107**, 718–747.
16 K. K. Baldridge and J. S. Siegel, *Angew. Chem. Int. Ed.*, 2013, **52**, 5436.
17 M. Ball, Y. Zhong, Y. Wu, C. Schenck, F. Ng, M. Steigerwald, S. Xiao and C. Nuckolls, *Acc Chem Res*, 2015, **48**, 267.
18 W. Pisula, X. L. Feng and K. Müllen, *Chem Mater*, 2011, **23**, 544.
19 Y. Morita, S. Suzuki, K. Sato and T. Takui, *Nat Chem*, 2011, **3**, 197.
20 K. Ozaki, K. Kawasumi, M. Shibata, H. Ito and K. Itami, *Nat. Commun.*, , DOI:10.1038/ncomms7251.
21 K. Kawasumi, Q. Zhang, Y. Segawa, L. T. Scott and K. Itami, *Nat. Chem.*, 2013, **5**, 739.
22 J. K. Stille, G. K. Noren and L. Green, *J Polym Sci Part -1 Polym Chem*, 1970, **8**, 2245.
23 K. Chmil and U. Scherf, *Makromol Chem Rapid Commun*, 1993, **14**, 217.
24 K. Chmil and U. Scherf, *Acta Polym*, 1997, **48**, 208.
25 M. D. Watson, A. Fechtenkötter and K. Müllen, *Chem. Rev.*, 2001, **101**, 1267–1300.
26 R. Dorel, C. Manzano, M. Grisolia, W.-H. Soe, C. Joachim and A. M. Echavarren, *Chem Commun*, 2015, **51**, 6932.
27 A. Matsumoto, M. Suzuki, D. Kuzuhara, H. Hayashi, N. Aratani and H. Yamada, *Angew Chem Int Ed*, 2015, **54**, 8175.
28 X. Yang, X. Dou, A. Rouhanipour, L. Zhi, H. J. Rader and K. Mullen, *J Am Chem Soc*, 2008, **130**, 4216.
29 J. Sakamoto, M. Rehahn, G. Wegner and A. D. Schluter, *Macromol Rapid Commun*, 2009, **30**, 653.
30 K. Ozaki, K. Kawasumi, M. Shibata, H. Ito and K. Itami, *Nat Commun*, 2015, **6**, 6251.
31 M. Shimizu and T. Hiyama, *Eur J Org Chem*, 2013, 8069.
32 C.-N. Feng, Y.-C. Hsieh and Y.-T. Wu, *Chem Rec*, 2015, **15**, 266.
33 D. M. Hitt and J. M. O'Connor, *Chem Rev*, 2011, **111**, 7904.
34 M. Grzybowski, K. Skonieczny, H. Butenschön and D. T. Gryko, *Angew. Chem. Int. Ed.*, 2013, **52**, 9900.
35 H. Omachi, Y. Segawa and K. Itami, *Acc. Chem. Res.*, 2012, **45**, 1378.
36 A. Yagi, Y. Segawa and K. Itami, *J. Am. Chem. Soc.*, 2012, **134**, 2962.
37 K. Matsui, Y. Segawa, T. Namikawa, K. Kamada and K. Itami, *Chem Sci*, 2013, **4**, 84.
38 L. T. Scott, *Pure Appl Chem*, 1996, **68**, 291.
39 V. M. Tsefrikas and L. T. Scott, *Chem Rev*, 2006, **106**, 4868.
40 L. T. Scott, *Polycycl Aromat Compd*, 2010, **30**, 247.
41 X. Feng, W. Pisula and K. Müllen, *Pure Appl. Chem.*, 2009, **81**, 2203.
42 Q. Zhang, H. Peng, G. Zhang, Q. Lu, J. Chang, Y. Dong, X. Shi and J. Wei, *J Am Chem Soc*, 2014, **136**, 5057.
43 P. Y. Huang, C. S. Ruiz-Vargas, A. M. van der Zande, W. S. Whitney, M. P. Levendorf, J. W. Kevek, S. Garg, J. S. Alden, C. J. Hustedt, Y. Zhu, J. Park, P. L. McEuen and D. A. Muller, *Nature*, 2011, **469**, 389.
44 K. Kim, Z. Lee, W. Regan, C. Kisielowski, M. F. Crommie and A. Zettl, *ACS Nano*, 2011, **5**, 2142.
45 J. Lahiri, Y. Lin, P. Bozkurt, I. I. Oleynik and M. Batzill, *Nat Nanotechnol*, 2010, **5**, 326.
46 S. Hagen, M. S. Bratcher, M. S. Erickson, G. Zimmermann and L. T. Scott, *Angew Chem Int Ed*, 1997, **36**, 406.
47 G. Mehta, G. Panda and P. V. V. Srirama Sarma, *Tetrahedron Lett*, 1998, **39**, 5835.
48 M. A. Brooks and L. T. Scott, *J Am Chem Soc*, 1999, **121**, 5444.
49 R. A. Nistor, D. M. Newns and G. J. Martyna, *ACS Nano*, 2011, **5**, 3096.
50 P. A. Denis, *Chem. Phys. Lett.*, 2010, **492**, 251–257.
51 S. Wang, L. Zhang, Z. Xia, A. Roy, D. W. Chang, J.-B. Baek and L. Dai, *Angew. Chem. Int. Ed.*, 2012, **51**, 4209.
52 X. Wang, X. Li, L. Zhang, Y. Yoon, P. K. Weber, H. Wang, J. Guo and H. Dai, *Science*, 2009, **324**, 768.
53 A. Lherbier, X. Blase, Y.-M. Niquet, F. Triozon and S. Roche, *Phys. Rev. Lett.*, 2008, **101**, 036808.
54 V. M. Hertz, J. G. Massoth, M. Bolte, H.-W. Lerner and M. Wagner, *Chem. - Eur. J.*, 2016, **22**, 13181.
55 C. Tönshoff, M. Müller, T. Kar, F. Latteyer, T. Chassé, K. Eichele and H. F. Bettinger, *ChemPhysChem*, 2012, **13**, 1173.
56 G. Giovannetti, P. Khomyakov, G. Brocks, P. Kelly and J. van den Brink, *Phys. Rev. B*, 2007, **76**, 073103.
57 M. J. D. Bosdet, W. E. Piers, T. S. Sorensen and M. Parvez, *Angew. Chem. Int. Ed.*, 2007, **46**, 4940.
58 A. J. V. Marwitz, A. N. Lamm, L. N. Zakharov, M. Vasiliu, D. A. Dixon and S.-Y. Liu, *Chem Sci*, 2012, **3**, 825.
59 A. J. V. Marwitz, M. H. Matus, L. N. Zakharov, D. A. Dixon and S.-Y. Liu, *Angew. Chem.*, 2009, **121**, 991.
60 C. Zhi, Y. Bando, T. Terao, C. Tang, H. Kuwahara and D. Golberg, *Adv. Funct. Mater.*, 2009, **19**, 1857.
61 M. J. D. Bosdet, C. A. Jaska, W. E. Piers, T. S. Sorensen and M. Parvez, *Org. Lett.*, 2007, **9**, 1395.
62 L. R. Thorne and R. D. Suenram, *Chem Phys Lett*, 1981, **78**, 157.
63 A. Haaland, *Angew Chem Int Ed*, 1989, **28**, 992.
64 K. Niedenzu and J. Dawson, *Boron-nitrogen compound*, Springer-Verlag, 1965.
65 F. Baitalow, J. Baumann, G. Wolf, K. Jaenicke-Rossler and G. Leitner, *Thermochim Acta*, 2002, **391**, 159.
66 J. S. Wang and R. A. Geanangel, *Inorg Chim Acta*, 1988, **148**, 185.

67 W. J. Shaw, J. C. Linehan, N. K. Szymczak, D. J. Heldebrant, C. Yonker, D. M. Camaioni, R. T. Baker and T. Autrey, *Angew Chem Int Ed*, 2008, **47**, 9600.
68 B. L. Davis, D. A. Dixon, E. B. Garner, J. C. Gordon, M. H. Matus, B. Scott and F. H. Stephens, *Angew. Chem. Int. Ed.*, 2009, **48**, 6812.
69 D. W. Himmelberger, C. W. Yoon, M. E. Bluhm, P. J. Carroll and L. G. Sneddon, *J Am Chem Soc*, 2009, **131**, 14101.
70 W. C. Ewing, P. J. Carroll and L. G. Sneddon, *Inorg Chem*, 2013, **52**, 10690.
71 H. A. Kalviri, F. Gärtner, G. Ye, I. Korobkov and R. T. Baker, *Chem Sci*, 2015, **6**, 618.
72 T. B. Marder, *Angew. Chem. Int. Ed.*, 2007, **46**, 8116.
73 A. Staubitz, A. P. M. Robertson, M. E. Sloan and I. Manners, *Chem. Rev.*, 2010, **110**, 4023.
74 V. Pons, R. T. Baker, J. Linehan, M. H. Matus and D. A. Dixon, *Chem Commun*, 2008, 6597.
75 A. Kumar, H. C. Johnson, T. N. Hooper, A. S. Weller, A. G. Algarra and S. A. Macgregor, *Chem Sci*, 2014, **5**, 2546.
76 W. R. Nutt and M. L. Mckee, *Inorg Chem*, 2007, **46**, 7633.
77 P. M. Zimmerman, A. Paul, Z. Zhang and C. B. Musgrave, *Inorg Chem*, 2009, **48**, 1069.
78 J. L. Gay-Lussac, *Mem Phys Chim Soc D'Arcueil*, 1809, **2**, 211.
79 E. L. Muetterties, *Boron Hydride Chemistry*, Academic Press NewYork, 1975.
80 A. B. Burg and H. I. Schlesinger, *J. Am. Chem. Soc.*, 1937, **59**, 780.
81 P. Atkins, *Shriver and Atkins' Inorganic Chemistry*, Oxford University Press, 2010.
82 M. Potyen, K. V. B. Josyula, M. Schuck, S. Lu, P. Gao and C. Hewitt, *Org. Process Res. Dev.*, 2007, **11**, 210.
83 J. V. B. Kanth, *Aldrichimica Acta*, 2002, **35**, 57.
84 O. T. Jr. Beachley and B.Washburn, *Inorg Chem*, 1975, **14**, 120.
85 G. W. Schaeffer and E. R. Anderson, *J Am Chem Soc*, 1949, **71**, 2143.
86 D. J. Heldebrant, A. Karkamkar, J. C. Linehan and T. Autrey, *Energy Env. Sci*, 2008, **1**, 156.
87 J. C. Catlin and H. R. Snyder, *J. Org. Chem.*, 1969, **34**, 1664.
88 S. Kotha, K. Lahiri and D. Kashinath, *Tetrahedron*, 2002, **58**, 9633.
89 M. C. Whisler, S. MacNeil, V. Snieckus and P. Beak, *Angew. Chem. Int. Ed.*, 2004, **43**, 2206.
90 M. Kauch and D. Hoppe, *Synthesis*, 2006, **10**, 1575.
91 W. E. Parham and L. D. Jones, *J Org Chem*, 1976, **41**, 16.
92 M. Scheideman, G. Wang and E. Vedejs, *J. Am. Chem. Soc.*, 2008, **130**, 8669.
93 E. Wiberg, *Naturwissenschaften*, 1948, **35**, 212.
94 H. J. Becher and J. Goubeau, *Z Anorg Allg Chem*, 1952, **268**, 133.
95 J. Goubeau, M. Rahtz and H. J. Becher, *Ibid.*, 1954, **275**, 161.
96 K. Niedenzu and J. W. Dawson, *J Amer Chem Soc*, 1960, **82**, 4223.
97 H. A. McGee and C. T. Kwon, *Inorg Chem*, 1970, **9**, 2458.
98 E. Wiberg, A. Bolz and P. Buchheit, *Z Anorg Chem*, 1948, **256**, 301.
99 A. B. Burg and C. L. Randolph, *J. Am. Chem. Soc.*, 1949, **71**, 3451.
100 E. Wiberg, K. Hertwig and A. Bolz, *Z Anorg Chem*, 1948, **265**, 177.
101 G. W. Shaeffer and E. R. Anderson, *Ibid.*, 1949, **71**, 2143.
102 A. Michaelis and K. Luxembourg, *Ber Dtsch Chem Ges*, 1896, **29**, 710.
103 J. F. Brown, *J. Am. Chem. Soc.*, 1952, **74**, 1219.
104 K. Niedenzu and J . W. Dawson, *ibid.*, 1959, **81**, 5553.
105 K. Niedenzu and J . W. Dawson, *ibid.*, 1960, **82**, 4223.
106 P. G. Campbell, A. J. V. Marwitz and S.-Y. Liu, *Angew. Chem. Int. Ed.*, 2012, **51**, 6074.
107 M. J. S. Dewar, V. P. Kubba and R. Pettit, *J. Chem. Soc.*, 1958, 3073.
108 M. J. Dewar, G. J. Gleicher and B. P. Robinson, *J. Am. Chem. Soc.*, 1964, **86**, 5698.
109 M. Dewar and R. Jones, *J. Am. Chem. Soc.*, 1968, **90**, 2137.
110 F. A. Davis, M. J. Dewar, R. Jones and S. D. Worley, *J. Am. Chem. Soc.*, 1969, **91**, 2094.
111 A. J. Ashe and X. D. Fang, *Org Lett*, 2000, **2**, 2089.
112 A. J. Ashe, X. Fang and J. Kampf, *Organometallics*, 2001, **20**, 5413.
113 J. Pan, J. W. Kampf and A. J. Ashe, *Organometallics*, 2004, **23**, 5626.
114 J. Pan, J. W. Kampf and A. J. Ashe, *Organometallics*, 2008, **27**, 1345.
115 J. Pan, J. W. Kampf and A. J. Ashe, *Organomet Chem*, 2009, **694**, 1036.
116 X.-Y. Wang, J.-Y. Wang and J. Pei, *Chem. - Eur. J.*, 2015, **21**, 3528.
117 D. J. H. Emslie, W. E. Piers and M. Parvez, *Angew Chem Int Ed*, 2003, **42**, 1252.
118 C. A. Jaska, D. J. H. Emslie, M. J. D. Bosdet, W. E. Piers, T. S. Sorensen and M. Parvez, *J. Am. Chem. Soc.*, 2006, **128**, 10885.
119 T. Hatakeyama, S. Hashimoto, S. Seki and M. Nakamura, *J. Am. Chem. Soc.*, 2011, **133**, 18614.
120 A. Saeki, S. Seki, T. Takenobu, Y. Iwasa and S. Tagawa, *Adv Mater*, 2008, **20**, 920.
121 T. Taniguchi and S. Yamaguchi, *Organometallics*, 2010, **29**, 5732.
122 T. Agou, J. Kobayashi and T. Kawashima, *Org Lett*, 2006, **8**, 2241.
123 J. S. A. Ishibashi, J. L. Marshall, A. Mazière, G. J. Lovinger, B. Li, L. N. Zakharov, A. Dargelos, A. Graciaa, A. Chrostowska and S.-Y. Liu, *J. Am. Chem. Soc.*, 2014, **136**, 15414.
124 A. Stock and E. Poland, *Ber Dtsch Chem Ges*, 1926, **59**, 2215.
125 E. Wiberg and A. Bolz, *ibid.*, 1940, **73**, 209.
126 G. W. Schaeffer, R. Schaeffer and H. I. Schlesinger, *ibid.*, 1951, **73**, 1612.
127 D. T. Haworth and L. F. Hohnstedt, *Chem Ind*, 1960, **65**, 559.
128 C. A. Brown and A. W. Laubergayer, *J Am Chem Soc*, 1955, 3699.
129 A. Stock and R. Wierl, *Z Anorg Allg Chem*, 1931, **203**, 228.
130 S. H. Bauer, *J. Am. Chem. Soc.*, 1938, **60**, 524.
131 W. Harshbarger, G. Lee, R. F. Porter and S. H. Bauer, *Inorg Chem*, 1969, **8**, 1683.
132 V. D. Yumatov, E. A. Ilinchik and V. V. Volkov, *Usp Khim*, 2003, **72**, 1141.
133 E. L. Muetterties, *The Chemistry of Boron and Its Compounds*, Wiley, NY, 1967.
134 F. N. Tavadze, G. V. Samsonov and G. V. Tsagareyshvili, *IV Mezhdunar Simp Po Boru Proc.*
135 V. V. Volkov, K. G. Myakishev and E. A. Ilinchik, *Chem. Sustain. Dev.*, 2009, **17**, 227.
136 B. Kiran, A. K. Phukan and E. D. Jemmis, *Inorg Chem*, 2001, **40**, 3615.
137 R. Islas, E. Chamorro, J. Robles, T. Heine, J. C. Santos and G. Merino, *Struct Chem*, 2007, **18**, 833.

138 S. H. Bauer, *J. Am. Chem. Soc.*, 1938, **60**, 524.
139 A. Kaldor, *J. Chem. Phys.*, 1971, **55**, 4641.
140 B. L. Crawford and Jr. and J. T. Edsall, *J Chem Phys*, 1939, **7**, 223.
141 W.C. Price, R.D.B. Fraser, T.S. Robinson and H.C. Longuet-Higgins, *Disc Faraday Soc*, 1950, **9**, 131.
142 D. W. Davies, *Trans Faraday Soc*, 1960, **56**, 1713.
143 H. Watanabe, K. Ito and M. Kubo, *J Am Chem Soc*, 1960, **82**, 3294.
144 R.A. Spurr and S. Chang, *J Chem Phys*, 1951, **19**, 528.
145 G. Mamantov and J. L. Margrave, *J. Inorg. Nucl. Chem.*, 1961, **20**, 348.
146 C. K. Narula, R. Schaeffer, A. Datye and R. T. Paine, *Inorg Chem*, 1989, **28**, 4053.
147 L. Maya, *Appl Organomet Chem*, 1996, **10**, 175.
148 I. H. T. Sham, C.-C. Kwok, C.-M. Che and N. Zhu, *Chem. Commun.*, 2005, 3547.
149 H. I. Schlesinger, D. M. Ritter and A. B. Burg, *Ibid.*, 1938, **60**, 1296.
150 H. J. Emelus and K. Wade, *J Chem Soc*, 1960, 2614.
151 D. Bonifazi, F. Fasano, M. M. Lorenzo-Garcia, D. Marinelli, H. Oubaha and J. Tasseroul, *Chem. Commun.*, 2015, **51**, 15222.
152 S. J. Groszos and S. F. Stafiej, *J Am Chem Soc*, 1958, **80**, 1357.
153 J. H. Smalley and S. F. Stafiej, *Ibid.*, 1959, **81**, 582.
154 L. F. Hohnstedt and D. T. Haworth, *Ibid.*, 1960, **82**, 89.
155 C. A. Brown and A. W. Laubengayer, *J. Am. Chem. Soc.*, 1955, **77**, 3699.
156 K. Niedenzu, *Inorg Chem*, 1962, **1**, 943.
157 A. W. Laubengayer, K. Watterson, D. R. Bidinosti and R. F. Porter, *Inorg. Chem.*, 1963, **2**, 519.
158 K. Niedenzu, *Inorg. Chem.*, 1962, **1**, 943.
159 H. Beyer, J. B. Hynes, H. Jenne and K. Niedenzu, *Adv. Chem.*, 1964, **42**, 266.
160 X.-Y. Wang, H.-R. Lin, T. Lei, D.-C. Yang, F.-D. Zhuang, J.-Y. Wang, S.-C. Yuan and J. Pei, *Angew. Chem. Int. Ed.*, 2013, **52**, 3117.
161 X.-Y. Wang, F.-D. Zhuang, X. Zhou, D.-C. Yang, J.-Y. Wang and J. Pei, *J Mater Chem C*, 2014, **2**, 8152.
162 X.-Y. Wang, F.-D. Zhuang, R.-B. Wang, X.-C. Wang, X.-Y. Cao, J.-Y. Wang and J. Pei, *J. Am. Chem. Soc.*, 2014, **136**, 3764.
163 S. Kervyn, O. Fenwick, F. Di Stasio, Y. S. Shin, J. Wouters, G. Accorsi, S. Osella, D. Beljonne, F. Cacialli and D. Bonifazi, *Chem. Eur. J.*, 2013, **19**, 7771.
164 L. Barreto, A. Makahira and K. Riahi, *Int J Hydrog. Energy*, 2003, **28**, 267.
165 G. W. Crabtree, M. S. Dresselhaus and M. V. Buchanan, *Phys Today*, 2004, **57**, 39.
166 C. W. Hamilton, R. T. Baker, A. Staubitz and I. Manners, *Chem Soc Rev*, 2009, **38**, 279.
167 W. R. H. Wright, E. R. Berkeley, L. R. Alden, R. T. Baker and L. G. Sneddon, *Chem. Commun.*, 2011, **47**, 3177.
168 W. Luo, P. G. Campbell, L. N. Zakharov and S.-Y. Liu, *J. Am. Chem. Soc.*, 2011, **133**, 19326.
169 T. E. Reich, K. T. Jackson, S. Li, P. Jena and H. M. El-Kaderi, *J. Mater. Chem.*, 2011, **21**, 1629.
170 K. T. Jackson, M. G. Rabbani, T. E. Reich and H. M. El-Kaderi, *Polym. Chem.*, 2011, **2**, 2775.
171 H. Furukawa and O. M. Yaghi, *J. Am. Chem. Soc.*, 2009, **131**, 8875.
172 M. G. Schwab, A. Lennert, J. Pahnke, G. Jonschker, M. Koch, I. Senkovska, M. Rehahn and S. Kaskel, *J Mater Chem*, 2011, **21**, 2131.
173 D. H. Knack, J. L. Marshall, G. P. Harlow, A. Dudzik, M. Szaleniec, S.-Y. Liu and J. Heider, *Angew. Chem. Int. Ed.*, 2013, **52**, 2599.
174 S. Kervyn, N. Kalashnyk, M. Riello, B. Moreton, J. Tasseroul, J. Wouters, T. S. Jones, A. De Vita, G. Costantini and D. Bonifazi, *Angew. Chem. Int. Ed.*, 2013, **52**, 7410.
175 M. Müller, S. Behnle, C. Maichle-Mössmer and H. F. Bettinger, *Chem. Commun.*, 2014, **50**, 7821.
176 R. Kçster, S. Hattori and Y. Morita, *Angew Chem*, 1965, **77**, 719.
177 M. Müller, C. Maichle-Mössmer, P. Sirsch and H. F. Bettinger, *ChemPlusChem*, 2013, **78**, 988.
178 R. Koster, H. Bellut and S. Hattori, *Liebigs Ann Chem*, 1968, **720**, 1.
179 R. Koster, K. Iwasaki, S. Hattori and Y. Morita, *Liebigs Ann Chem*, 1968, **720**, 23.
180 M. Krieg, F. Reicherter, P. Haiss, M. Ströbele, K. Eichele, M.-J. Treanor, R. Schaub and H. F. Bettinger, *Angew. Chem. Int. Ed.*, 2015, **54**, 8284.
181 C. Sánchez-Sánchez, S. Brüller, H. Sachdev, K. Müllen, M. Krieg, H. F. Bettinger, A. Nicolaï, V. Meunier, L. Talirz, R. Fasel and P. Ruffieux, *ACS Nano*, 2015, **9**, 9228.
182 J. Eichhorn, T. Strunskus, A. Rastgoo-Lahrood, D. Samanta, M. Schmittel and M. Lackinger, *Chem Commun*, 2014, **50**, 7680.
183 J. Dosso, J. Tasseroul, F. Fasano, D. Marinelli, N. Biot, A. Fermi and D. Bonifazi, *Angew. Chem. Int. Ed.*, 2017, **56**, 4483.
184 O. Allemann, S. Duttwyler, P. Romanato, K. K. Baldridge and J. S. Siegel, *Science*, 2011, **332**, 574.
185 D. Marinelli, F. Fasano, B. Najjari, N. Demitri and D. Bonifazi, *J. Am. Chem. Soc.*, 2017, **139**, 5503.
186 A. Narita, X.-Y. Wang, X. Feng and K. Müllen, *Chem. Soc. Rev.*, 2015, **44**, 6616.
187 F. Goubard and F. Dumur, *RSC Adv.*, 2014, **5**, 3521.
188 Y. N. Oded and I. Agranat, *Tetrahedron Lett.*, 2014, **55**, 636.
189 Ó. de Frutos, B. Gómez-Lor, T. Granier, Á. Monge, E. Gutiérrez-Puebla and A. M. Echavarren, *Angew. Chem. Int. Ed.*, 1999, **38**, 204.
190 E. V. Dehmlow and T. Kelle, *Synth. Commun.*, 1997, **27**, 2021.
191 O. De Frutos, T. Granier, B. Gómez-Lor, J. Jiménez-Barbero, Á. Monge, E. Gutiérrez-Puebla and A. M. Echavarren, *Chem. Eur. J.*, 2002, **8**, 2879.
192 K.-H. Lin, A. Prlj and C. Corminboeuf, *J. Phys. Chem. C*, 2017, **121**, 21729.
193 X. Zong, M. Liang, C. Fan, K. Tang, G. Li, Z. Sun and S. Xue, *J. Phys. Chem. C*, 2012, **116**, 11241.
194 W. Huang, E. Smarsly, J. Han, M. Bender, K. Seehafer, I. Wacker, R. R. Schröder and U. H. F. Bunz, *ACS Appl. Mater. Interfaces*, 2017, **9**, 3068.
195 B. Walker, C. Kim and T. Q. Nguyen, *Chem Mater*, 2011, **23**, 470.
196 E. Anthony, *Chem Mater*, 2011, **23**, 583.
197 M. Zhu and C. Yang, *Chem Soc Rev*, 2013, **42**, 4963.
198 D. R. Vinayakumara, M. Kumar, P. Sreekanth, R. Philip and S. Kumar, *RSC Adv.*, 2015, **5**, 26596.
199 T.-C. Lin, B.-K. Tsai, T.-Y. Huang, W. Chien, Y.-Y. Liu, M.-H. Li and M.-Y. Tsai, *Dyes Pigments*, 2015, **120**, 99.
200 A. Mishra, C.-Q. Ma and P. Bäuerle, *Chem Rev*, 2009, **109**, 1141.
201 C. Wang, H. Dong, W. Hu, Y. Liu and D. Zhu, *Chem Rev*, 2011, **112**, 2208.
202 X.-Y. Cao, W.-B. Zhang, J.-L. Wang, X.-H. Zhou, H. Lu and J. Pei, *J. Am. Chem. Soc.*, 2003, **125**, 12430.
203 L. Wang, Y. Jiang, J. Luo, Y. Zhou, J. H. Zhou, J. Wang and J. Pei, *Adv Mater*, 2009, **47**, 4854.
204 J.-M. Koenen, S. Jung, A. Patra, A. Helfer and U. Scherf, *Adv Mater*, 2012, **24**, 681.
205 K.-P. Tseng, M.-T. Kao, T. W. T. Tsai, C.-H. Hsu, J. C. C. Chan, J.-J. Shyue, S.-S. Sun and K.-T. Wong, *Chem. Commun.*, 2012, **48**, 3515.
206 S. Gomez-Esteban, M. Pezella, A. Domingo, G. Hennrich and B. Gómez-Lor, *Chem. Eur. J.*, 2013, **19**, 16080.

207 C. Destrade, H. Gasparoux, A. Babeau, N. H. Tinh and J. Malthete, *Mol Cryst Liq Cryst*, 1981, **67**, 37.
208 K. Isoda, T. Yasuda and T. Kato, *Chem. Asian J.*, 2009, **4**, 1619.

CHAPTER 2

Synthesis and Characterization of Borazatruxene and derivatives

2.1 Introduction

This work is directed towards the synthesis of innovative hybrid functional materials obtained by chemical doping of polycyclic aromatic hydrocarbons (PAHs) with boron and nitrogen atoms. Specifically, this chapter will be focused on the BN-doping of truxene. This molecule was chosen as target building block among various PAHs known species because recently F. Dumur *et al.* reported[1] that well-designed truxene derivatives are emerging as promising functional materials for high technology applications in the organic electronic field. We believed that the BN doping of truxene could be achieved replacing the C=C double bonds of the central aromatic core with the isoelectric and quasi-isosteric B-N covalent bond providing the borazine six membered ring following a bottom-up synthetic method. The project, started by Dr. Emmett with the synthesis of borazatruxene (BN-doped truxene) and borazatruxene derivatives.[2] He reported the synthesis of six differently substituted borazatruxene derivatives on the peripherals aromatic rings as shown in Figure 2.1.

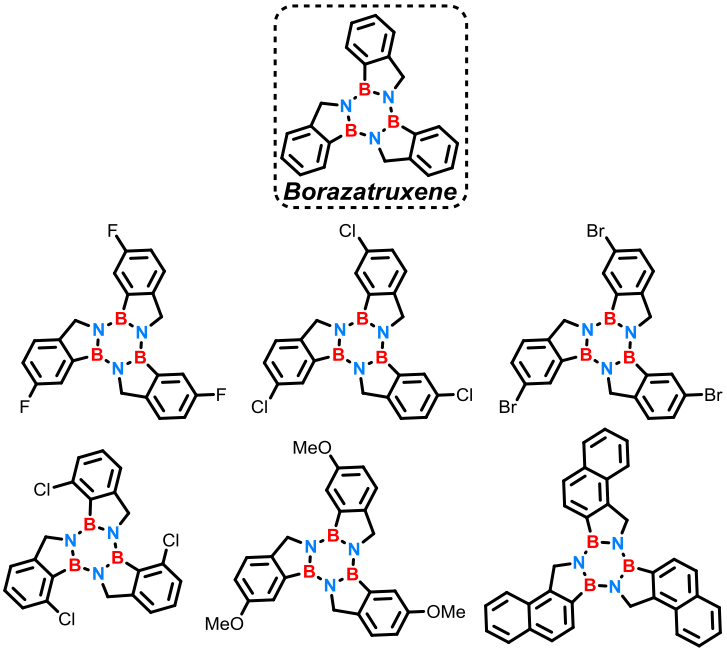

Figure 2.1 Representation of functionalized borazatruxenes on the peripheral aromatic rings.[2]

The synthetic pathway was strategically developed by a retrosynthetic approach (Scheme 2.1). It was envisioned that the key step to have access to the borazine framework **2** could be the condensation of three molecules of amine-boranes (ABs) **3**. These molecules, characterized by the dative N→B bond, when subjected to a thermolysis process led to the borazine ring formation via trimerization with the loss of six molecules of hydrogen. Retrosynthetically we envisaged to have access to aromatic amine-borane molecules by one-step reduction of *o*-benzonitrile boronic ester species **4** due to the cyano and boronic ester groups which are masked amine and borane functions. The regioselective *o*-borylation, which is a necessary requisite for the AB formation, could be conceived by lithiation-borylation of benzonitriles **5**.

This first approach was initially used by Dr. Emmett, however for some specific substrates it revealed to be ineffective in terms of regioselectivity. To this end we overcame this problem synthesising *o*-benzonitrile boronic ester species by Miyaura cross-coupling reaction of *o*-bromobenzonitriles **6**. Also, the reduction protocol was further developed by replacing the conventional heating with a microwave dielectric heating method. The latter revealed to be more efficient especially in reducing robust protecting groups such as neopentyl glycol or pinacol to the boron atom.

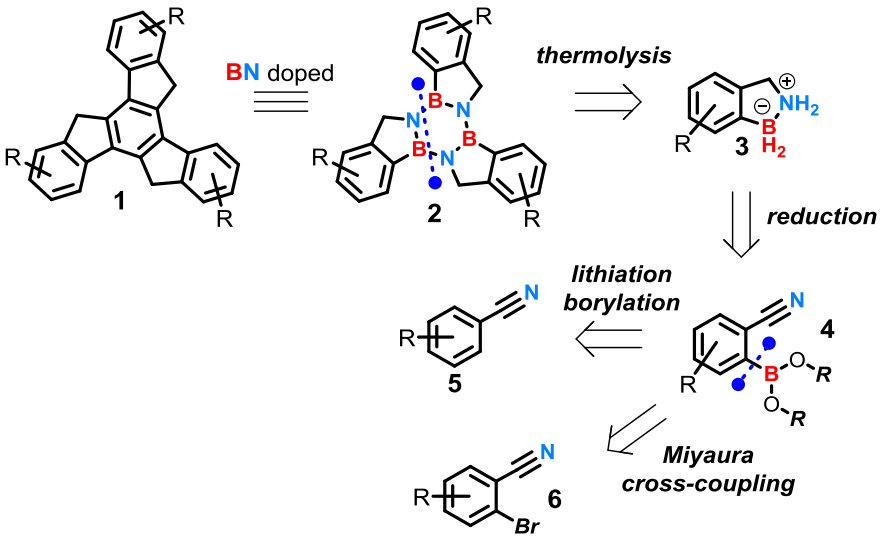

Scheme 2.1 Retrosynthetic analysis of borazatruxene.

Another way to synthesise the ABs is the reduction of (2-((methoxyimino)methyl) **8a** and (2-((methoxyimino)alkyl/aryl) **8b** phenylboronic acids. These species can be synthesised *via* condensation of methoxylamine hydrochloride with 2-formyl **9a** or 2-alkyl/aryl **9b** phenylboronic acids in water under physiological conditions as reported by Scouten and co-workers. This method was initially used by Dr. Emmett as an alternative route to have access to aryl substituted amine-boranes starting from 2-formylphenylboronic acid derivatives **9a**. Instead we envisaged this second strategy as an alternative way to functionalize amine-boranes in a different position than the aromatic ring. In fact, this method allows to have access to ABs functionalised in also in the benzylic position **7b** when 2-alkyl/aryl phenylboronic acids **9b** are employed in the synthetic process (Scheme 2.2).

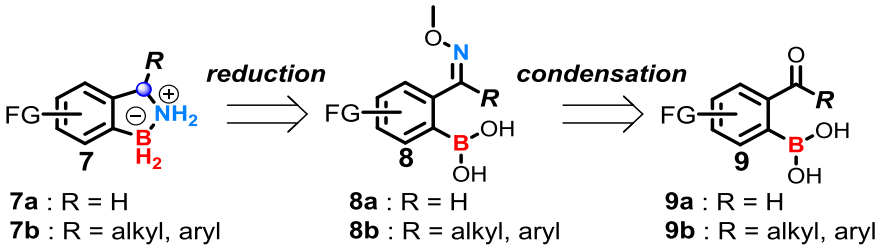

Scheme 2.2 Retrosynthetic analysis of amine-borane **7a-b**.

However, for the synthesis of aryl substituted borazatruxenes **1**, despite this method being faster, we mainly considered the first synthetic approach described. In fact, starting from benzonitrile derivatives **5** rather than 2-formyl or 2-acetyl phenylboronic acids **9** led to many more advantages. Benzonitrile species are cheaper than 2-formyl or 2-acetyl phenylboronic acids also, there are more derivatives commercially available so that we could expand the scope of studying the effect of substituents on the borazatruxene framework. Moreover, the presence of the carbonyl and boronic acid groups makes these molecules difficult to handle since they are highly reactive and very susceptible to nucleophilic attacks. Attempts to introduce functional groups at the stage of amine-borane or borazine species led them to decompose due to the higher sensitivity of the B-N bond with respect to the C=C bond.

2.2 Self-assembly process of Borazatruxenes

Early on in our study we also became interested in studying the supramolecular interactions involved in the self-assembly process of borazatruxene in solution and in the solid state. Borazine base material and especially aryl borazines can engage in non-covalent intermolecular interactions, such as π-π stacking and hydrogen bonding interactions.[3] However preliminary molecular modelling calculations studied by Dr. Emmett[2] suggested that borazines can also form supramolecular aggregates through intermolecular interaction between two borazine rings one on top of one another leading to columnar aggregates. Whether this is true, borazine rings should preferentially adopt a staggered conformation to stack, rather than to an eclipsed arrangement.

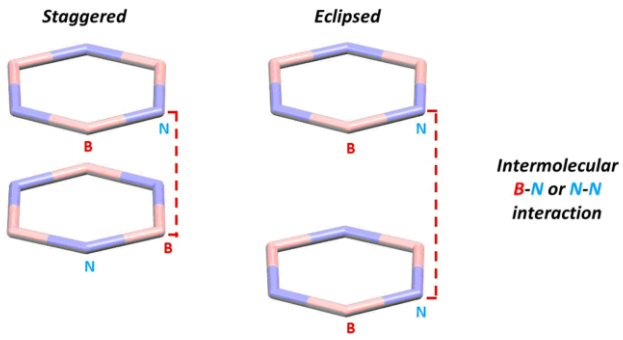

Figure 2.2 Representation of staggered and eclipsed arrangements of borazine stacks highlighting intermolecular and intramolecular bond distances.

Theoretical study highlighted that the staggered conformation adopted from borazatruxene in the crystalline packing is energetically more favourable respect to an eclipsed arrangement. In fact, when the latter was simulated, the distance calculate between two borazine ring was higher than a classic π-π

staking interaction distance, suggesting that borazines are unlikely to aggregate in this fashion. While, on the contrary, in the case of a staggered arrangement simulation the overall energy calculated resulted to be lower and distances between borazine rings shorter confirming the formation of a π-stack aggregation. Exploiting these non-covalent intermolecular interactions between borazine rings and driving molecules somehow to pack one on top of another it might be possible to direct the molecular self-assembly towards the formation of columnar aggregates. Columnar supramolecular assemblies can be obtained either by a disordered or by a cooperative self-assembly process of monomeric units that aggregate in a stereospecific fashion. In the latter case chiral structural shapes, such as helical fibres, twisted wires or ribbons, helical tubes, or coiled ribbons can be obtained. Specifically, in the case of helical aggregates, is possible to drive the self-assembly process preferentially towards a right-handed or a left-handed helical supramolecular structure.

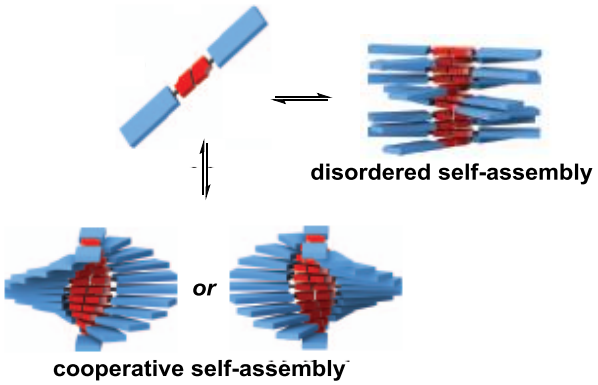

Figure 2.3 Examples of isodesmic and cooperative supramolecular self-assembly.

A promising way to enhance a cooperative self-assembly process and to specifically address the formation of one chiral helix rather than the other is to introduce functional groups with specific properties onto the molecular unit. It has been experimentally proved that chiral functional groups are very efficient to drive the molecular self-assembly aggregation towards an excess of a single-handed helix. Along with this idea we had a careful review of the literature and we came across with an interesting report by D. B. Amabilino.[4] He utilized a C_3-Symmetrical functional tris(tetrathiafulvalenes) as main structural motif of the trimeric cyclic arrangement and then he prepared helical columns with a controlled helix sense introducing chiral lipophilic chains on the peripheral 1,3-dithiole-2-thione moiety.

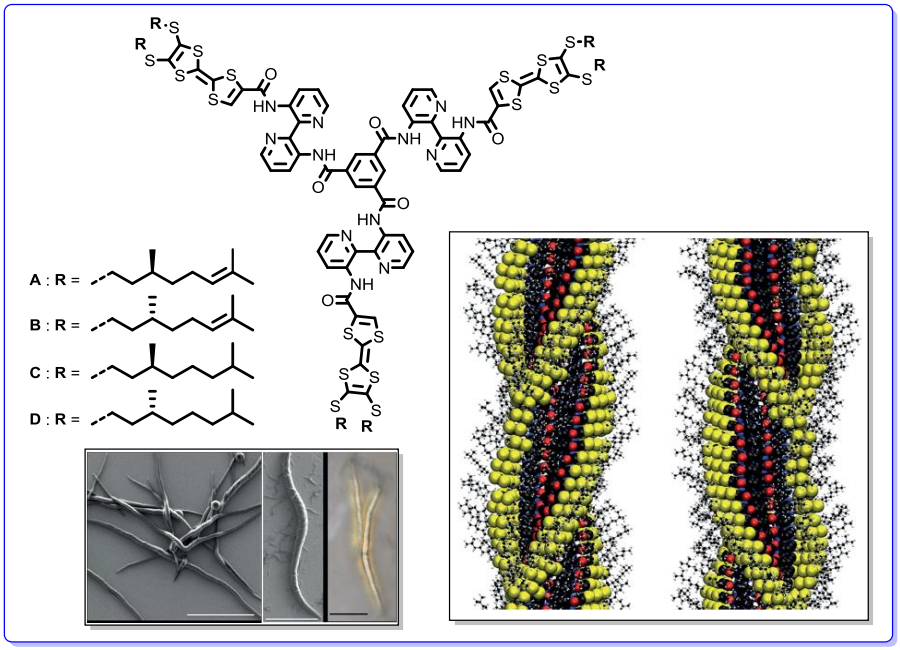

Figure 2.4 C_3-symmetric tris-tetrathiafulvalene (TTF) compounds with models of supramolecular elical rearrangement clock and anticlockwise depnding on the chirality of the alkyl chains.[4]

Likewise, borazatruxene is a C_3-symmetrical flat molecule therefore we envisioned a similar behaviour if properly functionalized with chiral alkyl chains.

2.3 Synthesis of BN [2,3]dihydroindenes

2.3.1 *Ortho*-lithiation-borylation of benzonitriles

As outlined, the synthesis of borazatruxenes **1** began with the preparation of differently substituted *o*-benzonitrile boronic esters **4** either *via* direct *ortho*-lithiation borylation of benzonitriles **5** or Miyaura cross-coupling reaction of *o*-bromobenzonitriles **6**. In those cases where benzonitriles with specific functional groups were not commercially available they were synthetized from commercially available sources adding additional steps at the beginning of the designed synthetic pathway. For the preparation of *o*-benzonitrile boronic esters following the *ortho*-lithiation borylation protocol, we started from benzonitrile derivatives differently substituted on the aromatic ring.

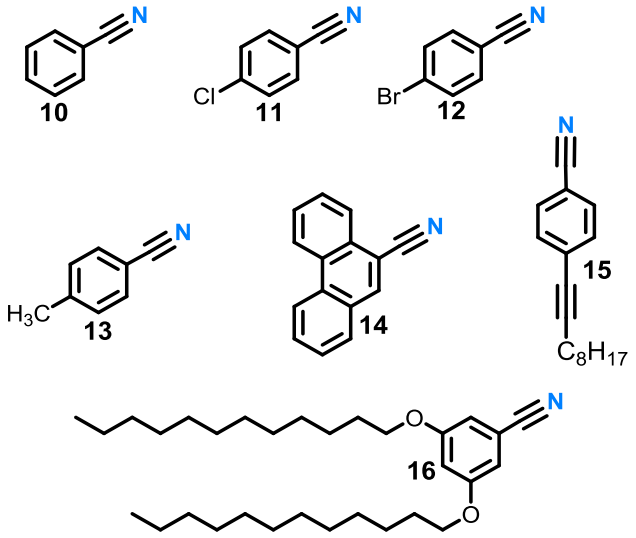

Figure 2.5 Representation of starting materials used in the synthesis of BN-doped truxene derivatives.

Starting materials **10-14** were commercially available sources while **15** was synthesised by Sonogashira cross coupling reaction between **12** and 1-decyne **17** as showed in Scheme 2.3, while **16** was synthesised by nucleophilic substitution between 3,5-dihydroxybenzonitrile **18** and 1-bromododecane **19**.

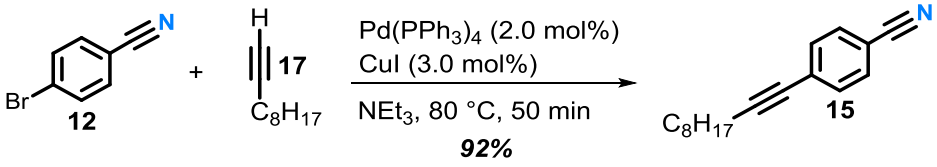

Scheme 2.3 Alkylation of 4-bromobenzonitrile by Sonogashira cross coupling reaction.

The general Sonogashira protocol for the coupling of terminal alkynes with aryl or alkenyl halides (or triflates), usually, involves an organic solvent, a Pd(0)/Cu(I) catalytic system, and a stoichiometric amount of a base.[5] The generally accepted catalytic cycle is showed in Scheme 2.4. The first step is the oxidative addition of the organic halide R^1-X to the active complex LnPd(0) (where Ln is the number (n) of ligands (L) coordinated to Pd) giving the intermediate LnPdR^1X. At this point, a transmetalation with an organometallic reagent (copper alkyne) occurs giving the adduct LnR^1Pd-CΞC-R^2. The Cu-C bond formation is promoted by the base through removal of the terminal hydrogen atom of the **H**-CΞC- bond. The copper atom, which previously was coordinated at the triple bond, can form the new bond with the terminal sp carbon atom to give Cu-CΞC-R^2. The last step involves the reductive elimination to provide the desired product and to reform the active catalyst which will be involved in a further catalytic cycle.

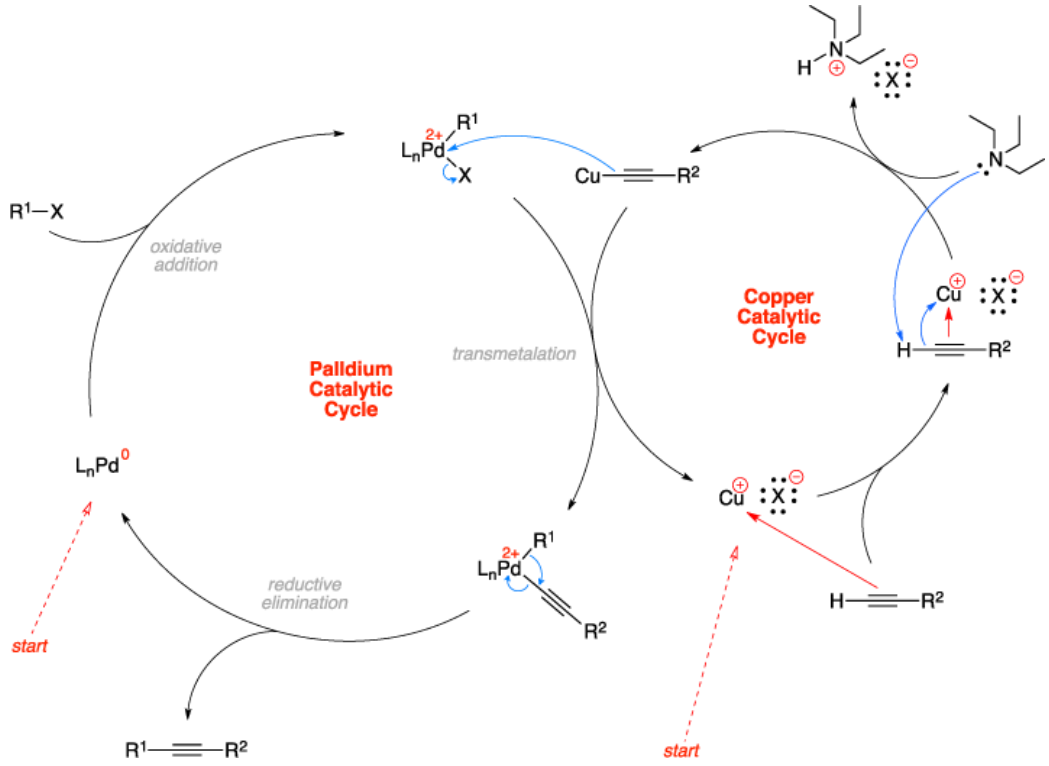

Scheme 2.4 General mechanism proposed for the Sonogashira cross coupling reaction.

The synthesis followed a literature procedure,[6] where upon treatment of **12** with 1-decyne **17** in presence of 2 mol% $Pd(PPh_3)_4$ and 3 mol% CuI in NEt_3 at 80 °C, under inert atmosphere (argon), led to the desired product **15** in high yield. The ^{1}H-NMR analysis spectra in $CDCl_3$ displayed matching signals related to both aromatic and alkyl chain protons. The absence of the singlet at 1.93 ppm, related to the terminal hydrogen atom of the alkyne (**H**-CΞC-) functional group was diagnostic in confirming structure **15**. The ^{13}C-NMR spectrum also matched with that reported in literature, showing peaks at 96.0 and 79.0 ppm corresponding to the two sp carbon atoms. Compound **16** was synthesized following a literature procedure[7] starting from the commercially available 3,5-dihydroxybenzonitrile **18**, which upon treatment with K_2CO_3 in DMF, followed by the addition of **19** led to the nucleophilic substitution product **16** in high yield (Scheme 2.5).

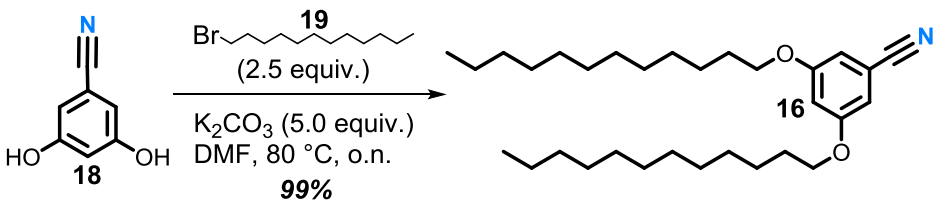

Scheme 2.5 Synthesis of 3,5-bis(dodecyloxy)benzonitrile.

Having all the desired benzonitrile derivatives in hands we could proceed with the preparation of *o*-benzonitrile boronic esters following, as outlined before, the *ortho*-lithiation borylation procedure. The

synthetic strategy was adapted from J. L. Kristensen's original protocol[8] where exposure of benzonitriles to the Li-TMP adduct **29** beforehand prepared in situ, resulted in the lithiation of the benzene ring in *ortho* position respect to the nitrile group. A subsequent nucleophilic attack occurs between the lithiated species **30** and the Lewis acid boronic ester species leading to the *ortho* borylated desired product (Table 2.1).

Table 2.1 Lithiation-borylation of benzonitriles for the preparation of substituted 2-cyanoarylboronic esters.

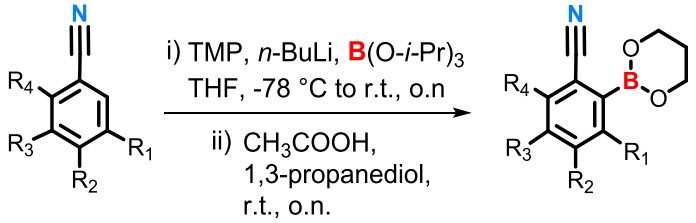

Entry	R_1	R_2	R_3	R_4	Product	%yield
10	H	H	H	H	**20**	75
11	H	Cl	H	H	**21**	85
12	H	Br	H	H	**22**	86
13	H	CH_3	H	H	**23**	-
14	Phenanthrene				**24**	95
15	H	-C≡C-C_8H_{17}	H	H	**25**	90
16	-$OC_{12}H_{25}$	H	-$OC_{12}H_{25}$	H	**26**	30

(*) All reactions have been performed initially starting from a quantity of 100 mg of starting materials

The high regioselectivity is mainly driven to the ability of nitrogen atom to form a coordinating complex with lithium atom of the Li-TMP adduct **29**.[9] This make possible the lithium-hydrogen exchange with the proximal hydrogen atom (*ortho* position in this case) avoiding that this reaction occurs in other parts of the aromatic ring. The key step involves the addition of a lithium-coordinating steric hindered base species as 2,2,6,6- tetramethylpiperidine (TMP) **27** to the alkyllithium species (*n*-BuLi) **28** (Scheme 2.6). The main role of the base is to break up the hexameric aggregated structure of the alkyllithium to give the Li-TMP adduct **29** which is more reactive towards the *ortho* lithiation. Also, the use of a highly sterically hindered base as TMP prevent the latter to be involved in a nucleophilic attack avoiding secondary reactions occurring.

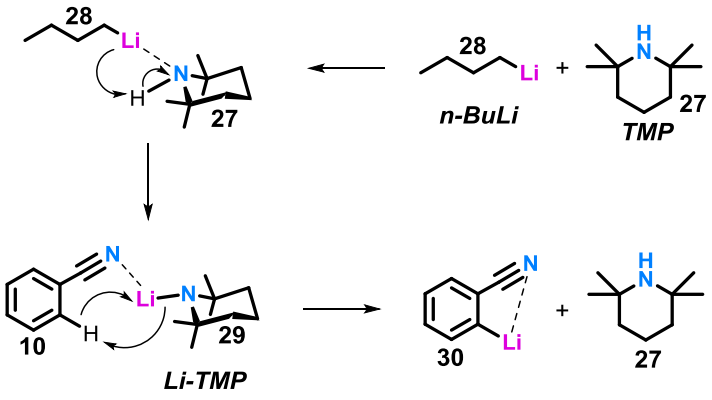

Scheme 2.6 Mechanism of *ortho* lithiation.

Li-TMP complex **29** was prepared in situ upon slow addition of a solution of *n*-BuLi **28** to a solution of TMP **27** in anhydrous THF cooled to -10 °C. The mixture was further cooled to -78 C° then $B(O\text{-}i\text{-}Pr)_3$ and benzonitrile were subsequently added in this order. The lithiation is the first reaction that occurs, followed by the nucleophilic attack to the electrophilic boronic ester species, thereby providing to the corresponding benzonitrile boronic ester derivative. The isopropyl boronic ester intermediate obtained was subsequently hydrolysed to boronic acids by acidic treatment and then converted into the cyclic 1,3-propanediol boronic ester derivative. This resulted in a more stable boronic ester species easier to isolate and characterize. This reaction proved to be highly regioselective, giving the *ortho*-borylated species as main products in high yields (75-95%) in most of the examples reported. However, a full conversion of **14** was possible only increasing the equivalents of *n*-BuLi from 1.5 (generally used) to 2.2 leading to a high product yield. The lower reactivity of **14** towards Li-TMP **29** might be associated with steric effects due to the bulky structure of both phenantrene and Li-TMP **29** which makes the lithiation in the 10th position difficult (Figure 2.6).

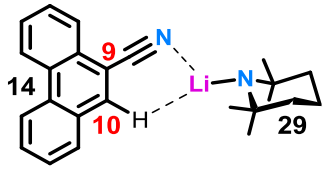

Figure 2.6 Representation of the adduct between 9-cyanophenantrene and Li-TMP.

This reaction was less successful for compounds **13** and **16** since after purification resulted in a complex mixture of different products, suggesting a loss in regioselectivity. Purification of all products was carried out by washing the crude mixture several times with an aqueous solution of KH_2PO_4. The isopropyl boronic esters obtained were hydrolysed to boronic acids by treating the mixture with CH_3COOH and then converted into the cyclic 1,3-propanediol boronic ester derivatives using an excess of 1,3-propanediol. Generally chromatographic purification was avoided, because the B-OR ester group readily reacted with the acidic OH groups of silica gel converting the boronic ester into the boronic acid (BOH) group which remained stuck on the column. Compounds **25** and **26** could be easily purified by flash chromatographic purification because the lipophilic long alkyl chains conferred a reasonable affinity to the eluent utilized. After purification of the crude mixture of **26** were isolated four different compounds therefore a series of NMR spectra were collected in an attempt to identify each component of the mixture. The ^{1}H-NMR spectrum of the first compound isolated at highest R*f* (0.73) displayed identical peak patterns observed for starting material **16**, while the last compound at lowest R*f* (0.1) was identified to be the desired product **26** obtained in very low yield (30%). To the second compound isolated (R*f* = 0.53) was assigned the structure of the other possible regioisomer *para* borylated respect to the nitrile group, since the ^{1}H-NMR spectra showed only one peak at 6.84 ppm related to the two chemically equivalent aromatic hydrogen

atoms. Moreover, no splitting in chemical shift related to the hydrogen atoms of the long alkyl chains was observed, therefore the system was symmetrical. The NMR spectra associated to the last compound isolated was very complex therefore we could not assign a correct structure for it. The isolation of boronic ester **23** was complicated especially by chromatography purification that resulted in product decomposition. At a later stage we evaluated the possibility of scaling up this reaction to grams scale, however first attempt with the unsubstituted benzonitrile 1**0** resulted in a significant decreasing in % yield. The observed outcome can be rationalized by considering the negative effect on keeping the solution homogeneous due to the large amount of 1,3-propanediol used which made the resulting mixture to gel out therefore becoming difficult to stir.

2.3.2 Borylation of o-bromobenzonitriles by Miyaura cross-coupling reaction

We deduced that complications encountered in the *ortho*-lithiation-borylation procedure, especially for compounds **13** and **16**, might potentially be overcome following a different synthetic pathway. Indeed, we envisioned that boron atom could be installed with high regioselectivity in *ortho* position using the Miyaura cross-coupling reaction starting from *o*-bromobenzonitriles. However, one of the main challenges in the synthesis was related to the commercial availability of *o*-bromobenzonitriles **6**, especially for substrates that we were interested in. Indeed, during our study, we became interested in synthesising molecules bearing pendant lipophilic alkyl chains, to increase the solubility of borazatruxene and to control the molecular assembly for supramolecular engineering purposes. To by-pass this problem, we evaluated the possibility of using a general method to introduce regioselectively halogen atoms in *ortho* position to the nitrile group. Recently Sun *et al*. reported a synthetic procedure for the regioselective *ortho* halogenation of arylnitriles **10** via Pd(II)-mediated sp^2 C−H bond activation.[10] The mechanism proposed (Scheme 2.7) presume the formation of adduct **31** where Pd is coordinated to the π-electrons between carbon and nitrogen atoms of cyano group. At the same time oxygen atom of the carboxylate group of the palladium catalyst forms a weak CH···O H-bond with the proximal aromatic hydrogen weakening the C−H bond. At this stage Pd-C bond is formed and a molecule of acetic acid is released, leading to an aryl palladium intermediate **32**. This step is followed by an oxidative addition by *N*-alogenosuccinimide (NXS, X = Cl, Br, I) **33** on palladium atom leading intermediate **32** to intermediate **34**. The desired *ortho*-halogenated product **35 is** generated *via* typical reductive elimination regenerating Pd(II) catalyst.

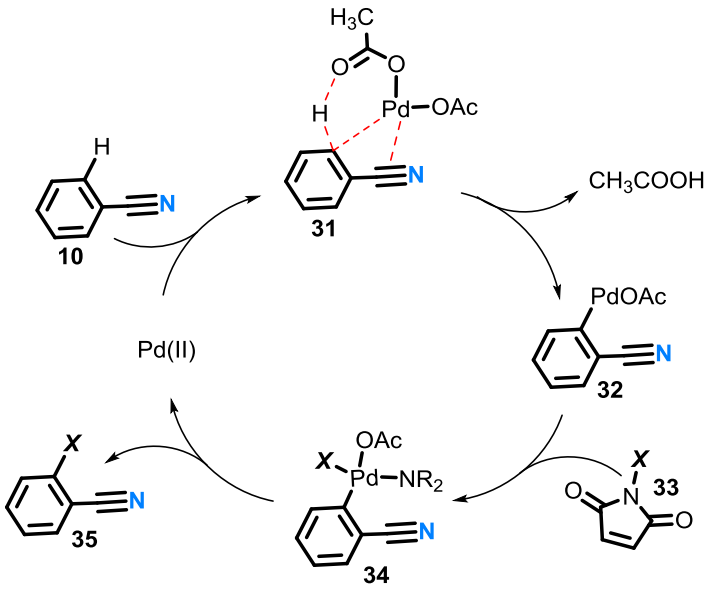

Scheme 2.7 Mechanism proposed for the Pd-catalyzed ortho halogenation of benzonitriles.

Starting material **13**, already available in our lab, was used in our initial evaluation of this method (Scheme 2.8). The reaction was carried out under the same reaction conditions reported in the literature providing **37** in high yield (90%). This promising result allowed us to access a wide range of *ortho*-brominated benzonitrile species to employ in the next step of the Miyaura reaction. This method was highly efficient also with compound **16** which delivered the corresponding *ortho*-brominated species **38** in 78% yield.

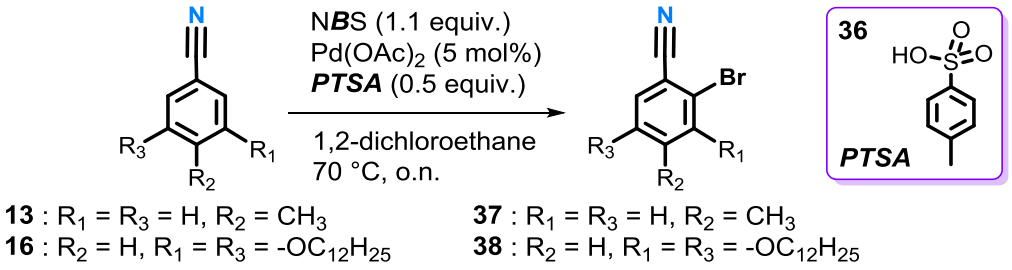

13 : $R_1 = R_3 = H$, $R_2 = CH_3$ **37** : $R_1 = R_3 = H$, $R_2 = CH_3$

16 : $R_2 = H$, $R_1 = R_3 = -OC_{12}H_{25}$ **38** : $R_2 = H$, $R_1 = R_3 = -OC_{12}H_{25}$

Scheme 2.8 Synthesis of *ortho* brominated benzonitriles **37** and **38**.

Attempts to scale-up this reaction for **38** to gram scale made workup and purification very difficult resulting in a very low yield reaction. The extraction with ethyl acetate from water caused the formation of a persistent emulsion which led to a partial loss of product. Unable to avoid this problem we decided to purify the crude mixture directly by flash column chromatography which successfully provided **38** in 65-75% yield. We were so pleased of this high regioselectivity degree obtained for both compounds **37** and **38**; the only possible by-product achievable with this method was the dibrominated species. Curiously we noticed that the amount of impurities presents in the *N*-bromosuccinimide (NBS) affected the outcome of this reaction making favourable the second bromination. In this regard commercial NBS was further purified by recrystallization from water in order to remove all the impurities. With this method in hand,

capable to install halogen atoms regioselectively on benzonitrile derivatives, we moved on the next step of Miyaura cross-coupling reaction. The well-known catalytic cycle is shown in Scheme 2.9, detailing the generic three-stage "*oxidative addition, transmetalation and reductive elimination*" sequence.[11]

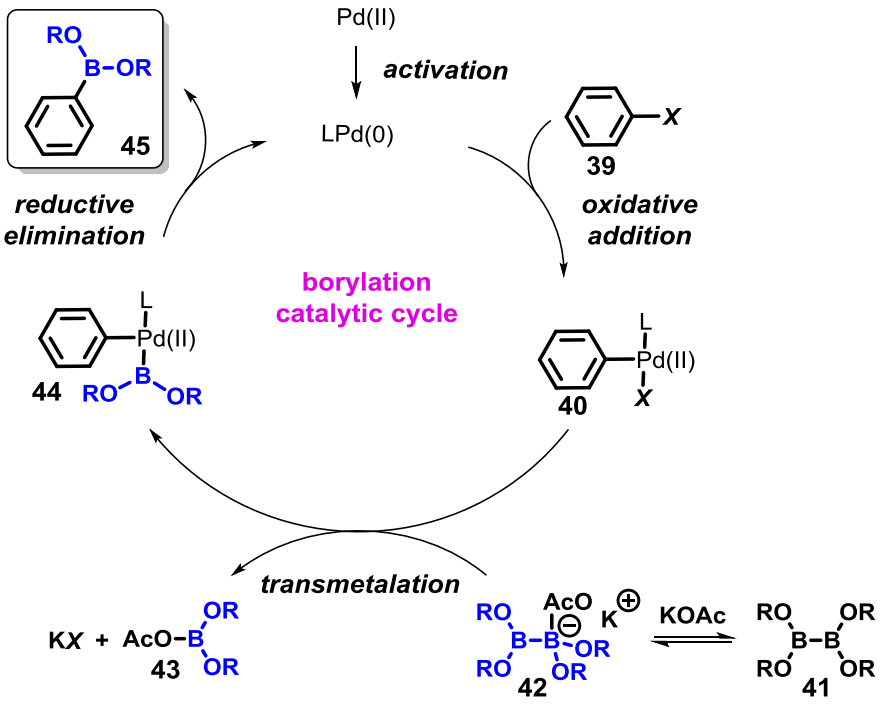

Scheme 2.9 Proposed mechanism for the Miyaura cross coupling reaction.

In parallel to the *ortho*-bromination of **13** and **16**, commercially available **46** was used to test the Miyaura reaction. The synthetic strategy was adapted from C. Rochais' s original protocol[12] to our substrate modifying equivalents of reactants used, work up and purification procedure.

Table 2.2 Synthesis of substituted 2-cyanoarylboronic esters **48-50** by Miyaura cross coupling reaction.

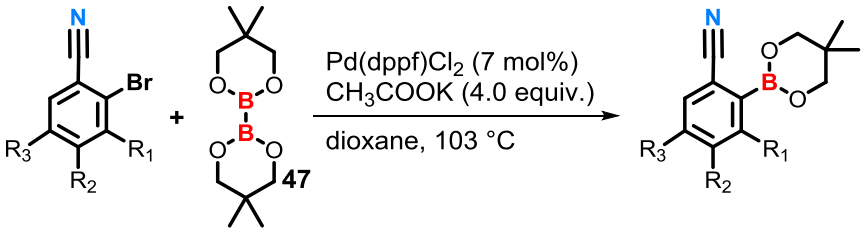

Entry	R_1	R_2	R_3	Product	%yield
46	CH_3	H	H	**48**	89
37	H	CH_3	H	**49**	90
38	$-OC_{12}H_{25}$	H	$-OC_{12}H_{25}$	**50**	60

The best result was obtained when the amount of bis(neopentyl glycolato)diboron 4**7** was increased to 1.5 equivalents and potassium acetate decreased to 4.0 equivalents. Also, the work up procedure was revised,

indeed the crude mixture was dissolved in ethyl acetate rather than diethyl ether and washed with water and brine. The best conditions found for the column chromatography purification was to use a mix of *n*-hexane/CH_2Cl_2 (60:40) and then pure CH_2Cl_2 to afford the desired **48** in 89% yield. With these conditions in hand, we extended this method to substrate **37** and **38**, however, while **37** provided the corresponding borylated species **49** in high yield (90%), **38** resulted in a complex mixture of products. Chromatographic purification allowed the isolation and identification of the components of the mixture. Unexpectedly, ^{1}H-NMR analysis of pure **50** revealed to be, in realty, a mix of boronic ester **50** and the corresponding boronic acid **58** in 6:4 ratio. Instead, surprisingly, one of the main by-product isolated was identified in **16**. This result suggested that a side reaction occurred in this particular case favouring the formation of by-products rather than the desired **50**. One of the possible decomposition pathways frequently observed for boronic acid species when employed in metal-catalysed cross-coupling reactions is the protodeboronation. This reaction has been well studied[13–15] in the past proving that it can occur in both acidic and alkaline conditions (commonly used in Miyaura reactions), following two different mechanisms (Scheme 2.10).

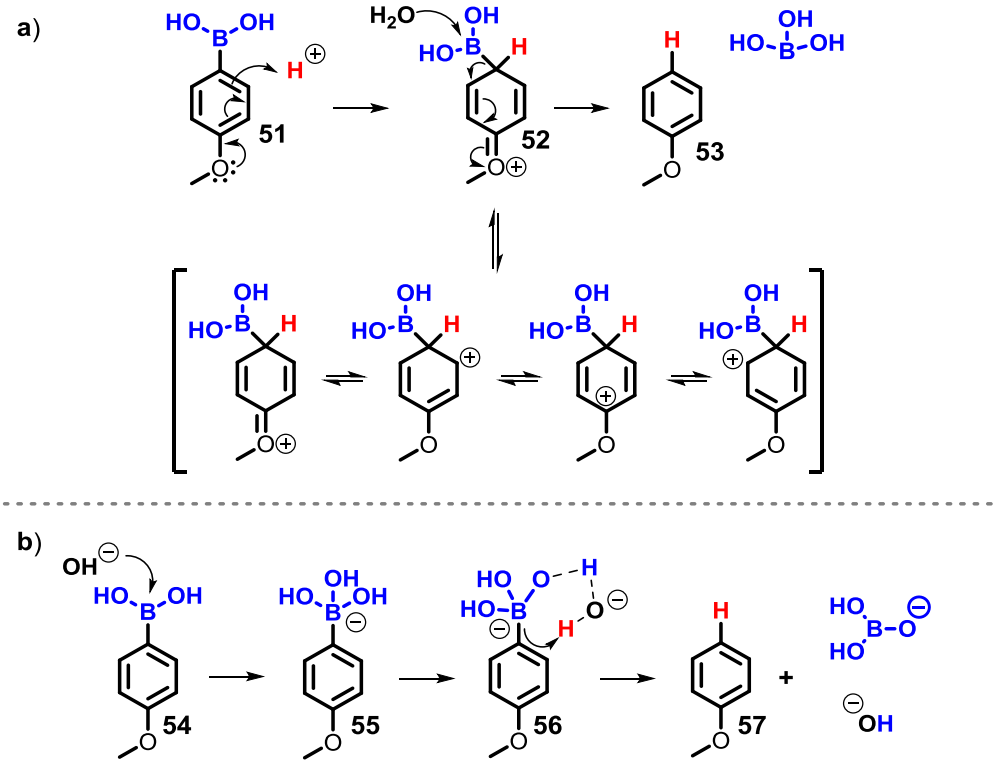

Scheme 2.10 Proposed mechanism for the protodeboronation of p-anisoleboronic acid under a) acidic conditions, b) basic conditions.

Studies reported in literature based on the Hammett constant evaluation[14] revealed that electron withdrawing (EWG) groups slowed down the acid-catalysed protodeboronation while, electron donating (ED) groups promoted this reaction stabilizing the positive charge in the Weland resonance forms. Instead, presumably, in alkaline conditions the excess of negative charge on the boron atom, due to the boronate adduct **55** formed, plus the presence of an electron donating group such as methoxy (MeO) group

conjugated either in *ortho* or *para* position to the boron atom destabilize intermediate **55** promoting the protodeboronation **56-56**. This explanation is in line with what we observed indeed, in our case, this phenomenon was even more enhanced because of the presence of two ED alkoxy groups in *ortho* or *para* position to the boron atom thus making more favourable the protodeboronation process. Considering that most of the examples reported in literature of protodeboronation occurs in presence of the boronic acid group, we believed that this side reaction occurred upon hydrolysis of **50** to the corresponding boronic acid species **58** which in turn underwent to protodeboronation (Scheme 2.11).

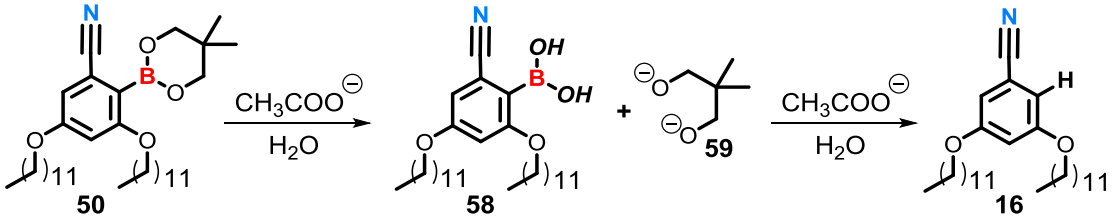

Scheme 2.11 Proposed mechanism for the protodeboronation of boronic ester **50.**

Clearly this problem was due to two main factors, the use of a solvent not perfectly anhydrous and an excess of base utilized. In an attempt to improve in the yield of **50** and minimize the protodeboronated by-product **16** formed, we decide to repeat the reaction halving the amount of base used; unfortunately, the outcome was the same. To this end we evaluated the possibility of keeping the same equivalents of base previously used and make a screening of different solvents. To examine the effect of the solvent we initially replaced 1,4-dioxane with toluene which is widely used in the common cross-coupling reactions. However, preliminary results obtained suggested that toluene had an inhibiting effect on the reaction because no product was formed but only starting material **38** was recovered. In a second attempt at the synthesis of **50** we followed a literature procedure[16] introduced by B. Wang using DMSO instead of 1,4-dioxane. They reported similar problems when similar aryl substituted boronic esters were subjected to the Miyaura reaction. According to the paper both 1,4-dioxane and toluene promoted the protodeboronation of these species while, when DMSO was used the amount of this by-product formed was drastically reduced. Therefore, we proceeded with the Miyaura reaction following the reaction condition reported except for the catalyst used. Indeed, they reported that $[(t\text{-}Bu)_2P(OH)]_2\text{-}PdCl_2$ (**POPd**) works better than $Pd(PPh_3)_4$ and $Pd(dppf)Cl_2$ in DMSO giving the best yield in terms of borylated products, however because we wanted to test only the effect of the solvent without changing more than one parameter per time we kept using $Pd(dppf)Cl_2$ as catalyst.

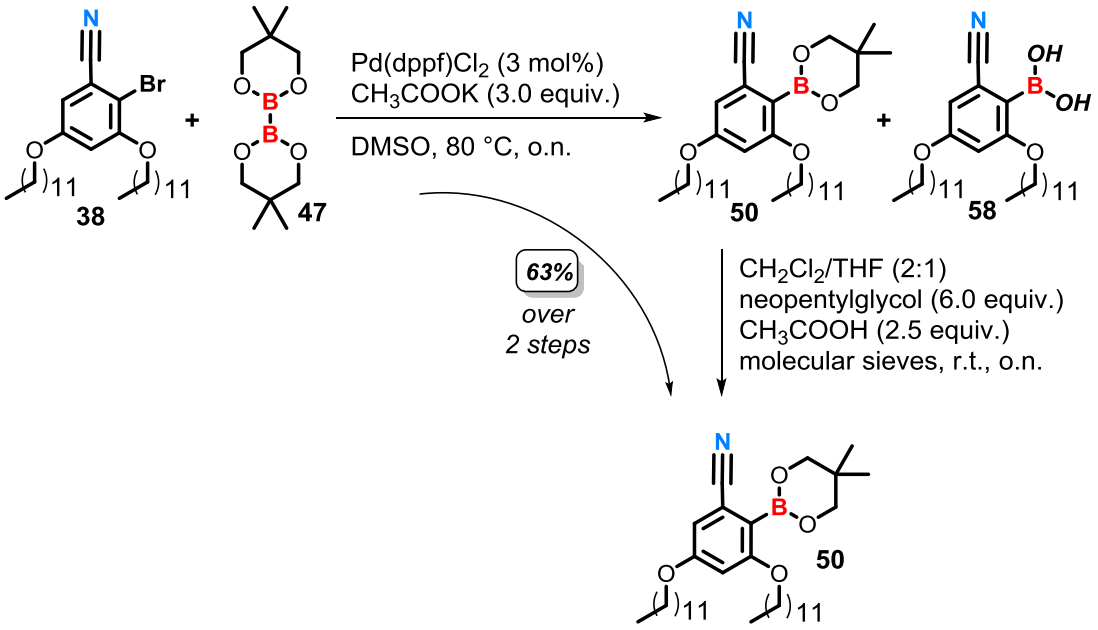

Scheme 2.12 Alternative synthesis of boronic ester **50.**

The reaction was performed in DMSO at 80 °C, overnight. After work-up, ^{1}H-NMR spectrum in $CDCl_3$ on the crude mixture displayed signals related to a mix of boronic ester and boronic acid species. In an attempt to obtain selectively the boronic ester **50**, the crude mixture was dissolved in a mix of CH_2Cl_2 : THF (2:1), under inert atmosphere (argon), and upon hydrolysis with acetic acid it was re-protected with neopentylglycol. Gratifyingly, after flash chromatography purification, the ^{1}H-NMR spectrum in $CDCl_3$ of the pure product displayed only peaks related to the boronic ester **50**, obtained in 63% yield. Despite this alternative synthetic pathway was highly efficient for the synthesis of **50**, it proved to be a tricky and time demanding procedure. In a later stage, we reviewed the option to use 1,4-dioxane following the standard procedure initially described. However, we decided to halve the amount of solvent used, working in higher concentration in order to reduce the amount of moisture in the reaction mixture. Also, potassium acetate usually kept in the oven at 200 °C was further dried under vacuum for 1 hour with bis(neopentyl glycolato)diboron and the catalyst before to start the reaction. Pleasingly, with all these precautions to minimize the amount of moisture in the reaction mixture in place, we noticed a remarkable improvement in the reaction yield of **50**. Indeed, **50** was provided in 60% yield after chromatography purification and the ratio of boronic ester/acid detected by NMR analysis increased to 8:2. Pleased to have found the right conditions for the synthesis of **50**, we decided to attempt at the scale-up of this reaction but, unfortunately, as expected, **50** was obtained in very low yields. Presumably the larger amount of solvent and base used, containing a significant amount of moisture difficult to remove, made more favourable the hydrolysis and thus the protodeboronation of **50**. A series of NMR spectra (^{1}H, ^{11}B and ^{13}C) were collected to proof molecular structure of **50** which was also confirmed by mass spectroscopy analysis that displayed a good match between the predicted isotope pattern distribution and the observed data.

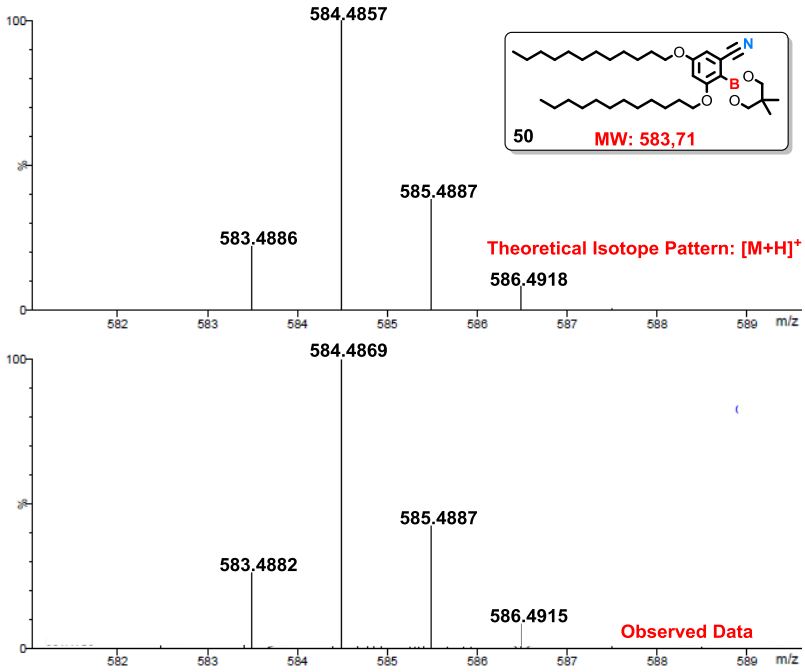

Figure 2.7 Mass Spectrum of compound **50** from Swansea University.

2.3.3 Synthesis of (2-((methoxyimino)methyl) 63 and (2-((methoxyimino) ethyl) 72 phenylboronic acids

As mentioned before another way to synthesise amine-borane building blocks **3** is the reduction of (2-((methoxyimino)methyl) **8a** and (2-((methoxyimino)alkyl/aryl) **8b** phenylboronic acids obtained *via* condensation of methoxylamine hydrochloride with 2-formyl **9a** or 2-alkyl/aryl **9b** phenylboronic acids. Specifically, we considered this synthetic approach a convenient way to have access to a wide range of borazatruxenes functionalized only in the benzylic 7, 14, 21 positions **60** rather than in the aromatic ring using 2-alkyl/aryl phenylboronic acids **61** in the synthesis (Scheme 2.13).

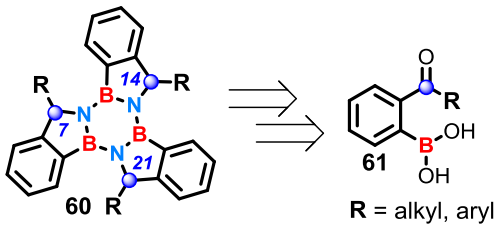

Scheme 2.13 Retrosynthetic analysis of borazatruxene **60.**

This elegant method to functionalize indirectly the internal bridging -CH_2- groups of borazatruxene, allowed us to by-pass problems encountered in the functionalization of both ABs and borazatruxenes. Indeed, our attempts at the bromination or deprotonation of the benzylic position (internal -CH_2- bridge) led only to decomposition, despite mild and inert reaction condition were adopted. The difficulties

surrounding the synthetic methodology mainly associated with the stability of these material when exposed to specific reactants limited their applications as substrates for many different types of reactions. This new strategy gave us the opportunity of synthesising a new class of borazatruxenes functionalized in a different region of the molecule and to study how this effects the molecular assembly, the electronic and optical properties and the stabilization of the system. Also, these derivatives might be further manipulated to create 2D or 3D structures for instance by polymerization or dehydrogenation to promote the formation of new C-C bonds. Commercially available 2-formylbenzeneboronic acid **62** was used in our initial evaluation of the condensation reaction with methoxylamine hydrochloride **66** following a method introduced by Groziak.[21]

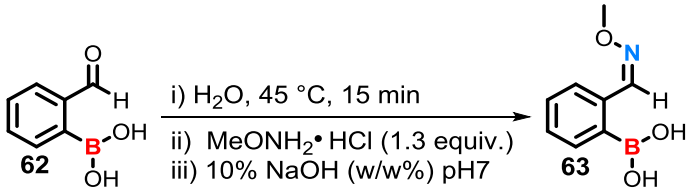

Scheme 2.14 Synthesis of (2-((methoxyimino)methyl)phenyl)boronic acid **63**.

As reported in the literature, boronic acids **64** can readily react with themselves by a self-condensation reaction,[22,23] resulting in the formation of a stable six membered ring boroxine **65** (B_3O_3)[24] as shown in Scheme 2.15. In our hands, this species prevented the imine formation on the neighbouring aldehyde group, therefore 2-formylbenzeneboronic acid **62** was stirred in water at 45 °C for 15 min before the use in order to ensure the quasi-complete hydrolysis.

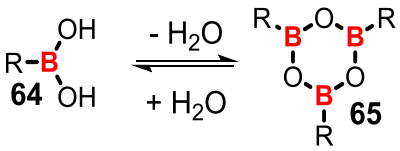

Scheme 2.15 Reversible synthesis of boroxine from boronic acids.

The methoxyamine hydrochloride **66** was added portion-wise at room temperature, resulting in the formation of a white precipitate representing a synthetic intermediate **68** proposed by J. Stress *et al.* as shown in Scheme 2.16.[25]

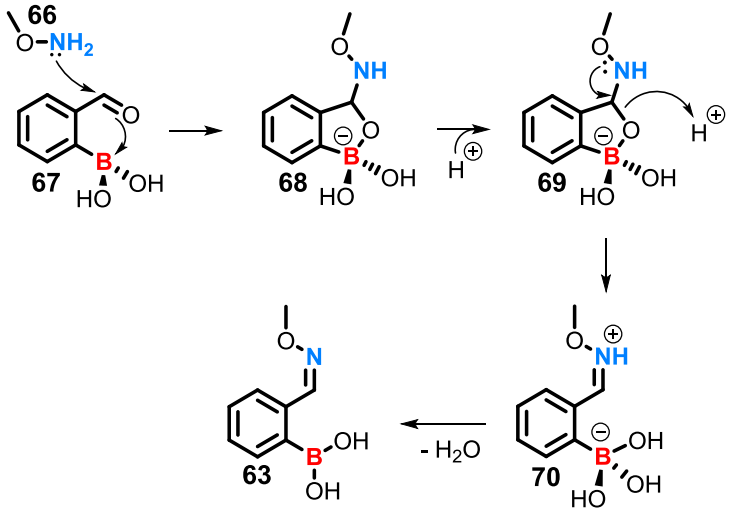

Scheme 2.16 Plausible mechanism for the aldehyde-methoxylamine boron assisted condensation.

The desired **63** was subsequently obtained by neutralizing the suspension with a solution of sodium hydroxide (10% v/v) until neutral pH and followed by heating at reflux for 15 min. At this stage the protonation of the cyclic boronate occurs, based on the pK_a of a boronate complexes (≈ 7), and the oxime functional group was formed at the expense of breaking the five-membered ring. We noticed that this method was entirely concentration dependent and the best condition found was starting from an initial concentration of starting material of 20 mg/mL providing to **63** in 83% yield. This is believed to be due to the imine's partial solubility in water. Attempts to isolate **63** by chromatography purification failed since it resulted in product decomposition, therefore only crystallization from water and filtration provided **63** as a pure sample. Characterization by NMR spectroscopy of **63** gave the same results reported in literature[21] confirming the molecular structure. Attempt at the synthesis of (2-((methoxyimino)ethyl)phenyl)boronic acid **72** following the same procedure resulted in substantial decomposition accompanied by unidentified side products which made difficult the work up and the purification. In this regard a careful review of the literature revealed an important report[26] by Gillingham detailing the synthesis of aldoxime and ketoxime in anhydrous methanol instead of water because moisture and pH sensible compounds. Also, they reported the synthesis of a similar compound bearing the benzyloxy group instead of methoxy group attached to the imine. Application of this protocol to our system, treating **71** with methoxyamine hydrochloride already available in our lab, necessitated to warm-up gently the solution to promote the reaction.

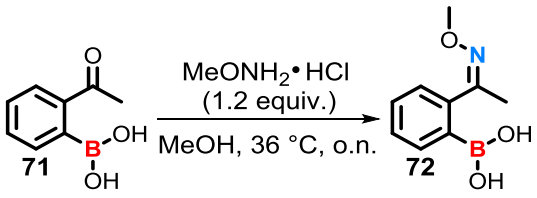

Scheme 2.17 Synthesis of (2-((methoxyimino)ethyl)phenyl)boronic acid **72**.

The reaction was completed after overnight, indeed the ^{1}H-NMR analysis spectrum on the crude mixture, displayed an overall shifting of the signals to lower ppm compared with starting material **71**. Specifically, the diagnostic singlet of the methyl group in α position to the carbonyl function shifted from 2.55 to 2.23 ppm, indicating a full conversion into the product. However, the NMR data displayed also signal not related to the desired **72** suggesting that the crude was impure. Attempts to isolate **72** by chromatography purification failed. Replication of the reversed phase chromatography conditions detailed in literature[26] resulted in an inseparable mixture containing the desired **72**, while using the normal chromatography condition with silica gel it resulted in product decomposition. Purification by crystallization from water as for **63** was excluded, also attempts at the recrystallization of **72** from methanol and dichloromethane was a failure. Unfortunately, our efforts to isolate **72** as an analytically pure sample for full characterization purposes failed, thus the only alternative was to use the crude product directly in the next step.

2.3.4 Reduction of boronic esters 20-22, 24-25, 48-50 and boronic acids 63 and 72

The subsequent step towards the synthesis of borazatruxenes involves the reduction of boronic esters **20-22, 24-25, 48-50** and boronic acids **63** and **72** into the corresponding amine-borane derivatives. Notoriously one of the classic ways to afford primary amines is the reduction of nitrile, nitro or oxime functional groups either with strong reducing agents, as for instance $LiAlH_4$, or by using metal catalysed reduction conditions.[27] Generally, these functional groups, with a particular attention to nitriles, can be considered as protected (latent) primary amines. Concerning the reaction mechanism involved in the nitrile reduction by hydride, the literature is rather vague, however the most popular mechanism academically accepted proceeds via initial formation of an iminium salt **74** (Scheme 2.18).[27] The formed **74** can in turn react with another molecule of starting material to give the dimeric species bis(iminoaluminate) **75**. Despite this intermediate has never been isolated, this step can be envisioned as the consequence of the formation of adduct **76** provided by a further reduction of **75** with an additional hydride as reported by Soffer and Katz.[28] The desired primary amine **77** is finally obtained upon addition of water or acid to the solution to hydrolyse adduct **76** cleaving the nitrogen-aluminium bonds.

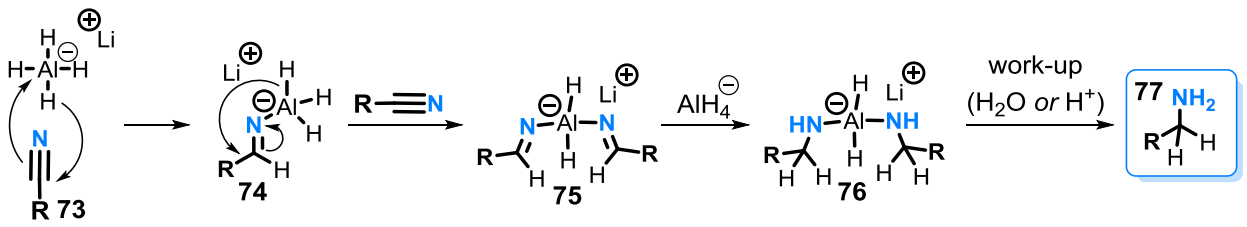

Scheme 2.18 Proposed mechanism for the reduction of nitrile function into primary amine.

Borane functional groups can be in turn obtained by reduction of boronic acids and esters in presence of $LiAlH_4$.[29–33] To this end, as both nitriles\oximes and boronic acids\esters could be reduced in the same manner we planned to synthesize amine-boranes exposing building blocks previously mentioned to an access of $LiAlH_4$. Following a procedure introduced by Snyder for the preparation of cyclic amine-boranes and their catechol derivatives,[34] we attempted at the synthesis of benzo[c][1,2]azaborole **80** reacting boronic ester **20** with 3 equivalents of 1 M solution of $LiAlH_4$ in THF.

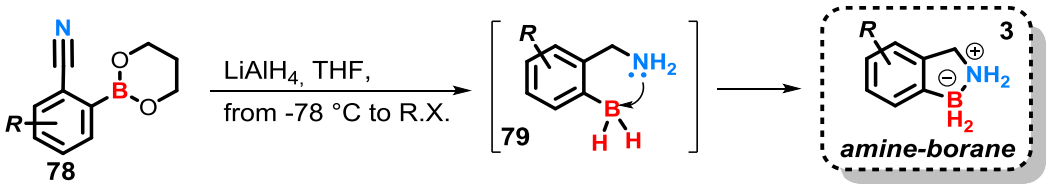

Scheme 2.19 Mechanism proposed for the synthesis of amine-boranes **3**.

The reaction was performed under inert atmosphere (Argon) and $LiAlH_4$ was slowly added dropwise to a solution of **20** in anhydrous THF at -78 °C. During the addition a gas evolution was observed and when it was entirely released the resulting mixture was allowed to warm to room temperature, this was accompanied by a change in colour, the protocol continued by heating the reaction mixture to reflux. According to the reported procedure[34] after 1h of refluxing the entire starting material should be converted into the desired amine-borane, however in our case a full conversion was achieved after 3 h of refluxing.

Table 2.3 Reduction of boronic esters **20-25**.

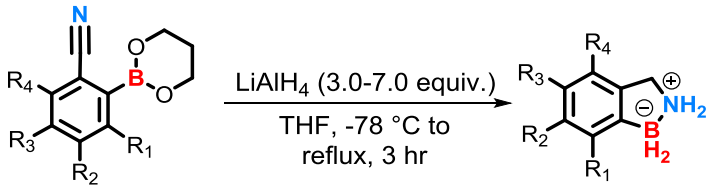

Entry	R_1	R_2	R_3	R_4	Product	%yield
20	H	H	H	H	**80**	53
21	H	Cl	H	H	**81**	56
22	H	Br	H	H	**82**	53
24	Phenanthrene				**83**	57
25	H	-CΞC-C_8H_{17}	H	H	**84**	34

(*) All reactions have been performed initially starting from a quantity of 100 mg of starting materials

The reaction was followed by TLC chromatography analysis, in which a sample of reaction beforehand quenched with a drop of water was extracted with ethyl acetate and then eluted with CH_2Cl_2. Generally, amine-borane species displayed a diagnostic spot at roughly R_f = 0.4 however a diagnostic test to confirm the presence of these species was the changing in colour to dark blue when reacted with a cerium-

ammonium-molybdate staining solution (mainly sensitive for amines and amides). The reaction was quenched by the careful addition of cold water to the mixture under vigorous stirring in order to decompose the excess of $LiAlH_4$. The white precipitate formed, composed by lithium\aluminium hydroxides, was filtered over a plug of anhydrous magnesium sulfate and the residue was washed with THF and ethyl acetate. Purification of the crude product by silica gel chromatography resulted in product decomposition. Amine-borane **80** readily reacted with the acidic OH groups of silica therefore the B-N dative bond was cleaved, and the borane functional group was converted into the more stable boronic acid $-B(OH)_2$ species. Another attempt at the purification of **80** was to dissolve the crude mixture in CH_2Cl_2 and wash the resulting solution with 1 M solution of HCl, however this procedure resulted in a large amount of product loss. During the course of our studies we noticed that amine-boranes in CH_2Cl_2 solution underwent to partial decomposition, suggesting that these molecules are not fully stable in this solvent. This might be due to the radical formation generated from the partial decomposition process of CH_2Cl_2 when prolonged exposed to the UV light.[35] A careful review of the literature to overcome these problems revealed that for similar molecules EtOAc was the best solvent to use in the work-up step. Following this procedure, we dissolved the crude mixture in EtOAc and the resulting solution was washed several times with deionized water. Analysis of ^{1}H-NMR in $CDCl_3$ revealed **80** to be an analytically pure sample to use for further characterization purposes proving this work up method to be highly efficient in purifying amine-borane species. Also, with this work-up method we did not detected any side products due to the decomposition process, moreover the amount of product lost during the work-up process was significantly lower than that previously described, thereby providing **80** in 53% yield. Pleased to have developed a suitable procedure to synthesise and purify **80**, we became interested in having access to the other amine-borane derivatives. Reduction of boronic esters **21** and **22** under the same reaction conditions delivered the corresponding amine-boranes **81** and **82** in 56% and 53% respectively. Application of this protocol for the reduction of **24** and **25** resulted in a complex mixture of by-products difficult to isolate. In an attempt to optimize the reaction conditions, we initially prolonged the reaction time to overnight, however no great changes were observed. Subsequently we increased also the equivalents of $LiAlH_4$ used to 6.5 for **24** and 7.0 for **25** obtaining the desired reduced species **83** and **84** in 57 and 34% yield. Surprisingly this protocol was unsuccessful when applied for building-blocks **48-50**. Compounds **48** and **49** were partially reduced with the primary amine formed and the boronic ester undisturbed leading to the typical complex[36] displayed in Figure 2.8, while in the case of **50** only starting material was recovered.

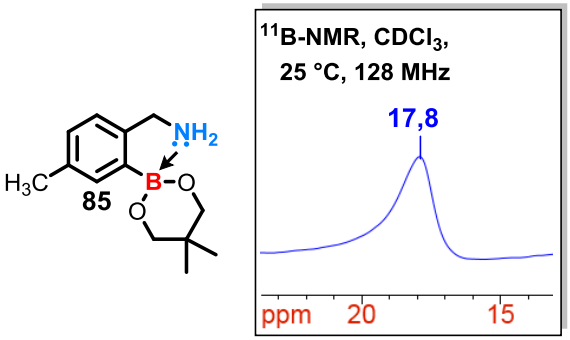

Figure 2.8 Example of a partially reduced 2-cyanoarylboronic ester.

In an attempt to elaborate a general protocol for the synthesis of amine-boranes independently of starting materials employed and functional groups present on the aromatic ring, we developed a more efficient reducing method based on the use of microwave assisted conditions. The advantage of using these heating conditions rather than the conventional thermal heating is that the energy is more efficiently transferred into the system allowing the temperature to rise homogeneously into the whole volume minimizing the reaction times.[37] Also, the ability to work at higher pressures than 1 atm allowed us to carry on reactions in solvents heated up at temperatures above their boiling points. The lab protocol developed requires the use of a flame-dried µW tube sealed with a plastic µW septum to ensure an inert atmosphere inside the vessel and to allow to add *via* cannula the anhydrous solutions in THF of boronic acid/esters and $LiAlH_4$. The latter is added dropwise at -78°C and then the resulting mixture is allowed to slowly warm to room temperature and then irradiated by microwave dielectric heating at 90 °C. this new method was initially tested on boronic ester **20**. By direct comparison of the conventional heating protocol with this method for the reduction of **20**, the latter revealed to be more efficient since the desired **80** was obtained in 67% yield after only 1.5 hour reaction rather than three. Application of this protocol to **21** and **22** successfully led us to obtain the desired pure amine-boranes **81** and **82** in 70% yield.

Table 2.4 Reduction of boronic esters **20-22** by microwave assisted conditions.

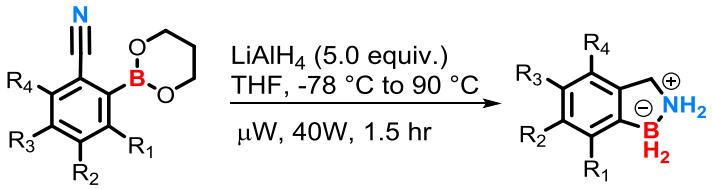

Entry	R_1	R_2	R_3	R_4	Product	%yield
20	H	H	H	H	**80**	67
21	H	Cl	H	H	**81**	70
22	H	Br	H	H	**82**	70

Pleased of these results obtained we subsequently decided to adopt this method to reduces also precursors **48-50**. Previous experiences in our group in the reduction of boronic esters following the initial

protocol, demonstrated that boronic acid protected with more robust protecting groups such as pinacol or neopentyl glycol, resulted in the only primary amine formation with the untouched boronic ester functionality leading to adducts similar to **85**. An interesting study was reported by Roy in 2007 to compare the stability of a range of boronic esters analysing the transesterification equilibrium of 2-(phenyl)-1,3,2-dioxaborolane **86** in presence of a free diol species to study (Scheme 2.20).[38] The progress of the reaction was monitored by ^{1}H-NMR spectroscopy in $CDCl_3$ determining the equilibrium composition between starting material **86** and the product **88** formed at the end of the transesterification reaction.

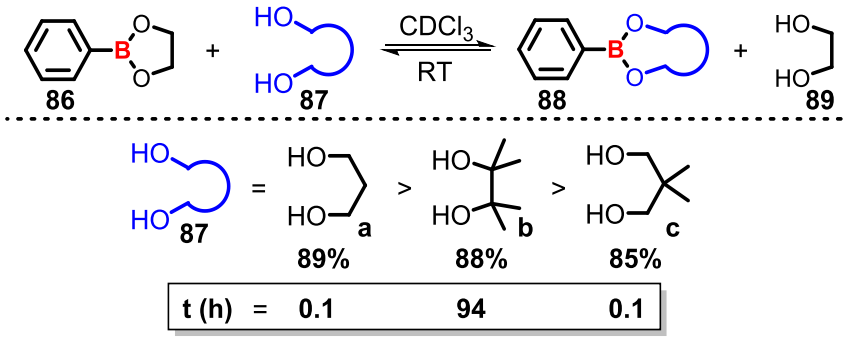

Scheme 2.20 General scheme for transesterification of 2-(phenyl)-1,3,2-dioxaborolane **86** with various diols **87a-c.**

The high yields of the transesterification products obtained suggested that boronic esters **88a-c** are thermodynamically more stable than the starting material **86**. However, another important aspect to consider is the steric hindrance of diols **87a-c** since it plays an important role in terms of reactivity. Indeed, pinacolboronic ester **88b** was formed after 94 h of reaction rather than 0.1 h as reported for **88a** and **88c**, in fact pinacol **87b**, being a sterically hindered diol, displaces ethylene glycol **89** very slowly, but produces a thermodynamically more stable boronic ester. Therefore, boronic esters protected with pinacol are less reactive and therefore more stable than those protected with **88a** and **88c** (Figure 2.9).

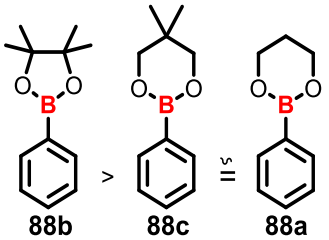

Figure 2.9 Classification of boronic esters from the most stable to the more labile.

However, with the new reducing method developed we could reduce the neopentyl glycol boronic ester derivatives to borane function without great efforts. In fact, boronic esters **48-50** synthesised *via* Miyaura cross-coupling reaction bearing the boron neopentyl glycolate group, when subjected to the reduction conditions developed, provided the corresponding amine-boranes in high yield (Table 2.5).

Table 2.5 Reduction of boronic esters **48-50** by microwave assisted conditions.

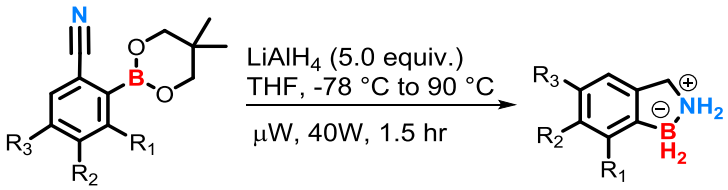

Entry	R_1	R_2	R_3	Product	%yield
48	CH_3	H	H	**90**	95
49	H	CH_3	H	**91**	75
50	$-OC_{12}H_{25}$	H	$-OC_{12}H_{25}$	**92**	30

Reduction of (2-((methoxyimino)methyl) **63** and (2-((methoxyimino) ethyl) **72** phenylboronic acids was performed following the same μW procedure developed. Pure **63** previously recrystallized from water was directly used in this step while on the contrary **72** was reacted with $LiAlH_4$ as a crude mixture because of difficulties encountered in the stage of purification as described before. Surprisingly in both cases the corresponding amine-boranes **80** and **93** were isolated in very good yield. Notably, **63** yielded amine-borane **80** in higher percentage (80%) in comparison with that obtained starting from **20** (53%), and amine-borane **93** was delivered in 70% yield over 2 steps. Interestingly, we noticed, by comparison of ^{1}H-NMR spectra, that the crude **80** obtained starting from **63** was much purer then that obtained from **20**. Clearly reduction of **63** leads to the formation of different reaction products than **20**, in fact in the first case only methanol and water are formed, and they can be easily removed by filtration over a plug of dry $MgSO_4$ followed by vacuum drying. In the second case instead, the free diol is formed therefore it can be removed only by washing the crude with deionized water and this implies a partial loss of the product due to decomposition.

Table 2.6 Reduction of boronic acids **63** and **72** by microwave assisted conditions.

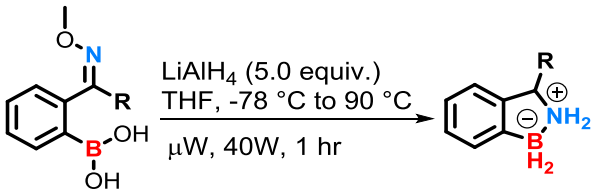

Entry	R	Product	%yield
63	H	**80**	80
72	CH_3	**93**	70

By analysis of the NMR data (^{1}H, ^{11}B and ^{12}C) it was possible to identify and characterize the amine-borane species. Generally, ^{1}H-NMR in $CDCl_3$ displayed an overall shifting of the aromatic protons to higher field in comparison with starting materials. More significant however, was the presence of diagnostic signals such as a triplet and a broad peak between 4.20 and 3.80 ppm related to the new internal -**CH_2**- and the

NH_2→BH_2- primary amine, meant the reduction went to the completion. In the case of boronic acids **63** and **72** also the absence of the peak at ≈ 10.00 ppm related to the $B(OH)_2$ group was diagnostic in confirming the success of the reaction. Also, ^{11}B-NMR analysis in $CDCl_3$ was diagnostic in confirming the molecular structure of amine-boranes displaying a triplet resonating at ≈-11.0ppm typical of boron-hydrogen coupling (*J*=96 Hz)[39] in which boron atom own a quaternary coordination negatively charged. The ^{13}C-NMR spectra in $CDCl_3$ were also collected for full characterization purpose displaying a new signal at ≈50.0ppm related to the -**CH_2**- group formed. Although IR spectra were not collected for all amine-borane synthesised, analysis carried out for compound **80-82** shown an intense and broad transmittance peak centred at ≈2300 cm^{-1} characteristic of the B-H stretching vibrations mode in line with that reported in literature.[40] Finally, mass spectroscopy analysis displayed a good match between the predicted isotope pattern distribution and the observed data for all amine-borane species.

2.3.5 X-ray structure of amine-borane 80

Structural proof of amine-borane **80** came from an X-ray diffraction analysis of single crystals grown by slow evaporation from an EtOAc solution. This compound crystallised in the centrosymmetric monoclinic space group $P2_{1/n}$ with four molecule units per unit cell packed in staggered array motif. The measured bond distances between carbon atoms of the aromatic ring are in line with that reported in literature[17]. The five-member heterocycle containing boron and nitrogen atoms adopt a half boat conformation ("envelop") with nitrogen atom pointing outwards of the plane containing the aromatic backbone of 26.3°. The distance measured between boron and nitrogen atom is 1.637(16) Å confirming the dative bonding interaction as reported in literature.[41] Regarding the distance between boron and carbon atoms B-C(7) was observed to be 1.600(17) Å, slightly longer than a C-B bond in boronic acid/ester species (≈1.580 Å). The respective bond angles calculated for C(7)-B-N, B-N-C(1) and N-C(1)-C(2) are, 97.9(9)°, 108.2(9)° and 104.5(9)°.

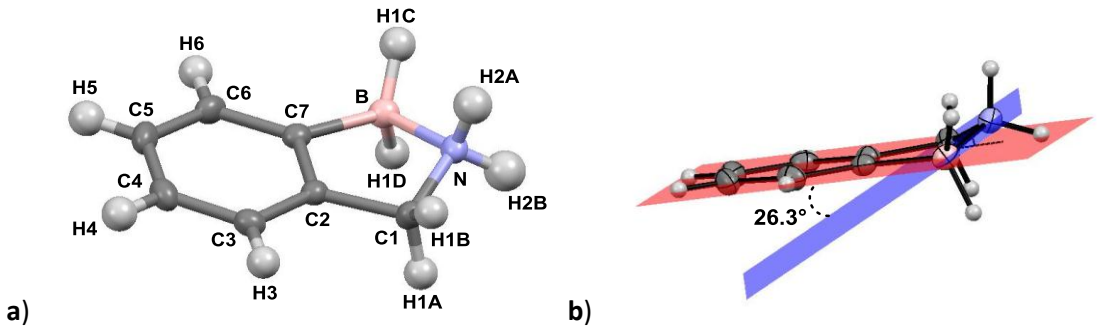

Figure 2.10 Crystal structure of **80**; a) top view, b) side-on view.

The crystalline lattice is mostly characterized by weak NH···π bonding interactions between the primary amine group with the aromatic ring of the closet amine-borane on the top N···Ph(C2-C7) with distance of 3.239 Å and the primary amine with the closest neighbouring benzene core N···Ph(C3, C4, C5) with distance of 3.339 Å (Figure 2.11).

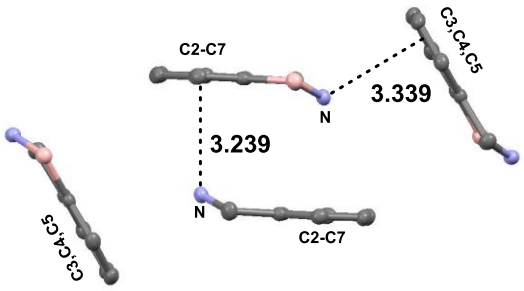

Figure 2.11 Unit cell characterizing the crystalline lattice of **80**.

A further significant contribution to the staggered array molecular packing is attributed to the intermolecular interaction B···C(4) between a unit of amine-borane and two symmetrically non-equivalent neighbouring molecules with a distance of 3.814 Å. The angle between two molecular units placed in the staggered array motif has been measured to be 57.3° (Figure 2.12).

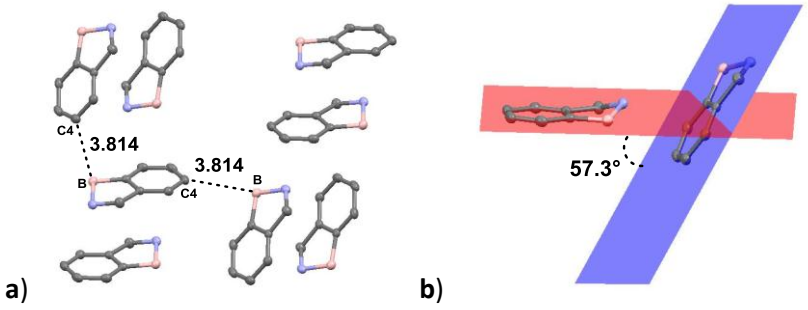

Figure 2.12 a) Intermolecular interactions, b) angle between two molecular units placed in the staggered array motif.

Finally Figure 2.13 shows the molecular packing characterizing the crystalline lattice of molecule **80** from two different perspectives.

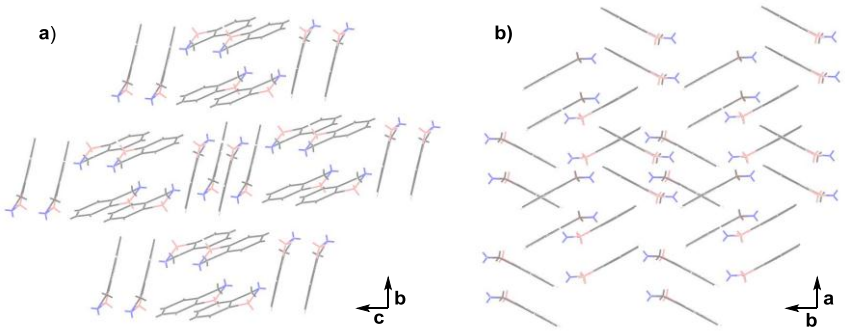

Figure 2.13 Crystal packing of **80** ; a) top view, b) horizontally translated view.

2.3.6 Outlook on amine-borane 93

Reduction of the prochiral sp^2-hybridized centre of **72** into the chiral sp^3 amine-borane **93** led to a new stereogenic centre in the benzylic position providing to a racemic mixture of the corresponding R and S enantiomers (Figure 2.14).

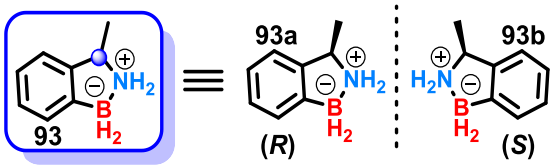

Figure 2.14 R and S enantiomers of chiral compound **93**.

Based on the experience in our group of using many different HPLC techniques we initially became interested in isolating enantiomers **93a** and **93b** by taking advance of the chiral chromatography methodology. We envisioned that by isolating the two enantiomers at this stage and employing them separately in the next step of the thermolysis process, theoretically, might provide to only an enantiomerically pure borazine (Scheme 2.21).

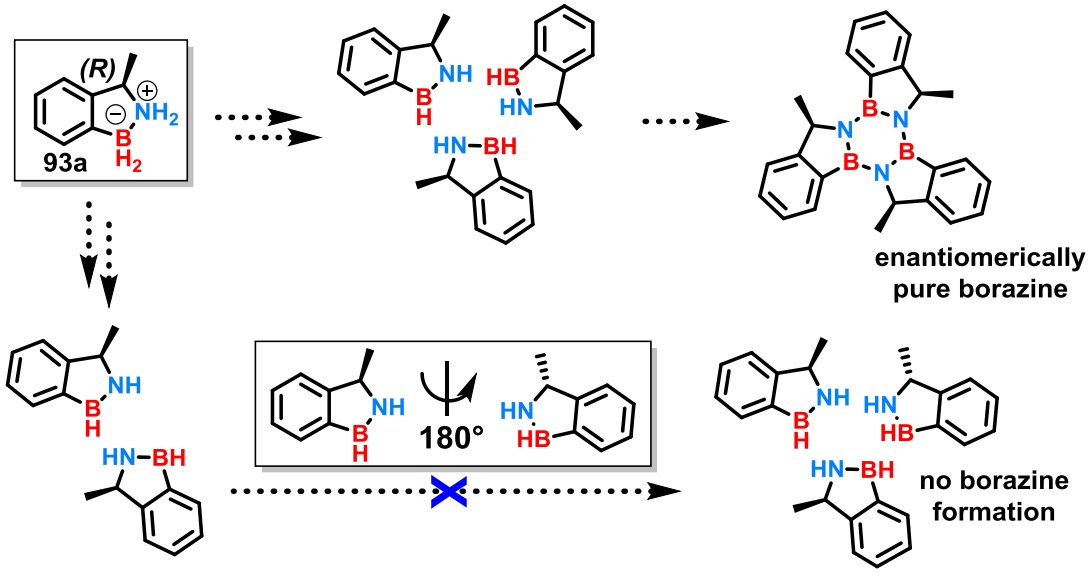

Scheme 2.21 Plausible method to synthesise an enantiomerically pure borazine.

However, after a careful evaluation of all factors involved in developing a valid method to isolate **93a** and **93b** as analytically pure samples we decided to attempt the chiral resolution in a later stage with the corresponding borazine.

2.4 Synthesis of borazatruxenes: trimerization of BN [2,3] dihydroindenes by a thermolysis process

Having secured access to amine-boranes **80-84** and **90-93** we explored the possibility of synthesising the corresponding borazine derivatives using a procedure developed in our group. The borazine ring is achieved by a thermolysis process involving the trimerization of amine-borane building-blocks proceeding with concomitant release of six molecules of hydrogen. Many examples based on the thermolysis process for the synthesis of the borazine ring have been reported in literature[42–46] in the past, mostly involving ammonia-borane for hydrogen storage purposes. However most of them use drastic reaction conditions and long reaction times making these procedures suitable only for certain types of substrates. One of the main disadvantages is that some amine-boranes are not fully stable and might decompose at high temperatures following a decomposition pathway that potentially generate side products that are toxic.[46] More recently, milder reaction conditions for the borazine synthesis have been developed by Liu and co-workers[42] employing the air and moisture stable 1,2-BN-5-methylcyclopentane **94** in a thermolysis process catalysed by Lewis acidic species (e.g. $FeCl_2$) at 80°C.

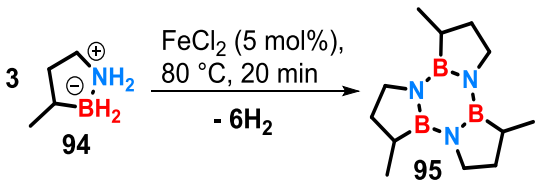

Scheme 2.22 A single-component liquid-phase hydrogen storage material.

We attempted the synthesis of the borazine ring following this protocol however, we found that it was not as efficient as described in literature[42] with our substrates. In this regard we developed another method based on the use of the microwave assisted conditions to promote the thermolysis process. Application of this protocol necessitated the choice of an appropriate solvent capable to dissolve amine-boranes building blocks and to ensure a good stability of both starting materials and products. Also, ideally, it had to be stable to the microwave irradiation. After a careful screening of different solvents made by Dr. Emmett,[2] toluene was found to be the most suitable solvent to use in our case. It is a quasi-inert aromatic compound that cannot take part at the thermolysis process leading to side products formation, and it can solubilize our substrates by π-π stacking interactions. Also halogenated aromatic solvents as chlorobenzene, 1,2 and 1,4-dichlorobenzene and hexafluoro benzene were screened to evaluate which could be better compatible with our system. However, we found that the thermolysis reaction, surprisingly, worked in the same manner independently from the solvent used since borazatruxene was obtained in the same yield in all cases considered. This outcome suggested that it might be a non-dependent solvent process, therefore

we kept using toluene in our protocol. Finally, during the developing of this procedure we noticed that this process is concentration dependent, indeed the best result obtained was when a solution 0.11 M of amine borane **80** in toluene was wormed up for 2 hours at 180°C under inert atmosphere at a power of 300 W.

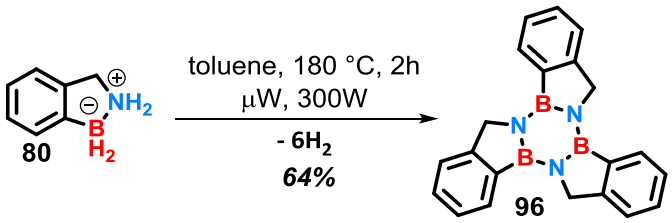

Scheme 2.23 Synthesis of borazatruxene **96**: trimerization of amine-borane **80** by a thermolysis process.

The reaction was performed in a flame-dried μW tube sealed with a plastic μW septum to ensure an inert atmosphere inside the vessel and equipped with a magnetic stir bar. A solution of **80** in anhydrous toluene (100mg in 3mL) was syringed into the μW tube and the mix was sonicated for 10 min before being placed into the microwave machine and reacted. After 2 hours of stirring at 180°C the reaction was cooled down to room temperature to yield a white precipitate which was isolated by gravity filtration and purified by washing with toluene and then with a solution of *n*-hexane/CH_2Cl_2 (80:20). Borazatruxene **96** was obtained in 64% yield after purification and the molecular structure was confirmed by ^{1}H-NMR analysis in $CDCl_3$, which displayed the disappearance of the peaks related to the -NH_2^+- group and a shift at lower field of the signal related to the internal bridging -CH_2- groups. Also, ^{11}B-NMR analysis in $CDCl_3$ was diagnostic in confirming structure **96** displaying a signal reasoning at 33.0 ppm characteristic of species containing a trivalent boron atom covalently bonded to a nitrogen atom.[45,47–50] Finally, mass spectroscopy analysis shown the molecular peak $[M+H]^+$ = 346.1843 consistent with that calculated (346.1853). Pleased to have developed a solid procedure for the synthesis of borazatruxene **96**, we next applied the same protocol for the synthesis of borazatruxenes **81-84** and **90-92**.

Table 2.7 Synthesis of substituted borazatruxenes **97-103**.

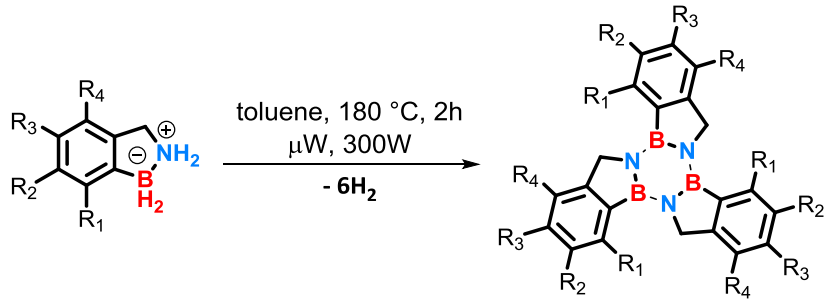

Entry	R_1	R_2	R_3	R_4	Product	%yield
81	H	Cl	H	H	**97**	45
82	H	Br	H	H	**98**	45
83	Phenanthrene				**99**	-
84	H	-CΞC-C_8H_{17}	H	H	**100**	-
90	CH_3	H	H	H	**101**	72
91	H	CH_3	H	H	**102**	70
92	-$OC_{12}H_{25}$	H	-$OC_{12}H_{25}$	H	**103**	13

(*) All reactions have been performed initially starting from a quantity of 100 mg of starting materials

Exposing building-blocks **81-83** and **90-91** to the same reaction conditions provided the corresponding borazines **97-99** and **101-102** as white solids after work up. For the synthesis of borazine **100** starting from **84**, we had to review the synthetic procedure since after 2 hours of heating only starting material was recovered, therefore in an attempt to promote the trimerization we prolonged the reaction time. However, after 17 hours no great changes were observed, in fact by TLC analysis eluted with a mix of *n*-hexane/CH_2Cl_2 (50:50) we mainly observed a spot attributable to starting material **84**. NMR (^{1}H, ^{11}B and ^{13}C) characterization of **97-99** and **101-102** resulted to be challenging because of their poor solubility in the most common organic solvents compared to borazatruxene. This might be attributed to their increased molecular weight and, especially in the anthracene derivative, to the formation of larger aggregates by π-π stacking interactions established between the extended aromatic areas. However, we overcame this problem by using high boiling point deuterated solvents, as for instance TCE-d_2 or DMSO-d_6. The ^{1}H-NMR spectra of **101** and **102** could be recorded using TCE-d_2 and worming up the suspension at 80 C° until complete solubilization, instead **97-99** necessitated the use of DMSO-d_6 at 100 C°. In all cases ^{1}H-NMR analysis displayed a shift to lower field of aromatic proton signals compared with starting materials in line with that previously observed with borazatruxene. Also, the ^{11}B-NMR spectra displayed peaks reasoning between 33.0-37.0 ppm and mass spectroscopy analysis displayed a good match between the predicted isotope pattern distribution and the observed data, confirming molecular structure of **97** and **98**. Unfortunately, this combination of solvents and temperatures was not sufficient to solubilize and analyze borazine **99**. However, a previous IR analysis displayed a sharp peak at 1450 cm^{-1} related to the B-N stretching vibrations mode and the absence of peaks at 2900 and 2300 cm^{-1} of N-H and B-H groups suggested that amine-borane reacted. To investigate in depth on the nature of **99** we sent samples of the

starting material **83** and the product **99** to the UK National Mass Spectrometry Facility & Service at Swansea University. Results obtained confirmed structure **83** displaying a good match between the predicted isotope pattern distribution and the observed data (Figure 2.15).

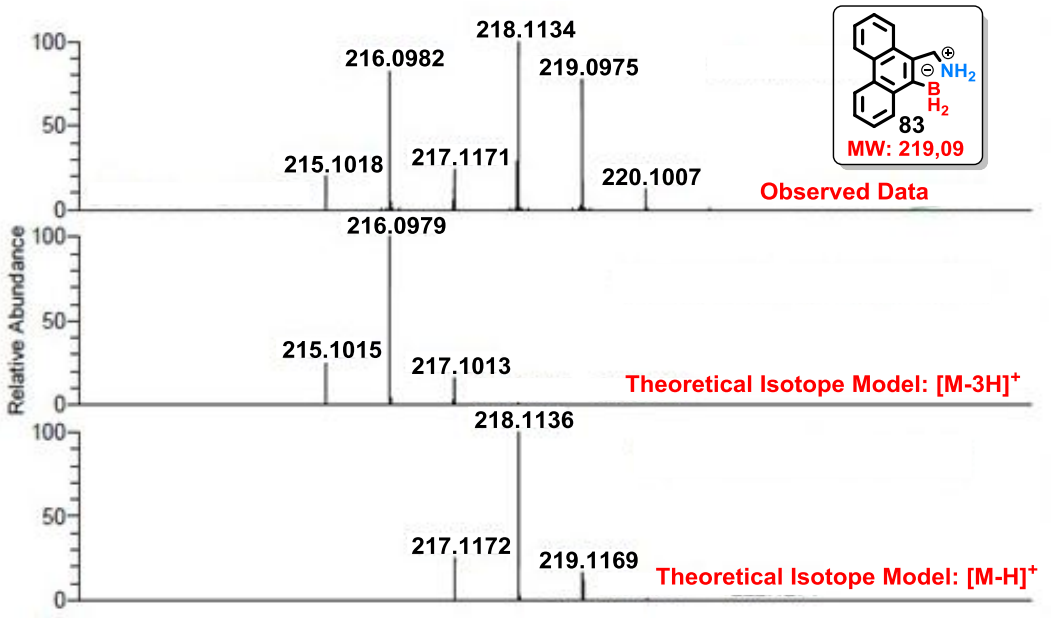

Figure 2.15 Mass Spectrum of compound **83** from Swansea University.

First attempt at the identification of the molecular ion of **99** failed therefore, in a later stage different technique as nanoelectrospray and MALDI have been unsuccessfully utilized, however further experiments are still on going to identify borazine **99**. A great improvement in solubility was achieved with borazine **103** bearing the peripheral long alkyl chains. After cooling the reaction to room temperature, we observed the mixture to be a transparent solution without any precipitate as in the previous cases described. To this end we revisited the work up and thus the purification procedure. Ensuring before of the stability of **103** in presence of silica using the 2D TLC technique, we later proceeded with the column chromatography purification to isolate **103** as a pure sample. The best conditions obtained for the purification was to elute the crude product with a mixture of *n*-hexane/CH_2Cl_2 (70:30) providing **103** in 13% yield. After separation a series of 2D NMR (HMBC, COSY and NOESY) were collected to prove the molecular structure. Analysis of ^{1}H-NMR in $CDCl_3$ revealed a general shifting of signals to lower field compared with starting material **92**, specifically, aromatic protons of **103** were more deshielded (6.54-6.36 ppm) respect to **92** (6.31 ppm). Also, the broad peak related to the primary amine disappeared whilst the triplet signal related to the -CH_2- bridge shifted to 5.02 ppm as a singlet. Figure 2.16 shows NOESY and COSY spectra overlapped, highlighting correlations between aromatic protons with the -CH_2- bridge and -OCH_2- groups of **103**.

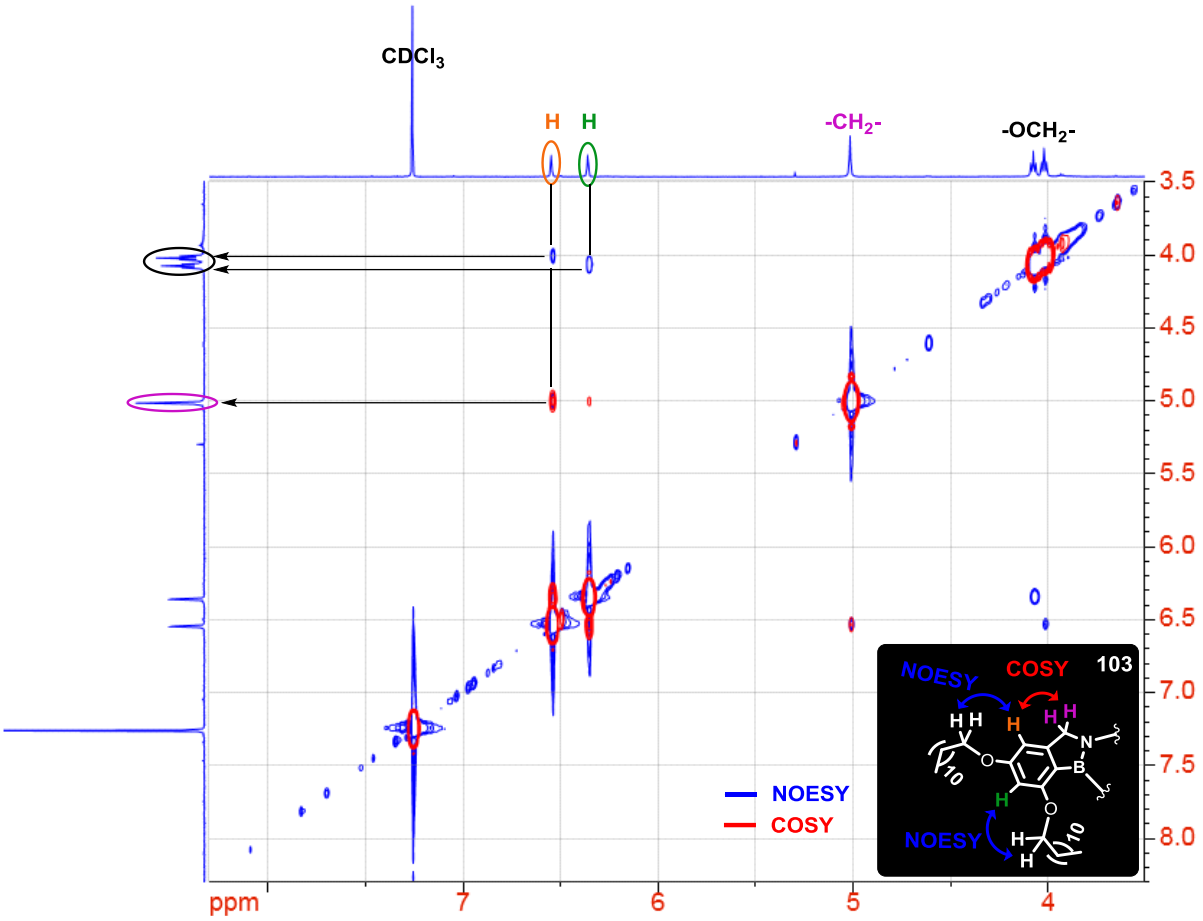

Figure 2.16 Representation of NOESY (blue) and COSY (red) NMR spectra of **103** overlapped.

Unfortunately, from ^{11}B-NMR we could not obtain any useful information because no signal was detected. This is typical of nuclei with spin I ≥ 1 that possess electric quadrupole moments.[39] The nonspherical electric charge distribution can interact with any electric field gradient present at the neighbouring nuclei leading to a very efficient relaxation mechanism which produces a collapse or reduce the output signal recorded. For these nuclei the quadrupolar relaxation mechanism is thought to be dominant compared with other relaxation mechanisms specific for nuclei with spin I = ½ as dipole-dipole relaxation, scalar coupling relaxation, or chemical shift anisotropy relaxation.[39] However, mass spectroscopy analysis displayed a good match between the predicted isotope pattern distribution and the observed data, confirming molecular structure of **103** (Figure 2.17).

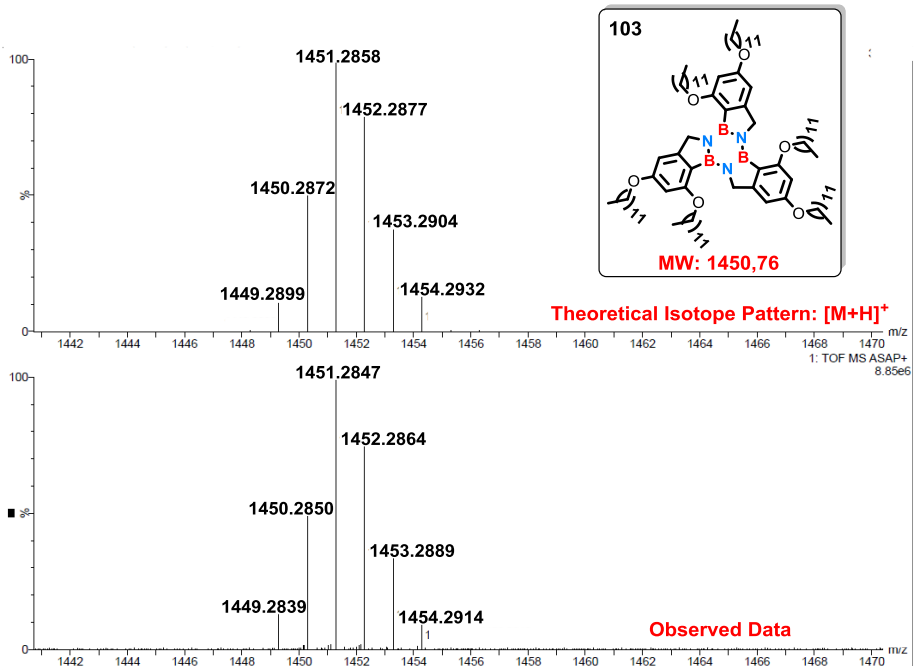

Figure 2.17 Mass Spectrum of compound **103** from Swansea University.

Alkyl and halogen substituted amine-boranes revealed to be were well tolerated under the thermolysis conditions developed and generally reactions proceeded well. However, we noticed that yields were strictly dependent on i) the nature and ii) the position of functional groups attached to the amine-borane backbone. Specifically, we observed that amine-boranes bearing weak electro donating groups with and inductive effect -I on the benzene ring (Cl, Br) lowered the yield of the corresponding borazine formed (45%) compared with the unsubstituted borazatruxene (64%). On the contrary electron donating methyl groups in 3 or 4 positions on the aromatic ring, as in the case of **90** and **91**, delivered the corresponding borazines **101** and **102** in very good yield (≈70%), higher than borazatruxene. Elongation of alkyl groups attached on the peripheral aromatic rings, as in the case of **84** and **92**, dropped the yield of the borazine obtained to 13% for **103** or it did not even form in the case of **100**. This might be due to the formation of supramolecular aggregates as micelles or vesicles which makes molecules less available to take part to the reaction. Another possible explanation could be that borazine ring is not the most thermodynamic stable species formed under these conditions therefore soluble borazines might further react to make other thermodynamically stable species as linear oligomers or polymers. Guided by this hypothesis, we decided to perform a reverse experiment exposing borazine **103** to the same reaction conditions used for the thermolysis process in presence of amine borane **80**. If our hypothesis would have been valid borazine **103** should undergo to the borazine ring opening followed by reaction with amine-borane **80**.

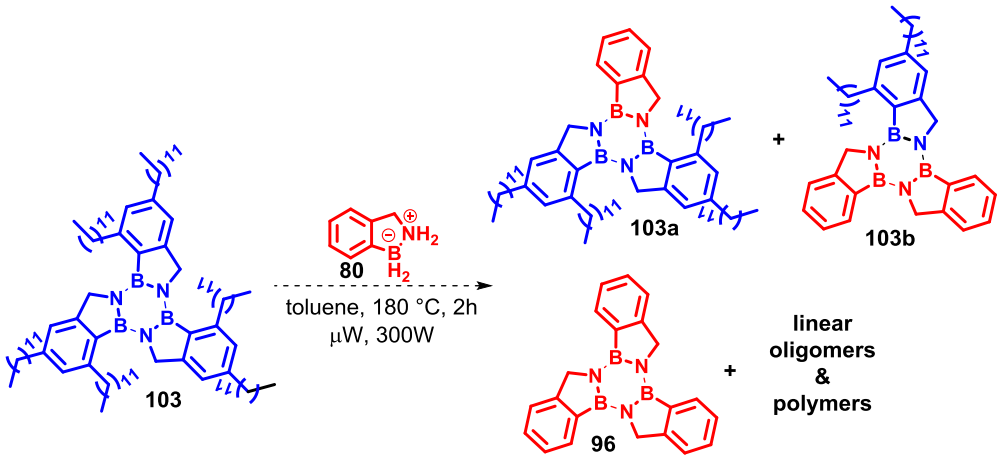

Scheme 2.24 Hypothetic products arising from the reaction between borazine **103** and amine-borane **80**.

This pathway should lead to a mixture of hybrid borazines **103a**, **103b** and linear oligomers and polymers. Preliminary results obtained by analysis of the NMR data revealed the major product to be the unreacted borazine **103** while a minor product was easily identified in borazatruxene **96**. However more analysis (i.e. mass spectroscopy analysis) need to be done in order to identify all by-products formed to validate our hypothesis.

2.4.1 Synthesis of chiral borazatruxene by trimerization of racemic amine-borane 93 mixture

Trimerization of the racemic mixture of amine-borane **93**, successfully delivered the corresponding borazine **104** in 93% yield. This remarkable result also proved that the functionalization in a different region of the molecule is decisive for the outcome of a reaction.

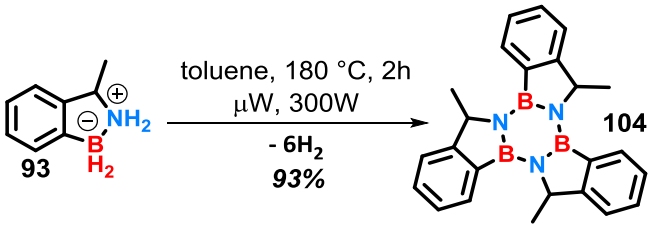

Scheme 2.25 Synthesis of chiral borazatruxene **104**.

The ^{1}H-NMR spectrum in $CDCl_3$ of the crude product displayed impurities arising from side reactions that clearly in this case were more limited. Moreover, we noticed that impurities were soluble in a mix of *n*-hexane/CH_2Cl_2 (95:5), therefore by washing the solid with this mixture they could be easily dissolved and removed after centrifugation as supernatant. As anticipated chiral amine-borane **93** was employed in the thermolysis process as a racemic mixture of the two enantiomers **93a** and **93b** therefore we expected to

obtain a mixture of diastereoisomers after the thermolysis process. Following the rules $\mathbf{2^n}$ (n = number of stereocenters in the molecule) to count the maximum number of possible stereoisomers formed, theoretically this reaction should provide to a mixture of eight stereoisomers due to the three stereocenters. However, due to the C_3 symmetry of borazatruxene four stereoisomers are identical, therefore the actual number of stereoisomers obtained is reduced to four: two *syn* **104a-b** and two *anti* enantiomers **104c-d** (Figure 2.18).

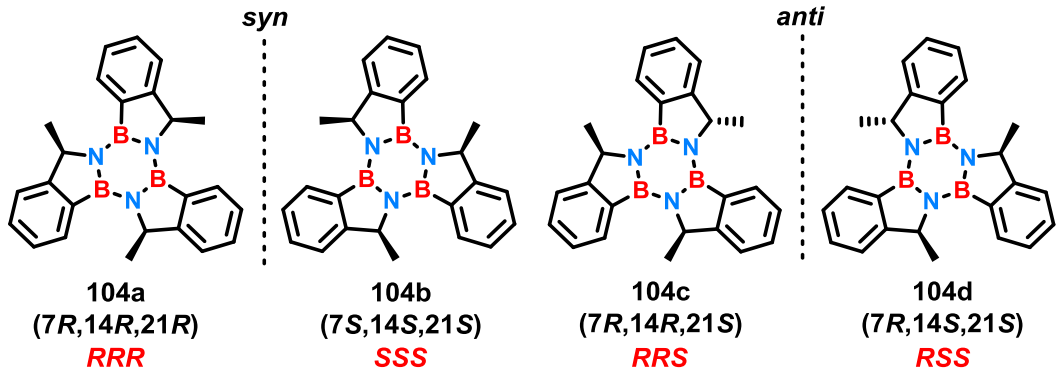

Figure 2.18 Representation of the four possible stereoisomers of borazatruxene **104** formed.

The two species were clearly recognizable in the ^{1}H-NMR spectrum of the crude mixture which displayed two different sets of signals. The diagnostic peaks assigned to the methyl groups in the range of 1.80-1.60 ppm were remarkably helpful in discriminating the *syn* from the *anti* diastereoisomers. Indeed, the *syn* species, still a C_3 symmetric molecule, displayed only a doublet integrating nine protons. On the contrary the *anti* species, because of the loss of the symmetry displayed three different doublets each corresponding to a methyl group thus integrating three protons. Remarkably we found that by washing the mixture of the two diastereoisomers with of *n*-hexane/CH_2Cl_2 (80:20) it was possible to isolate the *syn* from the *anti* species exploiting their different solubility in this mixture of solvents. Indeed, this procedure revealed to be extremely effective in solubilizing selectively the *syn* enantiomers, without dissolving the rest of the solid mainly composed by the *anti* derivatives. The two diastereoisomers isolated were fully characterized by NMR analysis (^{1}H, ^{11}B, ^{13}C, COSY and HMBC) and mass spec. analysis. Figure 2.19 shows a comparison between ^{1}H-NMR spectra in $CDCl_3$ of the mixture of the two diastereoisomers isolated.

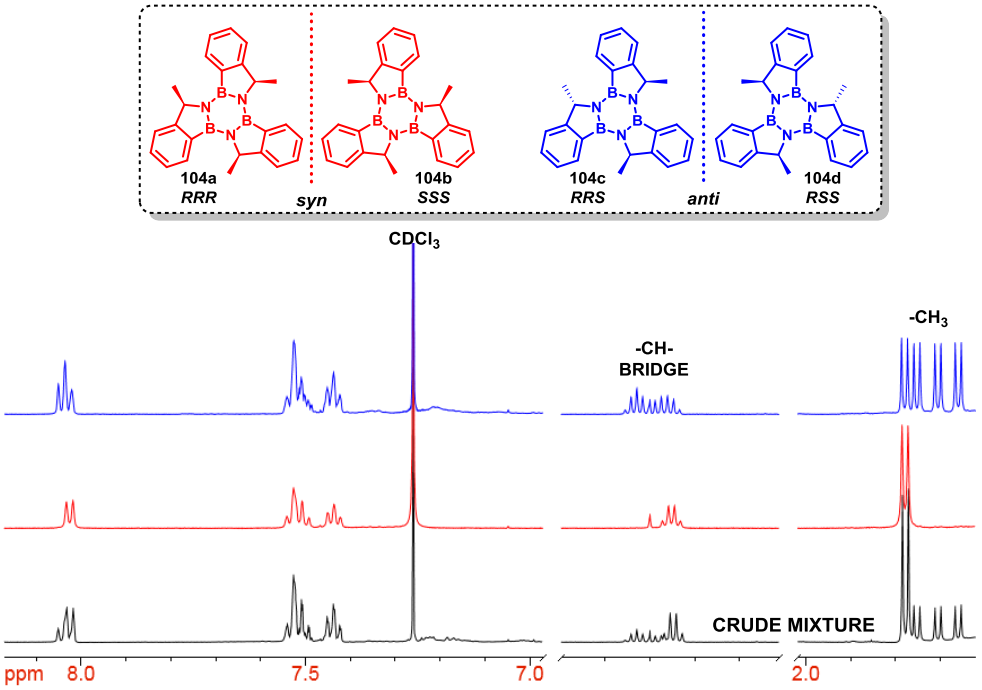

Figure 2.19 Comparison between ^{1}H-NMR spectra in $CDCl_3$ of the mixture of the two diastereoisomers isolated. To note, that the *anti* fraction isolated still contains impurities of the *syn* species but in a different ratio with respect to the crude mixture.

From the NMR spectra is possible to see how the *syn* enantiomers were isolated as a pure sample while the *anti* fraction still contained impurities of the *syn* enantiomers. However, signals related to the *anti* enantiomers are perfectly recognizable comparing both ^{1}H-NMR spectra. The ^{11}B-NMR displayed a signal reasoning at 34.4 ppm, while mass spec analysis shown the molecular peak $[M+H]^+$ = 388.2322 in line with that theoretically calculated (388.2322) confirming general structure of **104** (Figure 2.20).

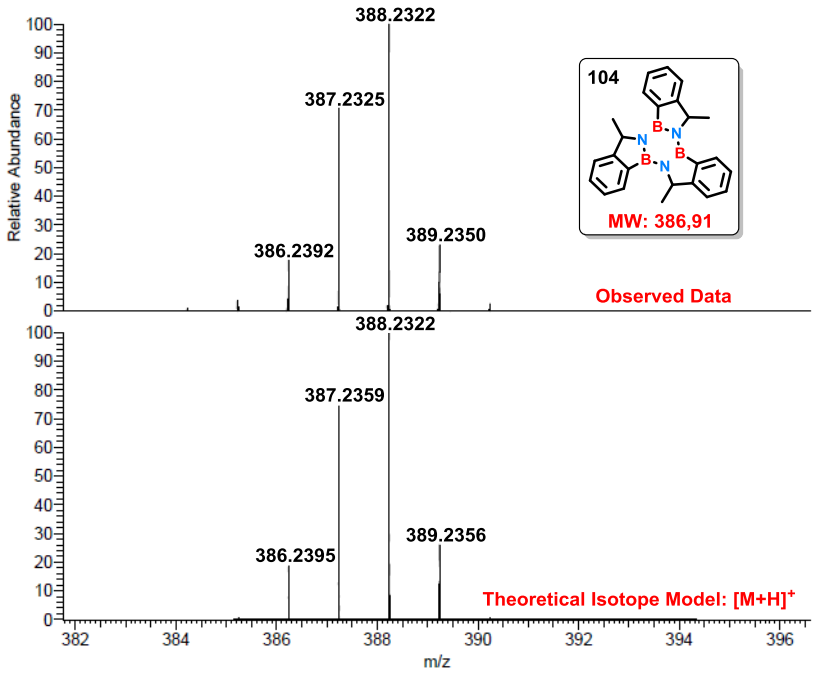

Figure 2.20 Mass Spectrum of compound **104** from Swansea University.

2.4.2 Chiral chromatography separation of the four isomers of borazatruxene 104

With the two fractions of *syn* and *anti* diastereoisomers isolated in hand we decided to attempt the chiral chromatographic separation in order to isolate all four optical isomers in the pure form. A sample of each pair of enantiomers was prepared with a concentration of 0.5mg/mL in a mixture of *n*-hexane/isopropyl alcohol (90:10). Initially we evaluated five readily available chiral HPLC columns with different polysaccharide-based chiral stationary phases (CSPs) under the same operating conditions. The *syn* solution was chosen for a full screening of the main parameters to have the best chiral resolution because purer and thus easier to separate than the *anti*. The best result obtained was using a Chiralcel OD chiral column (Figure 2.21).

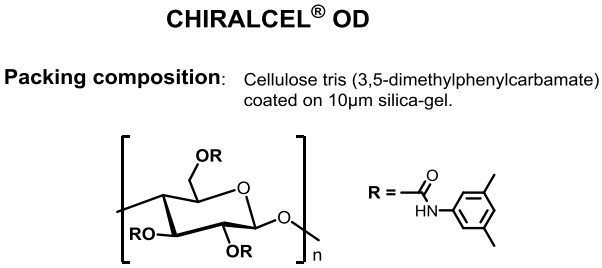

Figure 2.21 Packing composition of Chiralcel OD chiral column.

The optimal conditions found were to elute 30µL of the *syn* solution with a mobile phase composed by a mixture of *n*-hexane/isopropyl alcohol (98:2) at the flow rate of 0.5 mL/min. A UV detector was set up at 239 nm the optimum absorbance wavelength for the aromatic rings and at 279 nm, the optimum absorbance wavelength for the borazine ring. Figure 2.22 shows the chromatogram related to the mixture obtained with the conditions previously described.

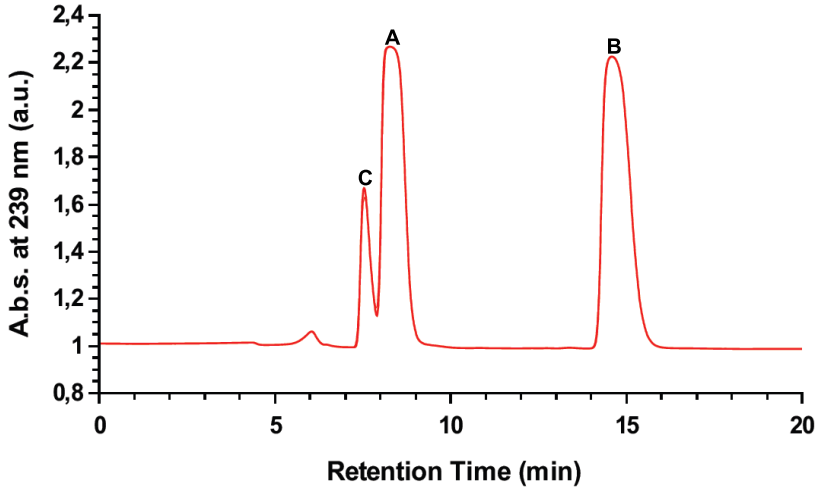

Figure 2.22 Chromatogram obtained eluting the fraction containing the *syn* species with *n*-hexane/isopropyl alcohol (98:2) at the flow rate of 0.5 mL/min. Peaks A and B with retention time of 8.3 and 14.6 min respectively, are related to the two enantiomeric species separated, while peak C at 7.5 min is related to impurities.

This chromatogram clearly suggested that there is a strong chiral recognition between the stationary phases and one of the two enantiomers. Indeed, the retention time of the first enantiomer was 8.3 min and the second was almost the double (14.6 min). Pleased of the high and efficient resolution obtained with this method developed, we later decided to proceed with a preparative procedure to isolate the two enantiomeric species. The volume injected was increased to 80µL maintaining the flow rate at 0.5mL/min and fractions were collected ten times. To prove the purity of each enantiomer, the fractions collected containing the same enantiomer were combined, reduced in volume and then reinjected separately. The chromatograms obtained for each enantiomer, after collection, are displayed in Figure 2.23 showing a high purity samples in both cases.

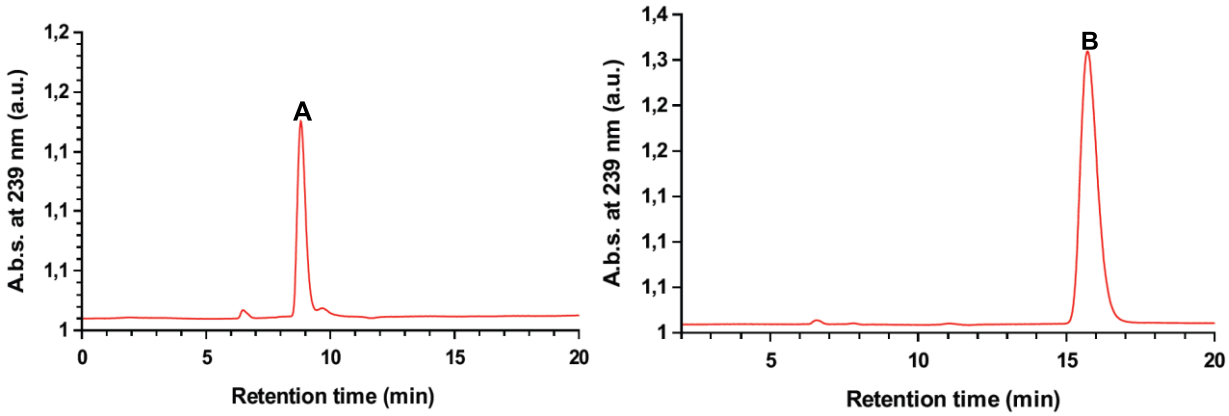

Figure 2.23 Chromatograms of the two pure *syn* enantiomers isolated with a preparative procedure.

From the chromatograms obtained is clear to see how the isolation of the two enantiomers using this method has been successful. Also, the amount of the enantiomeric species isolated was sufficient to proceed for further experiments such as the circular dichroism analysis (CD) to investigate in depth on the conformational and electronic structure of **104**. This is the first example of a chiral separation developed for a borazine species reported so far. Surprisingly, in the literature of functionalized truxenes on the -CH_2- bridge are described only few procedures concerning only the separation of the diastereoisomers[51,52] but no report detailing the chiral enantiomeric separation of the corresponding enantiomeric species. In this regard, we were very pleased to have developed the first efficient method for a chiral resolution of enantiomeric borazines. Application of this protocol to the less pure fraction containing the *anti* species necessitated a redevelopment of the procedure because the enantiomeric resolution was worse than the previous case. This preliminary result suggested that the stationary phase displayed almost the same affinity for both enantiomers. Initially we decrease the polarity of the eluent increasing the ratio of hexane to 99 to 1, however we needed to decrease also the flowing rate to 0.4 mL/min and the temperature to 12 °C to observe an improvement in resolution. Despite this revised method resulted to be valid for the separation of the pair *anti* enantiomers, we noticed, in the stage of collecting pure fractions of **104c** and

104d, that sort of impurities in the sample remained stuck on the stationary phase under these conditions. Because of the high retention time of these by-product, after every injection, their concentration increased poisoning the column and compromising the isolation of the pure enantiomers. Unable to avoid this we considered, as an alternative approach, to change the operating conditions from isocratic to gradient increasing the polarity (*n*-hexane/isopropyl alcohol (80:20)) and the flow rate (1.2 mL/min) of the eluent at the end of the separation to wash the column from the impurities. Figure 2.24 shows the chromatogram related to the chiral separation of the mixture containing the two *anti* enantiomers obtained with the gradient method previously described.

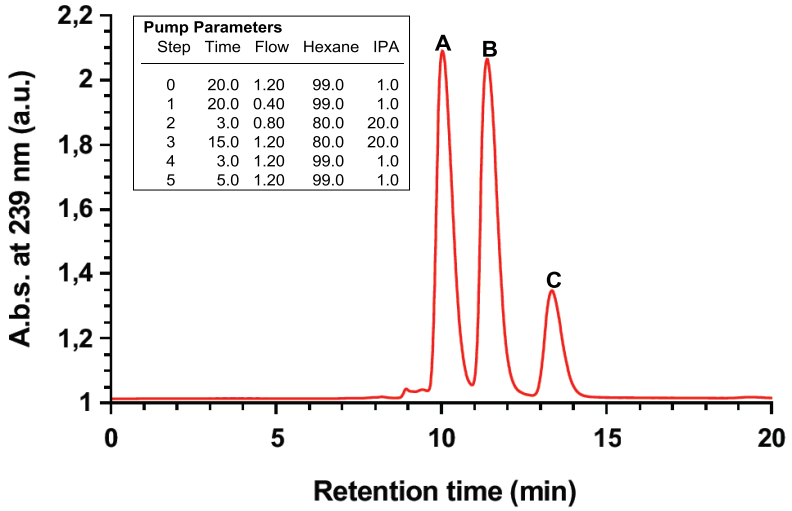

Figure 2.24 Chromatogram obtained eluting the fraction containing the *anti* species with the gradient method. Peaks A and B with retention time of 10.0 and 11.4 min respectively, are related to the two enantiomeric species separated, while peak C at 13.4 min is related to impurities.

With the cleaning procedure post elution necessary included, this method resulted to be longer than the first developed for the *syn* species, however it was very effective to collect pure fractions of the *anti* enantiomers.

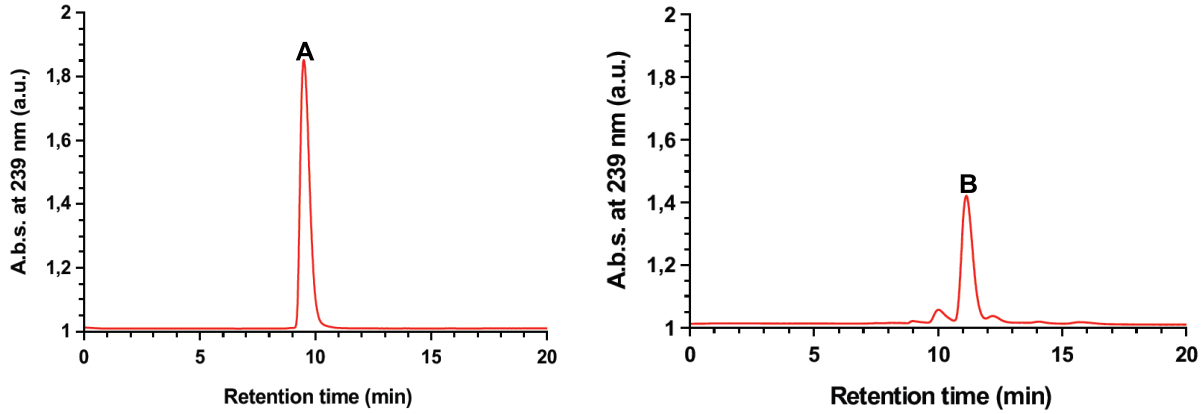

Figure 2.25 Chromatograms of the two pure *anti* enantiomers isolated with a preparative procedure.

Similarly, in this case we successfully achieved the purity desired for each enantiomer collected as proved by the chromatograms collected after reinjection of the pure fractions shown in Figure 2.25.

2.4.3 Optical studies of the four isomers of borazatruxene 104: UV-Vis and Circular Dichroism experiments

The great success achieved in the chiral separation of the four enantiomers allowed us to analyse the optical properties of **104a-d** by circular dichroism analysis. Samples were dissolved in 2.2 mL of *n*-hexane/isopropyl alcohol (90:10) and the CD spectra was recorded in parallel with the UV absorption from 200 nm to 400 nm. The window of wavelengths analysed was decided based on previous UV-Vis experiments on borazatruxene **96**, which displayed in chloroform a strong absorption at 239 nm associated to the peripheral aromatic rings followed by three distinct peaks of lower intensity at 265, 272 and 279 nm related to the central borazine ring (Figure 2.26).

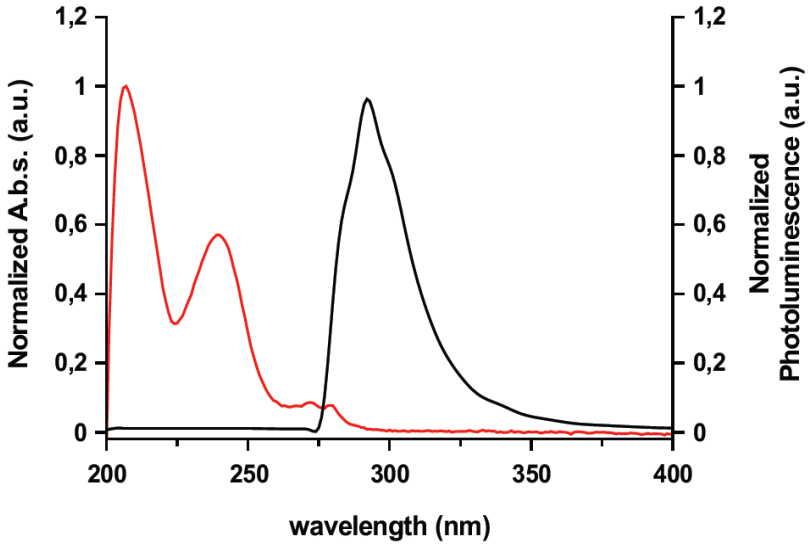

Figure 2.26 UV-Visible absorption (red) and emission (black) spectra of compound **104** in *n*-hexane/isopropyl alcohol (90:10).

The UV absorption (red) spectrum of **104** shows two very intense and broad absorbance at 207 and 239 nm attributed to the aromatic core in line with that observed for borazatruxene. Also, two distinct peaks of lower intensity were observed at higher wavelengths, centred at 272 and 279 nm diagnostics of the borazine ring. The fluorescence spectrum (black) was obtained exciting the sample at 279 nm because at this wavelength the photoluminescence intensity was higher compared to that obtained by exciting the sample either at 207 or 239 nm. The emission max resulted to be at λ_{em} = 291 nm and the overlap between the absorption and emission spectra was very small displaying a Stoke shift of $\Delta\lambda$ = 12 nm. The Circular Dichroism (CD) spectra of the *syn* enantiomeric species collected displayed a strong Cotton effects in both

aromatic and borazine regions as shown in Figure 2.27. The first enantiomer isolated (blue) displayed an intense induced CD signal, consisting of a positive band in the aromatic absorption region (239 nm) and a negative band in the borazine region (272-279 nm) while the second enantiomer (red) displayed opposite and symmetric CD maxima.

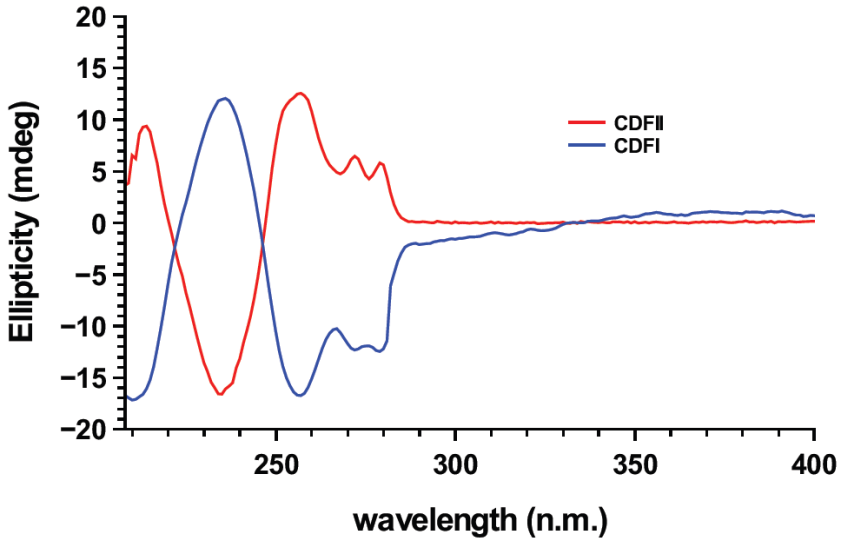

Figure 2.27 Circular Dichroism (CD) spectra of the *syn* enantiomeric species of **104** collected. The first fraction in blue is related to peak **A** in the chromatogram, while the second fraction in red is related to peak **B**.

The identification of the two *syn* enantiomers (*RRR* **104a** and *SSS* **104b**) was possible by comparing the experimental with the computed data. The latter were calculated using the TD-DFT method with M06-2X, exchange correlational with 6311G(dp) basis sets. The overlap of UV-Vis. absorption spectrum with the experimental and computed CD data is displayed in Figure 2.28.

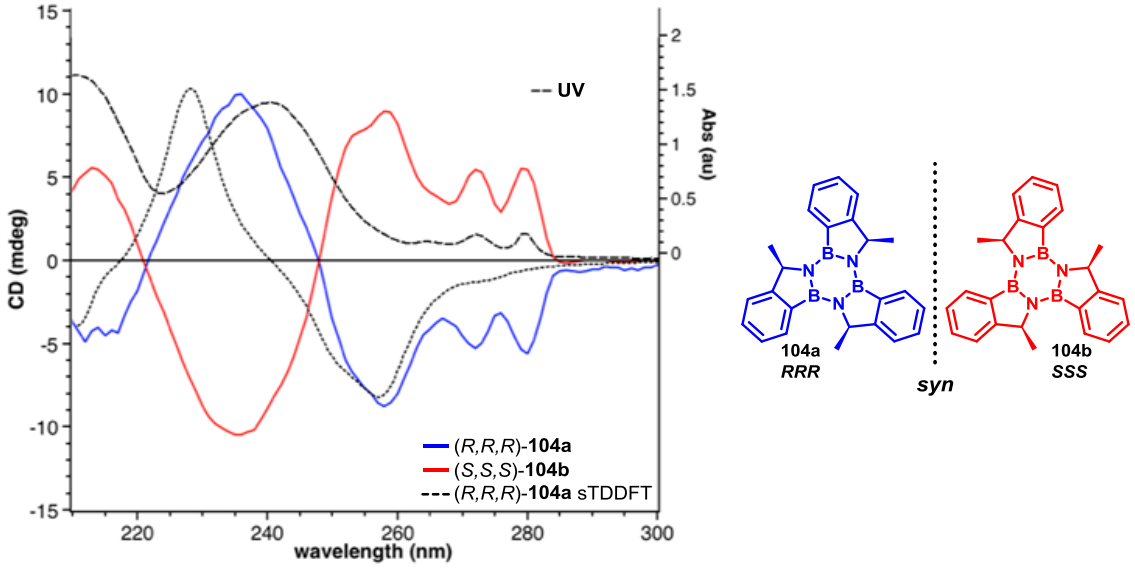

Figure 2.28 Comparison of the experimental (red and blue lines) with the computed (dots line) CD data to identify the two syn enantiomers *RRR* **104a** and *SSS* **104b**.

From data collected we could assign the absolute structure *RRR* **104a** to the first enantiomer isolated by preparative HPLC since experimental CD spectrum (blue) matched well that obtained by computational calculations (dashed green line). Consequently, the second fraction collected was related to the other enantiomer *SSS* **104b** isolated. The CD spectrum was also collected for both pure *anti* enantiomers isolated showing a similar trend just described. The two CD spectra overlaid are reported in Figure 2.29 displaying a symmetric pattern between the two enantiomers as previously observed.

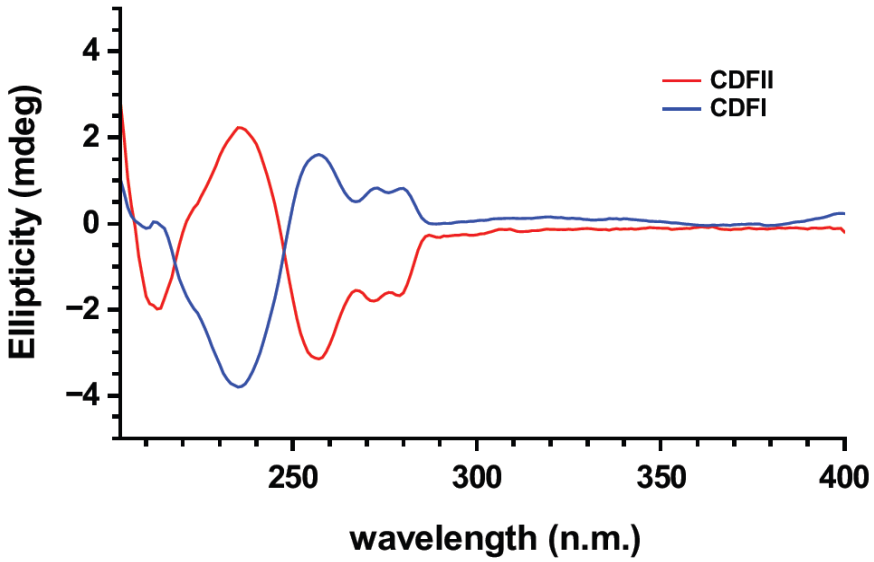

Figure 2.29 Circular Dichroism (CD) spectra of the *anti* enantiomeric species of **104** collected. The first fraction in blue is related to peak **A** in the chromatogram, while the second fraction in red is related to peak **B**.

To note that in this case signals were inverted compared with the syn pair. Indeed, the first fraction isolated (blue) displayed a negative band in the aromatic absorption region (239 nm) and a positive band in the borazine region (272-279 nm) and *vice versa* for the second enantiomer (red). At the moment DFT calculations for the CD spectra of the two *anti* enantiomers are still on going.

2.4.4 X-ray structure of the racemic mixture of *syn* borazatruxenes 104a-b

Structural proof of the *syn* enantiomers of borazine **104** was obtained from an X-ray diffraction analysis of single crystals grown by slow evaporation from a *n*-hexane/isopropyl alcohol (90:10) mixture. The *RRR* **104a** and *SSS* **104b** enantiomers co-crystallised in the rhombohedron trigonal R-3 space group with twelve molecule units per unit cell.

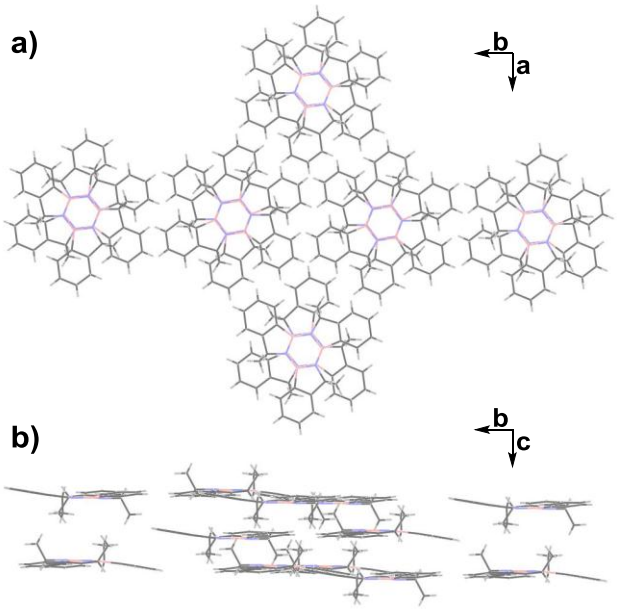

Figure 2.30 Crystal packing of **104a-b**; a) top view and b) layers and columns.

The measured bond distances between carbon atoms of the aromatic ring are 1.390(4) Å are in line with those reported in literature.[17] The distance calculated between boron and nitrogen atoms are B(1)-N(1) 1.448(4) Å and B(1)-N(2) 1.410(4) Å similar to those observed for borazatruxene.[2] These values matched very well with those reported in literature for a typical boron-nitrogen covalent bond characterizing the borazine ring system. While the corresponding bond angles calculated for the borazine ring are respectively 119.3(4)° for N(2)-B(1)-N(1) and 120.6(4)° for B(1)-N(1)-B(1). In good agreements with that predicted, and with that previously observed for borazatruxene, these molecules feature a flat shape configuration.

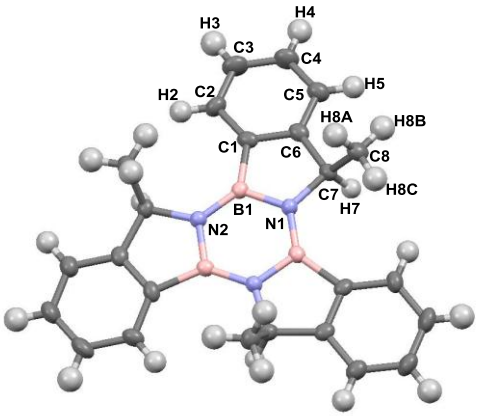

Figure 2.31 Crystal structure of syn **104.**

The two enantiomers packed into the crystalline lattice on top of one another adopting a 60° face-on stacking in which boron atoms interact with nitrogen atoms with the closest neighbouring borazine ring

with an average distance of 3.749 Å with methyl groups pointing outwards (Figure 2.32b). These close contact interactions observed, below to the sum of the van der Waals radii,[53] might be due to electrostatic interactions occurring between the lone pair on the nitrogen atoms and the empty p_z orbital on boron atoms. Also, in the crystal packing two enantiomers rearranges with methyl groups pointing inside in the same direction with distance measured of 4.905 Å (Figure 2.32c). This distance is higher than that observed before probably due to the steric hindrance effect of the methyl groups. On the other hand, these interactions mainly contribute to the off-set columnar arrangement between two sequential planes characterizing the crystallin lattice.

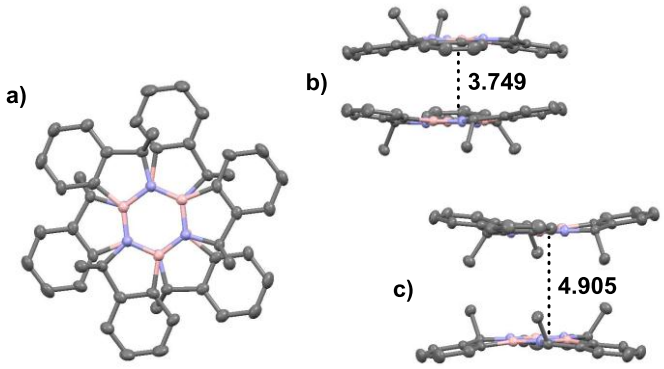

Figure 2.32 Stacking detail of the two enantiomers present in the structure highlighting a) top view and interlayers interactions between two enantiomers with methyl groups b) pointing outwards and c) pointing inside the cavity.

2.5 Synthesis of borazatruxene with chiral alkyl chains on the peripheral aromatic groups

2.5.1 Retrosynthetic approach

Our previous experience on installing alkyl chains as peripheral functional groups onto borazatruxene led us to consider the possibility of synthesising a chiral version **105** of **92**. The initial plan was therefore to follow the same procedure developed for the synthesis of **103**, starting from the same starting material **18** and to employ a chiral alkyl chain in the first step of the nucleophilic substitution.

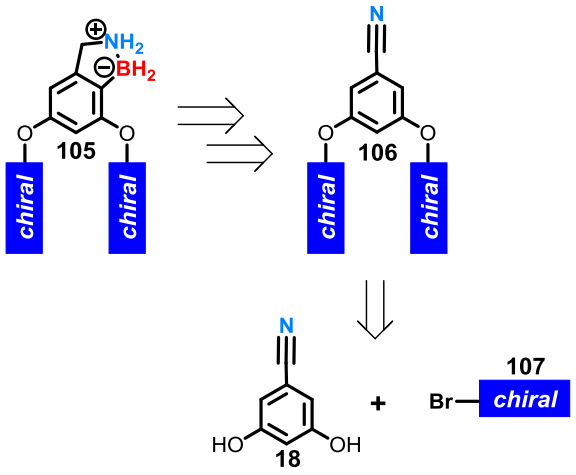

Scheme 2.26 Retrosynthetic analysis for the synthesis of amine-borane **105** bearing peripheral chiral alkyl chains.

Along with this plan we had a careful searching for commercially available 1-bromine chiral alkyl chains **107** to use in our synthetic pathway. Unfortunately, we found that few of them were suitable candidates for our synthesis and moreover all of them were very expensive therefore we decided to revisit our synthetic approach in order to overcome this problem. In an attempt to address this issue, we designed to build-up the chiral chain synthetically, at the expense to add one more step to the previous synthetic pathway envisioned. An interesting idea was that to connect covalently a short chiral linker in between the starting material **18** and a common aliphatic long alkyl chain **19** to preserve the solubility feature. To this end we found compound **108** to be the perfect candidate to employ in our synthesis since it possesses a central chiral carbon as we desired, also the bromine and hydroxyl functional groups at the extremity could be exploited in nucleophilic substitution reactions to bind the linker in between as we envisioned.

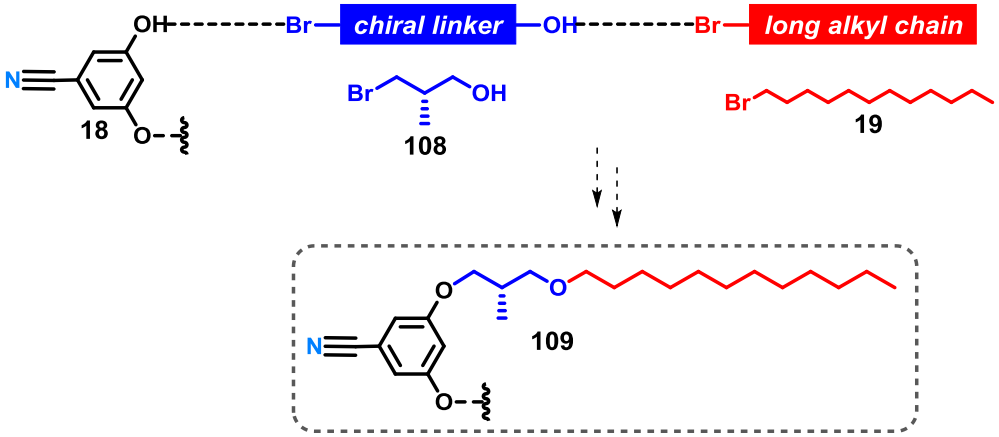

Scheme 2.27 Design of the chiral alkyl chain to link to starting material **18**.

2.5.2 Development of the synthesis using a non-chiral linker

To test the revisited synthetic pathway, however, we decide to use as linker the non-chiral version **110** since it was already available in our lab plus it was cheaper than **108**. Treatment of **18** with potassium carbonate in presence of **19** following the same procedure described for **16** resulted in a mixture of three different products. By chromatography purification and NMR analysis was possible to isolate and identify each compound. The desired **111** was obtained in very low yield (20%) while the rest was a mixture of starting material and monosubstituted intermediate suggesting that the reaction worked partially. However, when we repeated the reaction under forcing conditions (refluxing overnight in DMF) starting material **18** was fully converted into the product providing **111** in excellent yield (81%) (Scheme 2.28).

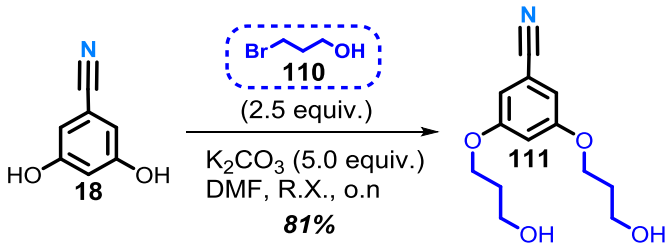

Scheme 2.28 Synthesis of compound **111**.

This first step was also successfully scaled-up to 10 mmol still resulting in high product yield. To alkylate the two-terminal aliphatic hydroxyl groups it was followed a method introduced by F. Heymans.[54] The intermediate di-alkoxide species formed upon treatment with NaH (60% dispersion in mineral oil) in DMF was subsequently reacted in presence of 1-bromododecane **19** leading to the desired **112** in >90%. Pleasingly even this reaction was successfully scaled-up to 10 mmol resulting in high product yield (Scheme 2.29).

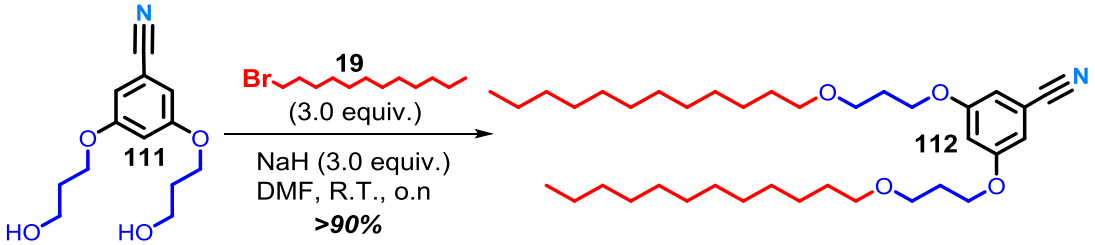

Scheme 2.29 Synthesis of compound **112**.

For the *ortho* bromination of **112** it was followed the same method described for the synthesis of **38**, however first attempt resulted in a complex mixture of products. Column chromatography purification to isolate and identify each component was particularly challenging because the retention time was very similar for each component of the mixture even when a low polar eluent (*n*-hexane/EtOAc 98:2) was

utilized. The development of a valid purification method was very time consuming. The best separation was obtained when ≈ 160 mg of crude product were purified using a 2.5 cm Ø column, filled with 15 cm of wetted silica gel and the best eluent found was a mixture of *n*-hexane/EtOAc (98:2). Three main compounds were isolated, ^{1}H-NMR analysis in $CDCl_3$ revealed the major product to be the mono brominated species **113** (48%) while the minor product was the unreacted starting material **112**. The third compound displayed a similar NMR pattern already encountered for **16**, therefore we tentatively assigned the molecular structure of the dibrominated species **114** which was later confirmed by mass spec analysis (Figure 2.33).

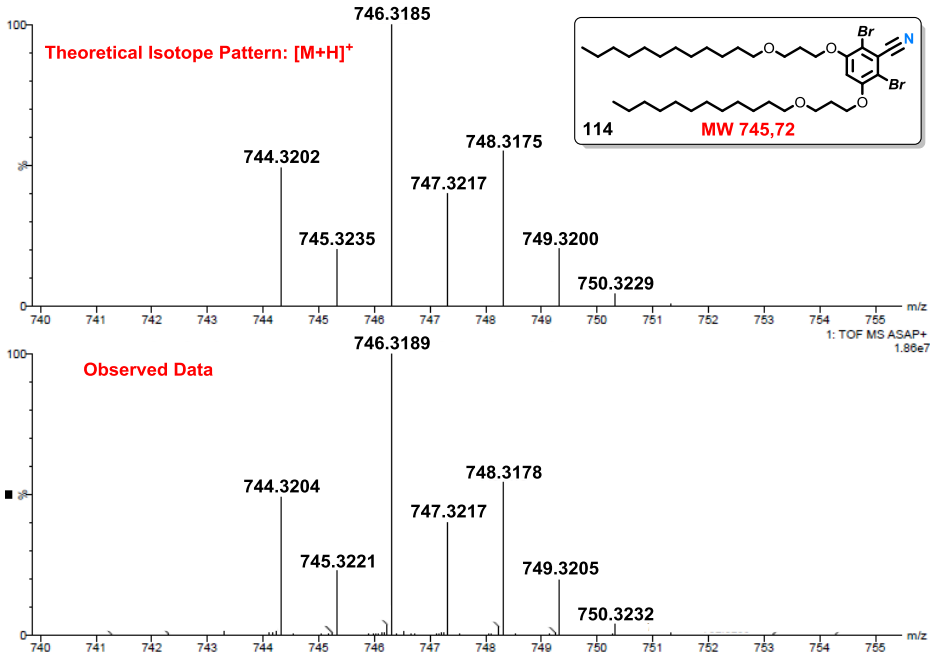

Figure 2.33 Mass Spectrum of compound **114** from Swansea University.

This outcome suggested that under the standard reaction conditions, the *ortho* bromination of substrate **111** was less effective since the reaction worked partially and also, the second bromination took place at the expense of the mono bromination of starting material still available in the reaction mixture. To avoid this side reaction, we attempted to optimize the process by screening different temperatures and different amount of NBS employed. Already aware of the problem involved with the impurities presents in commercial NBS that could drastically affect the yield of the reaction, we recrystallized pure NBS from water. Initially, in an attempt to optimize the reaction conditions, we screened different temperatures, setting the reaction at room temperature, 50 °C and reflux (83 °C, the maximum temperature achievable with 1,2-dichloethane). However, we did not notice any particular improvement with respect to the first attempt; still unreacted starting material and dibrominated species were isolated after column purification. In order to reduce the amount of dibrominated species **114** formed we later decided to reduce the number of equivalents of NBS from 1.1 to 0.9. In this case by-product **114** isolated was lower but still

starting material was recovered and this remained one of the key challenges in advancing the synthesis. A plausible explanation of a such behaviour of **112** towards the bromination could be associated to the tendency of it to form supramolecular aggregates, as for instance micelles, that could lead to a reduction of the amount of starting material readily available to react. Likewise, during the course of the reaction the amount of mono brominated species **113** increase: it become the predominant species at the expense of starting material **112** involved in supramolecular aggregates, therefore the side dibromination reaction occur. We reasoned that this problem could potentially be overcome by working in diluted conditions to avoid the formation of aggregates. Indeed, when we set the synthesis four times more diluted than the initial reaction (from 3.4 x 10^{-2} to 8.5 x 10^{-3} M) a notable improvement in yield was observed and **113** was provided in 70% yield. With this strategy also, we managed to cope with the problem of starting material unreacted, indeed, this time only mono and di brominated species were isolated after column purification.

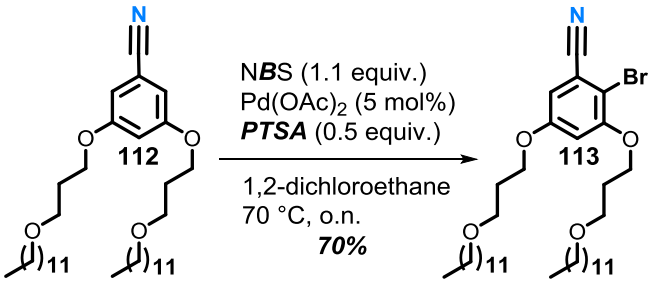

Scheme 2.30 Synthesis of compound **113**.

With intermediate **113** in hand to have access to the corresponding boronic ester **115** was rather straightforward based on our previous experience whit the synthesis of **50**. Indeed, when the Miyaura reaction was carried out under the same conditions previously developed for **50**, the desired **115** was obtained in 62% yield. On the contrary when this reaction was repeated in more diluted conditions the yield dropped to 35%, the amount of boronic acid in the mixture increased to 5:5 and also we isolated a significant amount of **112** due to the protodeboronation process.

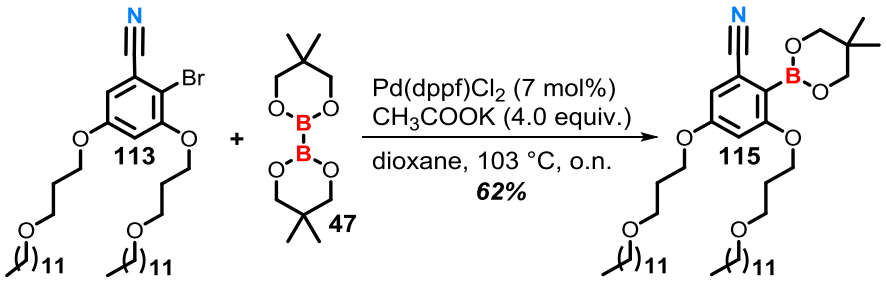

Scheme 2.31 Synthesis of compound **115**.

Pure **115** was obtained after column chromatography purification eluting with a mixture of *n*-hexane/EtOAc (85:15) and as we expected product **115** was isolated as a mixture of boronic ester and boronic acid in 7 : 3 ratio. However, the mixture was not subjected to the re-protection procedure since by our knowledge both boronic acids and esters could be reduced to borane functional group when treated in presence of an excess of $LiAlH_4$. Reduction of **115** following the standard protocol unexpectedly provided **116** in reasonable yield (64%) after work-up, furthermore it was reproducible.

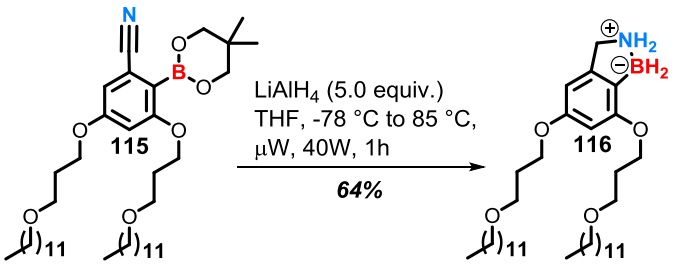

Scheme 2.32 Reduction of compound **115**.

The ^{1}H-NMR analysis spectrum in $CDCl_3$ shown in Figure 2.34 displayed a shift to higher field of aromatic signals compared with the starting material, in line with what previously observed for **92**. However, ^{11}B-NMR analysis spectrum was crucial in confirming molecular structure of **116**; it displayed the diagnostic peak at -11.2 ppm, typical of the amine-borane functional group.

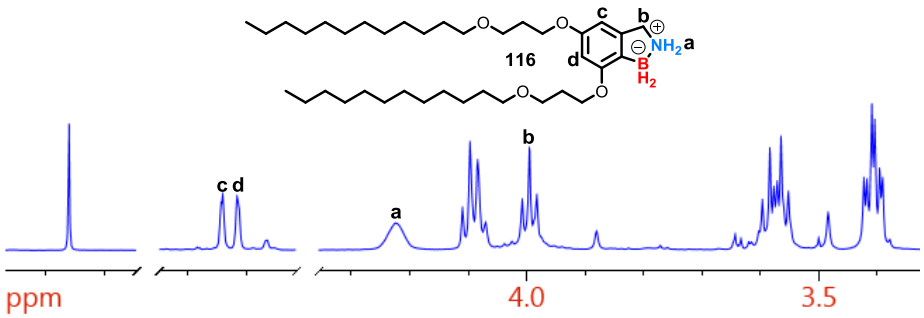

Figure 2.34 Representation of the ^{1}H-NMR analysis spectrum in $CDCl_3$ highlighting the diagnostic peaks to prove molecular structure of **116**.

A further confirmation of molecular structure of **116** came from mass spectroscopy analysis (Figure 2.35).

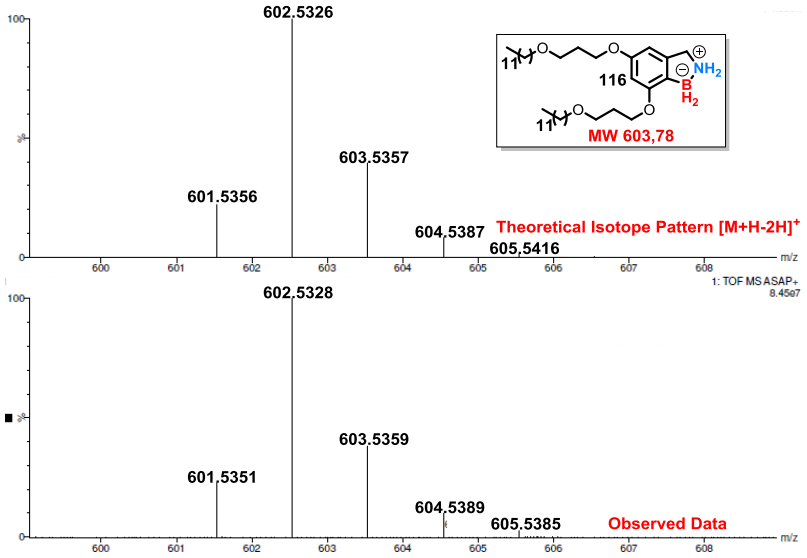

Figure 2.35 Mass Spectrum of compound **116** from Swansea University.

Having secured access to amine-borane **116**, we next explored the possibility of synthesising the corresponding borazine. Using the same synthetic approach based on the use of microwave assisted conditions described before, we successfully accomplished to borazine **117** in 26% yield after column chromatography purification (*n*-hexane/CH_2Cl_2 80:20).

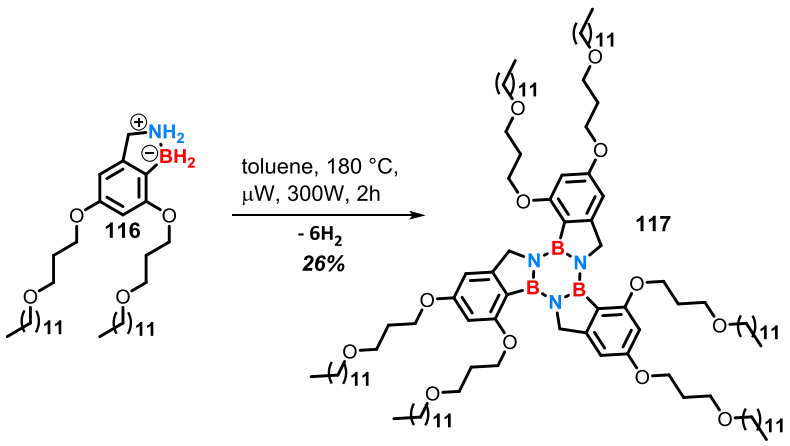

Scheme 2.33 Synthesis of borazine **117**.

Unfortunately, our efforts to isolate by-products failed since part of the mixture remained stuck on the silica gel at the beginning of the elution and later was challenging to remove even when high polar solvents were used. To isolate and characterize by-products would have been crucial in understating the reaction mechanism involved in the borazine formation for this substrate. In fact, surprisingly, even in this case the yield was lower than the average yields previously obtained for substituted borazatruxenes. Our initial hypothesis to explain this atypical outcome was associated to a difference in solubility between borazine **117** and borazatruxenes previously synthesised. In fact, both amine-borane **116** and borazine **117** were

much more soluble in toluene than the previous borazatruxene derivatives synthesised and the corresponding amine-boranes. The same trend was previously observed for both amine-borane **92** and borazine **103**. This difference in solubility might be a determining factor in directing the reaction towards a more kinetically controlled process rather than a thermodynamically controlled process and *vice versa*. The process leading to insoluble borazine is irreversible therefore once they are formed it is unlikely they take part to further side reactions, while the contrary in the case in which borazine is soluble, the process can be reversible leading the product to unexpected side rearrangements. After separation a series of 2D NMR spectra (HMBC, COSY and NOESY) were collected to proof molecular structure of **117**. Analysis of ^{1}H-NMR in $CDCl_3$ revealed a general shifting of signals to lower field compared with amine-borane **116**, specifically, aromatic protons were most deshielded (6.57-6.39 ppm) respect to **116** (6.32 ppm). Also, the broad peak related to the primary amine disappeared whilst the triplet signal related to the -CH_2- bridge shifted to 5.00 ppm as a singlet. COSY and NOESY NMR spectra obtained in TCE-d_2 are overlapped in Figure 2.36 displaying correlations between aromatic protons with the -CH_2- bridge and -OCH_2- groups of **117**.

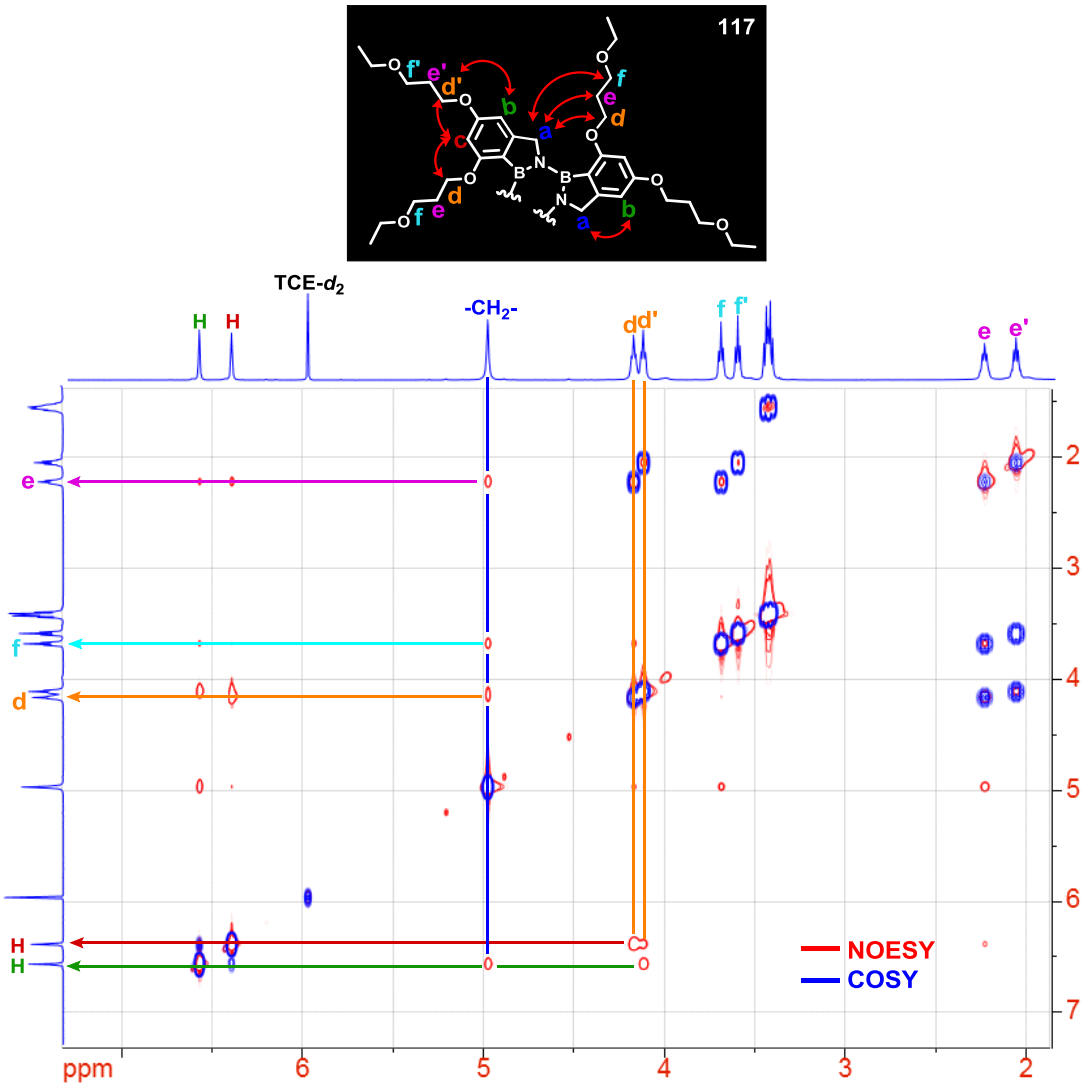

Figure 2.36 Representation of NOESY (rred) and COSY (blue) NMR spectra of **117** overlapped.

The ^{11}B-NMR spectrum was noisy when recorded at 298 K however we could observe the signal centered at 31.0 ppm of the borazine ring when we increased the number of acquisition scans and the temperature to 348 K in TCE-d_2. A further confirmation of molecular structure of **117** was obtained by mass spectroscopy analysis which displayed a good match between the predicted isotope pattern distribution and the observed data. The development of this synthesis required almost a year of work since the problems encountered especially in the bromination, borylation and reduction steps proved to be very challenging. Indeed, these reactions when performed with these particular substrates resulted to be highly dependent on many different factors such as temperature, moisture, concentration, reaction time, purification procedure etc. Scheme 2.34 shows a summary of the total synthesis of **117**.

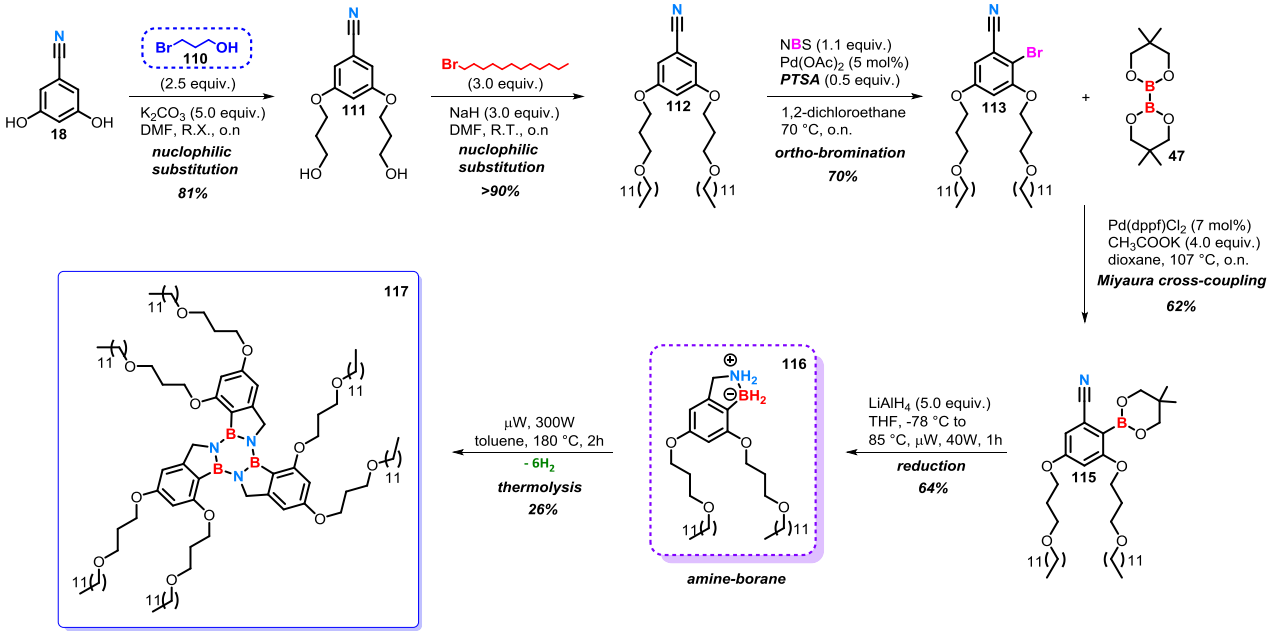

Scheme 2.34 Representation of the total synthesis of **117**.

2.5.3 Synthesis of borazatruxene chiral alkyl chains using the developed method

Satisfied of these results obtained we explored the possibility of synthesising the corresponding chiral analogue. In the first attempt to install the chiral linker **108** to 3,5-dyhdroxybenzonitrile **18** by following the same protocol previously described for **111**, unexpectedly provided **118** in very low yield. Indeed, TLC analysis after overnight reaction (eluent, *n*-hexane/EtOAc 70:30) displayed two different products therefore, by chromatography purification was possible to isolate and identify each compound. The desired **118** was obtained in 20% yield while the second product isolated was identified to be the monosubstituted intermediate suggesting that the reaction worked partially, however no starting material was recovered. Possibly an overnight reaction time in this case was not enough to get the reaction to the

completion. In fact, when we repeated the reaction for 17 h and we added 0.1 equivalent more of **108** after 8 h reaction, starting material **18** was fully converted into the product providing **118** in excellent yield (70%).

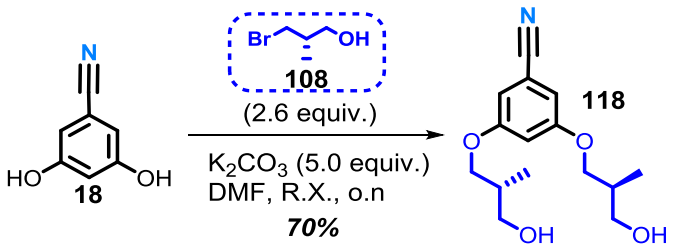

Scheme 2.35 Synthesis of compound **118**.

The resulting di-alcohol derivative **118** was then alkylated following the same procedure developed for **112**. The intermediate di-alkoxide species formed upon treatment with NaH (60% dispersion in mineral oil) in DMF was subsequently reacted in presence of an excess of 1-bromododecane **19** leading to the desired **119** in 70%.

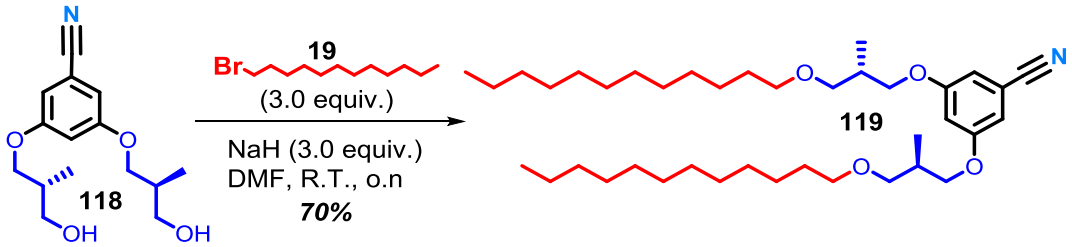

Scheme 2.36 Synthesis of compound **119**.

The *ortho* bromination of **119** was performed following the same method described before, using pure NBS beforehand recrystallized from water. Pleasingly with the application of the chromatography purification procedure previously developed for **113** we readily achieved **120** in very good yield (61%).

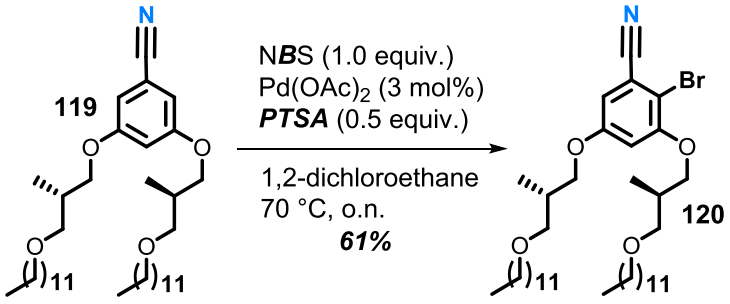

Scheme 2.37 Synthesis of compound **120**.

We observed that the bromination of **119** led to a smaller amount of by-products formed such as the dibrominated species, while unreacted starting material was not observed. This unusual outcome compared with that described for **16** and **112** with all the difficulties surrounding the selective mono bromination, can be explained in terms of different solubility in the organic solvents. Indeed, as we highlighted before, it is possible that both **16** and **112** easily form supramolecular aggregates as micelles because of the molecular structures similar to that of surfactants. Possibly the introduction of bulky methyl groups on the alky chain reduce the intermolecular hydrophobic Van der Waals interactions because of the steric hindrance, preventing the formation of these supramolecular aggregates, thus making these molecules more available to take part to the reaction. The ^{1}H-NMR analysis spectrum in $CDCl_3$ displayed a similar aromatic pattern observed for **113** confirming molecular structure of **120**. Borylation of **120** was performed following the same procedure described for **115**. In this reaction the concentration of starting material **120** in anhydrous dioxane was very important to achieve the desired **121** in good yields. Indeed, when the synthesis was carried out at a concentration of 0,058 M of **120** in dioxane, the desired **121** was delivered in 63% yield.

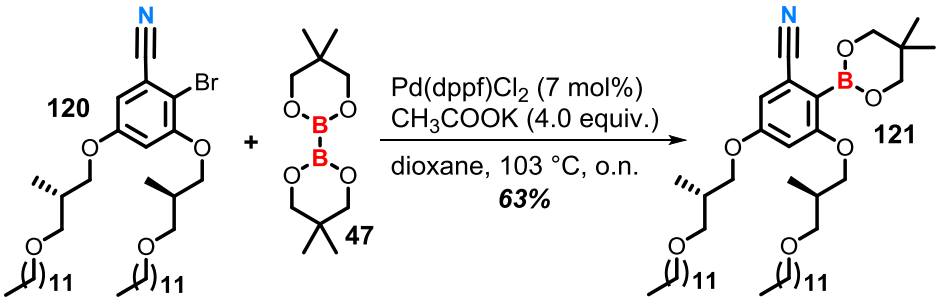

Scheme 2.38 Synthesis of compound **121**.

On the contrary, reactions performed at different concentrations proved to be less effective delivering **121** in very low yield. As we observed for the borylation of the previous alkylated 2-bromobenzonitriles species, after column chromatography purification **121** resulted to be a mixture of boronic ester and boronic acid in ratio 7 : 3. Considering that in the case of **115** we successfully achieved the corresponding amine-borane **116** directly employing the mixtures in the next step of the reduction, we decided to proceed in the same manner for **121**. After 1 hour of heating at 90 °C by microwave irradiation, the reaction was checked by TLC analysis which displayed the diagnostic blue spot of amine-borane compounds when treated with a cerium-ammonium-molybdate staining solution confirming the reduced form **122**. Following the standard work-up and purification protocol developed for amine-boranes we obtained pure **122** in 60% yield.

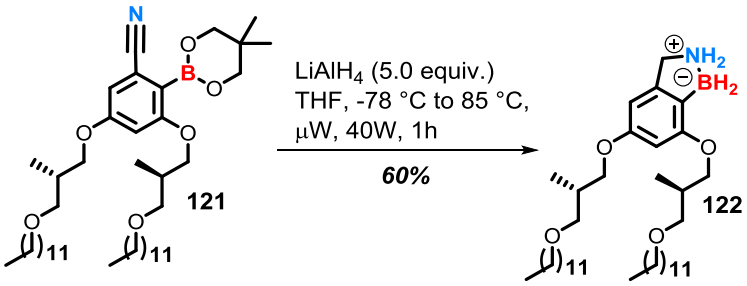

Scheme 2.39 Reduction of compound **121**.

By analysis of the NMR data (^{1}H, ^{11}B and ^{12}C) it was possible to identify and full characterize the desired **122**. The ^{1}H-NMR spectrum in $CDCl_3$ displayed the characteristic signals related to the -**NH_2**→BH_2- primary amine group and the internal -**CH_2**- bridge formed. Also, ^{11}B-NMR analysis confirmed the molecular structure of **122** displaying a signal resonating at -10.6 ppm. Unexpectedly when repeating the reaction under identical conditions, it led only to complex mixtures with partial decomposition. A subsequent attempt proved unsuccessful therefore we decide to force the reaction conditions stirring the solution at 100 °C for 3 hours. Preliminary TLC analysis revealed the desired **122** to be formed however, after work up NMR analysis of the crude mixtures proved to be inconclusive in determining the presence of **122** because of difficult interpretation due to the presence of a complex mixture of by-products. This result was quite surprising in that amine-borane was observed in solution after the reaction, but not after the work-up. At this juncture, we envisioned that compound **122** might be highly susceptible to the presence of water used in the work up procedure to neutralize the excess of $LiAlH_4$, thus undergoing to decomposition. After a careful review of the literature we found other ways to quench the excess of $LiAlH_4$, for example, by adding either less protic or non protic solvents such as alcohols, EtOAc or acetone, however one of the more efficient method reported in literature is the use of the Rochelle's salt. The latter is a saturated solution of sodium potassium tartrate salt in water which is well-known to be an excellent ligand for aluminium ion, breaking the aluminium emulsion formed upon water addition. Unfortunately, despite we attempted with all these quenching techniques described, the outcome was identical making this reaction not reproducible. Also repeating the reaction with 6.0 equiv. of $LiAlH_4$ and stirring the resulting mixtures at room temperature overnight proved to be unsuccessful leading only to the product decomposition **123**.

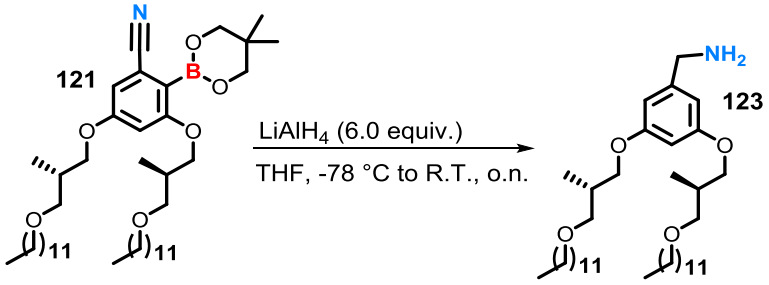

Scheme 2.40 Failed attempt at the synthesis of compound **121.**

With few milligrams of amine-borane **122** in hand we later attempted at the borazine synthesis following the same protocol before described. After two hours of reaction at 180 °C, removal of the solvent at high vacuum conditions led to a white glassy solid.

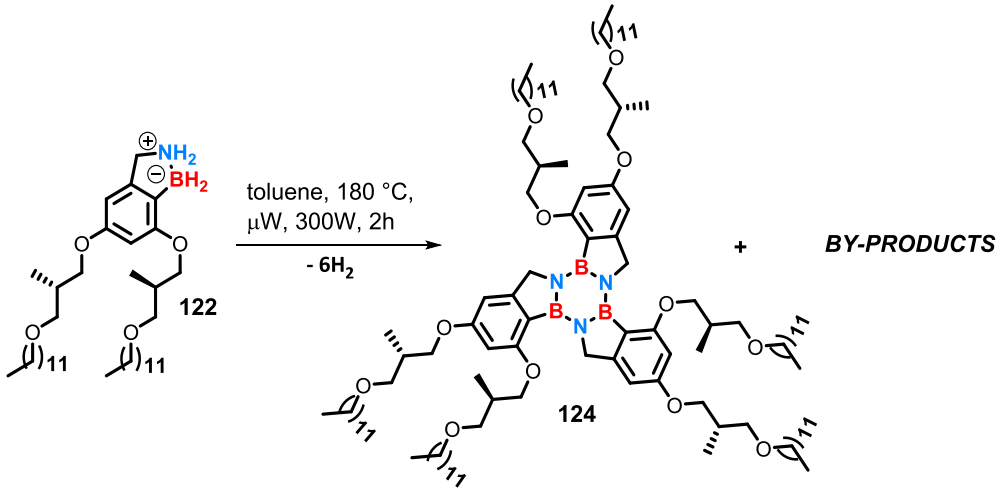

Scheme 2.41 Synthesis of borazine **124**.

Preliminary NMR analysis on the crude product suggested the presence of two different species, indeed the ^{1}H-NMR spectrum displayed two distinct set of signals. Unable to proceed with any purification procedure, due to the low quantities of product obtained, we decided to collect more NMR data (^{11}B, ^{13}C and COSY) and compare these results with NMR spectra obtained for **117**. Comparison of the ^{1}H-NMR spectra of borazine **124** and **117** displayed a good match between aromatic protons having identical chemical shift (Figure 2.37).

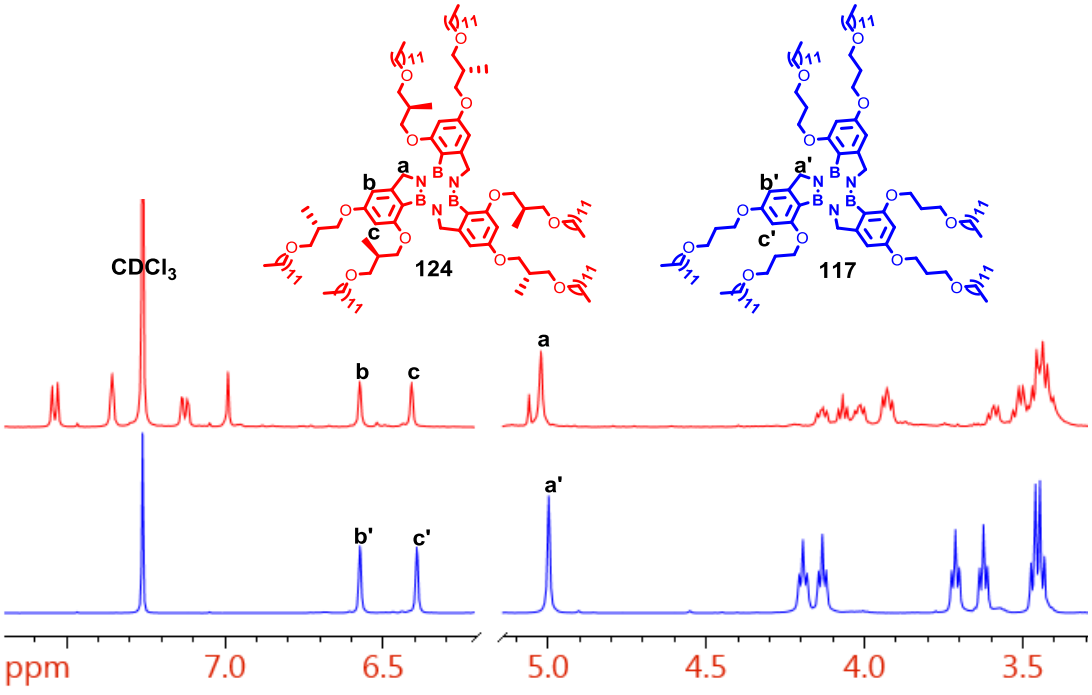

Figure 2.37 Comparison of the ^{1}H-NMR spectra in $CDCl_3$ of borazine **124** and **117**.

Also, the singlet of the internal -**CH_2**- bridge in both cases was centred roughly at 5.01 ppm. Regarding the aliphatic region, was more challenging to see match between signals of the two borazines, because the chiral linked of **124** made the signals splitting and moreover some of them were overlapped or even hidden by the presence of additional peaks of the unknown species.

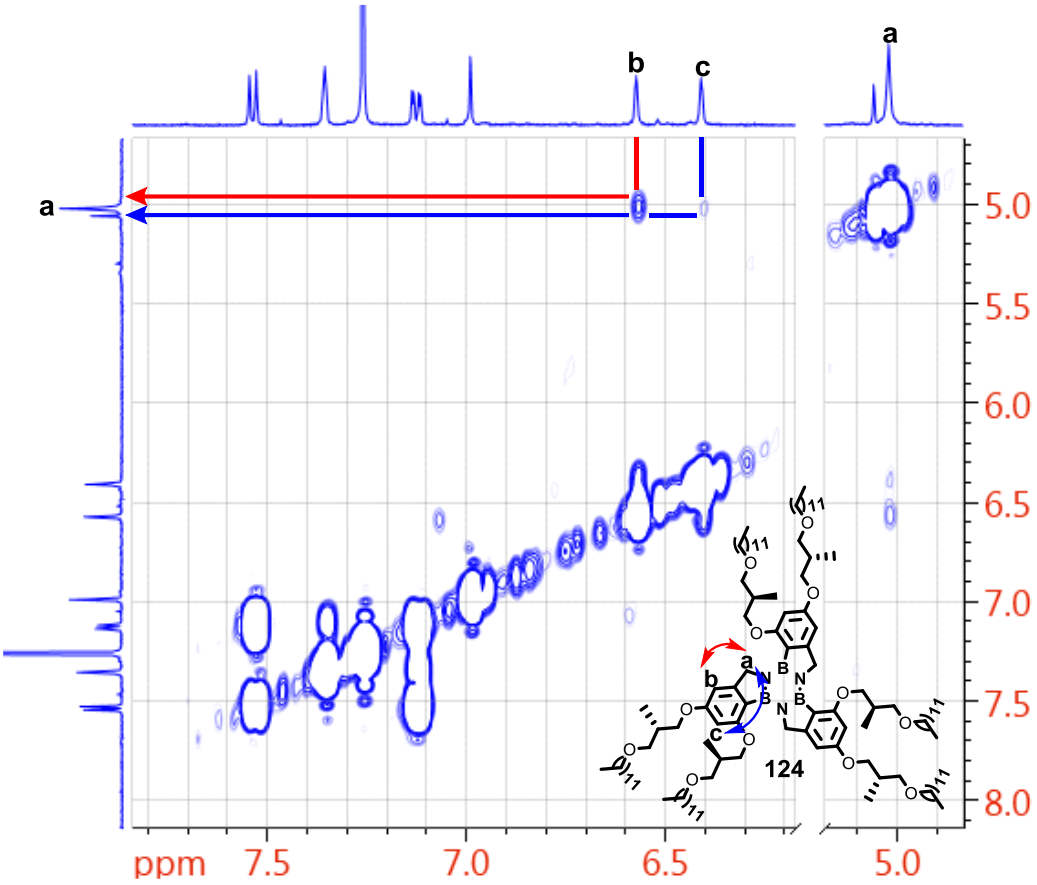

Figure 2.38 Representation of COSY NMR spectra of **124**.

The 2D COSY NMR analysis shown in Figure 2.38 was also helpful in the characterization of **124** since displayed correlations between aromatic protons with the benzylic -CH_2- bridge. We observed the same internal transfer magnetization during the relaxation process for borazine **124**, and this result made us more confident in believing to have synthesised borazine **124**. Also, this was a further prove to have a mixture of two different compounds since the aromatic signals between 7.5 and 7.0 ppm of the other unknown species did not display ant correlation with borazine **124.** However more analysis needs to be done for full characterization to confirm structure **124**. Speculating on the nature of the second product, we later attempted to assign a molecular structure to the unknown compound, but unfortunately all our effort resulted to be inconclusive.

2.6 Optical studies of borazatruxenes

Solutions of borazines **96-98**, **101-103** and **117** for UV-Visible and fluorescence analysis were prepared dissolving these compounds in HPLC grade CH_2Cl_2. We decided to use CH_2Cl_2 rather than $CHCl_3$ because we wanted to increase the window of wavelengths analysed to investigate better the middle-UV region (200-300 nm) were aromatic systems usually absorbs. Indeed, the UV cut off wavelength of chloroform is at 245 nm while for CH_2Cl_2 is at 233 nm allowing thus to analyse roughly 10 nm more in the UV region. Fluorescence spectra were obtained exciting samples at the lowest-energy absorption peak centred between 280 and 290 nm characterizing the borazine ring absorption because at this wavelength the photoluminescence intensity was higher compared to that obtained by exciting the sample at the λ_{max}. Also, solutions at different concentrations were prepared to determine the molar extinction coefficient ε of borazine species. Spectroscopy properties of borazine **96-98** have already been described by Dr. L. Emmett in his PhD thesis.[2] However, we repeated the UV-Visible absorption and fluorescence analysis with the only purpose to confirm the trend already observed. Indeed, as previously reported, borazatruxene **96** shown a max wavelength of absorption centred at 239 nm related to the peripheral aromatic rings while three further absorption peaks of lower intensity were observed at 265, 272 and 280 nm related to the borazine ring absorption (Figure 2.39). The emission spectrum (black) was obtained exiting the sample at 280 nm displaying a λ_{em} max centred at 304 nm and the overlap between the absorption and emission spectra was very small.

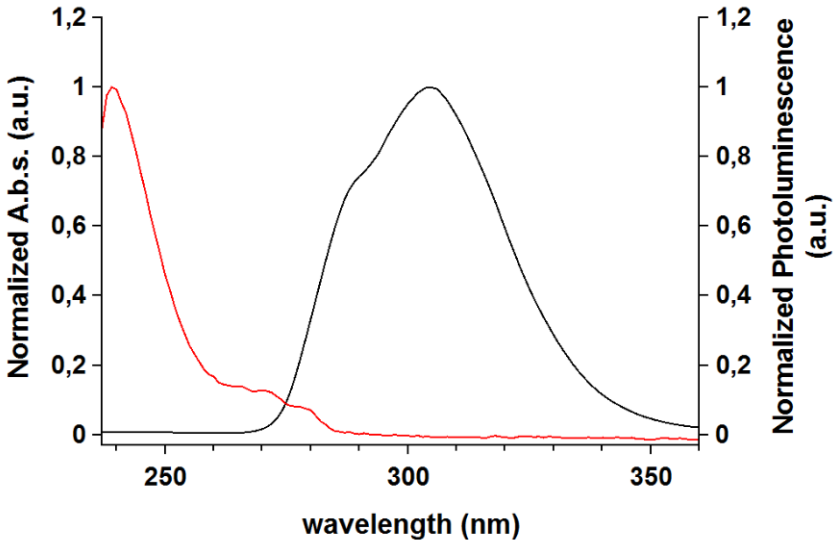

Figure 2.39 UV-Visible absorption (red) and emission (black) spectra of borazatruxene **96** in CH_2Cl_2.

In line with that reported in literature,[55] the isoelectronic substitution of CC units by BN units alters the electronic properties resulting in an increase of the HOMO-LUMO gap because of the more localized electron density due to the differences in polarity between boron and nitrogen atoms. This phenomenon

causes an hypsochromic effect in the absorption of the light radiation compared with the all-carbon system counterpart. Indeed, in a recent study Liu and co-workers reported a direct comparison between the absorption spectra of anthracene and BN-doped anthracenes.[56] The latter exhibited an hypsochromic shift of ≈ 30 nm when compared with the all-carbon analogue, moreover a further BN substitution blue shifted the λ_{max} of absorption of ≈ 20 nm more. We also observed this trend when the UV-Vis spectrum of borazatruxene was compared with that of truxene. Truxene (Figure 2.40 b) exhibited three distinct peaks with the lowest-energy absorption peak at 299 nm, while borazatruxene spectrum was blue shifted of ≈ 20 nm with the lowest-energy absorption peak at 280 nm.

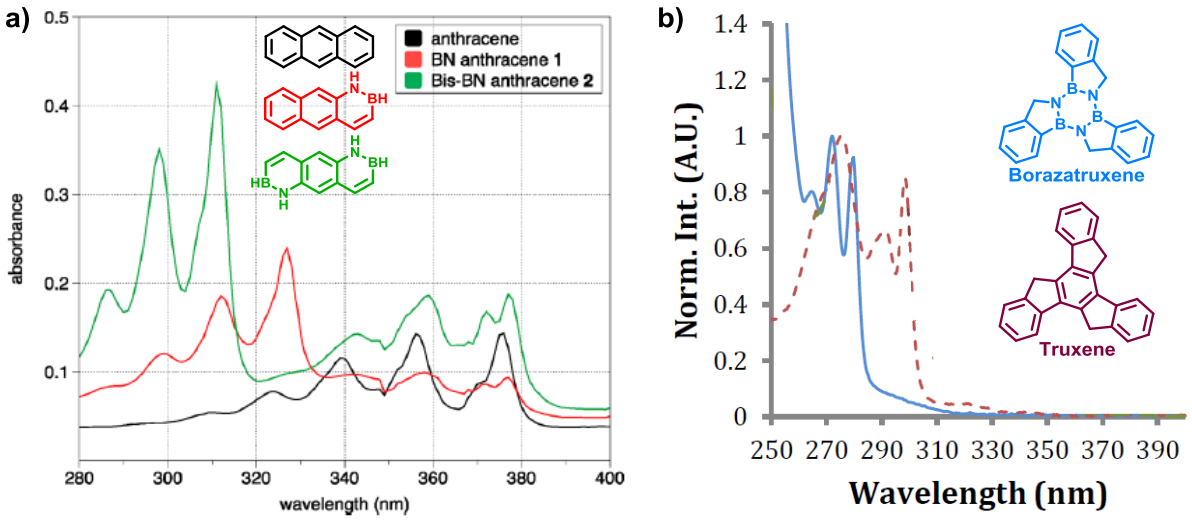

Figure 2.40 Comparison of absorption spectra of anthracene, BN anthracene, and bis-BN anthracene reported by Liu and co-workers[56] and b) truxene and borazatruxene reported by Dr. Emmett.[2]

In general, an hypsochromic shift was observed for all borazatruxene molecules synthesised respect to truxene, however the UV-Vis spectra displayed comparable peak patterns suggesting that the vibrational fine structure for the electronic transitions is similar for both species. Functionalization of the peripheral aromatic rings of borazatruxene caused a bathochromic shift of the UV-Vis spectra, indicating an increase of the electronic delocalization of the entire system. For example, introduction of chlorine atom on carbon 4 of the benzene ring **97**, resulted in a bathochromic shift of the lowest-energy absorption peak of ≈ 8 nm attributed to the increased n→π* interaction. Changing with bromine atom **98** marginal increased the lowest-energy absorption band of few nanometres. This is consistent with the similar inductive and mesomeric properties of two halogen species (**Br**: F = +0.45, R = –0.22 and **Cl**: F = +0.42, R = –0.19; F = field effect parameter, R = resonance parameter) behaving as moderately inductive (σ) electron-withdrawing groups and as weak π-donors.[57] By direct comparison of the UV-Vis spectra of borazatruxene with 3-methyl **101** and 4-methyl **102** substituted borazatruxenes we noticed a strong dependence of the absorption with respect to the substituents position. Indeed, the λ_{max} of absorption of 4-methyl substituted borazatruxene **102** was red shifted of only 1 nm while the lowest-energy absorption peak of the borazine band absorption

was red shifted of 6 nm. On the contrary 3-methyl substituted borazatruxene **101** UV-Vis spectrum displayed a general bathochromic shift of both aromatic and borazine absorption bands of ≈ 7 nm. In borazine **101** the methyl group being in *ortho* position respect to the boron atom, probably make more favourable the delocalization of the π-electrons of the aromatic system. The UV-Vis spectra recorded for borazines **103** and **117** bearing ether functional groups in 3 and 5 positions displayed a remarkable bathochromic shift of 35 nm of the λ_{max} of absorption (264 vs 239) and 10 nm of the lowest-energy absorption peak (290 vs 280). This observation can be attributed to the increase in conjugation in the borazatruxene system by this functionality.

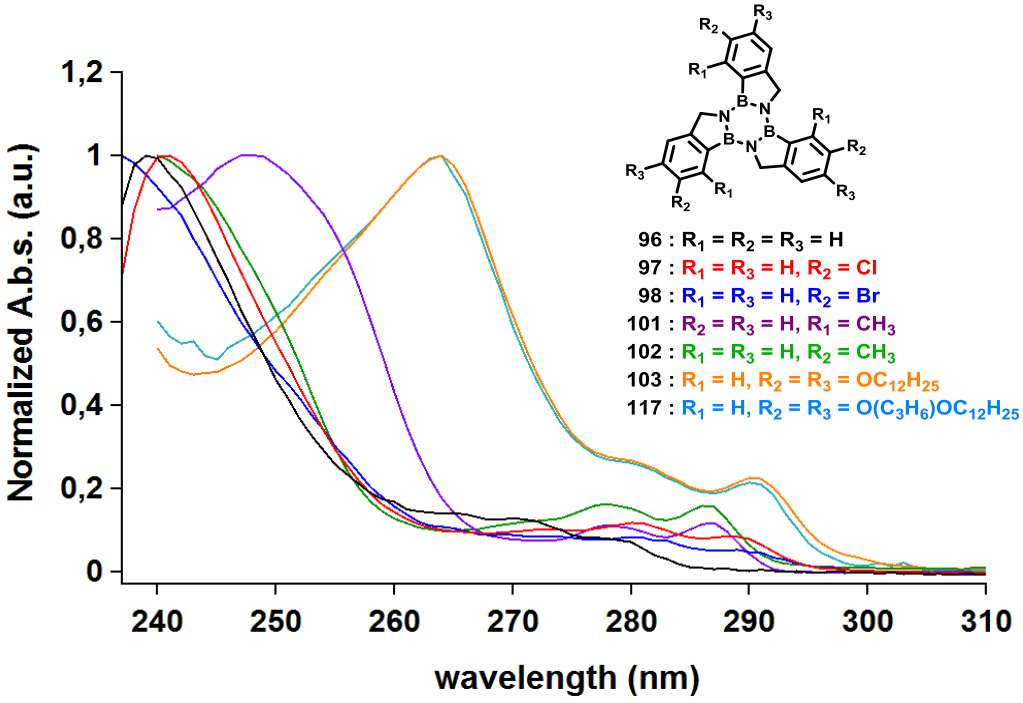

Figure 2.41 UV-Visible absorption spectra of borazatruxenes **96-98, 101-103** and **117** in CH_2Cl_2.

The emission spectra for all borazines were obtained by exiting samples at the lowest-energy absorption corresponding to the borazine absorption region (Figure 2.41). Although all borazine species when excited at either the low- or the high-energy absorption band the emission spectra resulted to be the same, excitation at the λ_{max} of absorption resulted in a lower intensity of the fluorescence spectra obtained. Borazines **96-97** and **101-102** displayed similar λ_{max} of fluorescence centred at ≈ 300 nm, while the bromine derivative **98** emitted at lower wavelength (294 nm). On the contrary borazine **103** and **117** bearing the ether functional groups displayed identical fluorescence spectra with a λ_{em} max centred at 391 nm with a second peak at similar intensity centred at 330 nm. Interesting to note that the Stoke shift decreased passing from the unsubstituted borazatruxene to the bromine derivative of almost five times (from 24 to 5), while ether derivative borazatruxenes **103** and **117** displayed the highest Stoke shift.

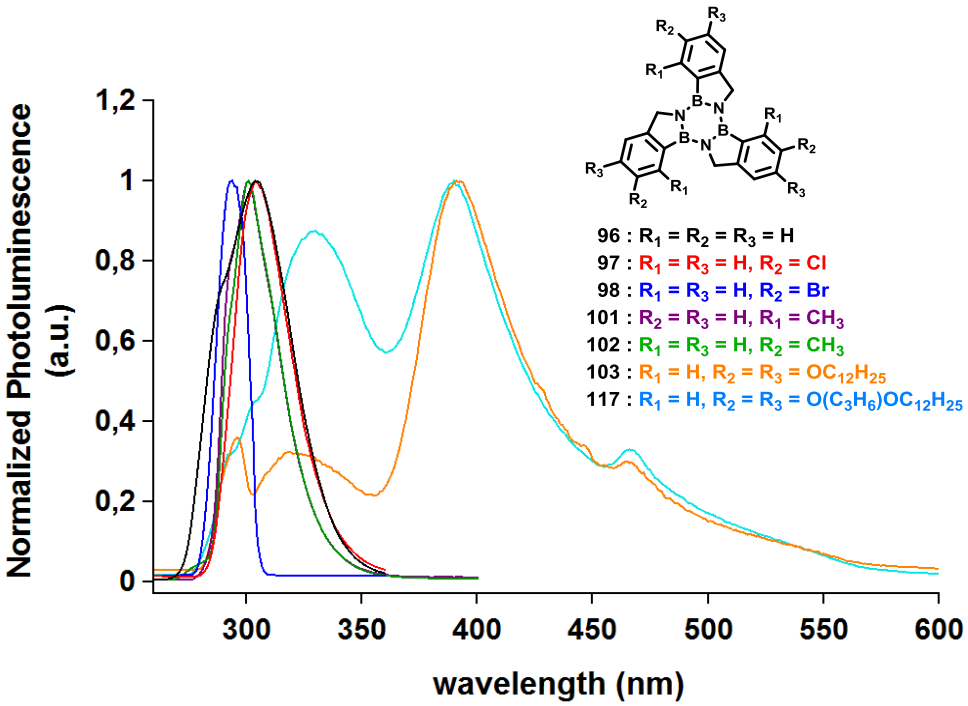

Figure 2.42 Emission spectra of borazatruxenes **96-98, 101-103** and **117** in CH_2Cl_2.

Solutions at different concentrations were prepared to determine the molar extinction coefficient ε of borazines **96-98**, **101-103** and **117**. Values obtained were then compared with those previously obtained for borazatruxene **96** and halogenated derivative borazine **97** and **98**. Unsubstituted borazatruxene **96** displayed an ε value of $1{,}06 \cdot 10^4$ mol · l^{-1} · cm^{-1}, five times less than the all carbon analogue truxene ($6{,}5 \cdot 10^4$ mol · l^{-1} · cm^{-1}) which can be attributed to their differing electronic structures. Descending group 7, from chlorine to bromine, we observed a decrease in the extinction coefficient values, suggesting an influence of the heavy atom affect. The same trend has been observed when the position of substituents changes alongside the aromatic ring. We noticed this effect with borazatruxenes **101** and **102**, which showed a three-fold disparity, indicating that a different position of the same functional group around the benzene ring greatly alters the electronic configuration of the borazine system. Introduction of strong electron donating groups such as ether groups in **103** and **117**, probably make more favourable the electronic delocalization of the entire system, thus increasing the extinction coefficient ε. Table 2.8 summarize the spectroscopic features of borazines **96-98**, **101-103** and **117**. The ϕ_f of borazatruxenes are also listed in Table 2.8. The increase in ϕ_f passing from borazatruxene to the chlorine derivative might be due to the presence of chlorine atom which make more rigid the system enhancing the emission quantum yield. The quenching of fluorescence observed with the introduction of bromine atom can instead be attributed to a more favourable intersystem crossing due to the heavy atom affect that increase the spin-orbital interaction. The same quenching of fluorescence is also observed for borazines bearing peripheral alkyl chains. This can be realistically attributed to nonradiative vibrational deactivations triggered by the peripheral alkyl chains.

Table 2.8 Experimental UV-Vis absorption and emission data for borazatruxenes **96-98, 101-103** and **117** in CH_2Cl_2.
(*) wavelength of excitation used to recorder the emission spectrum of each borazine.
(**) All quantum yields were calculated using anthracene in $CHCl_3$ as the standard (ϕ_{QS} = 0.11).

°n	Entry	λ_{max} (nm)	λ borazine band (nm)			λ_{PL} (nm)	$\Delta(\lambda_{PL} - \lambda^*)$ (nm)	ε ($mol \cdot l^{-1} \cdot cm^{-1}$)	ϕ^{**} (A)
96	**H**	239	265	272	280*	304	24	10648	0.065
97	**4-Cl**	241	272	280	288*	304	16	6738	0.099
98	**4-Br**	237	272	280	289*	294	5	2880	-
101	**3-CH_3**	247	-	278	287*	301	14	5886	0.039
102	**4-CH_3**	240	-	278	286*	301	15	8449	0.015
103	**3,5-$OC_{12}H_{25}$**	264	-	280	290*	391	101	15584	-
117	**3,5-$OC_3H_6OC_{12}H_{25}$**	264	-	280	290*	391	101	14047	-
	Truxene			298		400	102	65212	0.001

The quenching of fluorescence observed with the introduction of bromine atom can instead be attributed to a more favourable intersystem crossing mainly due to the formations of aggregates due to the poor solubility of the latter in organic solvents, even at very low concentrations. The same quenching of fluorescence is also observed for borazines bearing peripheral alkyl chains. This can be realistically attributed to nonradiative vibrational deactivations triggered by the peripheral alkyl chains, accompanied by the tendency of these species to form supramolecular aggregates.

2.7 VT-NMR isodesmic model[58] *for the aggregation studies*

The self-assembly processes of borazine **103** and **117** was studied by using temperature-dependent spectroscopic measurements. First investigation on the aggregation process for borazine **103** was carried out in 1,1,2,2-tetrachloroethane-d_2 as described by Dr. Hemmett. While in order to promote the self-assembly at room temperature, the aggregation processes for borazine **117** was studied in *n*-octane:1,1,2,2-tetrachloroethane-d_2 95:5. Temperature dependent ^{1}H NMR analysis of both borazines **103** and **117** was performed using a Bruker Advance 400 (^{1}H 400 MHz), on a 0.5 mL solution in a dry NMR tube of 10 mM concentration. Investigation of temperature ranging from -20 to 110 °C led to ^{1}H NMR spectra of borazine **103** shown in Figure 2.43.

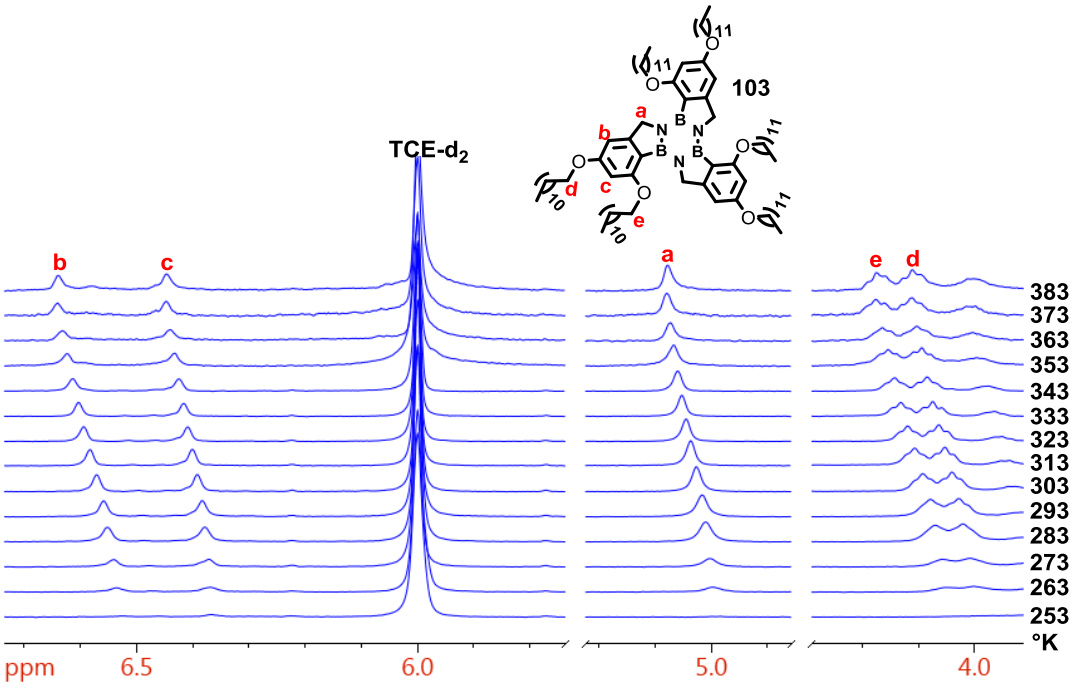

Figure 2.43 Variable temperature ^{1}H NMR spectra of **103**.

The chemical shift of all protons analysed (**a-e**) become more deshielded upon temperature increases. However, the full of both dissociation and aggregation of the polymeric species was not observed since no plateau was reached either at high or low temperatures. A more defined deshielding behaviour upon temperature increasing has been shown by protons **a, b** and **c,** which clearly are the more affected from the aggregation process characterizing borazine **103**. The temperature-dependant data calculated considering the chemical shift of **Ha** and **Hb** (**Hc** shown the same behaviour of **Hb**), were fitted to the isodesmic model using the Boltzmann equation.[59]

$$y = A_2 + \frac{A_2 - A_1}{1 + \exp\left[\frac{x - x_0}{dx}\right]}$$

Where:

A₁ = minimum value of the physical parameter monitored

A₂ = maximum value of the physical parameter monitored

x₀ = melting temperature (***T_m*** when $\emptyset_{agg}$ = 0.5)

dx = characteristic temperature that is related to the slope of the function at the melting temperature (***T****).

This slope is related to *ΔH* via:

$$T^* = \frac{-RT_m^2}{0.908\Delta H}$$

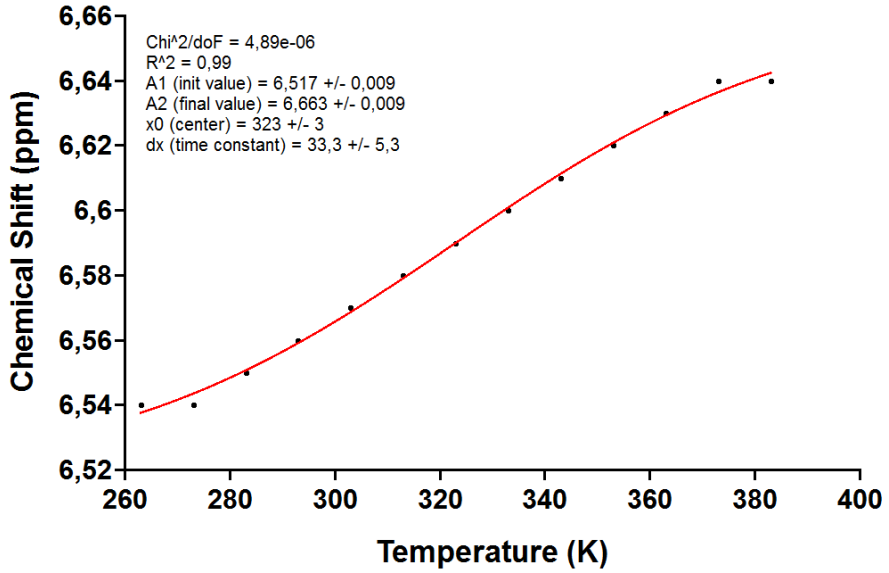

Figure 2.44 Plot of Hb chemical shift vs temperature of **103**.

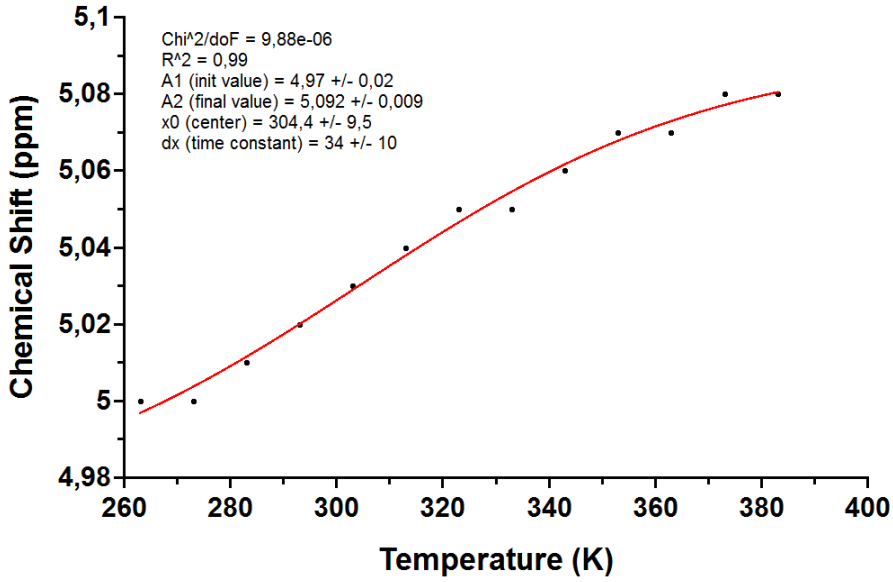

Figure 2.45 Plot of Ha chemical shift vs temperature of **103**.

The degree of aggregation, Ø, as a function of temperature, *T* is given by:

$$\emptyset(T) \approx \frac{1}{1 + exp\left[-0.0908\Delta H \frac{T - T_m}{RT_m^2}\right]}$$

From the degree of aggregation, the number-averaged degree of polymerisation DP_N can be calculated directly, via:

$$DP_n(T) = \frac{1}{\sqrt{1 - \emptyset(T)}}$$

The DP_N can then be related to the total concentration of molecules C_T, and the association constant K, via[60]:

$$DP_n(T) = \frac{1}{2} + \frac{1}{2}\sqrt{4KC_T + 1}$$

From this equation the distribution of material was calculated using the following equations.

$$C_1 = \frac{2KC_T + 1 - \sqrt{4KC_T + 1}}{2K^2C_T}$$

and $C_n = K^{n-1}C_1^n$

The number average aggregate size or the mean number of monomers per π-stack (*N*mers) can be calculated, via[59,61–64]:

$$N = \frac{C_T}{C_N} = \frac{C_1 + 2C_2 + 3C_3 + \ldots + nC_n}{C_1 + C_2 + C_3 + \ldots + C_n}$$

The association constant *K* can be calculated, via:

$$K = \frac{x}{2(C - 2x)}$$

Where:

C = initial concentration

x = *C*[ppm Hf (T)-ppm Hf (final)]/2[ppm Hf (initial)-ppm Hf (final)]

Finally using the Van't Hoff equation is possible to extrapolate the thermodynamic data.

$$lnK = \left(\frac{-\Delta H}{R}\right)\left(\frac{1}{T}\right) + \frac{\Delta S}{R}$$

The graph of ln*K* vs 1/*T* showed a linear relationship as consistent with Van't Hoff fitting, the slope of the graph is related to the ΔH while the intercept to the ΔS (Figure 2.46 and 2.47).

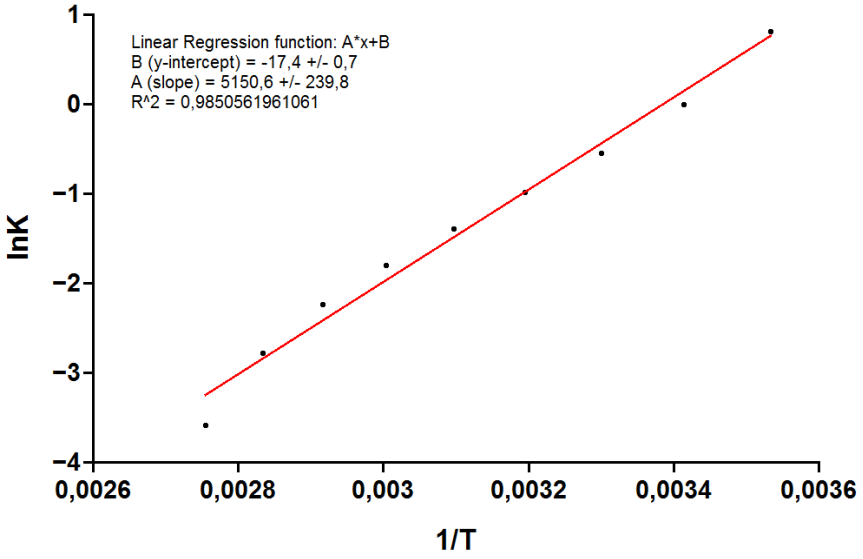

Figure 2.46 Plot of ln*K* vs 1/*T* for Hb of **103**.

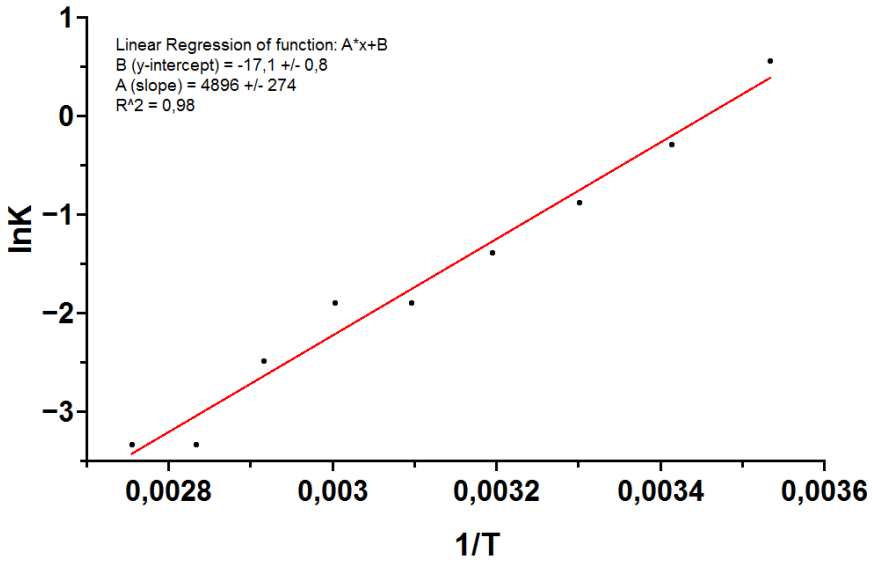

Figure 2.47 Plot of ln*K* vs 1/*T* for Ha of **103**.

The data collected were then fitted with the isodesmic polymerisation model described before with the corresponding equations and the graph shown in Figure 2.48 were obtained.

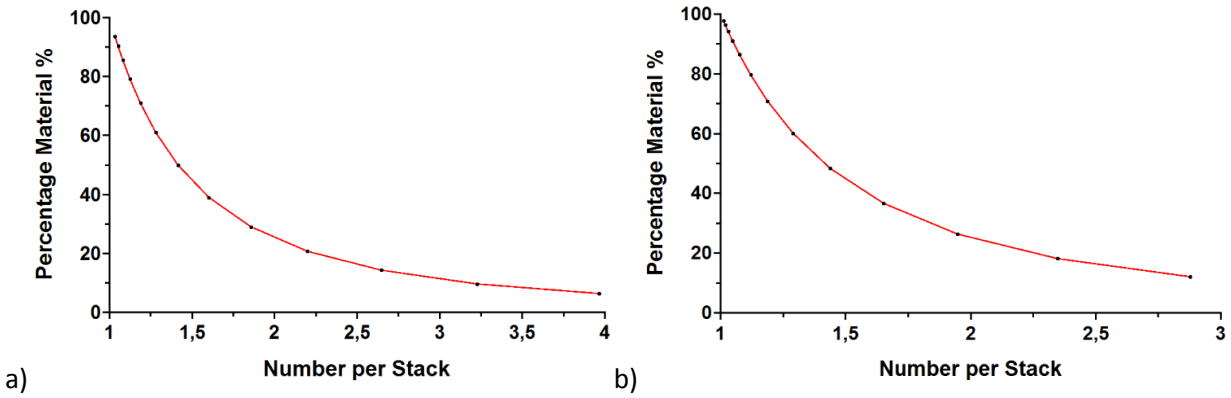

Figure 2.48 Distribution of species of **103** calculated by a)Hb and b) Ha.

The graphs obtained showed that at room temperature the majority of borazine **103** (≈95%) exists as a monomer along with the concentration analysed (10 mM) with 25% of dimers when calculated considering both Ha and Hb. Also, borazine **103** exist at 10-15% as tetrameric and trimeric species. These results suggested that the dimerization process of borazine **103** in 1,1,2,2-tetrachloroethane-d_2 is not dominant as we expected since most of the material is in the monomeric form. However, this process can be favoured by using less polar solvents thus increasing interactions between borazine rings. To this end, as described before, the same investigation was carried out for borazine **117**, which was studied in 10 mM solution of *n*-octane:1,1,2,2-tetrachloroethane-d_2 95:5. The variable temperature ^{1}H NMR spectra collected for borazine **117** at temperature ranging from -15 to 105 °C are shown in Figure 2.49.

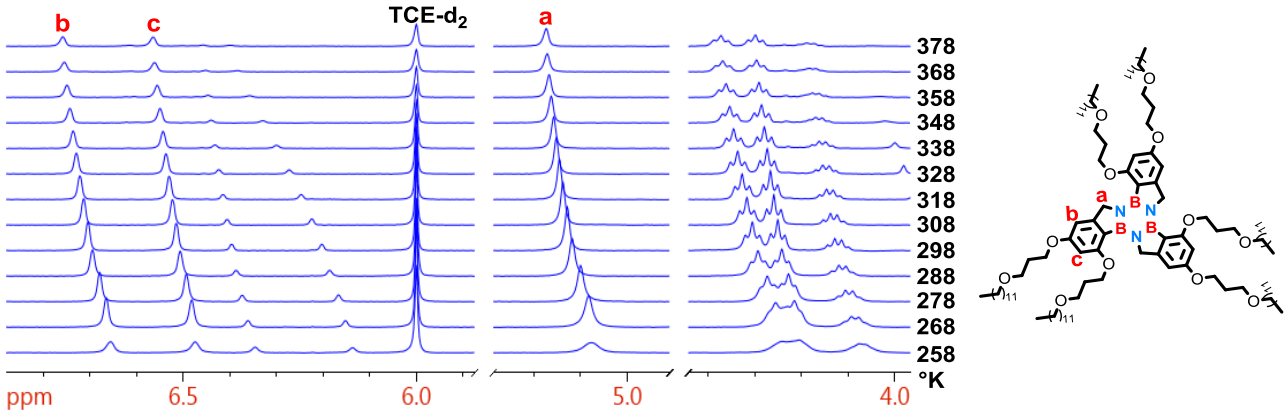

Figure 2.49 Variable temperature ^{1}H NMR spectra of **117**.

The temperature-dependant data calculated considering the chemical shift of **Hb**, was fitted to the isodesmic model using the Boltzmann equation.

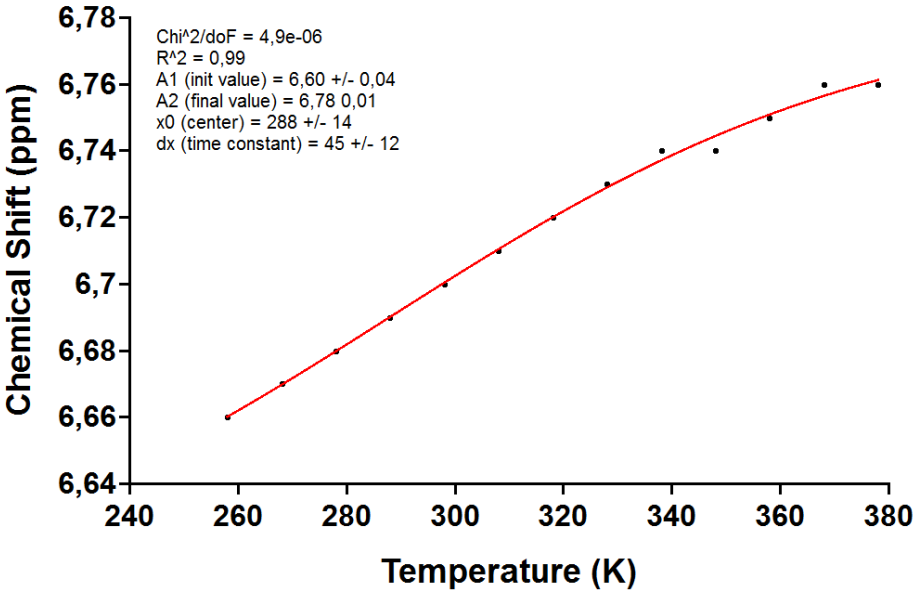

Figure 2.50 Plot of Hb chemical shift vs temperature of **117**.

The graph of ln*K* vs 1/*T* showed a linear relationship as consistent with Van't Hoff fitting (Figure 2.51).

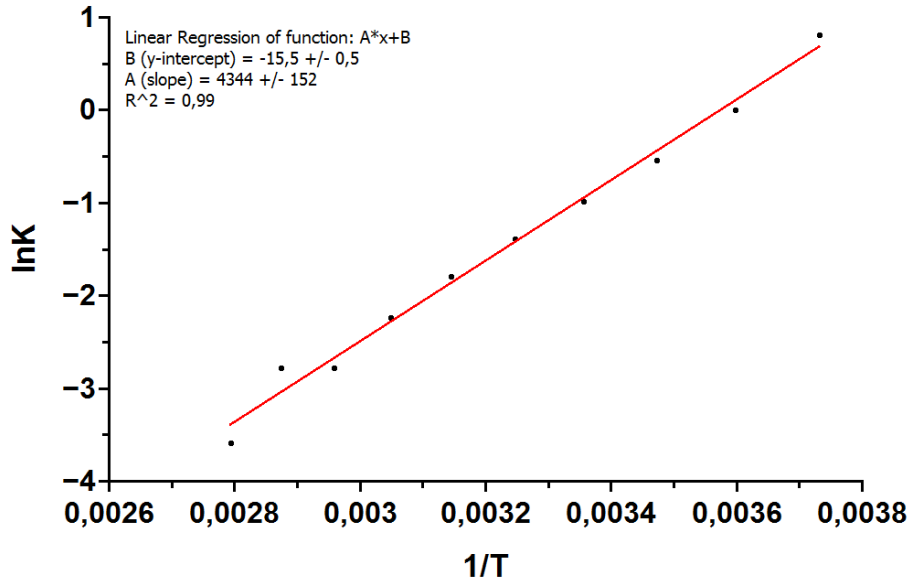

Figure 2.51 Plot of ln*K* vs 1/*T* of **117**.

The data collected were then fitted with the isodesmic polymerisation model described before with the corresponding equations and the graph shown in Figure 2.52 were obtained.

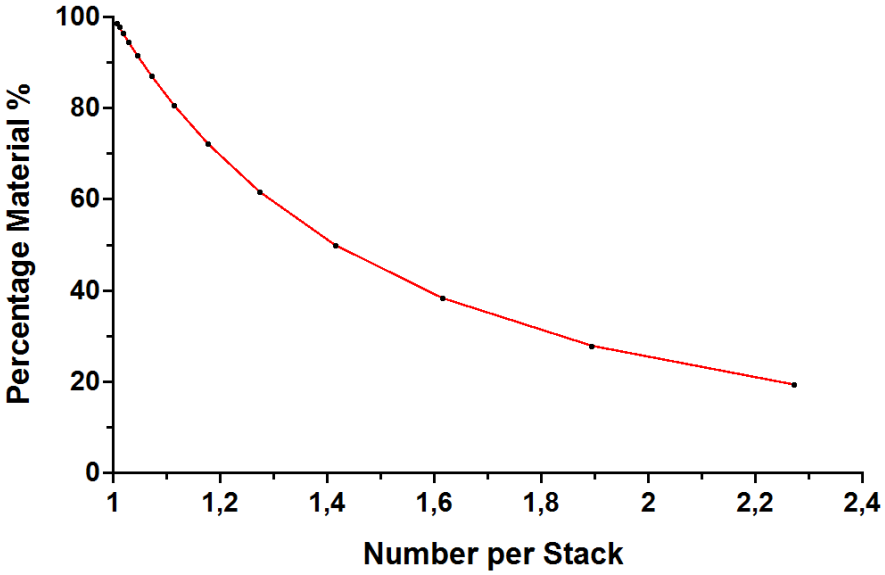

Figure 2.52 Distribution of species of **117.**

The graphs obtained showed that at room temperature the majority of borazine **117** (≈98%) exists as a monomer along with the concentration analysed (10 mM) with 30% of dimers.

REFERENCES

1 F. Goubard and F. Dumur, *RSC Adv.*, 2014, **5**, 3521.
2 Liam Emmett, Doctoral dissertation, University of Bath, 2015.
3 B. Anand, H. Nöth, H. Schwenk-Kircher and A. Troll, *Eur. J. Inorg. Chem.*, 2008, **2008**, 3186.
4 F. Pop, C. Melan, I. Danila, M. Linares, D. Beljonne, D. B. Amabilino and N. Avarvari, *Chem. - A Eur. J.*, 2014, **20**, 17443.
5 M. García-Melchor, M. C. Pacheco, C. Nájera, A. Lledós and G. Ujaque, *ACS Catalysis*, 2012, **2**, 135.
6 R. Singh and G. Just, *J. Org. Chem.*, 1989, **54**, 4453.
7 T. Nishimura, T. Matsuo and K. Sakurai, *Phys. Chem. Chem. Phys.*, 2011, **13**, 15899.
8 M. Lysén, H. M. Hansen, M. Begtrup and J. L. Kristensen, *J. Org. Chem.*, 2006, **71**, 2518.
9 J. Clayden, *Organolithiums: Selectivity for Synthesis*, Pergamon, First Edition., 2002.
10 B. Du, X. Jiang and P. Sun, *J. Org. Chem.*, 2013, **78**, 2786.
11 G. A. Molander, S. L. J. Trice, S. M. Kennedy, S. D. Dreher and M. T. Tudge, *J. Am. Chem. Soc.*, 2012, **134**, 11667.
12 C. Rochais, R. Yougnia, T. Cailly, J. Sopková-de Oliveira Santos, S. Rault and P. Dallemagne, *Tetrahedron*, 2011, **67**, 5806.
13 S.-J. Ahn, C.-Y. Lee, N.-K. Kim and C.-H. Cheon, *J. Org. Chem.*, 2014, **79**, 7277.
14 J. Lozada, Z. Liu and D. M. Perrin, *J. Org. Chem.*, 2014, **79**, 5365.
15 A. J. J. Lennox and G. C. Lloyd-Jones, *Chem. Soc. Rev.*, 2014, **43**, 412.
16 H. Fang, G. Kaur, J. Yan and B. Wang, *Tetrahedron Lett.*, 2005, **46**, 1671.
17 *International Tables for Crystallography*, Springer, 1965.
18 J. B. Moffat, *Can. J. Chem.,* 1964, **43**, 1323.
19 W. H. Scouten, X.-C. Liu, N. Khangin, D. F. Mullica and E. L. Sappenfield, *J. chem. cry.*, 1994, **24**, 621.
20 P. Rodríguez-Cuamatzi, O. I. Arillo-Flores, M. I. Bernal-Uruchurtu and H. Höpfl, *Crystal Growth & Design*, 2005, **5**, 167.
21 M. P. Groziak, L. Chen, L. Yi and P. D. Robinson, *J. Am. Chem. Soc.*, 1997, **119**, 7817.
22 M. Sana, G. Leroy and C. Wilante, *Organometallics*, 1991, **10**, 264.
23 K. Severin, *Dalton Trans.*, 2009, 5254.
24 D. G. Hall, *Boronic Acids*, Wiley-VCH Verlag & Co. KGaA, 2011.
25 C. J. Stress, P. J. Schmidt and D. G. Gillingham, *Org. Biomol. Chem.*, 2016, **14**, 5529.
26 P. Schmidt, C. Stress and D. Gillingham, *Chem. Sci.*, 2015, **6**, 3329.
27 M. B. Smith, *Organic Synthesis*, 3rd Edition., 2010.
28 L. M. Soffer and M. Katz, *J. Am. Chem. Soc.*, 1956, **78**, 1705.
29 M. Srebnik, T. E. Cole, P. V. Ramachandran and H. C. Brown, *J. Org. Chem.*, 1989, **54**, 6085.
30 D. A. Resendiz-Lara, N. E. Stubbs, M. I. Arz, N. E. Pridmore, H. A. Sparkes and I. Manners, *Chem. Commun.*, 2017, **53**, 11701.
31 D. Franz, M. Bolte, H.-W. Lerner and M. Wagner, *Dalton Trans.*, 2011, **40**, 2433.
32 Ö. Seven, M. Bolte, H.-W. Lerner and M. Wagner, *Organometallics*, 2014, **33**, 1291.
33 A. Ledoux, P. Larini, C. Boisson, V. Monteil, J. Raynaud and E. Lacôte, *Angew. Chem. Int. Ed.*, 2015, **54**, 15744.
34 J. C. Catlin and H. R. Snyder, *J. Org. Chem.*, 1969, **34**, 1664.
35 K. J. Doyle, H. Tran, M. Baldoni-Olivencia, M. Karabulut and P. E. Hoggard, *In. Chem.,* 2008, **47**, 7029.
36 S. Toyota, T. Futawaka, M. Asakura, H. Ikeda and M. Ōki, *Organometallics*, 1998, **17**, 4155.
37 C. O. Kappe, A. Stadler and D. Dallinger, *Microwaves in Organic and Medicinal Chemistry*, Wiley-VCH Verlag & Co. KGaA, Second, Completely Revised and Enlarged Edition., 2012.
38 C. D. Roy and H. C. Brown, *J. Organomet. Chem.*, 2007, **692**, 784.
39 H. Noth and B. Wrackmeyer, *Nuclear Magnetic Resonance Spectroscopy of Boron Compounds*, Springer-Verlag Berlin Heidelberg, 1 st edition., 1978.
40 J. L. Adcock and J. J. Lagowski, *In. Chem.,* 1973, **12**, 2533.
41 V. Jonas and G. Frenking, *J. Chem. Soc., Chem. Commun.*, 1994, 1489.
42 W. Luo, P. G. Campbell, L. N. Zakharov and S.-Y. Liu, *J. Am. Chem. Soc.*, 2011, **133**, 19326.
43 A. Staubitz, A. P. M. Robertson, M. E. Sloan and I. Manners, *Chem. Rev.*, 2010, **110**, 4023.
44 V. Pons and R. T. Baker, *Angew. Chem. Int. Ed.*, 2008, **47**, 9600.
45 M. Krieg, F. Reicherter, P. Haiss, M. Ströbele, K. Eichele, M.-J. Treanor, R. Schaub and H. F. Bettinger, *Angew. Chem. Int. Ed.,* 2015, **54**, 8284.
46 D. Bonifazi, F. Fasano, M. M. Lorenzo-Garcia, D. Marinelli, H. Oubaha and J. Tasseroul, *Chem. Commun.*, 2015, **51**, 15222.
47 S. Kervyn, N. Kalashnyk, M. Riello, B. Moreton, J. Tasseroul, J. Wouters, T. S. Jones, A. De Vita, G. Costantini and D. Bonifazi, *Angew. Chem. Int. Ed.*, 2013, **52**, 7410.
48 S. Kervyn, O. Fenwick, F. Di Stasio, Y. S. Shin, J. Wouters, G. Accorsi, S. Osella, D. Beljonne, F. Cacialli and D. Bonifazi, *Chem. - A Eur. J.*, 2013, **19**, 7771.
49 J. Dosso, J. Tasseroul, F. Fasano, D. Marinelli, N. Biot, A. Fermi and D. Bonifazi, *Angew. Chem. Int. Ed.*, 2017, **56**, 4483.
50 M. Müller, S. Behnle, C. Maichle-Mössmer and H. F. Bettinger, *Chem. Commun.*, 2014, **50**, 7821.
51 D. K. Frantz, J. J. Walish and T. M. Swager, *Org. Lett.*, 2013, **15**, 4782.
52 H. Norouzi-Arasi, A. K. Pal, S. Nag, D. Chartrand and G. S. Hanan, *Chem. Commun.*, 2016, **52**, 12159.
53 W.C. Hamilton, J.A. Ibers, and W.A. Benjamin, *Hydrogen Bonding in Solids*.
54 M. Touaibia, A. Djimdé, F. Cao, E. Boilard, S. Bezzine, G. Lambeau, C. Redeuilh, A. Lamouri, F. Massicot, F. Chau, C.-Z. Dong and F. Heymans, *J. Med. Chem.*, 2007, **50**, 1618.
55 X.-Y. Wang, J.-Y. Wang and J. Pei, *Chem. - A Eur. J.,* 2015, **21**, 3528.
56 J. S. A. Ishibashi, J. L. Marshall, A. Mazière, G. J. Lovinger, B. Li, L. N. Zakharov, A. Dargelos, A. Graciaa, A. Chrostowska and S.-Y. Liu, *J. Am. Chem. Soc.*, 2014, **136**, 15414.
57 A. L. Appleton, S. M. Brombosz, S. Barlow, J. S. Sears, J.-L. Bredas, S. R. Marder and U. H. F. Bunz, *Nat Commun*, 2010, **1**, 91.
58 N. Ponnuswamy, G. D. Pantoş, M. M. J. Smulders and J. K. M. Sanders, *J. Am. Chem. Soc.*, 2012, **134**, 566.
59 M. M. J. Smulders, M. M. L. Nieuwenhuizen, T. F. A. De Greef, P. van der Schoot, A. P. H. J. Schenning and E. W. Meijer, *Chem. -Eur. J.*, 2010, **16**, 362.
60 Z. Chen, A. Lohr, C. R. Saha-Möller and F. Würthner, *Chem. Soc. Rev.*, 2009, **38**, 564.
61 N. J. Baxter, M. P. Williamson, T. H. Lilley and E. Haslam, *J. Chem. Soc. Faraday Trans.*, 1996, **92**, 231.

62 A. Ciferri, *Supramolecular Polymers*, CRC Press, Boca Raton, Florida, 2nd edn., 2005.
63 J. R. Henderson, *J. Chem. Phys.*, 2000, **113**, 5965.
64 D. Zhao and J. S. Moore, *Org. Biomol. Chem.*, 2003, **1**, 3471.

CHAPTER 3

Synthesis and Characterization of Benzo(c)naphtho(2,1-p)borazachrysene and derivatives

3.1 Introduction

Along with the intriguing synthetic project for the preparation of functionalized borazatruxene derivatives, during the course of our study we have also been interested in exploring the possibility of creating BN-doped geodesic polyarenes. The latter is a specific family of polycyclic aromatic hydrocarbons (PAHs) characterized by the curved surface reminding of the surface of the earth (hence the term "geodesic"). The geodesic polyarenes curved shape is a result of 5 and 6-membered rings condensed together, which make up the faces of 3D-polyhedral structures where trigonal carbon atoms sit at the vertices and carbon-carbon bonds form the edges. Classic examples that reflects this description are fullerenes, classified as "closed" geodesic polyarenes and subunits of fullerenes that lack one or more of the rings remaining curved, classified as "opened" geodesic polyarenes (Figure 3.1). The latter are also defined in the literature as bowl-shaped PAHs, fullerene fragments, and buckybowls; corannulene is the smallest and simplest curved subunit of C_{60}.

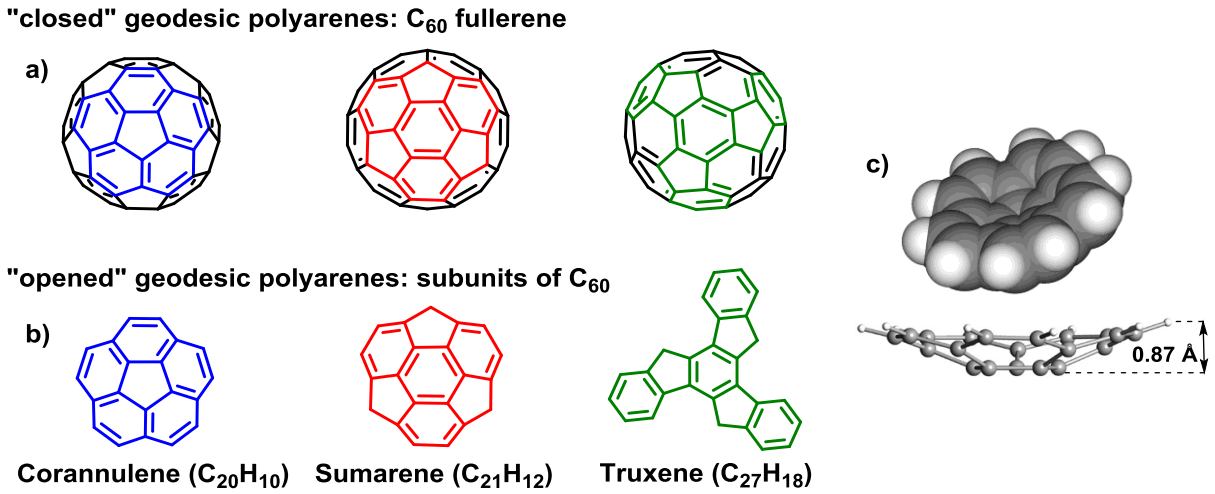

Figure 3.1 Representation of a) "closed" and b) "opened" geodesic polyarenes.

In the past, the synthesis of these material was very challenging since it required numerous reaction steps and purification processes.[1] Therefore, these molecules remained less well explored[1] until fullerene was discovered in 1985.[2] This discovery led to a great progress in the synthesis of these materials mainly attributed to the emergence of innovative techniques as the flash vacuum pyrolysis (FVP) or the chemical vapour deposition (CVD), which proved to be effective synthetic tools for constructing geodesic polyarenes.[3–5] Usually, planar PAHs derivatives are subjected to very high vacuum and temperatures, therefore, they react intramolecularly in the gas phase. These strong reaction conditions promote the formation of new C-C bond between the two closest sp^2 carbon atoms *via* radical pathway affording the rings closure.[1]

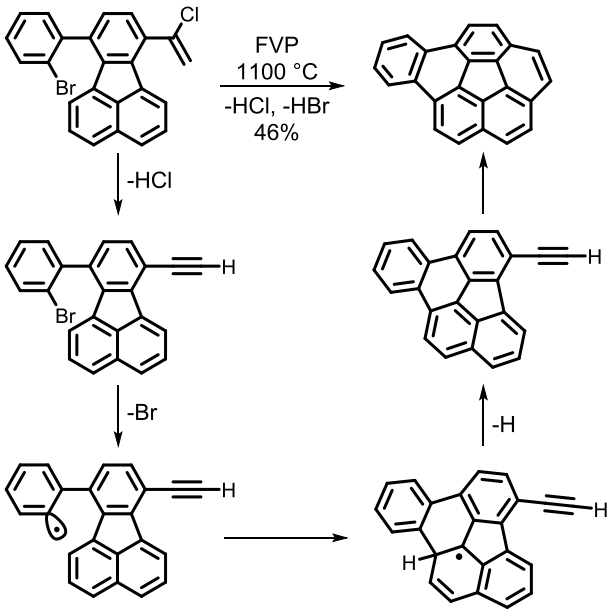

Scheme 3.1 Example of synthesis of corannulene derivatives by flash vacuum pyrolysis (FVP).

Corannulene and its derivatives are π-electron rich compounds featured by a dipole moment, since the electron density on the concave face is different from the one on the convex face.[6] Also, according to both theoretical and experimental studies, it has been established that corannulene is a flexible molecule and the bowl-to-bowl inversion barrier, passing through a planar structure configuration as a transitional state, ranges between 10-12 kcal mol^{-1} (Figure 3.2).[7]

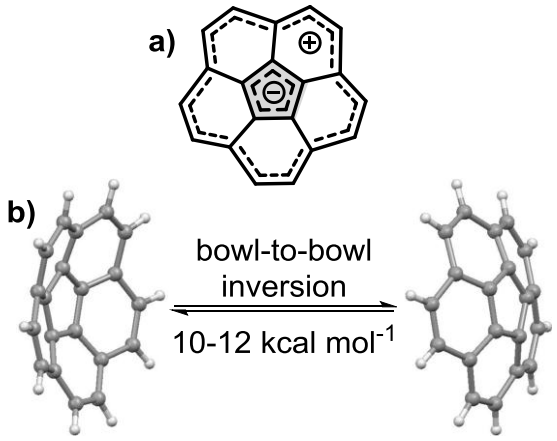

Figure 3.2 Representation of corannulene bowl-to-bowl inversion.

The electronic and structural properties are strongly influenced by the presence of substituted groups. Functionalization of these materials is becoming extremely attractive in the materials science and engineering areas.[6] The introduction of functional groups or the chemical doping of "fullerene fragments" is currently emerging as a powerful tool to tune their physicochemical and optoelectronic properties to design new molecules for organic electronic.[6] In addition, corannulene and more complex fused π-

conjugated derivatives have been utilized in supramolecular chemistry for the synthesis of complexes with alkaline and transition metals.[6] They have also been used in the host-guest chemistry for making C_{60} and C_{70} fullerenes-based molecules as the recently reported tetra-cationic cyclophane $ExBox^{4+}$ supramolecular complex[8] (Figure 3.3).

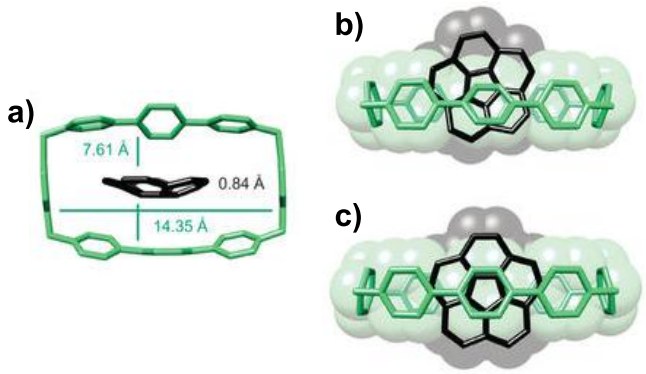

Figure 3.3 b-c) Top and a) side-on views of the X-ray crystallography superstructures of corannulene and $ExBox^{4+}$.[8]

These multifunctional materials are potential candidates for different applications in supramolecular chemistry, for instance in chemical encapsulation,[9] drugs-delivery and motors for future nanoscale machinery[10,11] or in organic electronic as photoemitters of electrons or active materials for electronical devices.[12] Also important is their use as precursors for the synthesis of fullerenes.[13,14]

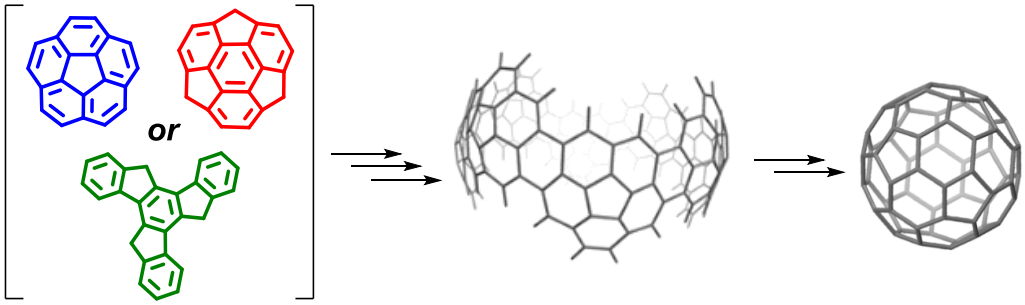

Scheme 3.2 Synthesis of fullerene fragments and Buckminsterfullerene C_{60} starting from flat and bowl-shaped PAHs.

Fascinated by all these intriguing features, we have reasoned that these materials might be also tunable, in terms of electronic properties, by replacement of C=C unit with the more polarized B-N covalent bond. We therefore assumed that our synthetic knowledge in doping truxene to achieve the corresponding BN-doped borazatruxene, would similarly allow us to produce BN-doped fullerene fragments with the borazine ring. A particular attention has been addressed to the BN-doping of $C_{30}H_{12}$ hemifullerene-C_3 (triindenotriphenylene) **1**, since the latter can be synthetized either starting from truxene derivative **2** as reported by Sygula and co-workers[7] or using benzo(c)naphtho(2,1-p) chrysene derivatives **3** and **4** as reported by Scott and co-workers.[15]

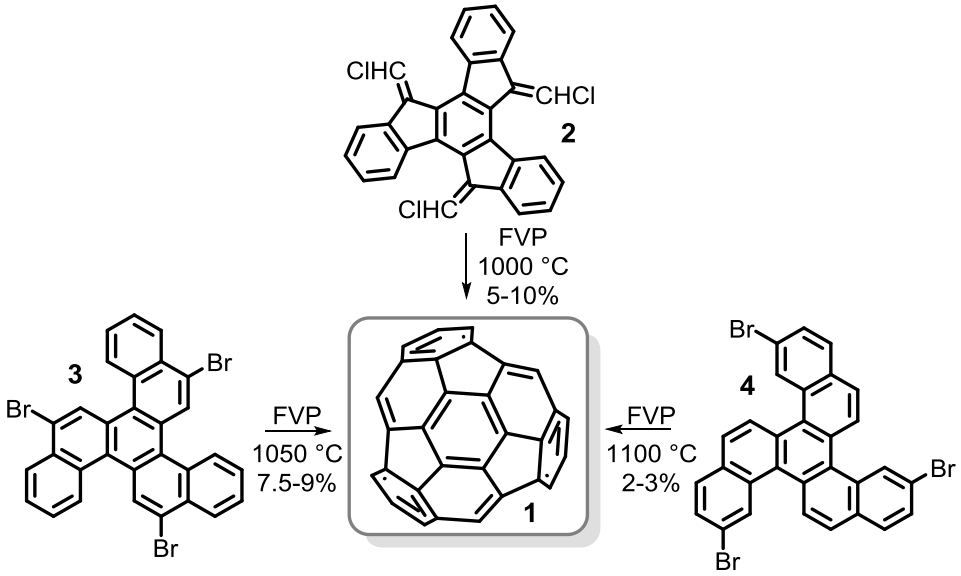

Scheme 3.3 Synthesis of hemifullerene **1** starting from different PAHs precursors.

3.1.1 Retrosynthetic analysis for the synthesis of BN-hemifullerene

We envisioned that the BN doping of hemifullerene could be achieved by replacing the C=C units of the central aromatic core with the BN unit providing that the 6 membered borazine ring following a bottom-up synthetic method. The synthetic pathway designed for the synthesis of BN-doped hemifullerene **5** was strategically developed by a retrosynthetic approach as shown in Scheme 3.4.

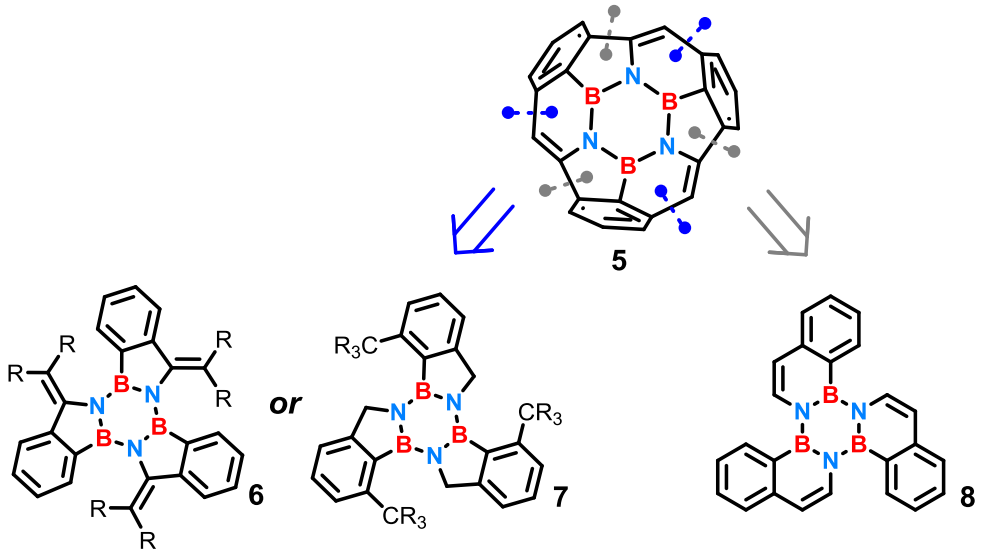

Scheme 3.4 Retrosynthetic analysis of BN-doped hemifullerene.

Disconnections of different areas of **5** led us to envisage the construction of the target molecule following two different synthetic pathways. In the first approach considered (blue), either vinyl functionalized

borazatruxenes **6** in the benzylic position or borazatruxenes ortho substituted respect to the boron atom **7** seemed to be valid precursors for the synthesis of **5**. A this point we decided to employ in this synthetic process the borazines **10** and **11** previously synthesised and described in Chapter 2. Despite the substituent in the benzylic position of borazine **10** was an sp^3 methyl group we considered to achieve the vinyl functional group by dehydrogenation in presence of Pd/C and then with the real precursor **9** in hand to proceed with the synthesis of **5**.

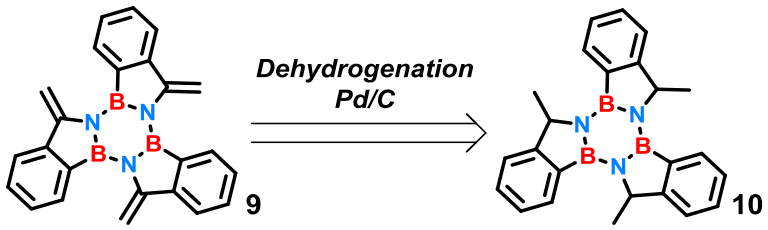

Scheme 3.5 Retrosynthetic analysis of compound **9**.

Regarding borazine **11**, we believed that under the drastic reaction conditions used in the flash vacuum pyrolysis (FVP) procedure, both benzylic positions might be susceptible to the radical formation which in turn could react internally closing the ring (Scheme 3.6).

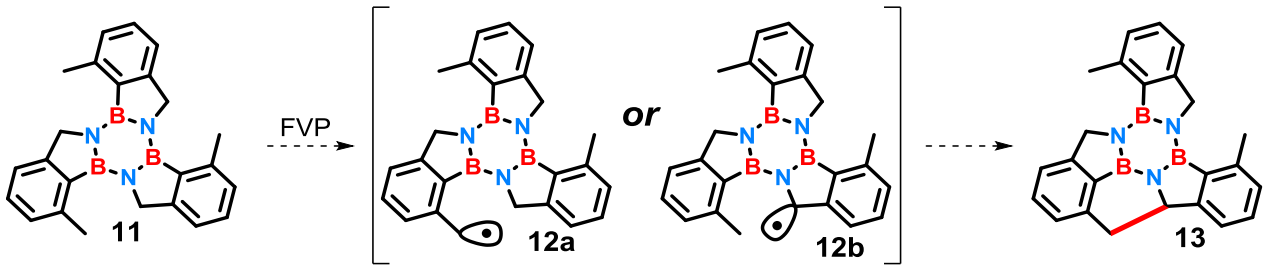

Scheme 3.6 Mechanism proposed for the ring closure of **10** by FVP.

For benzo(c)naphtho(2,1-p)borazachrysene **8** we also performed a retrosynthetic analysis. Initially, the disconnection of the borazine ring led to three molecules of 1,2-dihydroborazaronaphthalene **14**. However, this molecule is involved in the tautomeric equilibrium with the corresponding imine species **15** which unlikely go forward the borazine ring formation. This because during the borazine formation each couple on BN unit needs to lose two molecules of hydrogen to form the new B-N bonds. In the case of **15** this is not possible since only a molecule of hydrogen can be released. Also 1,2-borazaronaphthalene species **16**, that we envisioned to be an alternative substrate to utilize, is involved in the amine-imine tautomeric equilibrium[16,17] with the inactive imine species **17**.

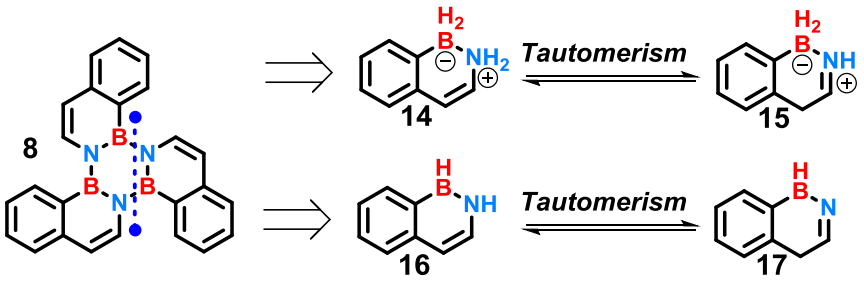

Scheme 3.7 Retrosynthetic analysis of compound **8.**

Given the fact that this first approach proved to be ineffective we considered an alternative tactic for the synthesis of **8**. Another route that we later explored started from saturated 1,2,3,4-tetrahydro-1,2-borazaronaphthalene **19** to synthesise the corresponding borazine **18** with the already developed thermolysis process and then to introduce instaurations in α and β positions by dehydrogenation in presence of Pd/C. In turn, amine-borane **19** could potentially be achieved by following the same synthetic procedure utilized for the synthesis of amine-boranes detailed in Chapter 2 for the synthesis of borazatruxenes. Indeed, from the retrosynthetic perspective, we could have access to amine-borane **19** by one-step reduction of *o*-phenylacetonitrile boronic ester derivatives **20** and boron atom would be regioselectively installed in *ortho* position to the acetonitrile group by Miyaura cross-coupling reaction of commercially available *o*-bromophenyl acetonitriles **21** (Scheme 3.8).

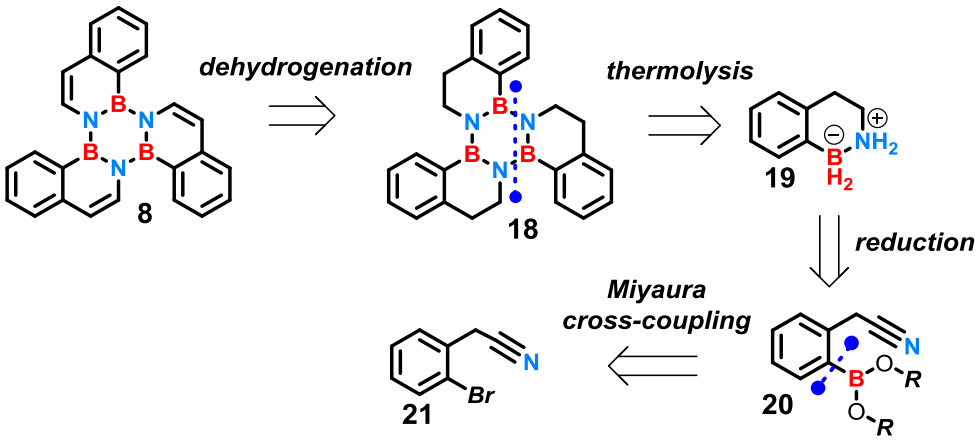

Scheme 3.8 Alternative approach for the synthesis of **9**.

3.2 Synthesis of 2,1-borazaronaphthalene derivatives

Simultaneously another alternative retrosynthetic pathway was envisaged for the synthesis of a similar borazine to **8**. To overcome the problem related to the amine-imine tautomeric equilibrium of species **14** and **16**, we hypothesized to use a similar building block **23** with boron and nitrogen atoms changed position.

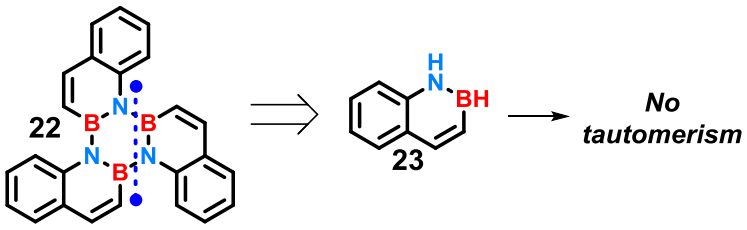

Scheme 3.9 Alternative approach for the synthesis of **9.**

This strategy seemed to be better compared with the first approach considered because the step of the dehydrogenation would be avoided; moreover 2,1-borazaronaphthalene **23** is a well-established molecule and the synthesis of this building block was pioneered by Dewar and co-workers in the 50s and 60s. Also, a great contribution in developing new synthetic methods to access BN heteroarenes in a more straightforward manner is addressed by Molander,[18–21] Piers,[22–24] Pei[25] and Liu and co-workers.[26] Indeed, for the synthesis of 2,1-borazaronaphthalene **23** and the corresponding derivatives we followed a method introduced by Liu and co-workers,[27] which consists of two steps reaction.

Table 3.1 Synthesis of 2-aminostyrene derivatives **27** and **28**.

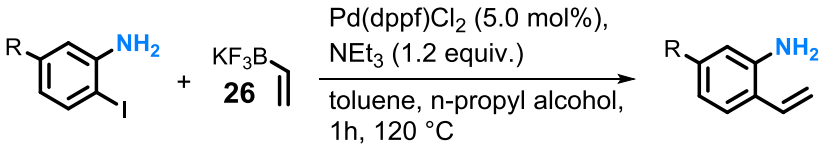

Entry	R	Product	%yield
24	H	**27**	87
25	Cl	**28**	70

Initially the Suzuki cross-coupling protocol was utilized to install the vinyl group in *ortho* position to the ammine group of commercially available starting materials **24** and **25**. Iodoaniline was chosen as test compound in our initial evaluation. The reaction was performed in a mixture of anhydrous toluene and degassed *n*-propyl alcohol under inert atmosphere (Argon). Compound **24** was reacted at 120 °C with potassium vinyltrifluoroborate **26** in presence of triethylamine and Pd(dppf)Cl_2. The reaction was followed by TLC chromatography analysis where a sample of reaction beforehand diluted with ethyl acetate was

eluted with *n*-hexane/CH_2Cl_2 (60:40). A full conversion of **24** was achieved after 1 h of refluxing, but unfortunately the attempt to reproduce the work-up procedure described in the literature[27] resulted in loss of product. Interestingly when the crude mixture was exposed to the air an immediate change in color passing from dark green to brown was observed. Considering that styrene spontaneously polymerizes when exposed to the atmospheric moist air and oxygen, we supposed that a similar side reaction occurred with product **28**. This assumption was later confirmed by a literature procedure,[28] which detailed about the spontaneous polymerization of aminostyrenes in presence of their corresponding salts.

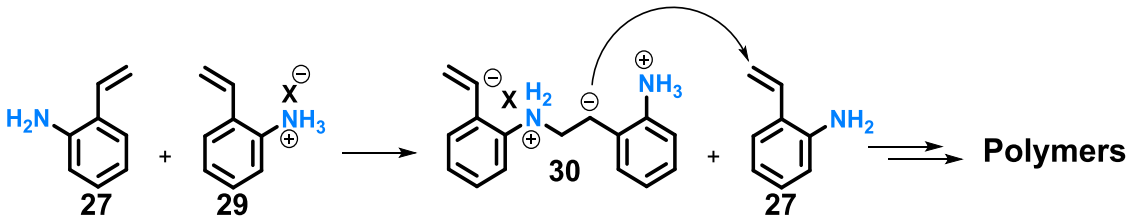

Scheme 3.10 Mechanism proposed for the aminostyrene ionic polymerization.

The initiation step is caused by the nucleophilic attack of 2-aminostyrene molecule **27** on the activated β-position of the double bond of the monomer salt **29** to give a zwitterionic propagating species **30**. On the other hand, the mechanism of propagation has been considered to occur through the nucleophilic addition of the zwitterionic propagating species **30** to a new monomer salt **27**. Thus, improvement in the work-up have been made by a rapid washing of the crude mixture dissolved in ethyl acetate with deionized water followed by a rapid removing of the organic solvent under reduced pressure. The crude product was then purified by flash silica gel chromatography eluting with a more polar eluent composed by *n*-hexane/EtOAc (80:20) in order to minimize the formation of oligomers. The desired compound **27** was obtained in 87% yield and the ^{1}H NMR spectrum perfectly matched with that reported in literature,[29] confirming the molecular structure. Attempt at the synthesis of **28** following the same procedure resulted in a partial conversion into the desired products even when the reaction time was increased at 3 hours. A notable improvement was observed when increasing the amount of both vinyltrifluoroborate **26** and triethylamine to 1.7 equivalents yielding products **28** in 70% yield. Analysis of the NMR data collected for **28** gave the same results reported in literature,[29] confirming the molecular structure. The synthesis of targeted compounds **23** and **35** was adapted from Dewar's original protocol for the preparation of 1,2-BN naphthalenes.[30] This method consists of two consecutive steps: in the first step the new covalent bond between boron and nitrogen atoms is formed closing the 6-membered ring. In the last step reduction with $LiAlH_4$ converted the resulting 2-chloro-2,1-borazaronaphthalene **33** into the more stable 2,1-borazaronaphthalene **23**. A plausible mechanism leading to the formation of 2-chloro-2,1-borazaronaphthalene **33** is shown in Scheme 3.11.

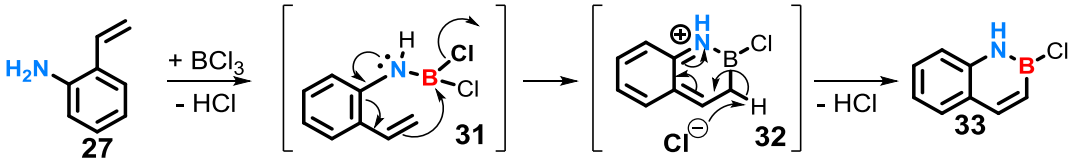

Scheme 3.11 Proposed mechanism for the synthesis of 2-chloro-2,1-borazaronaphthalene.

The first stage is a well-established reaction,[31] which involves an initial coordination of BCl_3 to the primary aromatic amine resulting in the formation of a covalent N–B bond with loss of HCl. This stage is followed by a nucleophilic attack of the terminal alkene to the boron atom, resulting in cyclization with loss of Cl^- yielding the iminium intermediate **32**. The driving force that promotes the formation of **33** (that otherwise should not happen for a loss of aromaticity), is mainly due to the resonance stabilization given by the amine group. The aromaticity is subsequently restored in the last stage by elimination of a molecule of HCl giving 2-chloro-2,1-borazaronaphthalene **33**. The latter is directly reduced in presence of $LiAlH_4$ yielding the desired 2,1-borazaronaphthalene **23**.

Table 3.2 Reduction of 2-chloro-2,1-borazaronaphthalenes **33** and **34**.

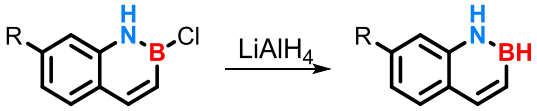

Entry	R	Product	%yield
33	H	**23**	43
34	Cl	**35**	43

The reaction was performed in anhydrous toluene under inert atmosphere (Argon) and a solution of BCl_3 (1M in heptane) was added dropwise to a solution of **27** at -30 °C. At the end of the addition, the resulting mixture was allowed to warm to room temperature accompanied by the formation of a white precipitate. The suspension was refluxed for 18 hours and then the resulting solution was cooled to room temperature. Toluene was removed under reduced pressure without opening the flask to avoid side reactions occurring between **33** and the air moisture. Indeed B-Cl bond **36** is highly susceptible to the moisture since it can easily react with water giving the corresponding more stable boronic acid form **37**.[30]

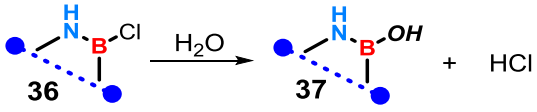

Scheme 3.12 Synthesis of boronic acid **36** by nucleophilic attack of water to the B-Cl bond.

The latter is an unusable substrate for the thermolysis process and also is very challenging to reduce B-OH back to the amino-borane functional group. Therefore, 2-chloro-2,1-borazaronaphthalene **33** was directly

used in the next step of the reduction dissolving the crude product in anhydrous THF and then cooling the resulting mixture to -78 °C. A solution of $LiAlH_4$ was added dropwise to the solution at -78 °C and the resulting mixture was allowed to warm to room temperature and then refluxed. A full conversion was achieved after 12 hours of refluxing. The reaction was followed by TLC chromatography analysis: a sample of reaction was quenched with 1 M HCl, extracted with ethyl acetate and then eluted with CH_2Cl_2. The diagnostic spot at roughly R*f*=0.4 was further confirmed by a changing in colour to dark blue when reacted with a cerium-ammonium-molybdate staining solution (mainly sensitive for amines and amides), confirming the presence of amino-borane product **23**. The crude amino-borane was obtained upon hydrolysis by careful addition of 1 M HCl to the mix at -5 °C in order to decompose the excess of $LiAlH_4$ and then extracted with CH_2Cl_2. The pure product was isolated by silica gel flash chromatography (*n*-hexane/EtOAc 80 : 20) in 43% yield over two steps. The desired **35** was subsequently obtained in the same yield percentage of **23** over two steps following the same synthetic procedure. The ^{11}B NMR spectrum confirmed the molecular structure of aminoboranes **23** and **35**, displaying a doublet resonating at 32.0 and 32.5ppm with a J_{BH} coupling of 130 Hz in line with that reported in literature for these species.[32]

3.3 Borazine synthesis by thermolysis of 2,1-borazaronaphthalene derivatives

With building blocks **23** and **35** in hand we proceeded with the synthesis of the corresponding borazines following the same thermolysis protocol described in Chapter 2.

Table 3.3 Attempt at the synthesis of borazines **37** and **38**.

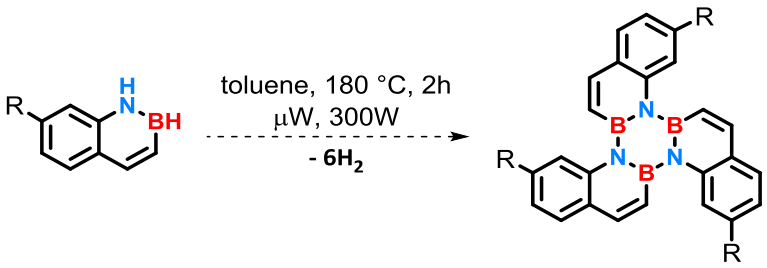

Entry	R	Product	%yield
23	H	**22**	-
35	Cl	**38**	-

Aminoborane **23** was employed as compound test in our initial evaluation of the reaction conditions. First attempt at the cyclotrimerization resulted in a complex mixture of products. Our efforts to isolate and identify part of the components of the mixture by chromatography purification failed. Unfortunately, most of the products were lost during the elution since they reacted with the acidic -OH groups of silica remained blocked on the column. Only few products were isolated; however, in most of the cases NMR

analysis (^{1}H, ^{11}B and COSY) was difficult to interpret, preventing us from a complete characterization. In an attempt to minimize the amount of by-products formed, we repeated the reaction using different reaction conditions. We initially explored the possibility to promote the intermolecular boron-nitrogen bonding formation by using a metal catalyzed procedure. Liu and co-workers reported a catalytic dehydrogenation using $FeCl_2$ for the synthesis of borazines starting from their corresponding amine-borane precursors.[33] Despite the starting material was different, we followed this procedure for the synthesis of borazine **22**. Microwave irradiation of aminoborane **23** in presence of 5 mol% of $FeCl_2$ catalyst in toluene at 180 °C for 2 hours, unfortunately resulted again in a complex mixture of products difficult to purify. Other attempts with different catalysts such as Pd/C, commonly used in the dehydrogenation procedures, or Lewis acids as Al_2O_3, were also not successful to convert **23** into the corresponding borazine **22**. We also tried to increase the reactivity of amino-borane **22** directly using 2-chloro-2,1-borazaronaphthalene **33** in the thermolysis process, since the loss of a molecule of HCl is more favourable then a molecule of hydrogen. However, the outcome was identical even when we forced the reaction conditions increasing the temperature to 190 °C or the reaction time to 10 hours.

Table 3.4 Reaction conditions used for the synthesis of borazines **37**

Reaction Conditions	***outcome***
180 °C, µW, 2h $FeCl_2$	✗
180 °C, µW, 2h Pd/C	✗
180 °C, µW, 2h Al_2O_3	✗
180 °C, µW, 2h starting form -NH-BCl- **33**	✗
180 °C, µW 10 h	✗
190 °C, µW 2h	✗

Unfortunately, this synthetic pathway was not successful for the synthesis of borazine **22**, therefore we reconsidered the first synthetic strategy initially planned starting from saturated 1,2,3,4-tetrahydro-1,2-borazaronaphthalene **19**.

3.4 Synthesis of 1,2,3,4-tetrahydro-1,2-borazaronaphthalene derivatives

As outlined at the beginning of the chapter 1,2,3,4-tetrahydro-1,2-borazaronaphthalene **19** and substituted derivatives can be obtained by one-step reduction of *o*-phenylacetonitrile boronic ester derivatives **20**. In turn, the latter could be synthesised by Miyaura cross-coupling reaction starting from commercially available *o*-bromophenyl acetonitriles **21**. However, before to begin with this synthetic procedure, we attempted the lithiation-borylation of 2-(3-chlorophenyl) acetonitrile **39** since it was already available in our lab. We envisioned that starting material **39**, if subjected to the standard lithiation-

borylation protocol[34] described in Chapter 2, would provide the two regioisomeric boronic esters derivatives **40** and **41**. Subsequent treatment with $LiAlH_4$ would deliver the corresponding amine-boranes **42** and **43**, which are both suitable building blocks for the synthesis of the corresponding borazines **44** and **45**.

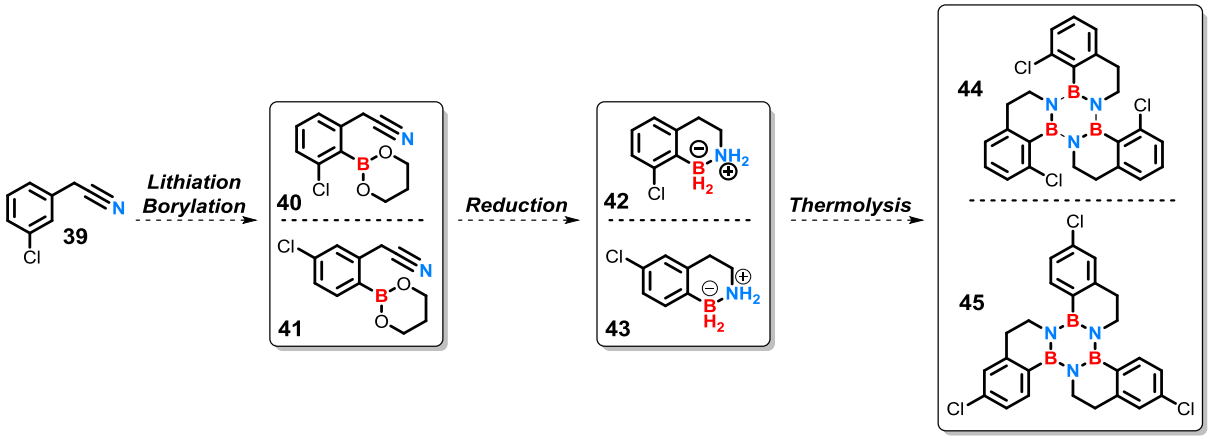

Scheme 3.13 Plane envisioned for the synthesis of borazines **44** and **45**.

Lithiation-borylation of **39** under the same reaction conditions reported in Chapter 2, led only to the recovery of starting material. Surprisingly no products or even by-products were observed. Therefore, to fully understand the reaction mechanism occurring between **39** and the lithiating agent species, we took advantages of the lithium-deuterium exchange experiment. The reaction was repeated under the same reaction conditions and once the lithiated species **47** was formed at -78 °C, the reaction was quenched with deuterated methanol **48** so that deuterium atom displaced lithium atom leading to the deuterated starting material **46**. After work-up the crude product was analysed by ^{1}H NMR, which displayed an attenuation of the singlet related to the Ph-CH_2- of the benzylic position, also the singlet became a triplet with a germinal H-D *J* coupling of 2.1 Hz in good agreement with that reported literature.[35]

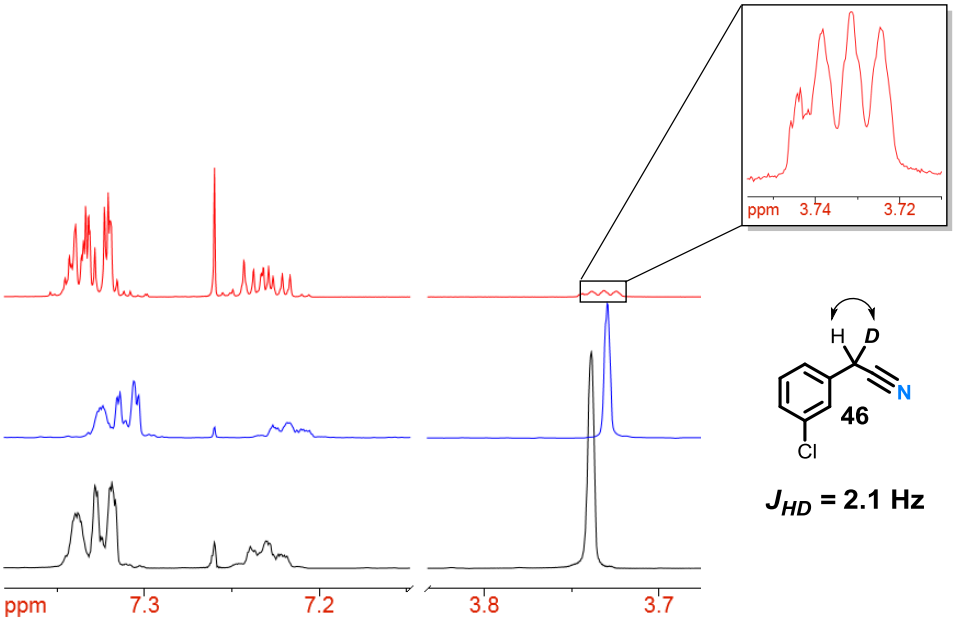

Figure 3.4 Comparison between ^{1}H-NMR spectra in $CDCl_3$ of starting material **39** (black), after lithiation-borylation of **39** (blue) and after lithiation of **39** quenched with deuterated methanol (red).

Therefore the lithiation of 2-(3-chlorophenyl)acetonitrile **39** evolved towards the formation of the lithiated species in the benzylic position **47** rather than on the benzene ring as shown in Scheme 3.14.

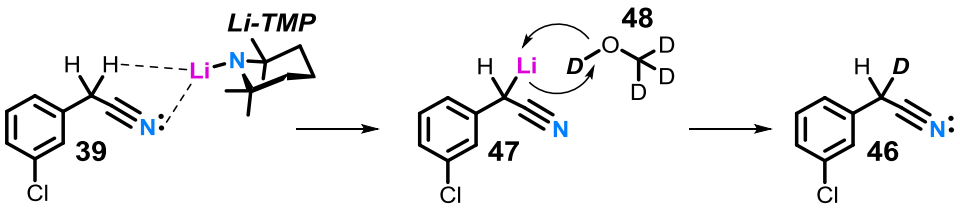

Scheme 3.14 Proposed mechanism for the synthesis of **46**.

Nitrogen atom of cyano group coordinated lithium atom of Li-TMP adduct and lithiation occurred on the closest nucleophilic centre: the benzylic position. This methodology could not be applied for the borylation of phenylacetonitriles so we moved towards the Miyaura cross-coupling reaction protocol as previously planned.

3.4.1 Borylation of *o*-bromophenyl acetonitriles by Miyaura cross-coupling reaction

Borylation of commercially available *o*-bromophenyl acetonitrile **21** followed the same literature procedure[36] described in Chapter 2 for the borylation *o*-bromobenzonitrile species. The reaction was carried out under the identical reaction conditions reported, giving **50** in 98% yield.

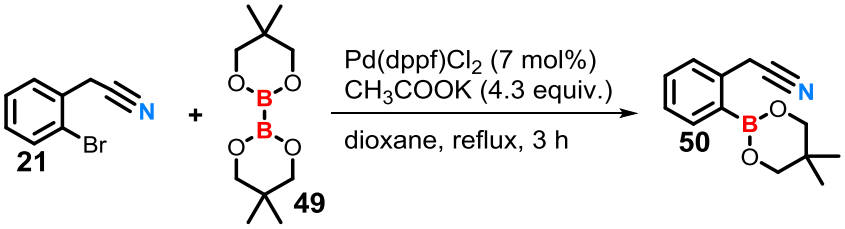

Scheme 3.15 Synthesis of compound **50**.

This promising result allowed us to have secured access to aryl substituted *o*-phenylacetonitrile boronic ester derivatives. In particular, we were interested in having chlorine atom in *para* position to the boron atom in order to make the radical formation more favourable, and so the closure of the ring in the last step of the hemifullerene synthesis. At this stage, we found 2-bromo-5-chlorophenylacetonitrile **52** to be a suitable commercially available source for our synthetic project. However, the too high cost of this material (> £450/ 1 g) made us to consider the option to prepare **52** starting from the cheaper 1-bromo-2-(bromomethyl)-4-chlorobenzene **51** precursor, by nucleophilic substitution in presence of CN^-.

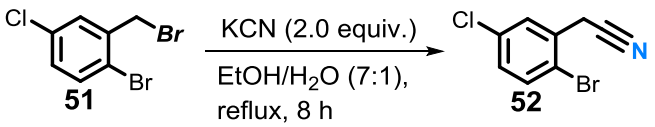

Scheme 3.16 Synthesis of **52**.

Following a literature pocedure introduced by Hsieh,[37] starting material **51** was refluxed 8 hours in presence of a solution of KCN in EtOH/H_2O (7:1). In order to avoid dangerous gas leaking (HCN), the top of the condenser was closed with a septum linked with a plastic tube to an aqueous solution of NaOH (20 w/w %). After work-up the ^{1}H NMR spectrum of the crude displayed the same pattern reported in literature[37] confirming molecular structure of **52**. Also, NMR analysis revealed the crude product to be an analytically pure sample, therefore it was used in the next step of the Miyaura cross-coupling reaction without any further purification. Exposure of **52** to the standard Miyaura cross-coupling reaction conditions described before, gave **53** in good yield (71%) after column chromatography purification (*n*-hexane/CH_2Cl_2 70:30 to pure CH_2Cl_2).

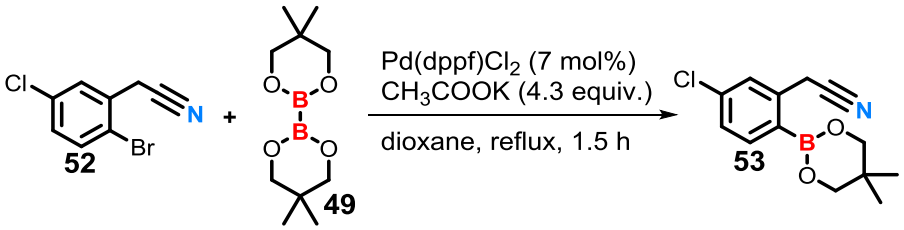

Scheme 3.17 Synthesis of compound **53**.

In order to expand the scope of the study to the analysis of the effect of substituents on the borazines, two additional *o*-phenylacetonitrile boronic esters **56** and **57** (Table 3.5) were synthesised starting from commercially available starting material **54** and **55**. Boronic esters **56** and **57** were obtained in 87% and 90% yield after column chromatography purification.

Table 3.5 Synthesis of substituted boronic esters **56** and **57**.

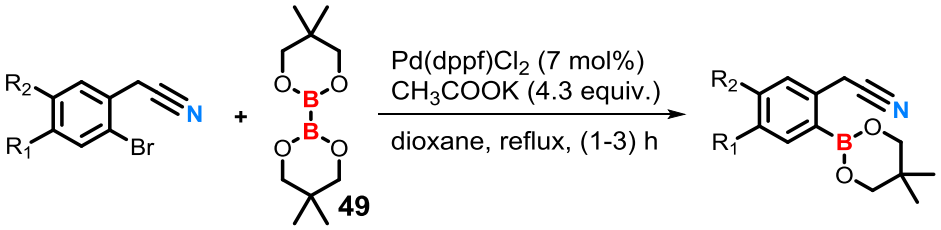

Entry	R_1	R_2	Product	%yield
54	CF_3	H	**56**	87
55	OMe	OMe	**57**	90

This procedure proved to be successful for the synthesis of *o*-bromophenyl acetonitrile, leading to high products yields with few by-products formed. Also, the chromatography purification proceeded smoothly.

3.4.2 Reduction of boronic esters 50, 53, 56 and 57

With four differently aryl substituted *o*-phenylacetonitrile boronic esters in hand we next explored the possibility of reducing these materials following the same protocol described in Chapter 2 based on the use of microwave assisted conditions.

Table 3.6 Reduction of boronic esters **50**, **53**, **56** and **57** by microwave assisted conditions.

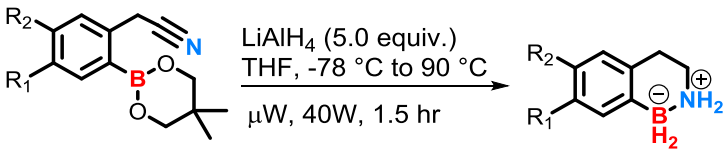

Entry	R_1	R_2	Product	%yield
50	H	H	**19**	56
53	H	Cl	**58**	47
56	CF_3	H	**59**	40
57	OMe	OMe	**60**	50

The reaction was performed in a flame-dried μW tube sealed with a plastic μW septum under inert atmosphere (Argon) and $LiAlH_4$ was added dropwise to solutions of **50**, **53**, **56** and **57** at -78 °C in anhydrous THF. A gas evolution was observed during the addition. When it was entirely released, the resulting mixture was allowed to warm to room temperature, a change in colour was observed, and then irradiated by microwave dielectric heating at 90 °C. After 1.5 hour, the reaction was checked by TLC analysis (eluent = CH_2Cl_2), which showed the disappearance of starting materials **50**, **53**, **56** and **57** and the formation of amine-borane species. The diagnostic spots at roughly R*f* = 0.4 was furthermore confirmed by a changing in colour to dark blue when reacted with a cerium-ammonium-molybdate staining solution. In all cases the reaction was quenched by careful addition of water to the mixture in order to decompose the excess of $LiAlH_4$. The white precipitate formed was filtered over a plug of anhydrous magnesium sulfate and the residue was washed with THF and ethyl acetate. Purification of amine-boranes by washing the crude dissolved in EtOAc with deionized water successfully led to the desired pure **19** and **58-60** in 40-56 % yield. By analysis of the NMR data (^1H, ^{11}B and ^{12}C) it was possible to identify and characterize the amine-borane species. Generally, ^1H NMR displayed an overall shifting of the aromatic protons to higher field in comparison with starting materials. More significant, however, was the disappearance of the signals related to the neopentyl glycol protecting group and the presence of the diagnostic signals as the broad peak of the **NH_2**→BH_2- primary amine group, the triplet related to the Ph-**CH_2**- on the benzylic position and a multiplet of the new internal -**CH_2**- bridge formed. This diagnostic sequence of signals confirmed the molecular structure of these amine-borane species. Comparison of ^1H NMR of starting material **50** and the corresponding amine-borane product **19** is shown in Figure 3.5.

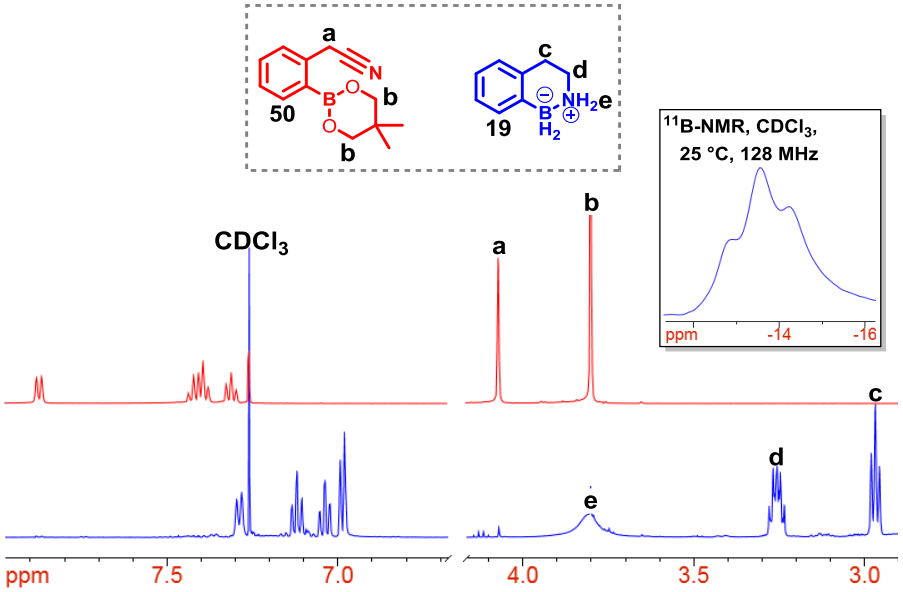

Figure 3.5 Comparison between ^{1}H-NMR spectra in $CDCl_3$ of starting material **50** and the corresponding reduced amine-borane **19**.

The ^{11}B NMR analysis was also important to confirm the molecular structure of amine-boranes **19** and **58-60** showing a triplet resonating at ≈-13.0ppm typical of boron-hydrogen coupling (*J*=96 Hz). ^{13}C NMR spectra were also collected for full characterization purpose displaying two new signals at ≈42.0 and 30.0 ppm related to the two internal -**CH_2**- bridge formed. Interestingly, the ^{1}H NMR spectrum of **59** (CF_3) displayed two distinct sets of signals related to two different products although the purification procedure was repeated twice. The ^{11}B-NMR spectrum of **59** showed only one signal resonating at -13.6 ppm, suggesting that only the amine-borane species was present.

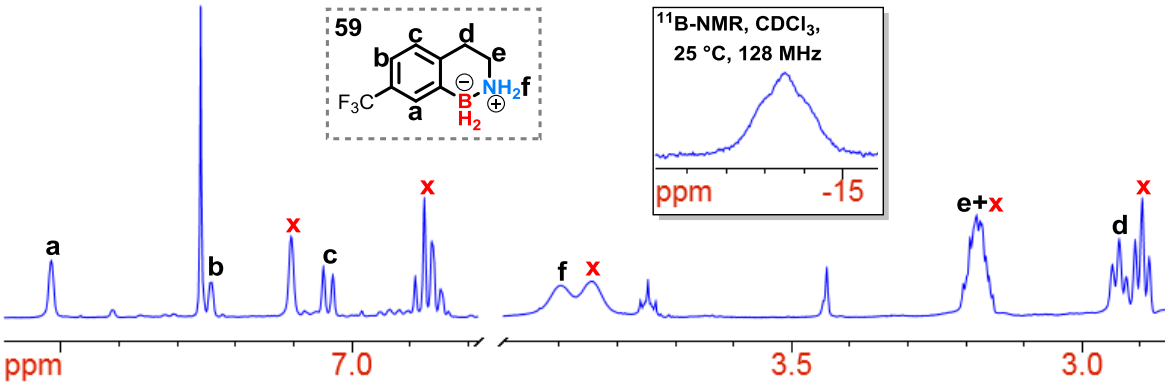

Figure 3.6 Representation of the ^{1}H and ^{11}B NMR spectrum in $CDCl_3$ of **59** containing impurities of a unknown compound with peaks highlighted in red.

In an attempt to determine the molecular structure of the second product, a series of NMR spectra (COSY, HMQC and HMBC) were collected, but unfortunately all our effort resulted to be inconclusive. Luckily, single crystals were grown by slow evaporation from an EtOAc solution, that allowed us to characterize the mixture by X-ray diffraction analysis. Unexpectedly, the results obtained showed that the other

component of the mixture was the corresponding reduced form of **59** to the -CF_3 functional group to -CH_3. Indeed, based on a literature precedent the CF_3 functional group could be easily reduced in presence of $LiAlH_4$ to methyl group as Akiyama and co-workers[38] described for the hydrodefluorination of fluorobenzenes, α,α,α-trifluorotoluenes and (trifluoromethyl)pyridines. They developed a selective and stepwise hydrodefluorination method to reduce a variety of α,α,α-trifluorotoluenes **61** by the combined use of 5 mol % of niobium (V) chloride and lithium aluminum hydride obtaining the corresponding toluenes **62** in good yields.

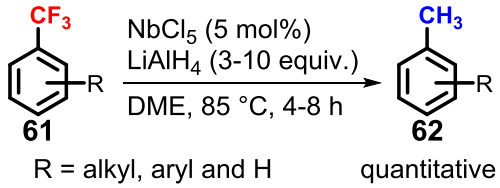

Scheme 3.18 Reduction of the CF_3 functional group into the corresponding methyl group when exposed to the reducing agent $LiAlH_4$.

In our case the reaction conditions used for the reduction of *o*-phenylacetonitrile boronic esters were very similar to those reported in literature, therefore the large excess of $LiAlH_4$ used promoted also the reduction of the -CF_3 group to the corresponding methyl group.

3.4.3 X-ray structure of amine-boranes 19, 58 and 59

As anticipated before, structural proof of amine-borane **59** and the corresponding methyl derivative came from an X-ray diffraction analysis of single crystals grown by slow evaporation from an EtOAc solution. Also, single crystals of **19** and **58** suitable for X-ray crystallography were grown by slow evaporation from an EtOAc solution. Unfortunately, attempts to grow crystal for **60** using either EtOAc or chlorinated solvents such as $CHCl_3$, CH_2Cl_2 failed. Amine-borane **19** crystallised in the orthorhombic space group $P2_12_12_1$ with four molecule units per unit cell packed in staggered array motif. The measured bond distances between carbon atoms of the aromatic ring are in line with that reported in literature[39], as well as the distance calculated between boron and nitrogen atoms (B-N 1.606(4) Å) reported in Chapter 2.

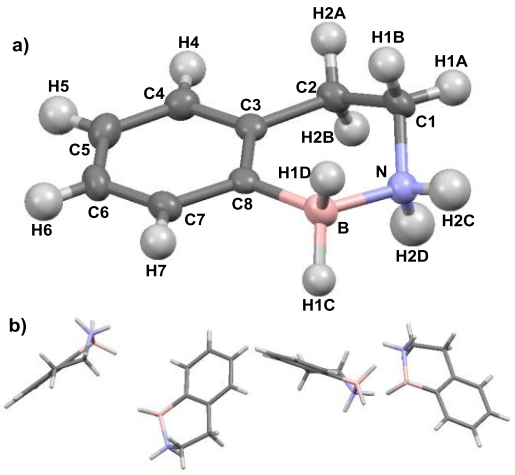

Figure 3.7 a) Crystal structure of **19**, b) unit cell characterizing the crystalline lattice.

Interestingly to note that the six-membered heterocycle containing boron and nitrogen atoms adopt a half chair conformation, typical of cyclohexene molecule, with carbon C(1) and nitrogen atoms pointing in the opposite direction outwards of the plane containing the aromatic backbone. Angles measured between the three planes are displayed below in Figure 3.8.

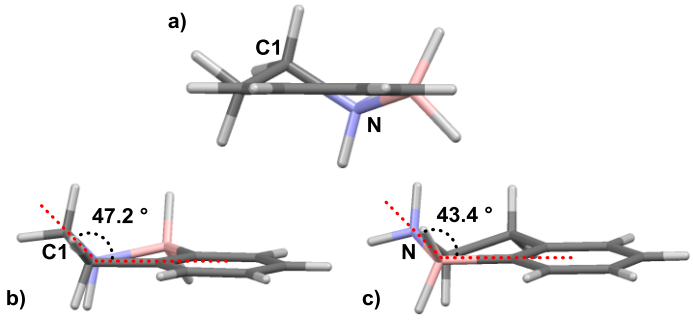

Figure 3.8 a) Side-on view of the X-ray structure of **19**, highlighting the angles of b) C1 and c) N with respect the plane laying the aromatic backbone.

Compound **58** crystallized in the triclinic space group P-1 arranging itself in a staggered L-shaped configuration with four molecules per unit cell. The measured bond distances between carbon atoms of the aromatic ring were similar to those observed for **19**, also distances calculated between boron and nitrogen atoms B(1)-N(1) and B(2)-N(2) were in line with the value observed for **19** (1.603(3) and 1.598(3) Å respectively). The distances calculated for chlorine-carbon bonds Cl(1)-C(5) and Cl(2)-C(13) were 1.751(2) and 1.747(2) Å respectively, in between of that calculated for chlorobenzene (1.725 Å) and methyl chloride (1.785 Å).[39] This result suggested that the mesomeric and inductive effect of chlorine atoms in this system have different contributions with respect to chlorobenzene and methyl chloride, therefore the partial double bond character due to the resonance is consequently less enhanced.

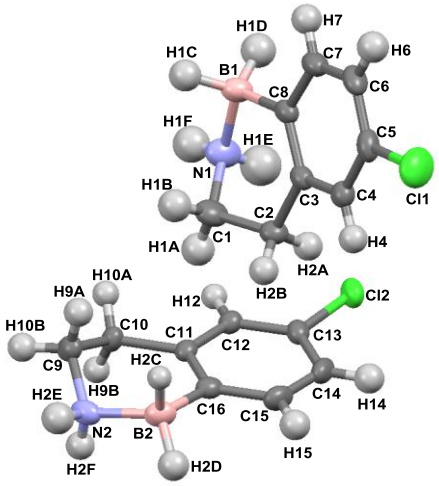

Figure 3.9 X-ray structure of **58**.

Staggered L-shaped dimer units interact one another with close contacts between carbon C(1) of a molecule of **58** and aromatic carbon atoms C(11) and C(16) of the other molecules with distances of 3.580 and 3.723 Å. Also, two dimeric units interact one another with symmetrical short contacts between nitrogen and aromatic carbon atoms C(7) and C(8) with distances being 3.404 and 3.382 Å defining the unit cell composing the crystalline lattice of **58**.

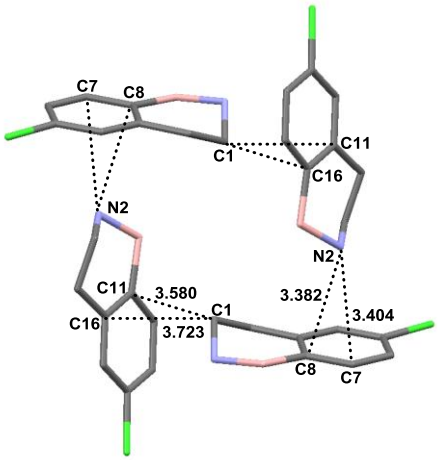

Figure 3.10 Unit cell characterizing the crystalline lattice of **58**.

Amine-borane **59** and the corresponding methyl derivative crystallised in the orthorhombic space group $Pca2_1$ with eight molecule units per unit cell packed in staggered array motif. The measured bond distances between carbon atoms of the aromatic ring and that calculated between boron and nitrogen atoms were similar with values previously described amine-boranes **19** and **58**. Interesting to note that fluorine atoms of the $-CF_3$ group are partially overlapped with hydrogen atoms of a molecule of amine-borane confirming the presence of two species in the crystalline lattice. However, considering that the size of hydrogen and fluorine atoms is very close, in the X-ray data processing for the calculation of the molecular packing of **59** has been used the hydrogen parameters.

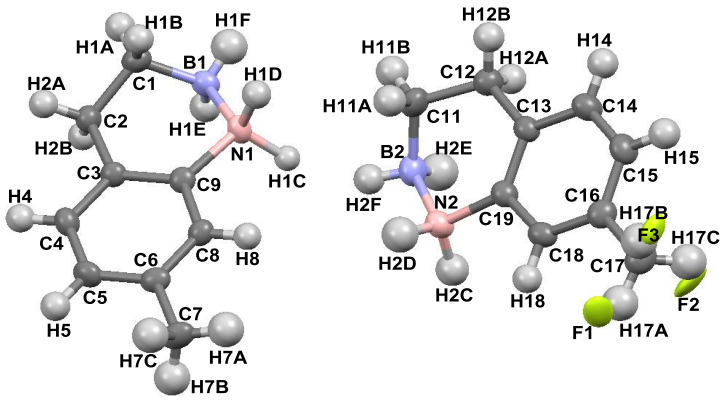

Figure 3.11 X-ray structure of **59**.

3.5 Borazine synthesis by thermolysis of amine-boranes 19, 58 and 60

With amine-borane building blocks **19** and **58-60** in hand, we next explored the possibility of synthesising the corresponding borazine derivatives using the same procedure described in Chapter 2 for the synthesis of borazatruxene. First attempt at the synthesis of borazine **18** under the same reaction conditions developed, resulted in partial conversion of **19** into the desired **18**. Indeed, after 2 h of reaction, TLC analysis eluted with CH_2Cl_2 showed two distinct spots corresponding to the borazine formed and to the amine-borane unreacted. However, when the reaction time was increased to 3 h, all the starting material was successfully converted in to the product.

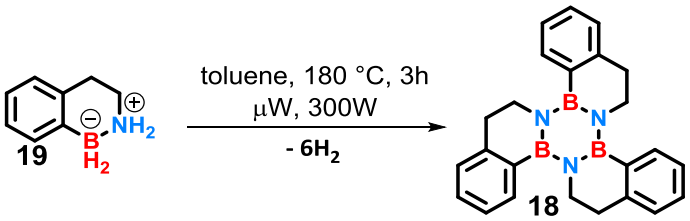

Scheme 3.19 Synthesis of borazine **18**: trimerization of amine-borane **19** by a thermolysis process.

After removing the solvent under reduced pressure, we evaluated the possibility of purifying the crude mixture by silica gel flash chromatography. At this stage, the stability of **18** in presence of silica was checked by using the 2D TLC technique, then we proceeded with the column chromatography purification. The best conditions consisted of eluting the crude with a mixture of *n*-hexane/CH_2Cl_2 (80:20) but unexpectedly the desired **18** was isolated in only 20% yield. After separation a series of NMR spectra (^{1}H, ^{11}B, ^{13}C, COSY, NOSY, HMQC and HMBC) were collected for full characterization purpose.

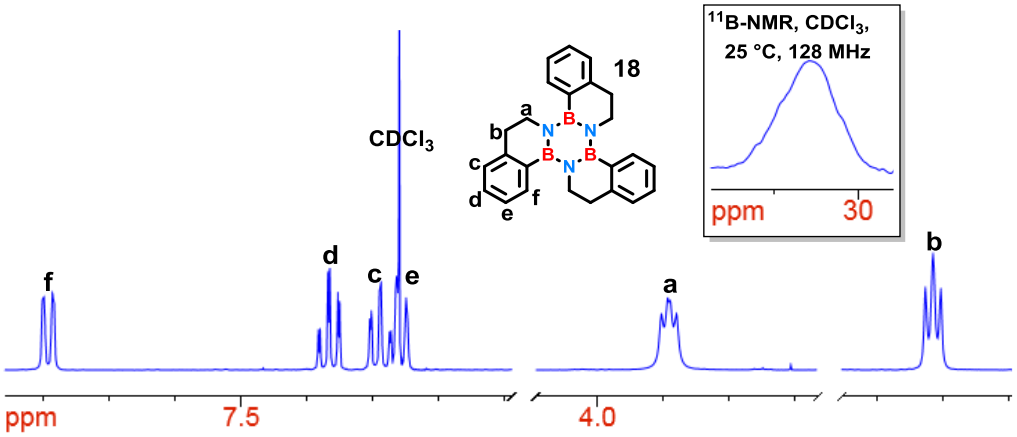

Figure 3.12 Representation of the ^{1}H and ^{11}B NMR spectrum in $CDCl_3$ of **18** highlighting the diagnostic peaks to confirm the molecular structure.

The ^{1}H NMR displayed an overall shifting of the aromatic protons to lower field compared with the starting material amine-borane **19**. Also, the broad peak related to the primary amine disappeared whilst the multiplet assigned to the -CH_2- bridge between nitrogen atom and the benzylic position shifted to 3.89 ppm as a triplet. The ^{11}B NMR spectrum showed the diagnostic peak resonating at 33.5 ppm confirming the borazine ring. Figure 3.13 shows the NOESY spectrum, highlighting correlations between aromatic protons with the two -CH_2- bridge groups of **18** and the closest aromatic protons through space.

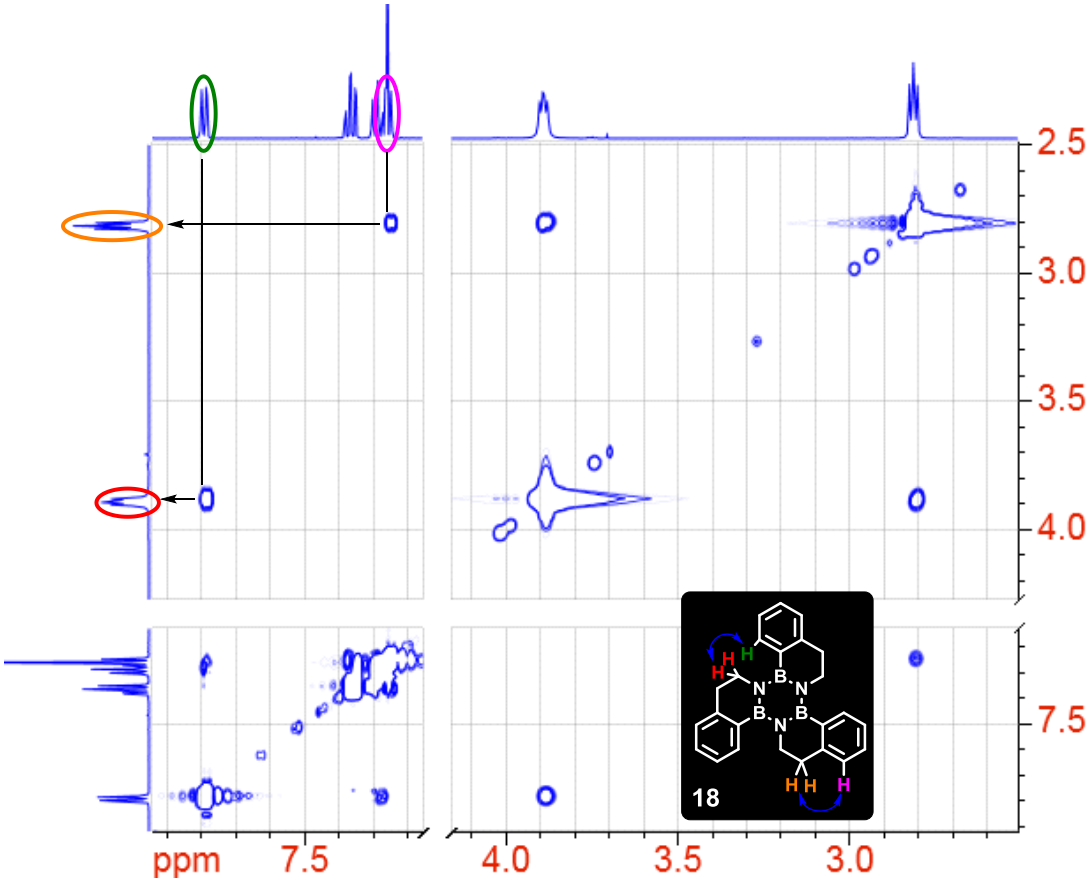

Figure 3.13 Representation of COSY NMR spectra of **18**.

Finally, mass spectroscopy analysis was in accordance with the predicted isotope pattern distribution, confirming molecular structure of **18**.

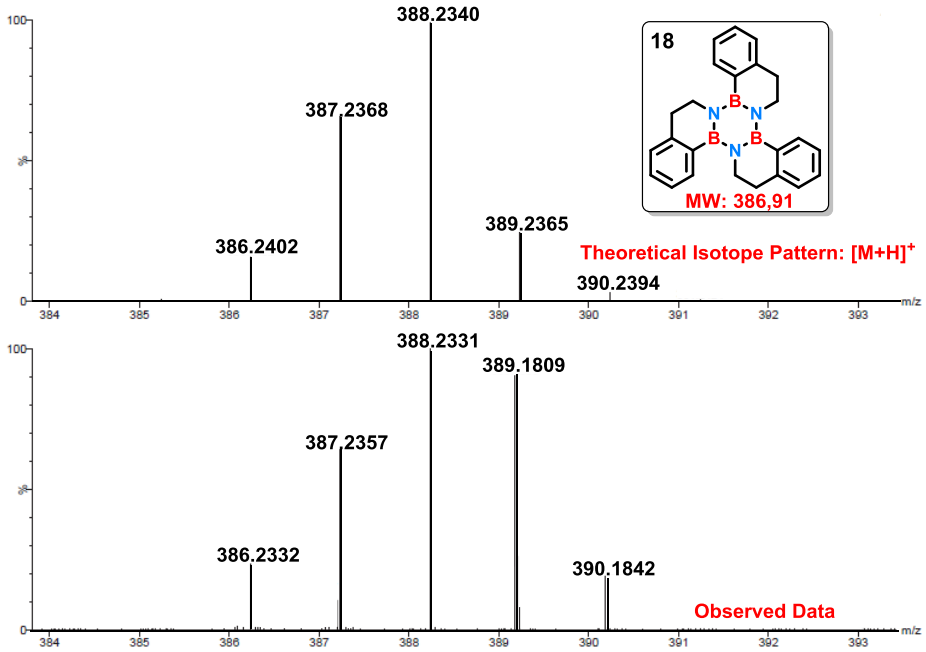

Figure 3.14 Mass Spectrum of compound **18** from Swansea University.

Distinctly form borazatruxenes, borazine **18** displayed excellent solubility features. Indeed, solubility tests revealed **18** to be soluble in the most common organic solvents used, even in a mixture of *n*-hexane/CH_2Cl_2 (50:50). This promising result was a considerable step towards the possibility of using these materials for the construction of new electronic devices. However, the low yield obtained was unexpected, since by TLC analysis, we observed that the intensity of the borazine spot was massively higher than that of impurities, therefore we expected to obtain **18** in higher yield. We initially though that the low polarity of the eluent used in the chromatography purification might have led to the precipitation of borazine **18** during the elution with consequent loss of material. To prove our hypothesis, the reaction was repeated under the same reaction conditions and then the crude mixture was purified by chromatography purification using only CH_2Cl_2. In this case the desired **18** was also isolated in the same yield. This outcome convinced us that the thermolysis of amine-borane **19** might proceed *via* a pathway that is mechanistically different from that proposed for the synthesis of borazatruxene. To get insight the issue with the poor yield of **18**, we decided to isolate and characterize the other products constituting the crude mixture. First attempt to isolate the side products by silica gel flash chromatography purification was unsuccessful because they reacted with the acidic OH groups of silica, remaining stuck on the surface from the beginning. Also, trials to remove these products with more polar eluents such as ethyl acetate and methanol failed. Therefore, the plan to isolate each component of the crude mixture was changed. Due to the strong interactions between these species and the stationary phases, we used the reversed-phase chromatography as an

alternative tactic. This chromatographic method uses a hydrophobic stationary phase; usually is a silica-based stationary phase supported with non-polar substances in order to minimise the hydrophilic interactions. The most commonly used column in the reverse-phase chromatography is a silica-based stationary phase supported with an octadecyl carbon chain (C18). To find the best purification conditions, we initially proceeded with the TLC analysis using silica gel C18 on TLC plates. The best separation was obtained when a mixture of *n*-hexane/EtOAc (80:20) was used; however, side-products could be eluted only by increasing the polarity. With the optimal conditions in hand, we then proceeded with the separation by taking advantage of the column machine as column cartridges for reversed-phase chromatography purification were already available in our lab. Using this method, we could isolate each component of the mixture and, by NMR analysis, it was possible to identify the major products. The ^{1}H NMR spectra of the last two fractions were difficult to interpret, and in both cases, peaks were broader compared with those previously observed for borazine **18**. We therefore believed that these two fractions isolated contained either oligomers or polymers of amine-borane **19**, however, to further confirm this hypothesis more analytical experiments need to be done. The second main product isolated, instead, displayed an unusual set of signals vaguely attributed to that observed for borazine **18**.

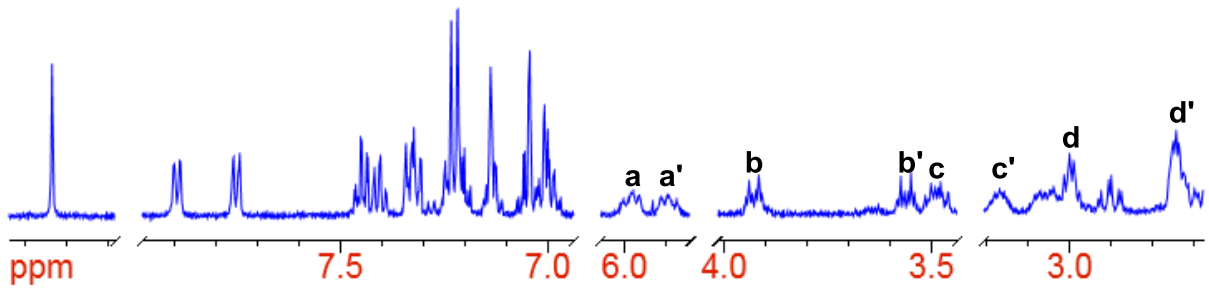

Figure 3.15 Representation of the ^{1}H-NMR analysis spectrum in $CDCl_3$ of the unknown compound isolated by column machine, obtained from the synthesis of borazine **18**.

Interesting to note that, in the area between 6.00 and 3.00 ppm, we observed the same pattern reported for **18**. For instance, broader triplets around 6.00 ppm and sharper triplets at lower ppm assigned to the two -CH_2- bridge groups are identified. However, they are also seen around 3.00 ppm, being split in set of doublets integrating to one proton each. The aromatic region displayed similar trend and the peak at 9.33 ppm was tentatively assigned to the B-OH group. The presence of both carboxylic acid and aldehyde groups is excluded because these would resonate at higher ppm; also, ^{13}C NMR spectrum has not displayed any peak in the carbonyl region. COSY and NOESY NMR analysis, revealed correlations between aromatic and aliphatic protons, suggesting that they belong to the same molecule. This allowed us to consider that the ^{1}H NMR spectrum can be attributed to a dimeric unit **63** composed of two amine-borane **19** bonded *via* a boron-nitrogen covalent bond with free N-H and B-OH groups at the two ends. The interesting splitting of

doublet of triplets signals resonating in the aliphatic region (6.00-3.00 ppm) of the four -CH_2- bridge groups could be explained in terms of anisotropic effect caused by the molecular rearrangement in space.

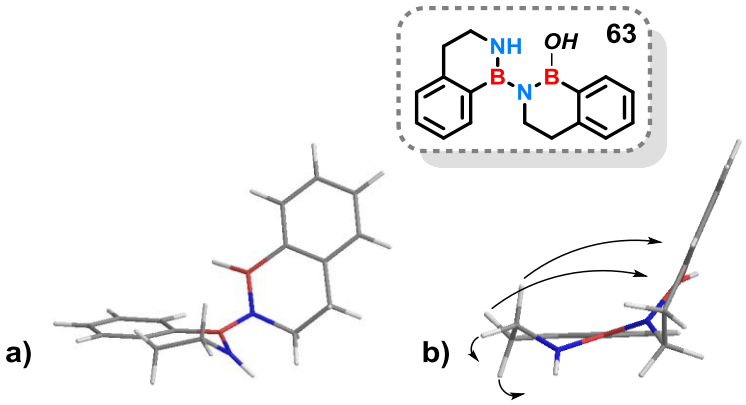

Figure 3.16 Molecular modelling calculations of compound **63**: a) angled and b) side-on view.

Indeed, molecular modelling calculations revealed each amine-borane to be perpendicularly aligned to the other therefore protons of the -CH_2- bridge are differently affected by the magnetic field because of an axial chirality probably due to restricted rotation on the BN bond. Our hypothesis about the dimer was confirmed by mass spectroscopy analysis, which displayed a good match between the predicted isotope pattern distribution and the observed data with the molecular peak $[M+H]^+$ = 277.1686 and the theoretically calculated at 277.1689, confirming the molecular structure of **63**.

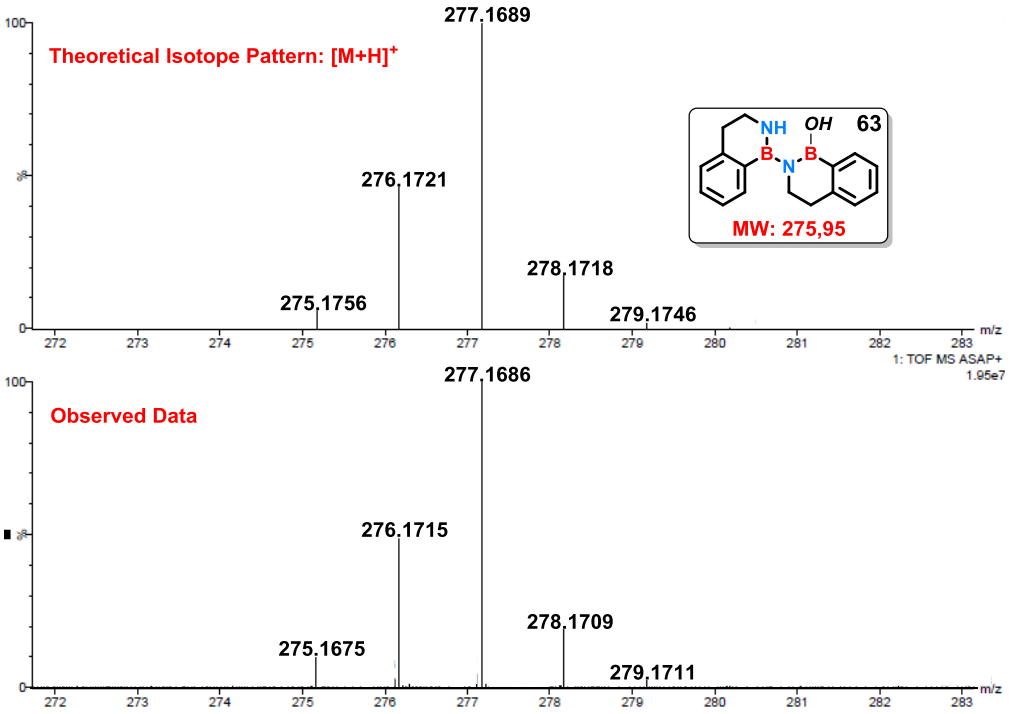

Figure 3.17 Mass Spectrum of compound **63** from Swansea University.

On the basis of this outcome, we speculated that the preference of amine-borane **19** to form dimers and oligomers rather than the borazine ring when exposed to the thermolysis process might be due to thermodynamic factors. Probably the process that led to the formation of dimer **63** and subsequently proceeded with the oligomerization might be thermodynamically more favourable than that related to the borazine formation. Possibly, steric hindrance limits the closure of three molecules of **19** to give **18**. Also, given the fact that borazine **18** is soluble in toluene, during the thermolysis process, **18** might further react to open the borazine ring leading to the formation of other thermodynamically stable species as oligomers or polymers. In an attempt to rationalize our hypothesis, borazine **18** was exposed to the same reaction conditions described for the thermolysis processes. In this sense if borazine **18** was not the most thermodynamically stable product, under these conditions, it would have reacted to give the expected dimer and oligomers as anticipated before. Unfortunately, the results obtained were inconclusive because NMR analysis of the crude product displayed only signals related to the starting borazine **18**. To this end we considered the possibility of limiting the formation of the dimer species **63** and oligomers using different solvents from toluene in the trimerization step. In fact, solvent dependent reactions can be manipulated and directed towards the formation of specific products than others when the right solvent is chosen. Therefore, we assumed that screening different solvents for the thermolysis of **19** would have been an important information on the nature and stability of the transition state leading to the formation of the borazine ring. Guided by this idea, we decided to compare the % yield of borazine **18** obtained depending on the different solvents used in thermolysis reaction (Table 3.7)

Table 3.7 Screening of different solvents for the synthesis of borazine **18**.

SOLVENTS	***REACTION CONDITIONS***	***% YIELD***
Toluene	μW, 180 °C, 2hrs	20
1,2-dichlorobenzene	μW, 180 °C, 2hrs	30
chlorobenzene	μW, 150 °C + cooling, 10hrs	20
α,α,α-trifluorotoluene	μW, 180 °C, 2hrs	16
hexafluorobenzene	μW, 180 °C, 3hrs	20
mesitylene	reflux, 165 °C, 4 days	20

This study demonstrated that the thermolysis process for the synthesis of borazine **18** starting from saturated 1,2,3,4-tetrahydro-1,2-borazaronaphthalene **19** is slightly solvent dependent. Indeed, we did not observe substantial changes in % yield when solvents of different polarities and steric hindrance were used, therefore we assumed that other factors affected the outcome of this reaction. However, because the study of the thermodynamic and kinetic factors characterizing a particular reaction is a time demanding process and our project was mainly focused on the synthesis of BN-doped hemifullerene, we decided to further investigate this reaction later. Therefore, we carried on with the synthesis of borazines

64 and **66** exposing amine-boranes **58** and **60** to the standard reaction conditions developed for the thermolysis.

Table 3.8 Synthesis of substituted borazines **64-66**.

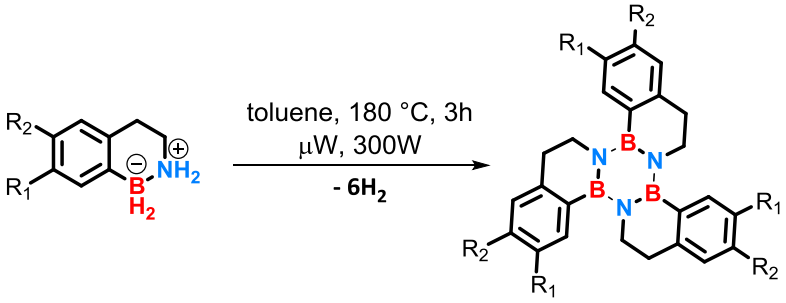

Entry	R_1	R_2	Product	%yield
58	H	Cl	**64**	15
60	OMe	OMe	**65**	20

Building block **59** was not employed in this step because of the mixture between the -CF_3 and -CH_3 derivatives. In fact, they can react together in a different ratio to theoretically give four different products thus making work-up and purification difficult.

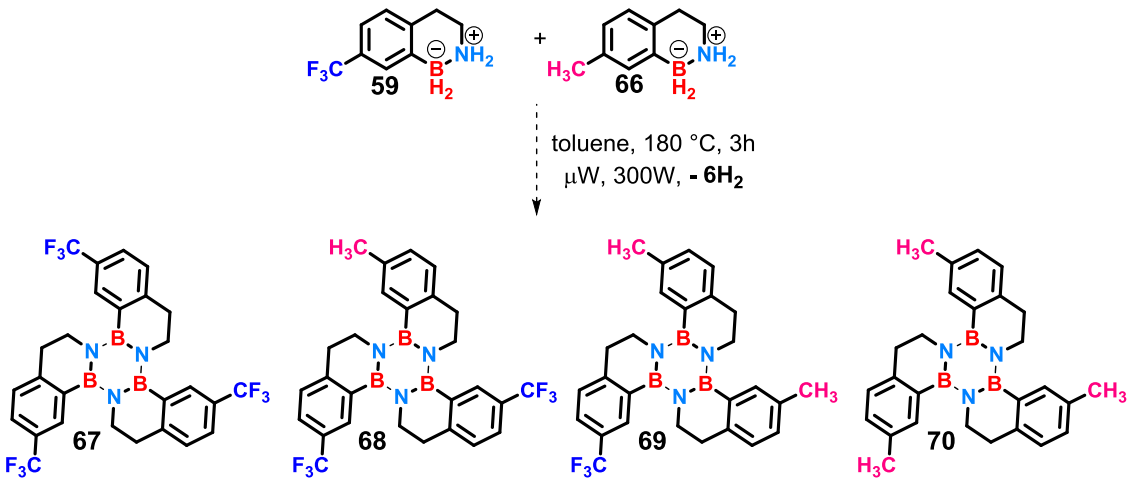

Scheme 3.20 Hypothetic products formed by the thermolysis of the mixture composed by amine-borane **59** and **67**.

As expected, borazines **64** and **65** were obtained in 15 and 20% yield respectively, after column chromatography purification using the same conditions described for borazine **18**. Analysis of the NMR data proved molecular structure of the desired **64** and **66**, displaying the same diagnostics peaks previously observed for **18**. Also, mass spectroscopy analysis of **64** displayed a good match between the predicted isotope pattern distribution and the observed data, confirming the molecular structure.

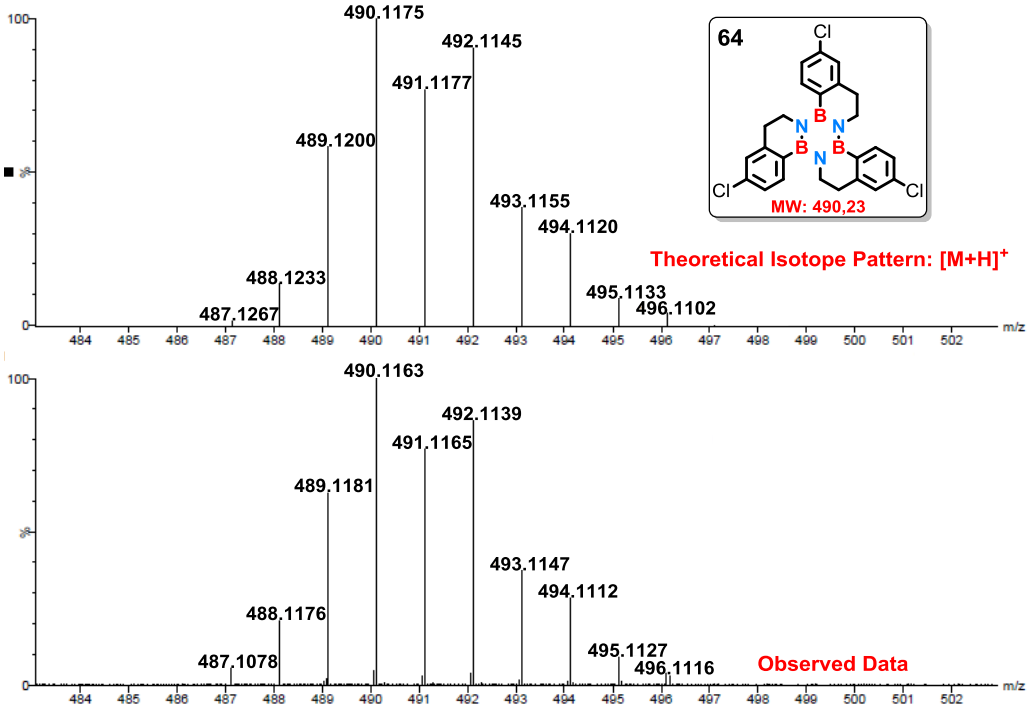

Figure 3.18 Mass Spectrum of compound **64** from Swansea University.

3.6 X-ray structure of borazines 18 and 64

Structural proof of borazines **18** and **64** came from an X-ray diffraction analysis of single crystals grown by slow evaporation from an $CHCl_3$ solution. Borazine **18** crystallised in the trigonal space group P-3 with two molecule units per unit cell packed in staggered array motif. The measured bond distances between carbon atoms of the aromatic ring are in line with the previously observed for borazatruxene molecules. Also, the distance calculated between boron and nitrogen atoms B-N and $B^{\#}$-N of 1.433(2) and 1.442(2) Å are very similar to those observed for borazatruxene. Comparable values were also observed for the B-N-$B^{\#}$ and N-B-N bond angles of the borazine ring.

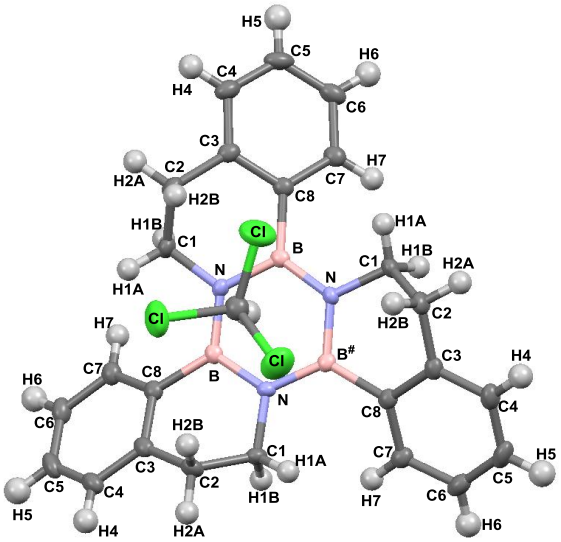

Figure 3.19 X-ray structure of **18**.

Interesting to note that molecules of $CHCl_3$ co-crystallized with borazine x remaining included in the crystal structure of **18**. In this case we observed that each borazine interacts *via* CH···π interactions with the hydrogen atom of $CHCl_3$ pointing inside the borazine ring. There are also electrostatic interactions with chlorine atoms of another molecule of $CHCl_3$ perpendicularly aligned with the borazine ring on the opposite face.

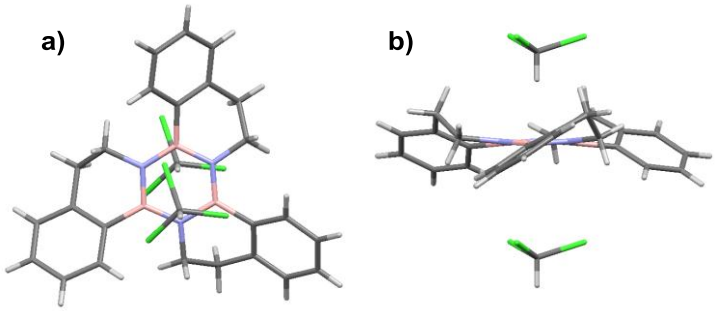

Figure 3.20 a) Top and b) side-on view of crystal structure of **18**.

Also, looking in depth at the crystal structure of **18**, we noticed that each molecule of $CHCl_3$ is surrounded by three molecules of **18** plus two more on top and below, making a sort of cage sufficiently large to accommodate a molecule of $CHCl_3$. This motif is the peculiar sequence repeating in space that characterizes the crystalline lattice of borazine **18**.

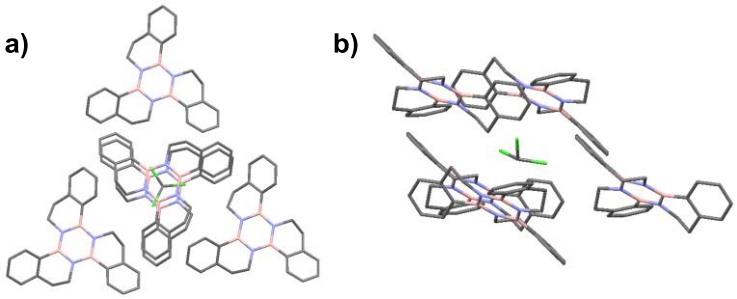

Figure 3.21 a) Top and b) side-on view of the cage embedding a molecule of $CDCl_3$ characterizing the crystal structure of **18**.

Borazine **64** crystallised in the triclinic space group P-1 with two molecule units per unit cell packed one on top of one another in a staggered array. The measured bond distances between carbon atoms of the aromatic ring displayed distances similar to those previously observed for borazine **64** and borazatruxene molecules. Also, the distances calculated between boron and nitrogen atoms are ranging between 1.428(5) and 1.442(5) Å, in line with the observed distances for the previous borazines. The bond distances observed between chlorine and carbon atoms resulted to be very similar to the previously observed for the corresponding ammine-borane starting material **58**, indeed Cl(1)-C(5) resulted to be 1.747(4) Å, while Cl(2)-C(13) and Cl(3)-C(21) of 1.748(4) and 1.745(4) Å, respectively.

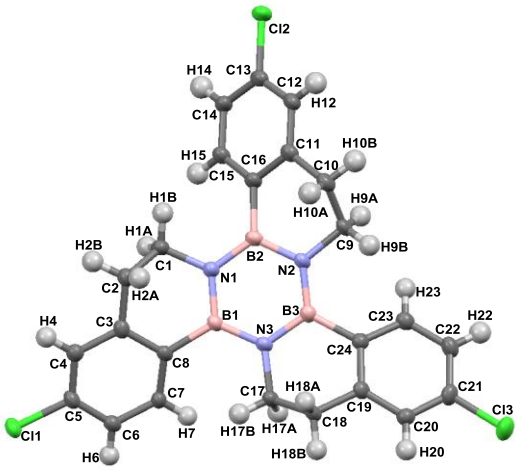

Figure 3.22 X-ray structure of **64**.

As anticipated, in the unit cell two molecules of **64** are arranged one on top of one another in a staggered array. Short contact interactions are seen between aromatic carbons C22 and C23 of the closest neighbouring aromatic ring and B(1) with distances of 3.490 and 3.249 Å, and also between two boron atoms B(3)-B(3) aligned parallel with distances of 3.906 Å.

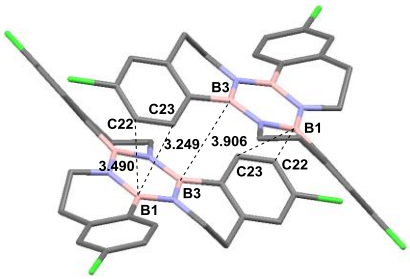

Figure 3.23 Unit cell characterizing the crystalline lattice of **64**.

The resulting molecular packing characterizing the crystalline lattice of borazine **64** is shown in Figure 3.24. displaying a top and two side views of the X-ray structure.

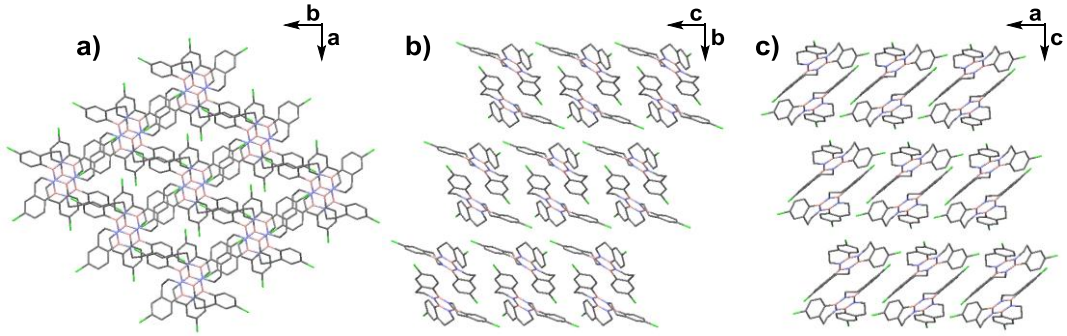

Figure 3.24 Representation of crystal packing of molecule **64** from different angles.

3.7 Optical studies of borazine 18 and 64

Solutions suitable for UV-Visible and fluorescence analysis were prepared by dissolving borazine **18** and **64** in HPLC grade THF rather than in $CHCl_3$ because we wanted to investigate, also, the middle-UV region (200-300 nm) were aromatic systems usually absorbs. We could not have access to this window of wavelengths by using $CHCl_3$ because the UV cut off wavelength of chloroform is at 245 nm and this is the limit of working wavelength within the errors admitted. In our case instead, because we used THF, we could scan as low as 212 nm (UV cut off value); however, the UV-Vis spectra were collected across 400 and 220 nm region to minimize the possible errors. Fluorescence spectra were obtained by exciting samples at the lowest-energy absorption peak centred around 280 nm characterizing the borazine ring because at this wavelength the photoluminescence intensity was higher compared to that obtained by exciting the sample at the λ_{max}. Also, solutions at different concentrations were prepared to determine the molar extinction coefficient ε of both borazines **18** and **64**. Borazine **18** displayed absorption and emission spectra similar to those previously reported for borazatruxene **71** in Chapter 2.

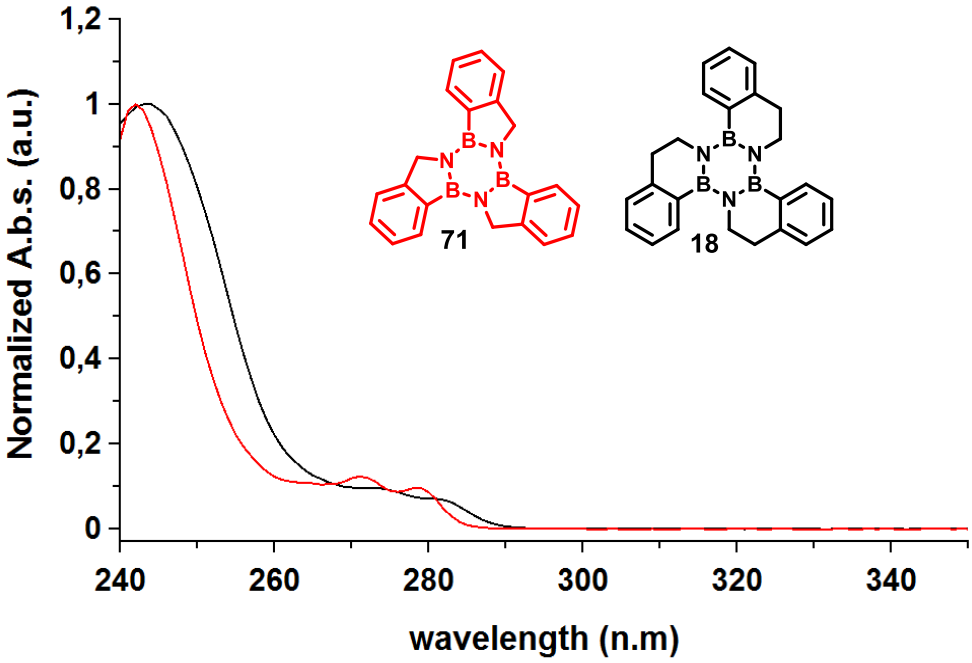

Figure 3.25 Comparison of absorption spectra of borazatruxene **72** (red) and borazine **18** in CH_2Cl_2.

A strong absorption at 244 nm was observed for the peripheral aromatic rings followed by two distinct peaks of lower energy centred at 272 and 281 nm related to the central borazine ring. As already highlighted for borazatruxene, the BN introduction into the all-carbon system caused a significant hypsochromic shift of the lowest-energy absorption band compared with truxene; however, with comparable peak patterns suggesting similar electronic structures. The more localized electron density due to the differences in polarity between boron and nitrogen atoms, which in turn reduces the electronic communication throughout the molecule, resulted in an increase in the HOMO-LUMO gap and a blue shift of the peaks. The emission spectrum (black) of borazine **18** was obtained exiting the sample at 281 nm with an emission wavelength λ_{max} at 302 nm with a Stoke shift of $\Delta\lambda$ = 21 nm, similar to that observed for borazatruxene. Excitation at this wavelength resulted in a higher photoluminescence intensity compared with that obtained when exciting at higher-energy absorption wavelengths. However, when borazine **18** was excited at either the low- or the high-energy absorption band, the emission spectra were the same without loss of vibrational fine structure.

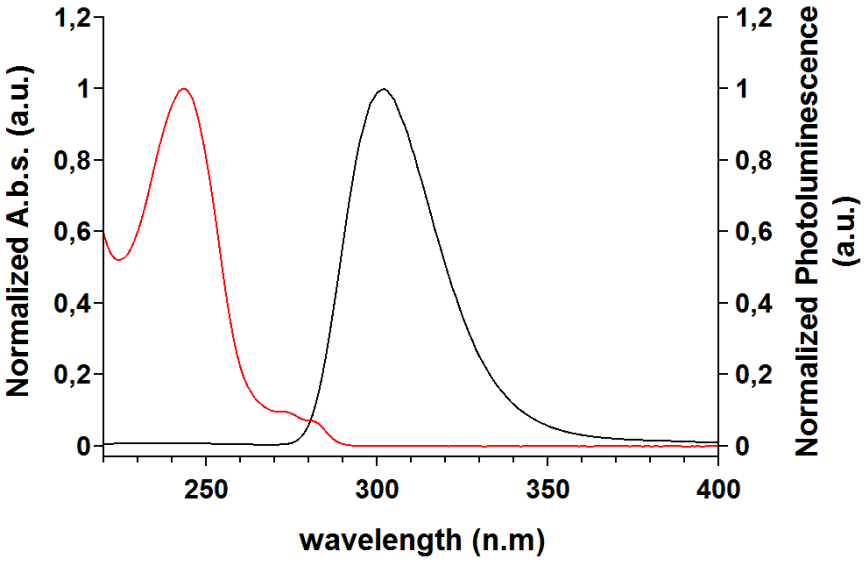

Figure 3.26 UV-Visible absorption (red) and emission (black) spectra of **18** in THF.

Introduction of chlorine atoms on the peripheral aromatic rings resulted in a bathochromic (red) shift attributed to the increased n→π* interaction as previously observed for halogenated borazatruxenes. Indeed, the λ_{max} of absorption was centred at 250 nm, 6 nm red shifted when compared with the unsubstituted **18**, while the borazine ring displayed two distinct peaks at 275 and 284 nm. The introduction of an n pair donor species as chlorine atom slightly increased the electronic delocalization of the system, resulting in a red shifted absorption spectrum towards lower energies. The emission spectrum in black, obtained exciting the sample at 284 nm, instead displayed a λ_{em} centred at 303 nm, very similar to that observed for **18**, suggesting that the ground level of the first excited state of both borazines **18** and **64** is of comparable energies. Also, for both **18** and **64**, when excited at either the low- or the high-energy absorption bands, the emission spectra were the same without loss of vibrational fine structure.

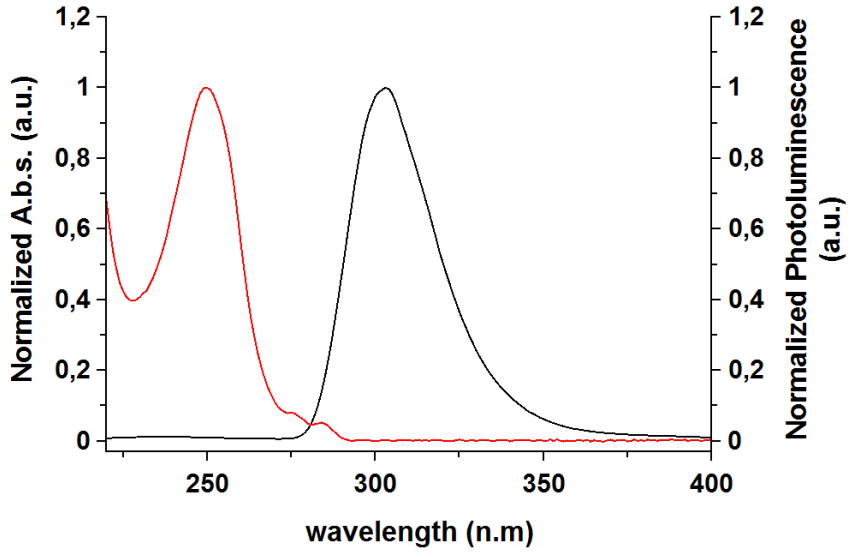

Figure 3.27 UV-Visible absorption (red) and emission (black) spectra of **64** in THF.

Comparison of the UV-Vis and fluorescence spectra of borazines **18** overlapped with **64** are displayed in Figure 3.28.

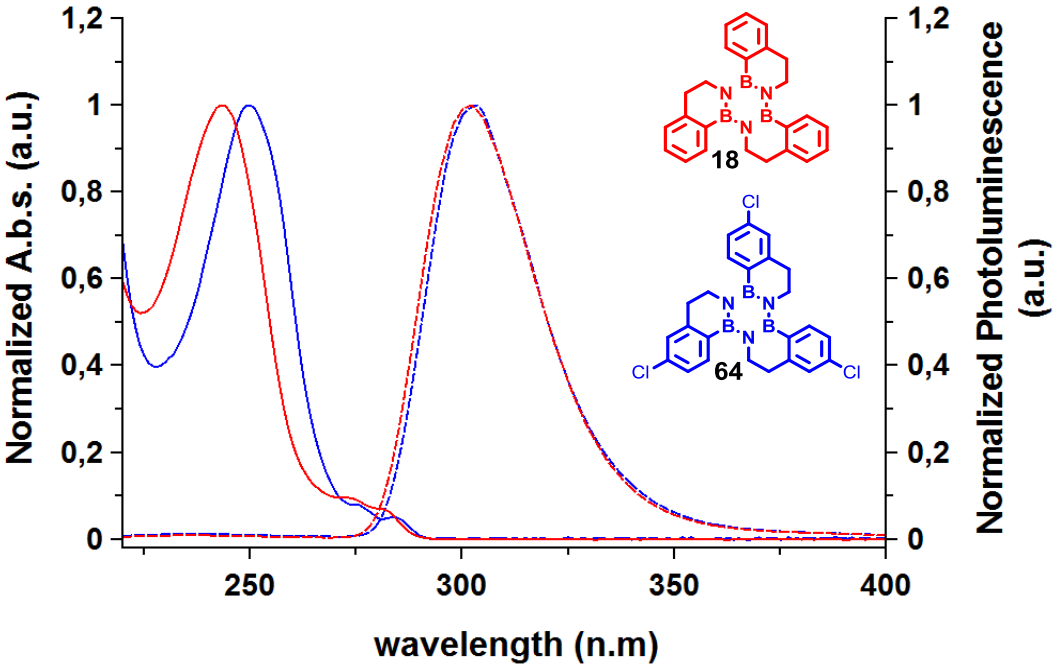

Figure 3.28 Comparison of UV-Visible absorption and emission spectra of borazine **18** (red) and **64** (blue) in THF.

The molar extinction coefficients ε of **18** and **64** were determined by linear regression of the curve obtained by plotting absorbance data recorded for different concentrations. The trend of the ε values calculated for borazines **18** and **64** was in line with the hyperchromic effect observed in the UV-vis spectra. Indeed, borazine **18** displayed an ε value of $3{,}8 \cdot 10^4$ mol · l^{-1} · cm^{-1}, while the ε of the chlorinated derivative **64** was of $5{,}7 \cdot 10^4$ mol · l^{-1} · cm^{-1}, almost the double of **18**.

Table 3.9 Experimental UV-Vis absorbtion and emission data for borazatruxenes **18** and **64** in THF.
(*) wavelength of excitation used to recorder the emission spectrum of each borazine.
(**) All quantum yields were calculated using anthracene in $CHCl_3$ as the standard ($\phi_{QS} = 0.11$).

°n	Entry	λ_{max} (nm)	λ borazine band (nm)		λ_{PL} (nm)	$\Delta(\lambda_{PL} - \lambda^*)$ (nm)	ε (mol · l^{-1} · cm^{-1})	ϕ** (A)
18	**H**	244	271	281*	302	21	38443	0.23
64	**5-Cl**	250	275	284*	303	19	57267	0.26

As explained earlier, the n→π* electronic transitions are less forbidden than the π →π*, therefore with the introduction of chlorine atoms, the probability to absorb a photon and to have an electronic transition is double than in the unsubstituted species **18**. Also, interesting to note that these molecules displayed extinction coefficient values almost four times higher than those observed for borazatruxene species, despite the UV-Vis and fluorescence spectra are very similar. We need to consider the various factors

involved as the different solvents used (regardless the limited dependence of ε from the latter) but more importantly the difference in solubility. In fact, borazatruxenes displayed significantly lower solubility in the common organic solvents compared with **18** and **64**, therefore this might have resulted in the formation of aggregates making the real concentration lower than that calculated. However, borazine species **18** and **64** showed interesting spectroscopic features since ε values were almost comparable with the extinction coefficient of truxene ($6{,}5 \cdot 10^4$ mol $\cdot$ $l^{-1} \cdot cm^{-1}$) and the HOMO-LUMO gap similar to that observed for borazatruxene. The ϕ_f of borazines **18** and **64** are also listed in Table 3.9. The increase in ϕ_f passing from borazatruxene to the chlorine derivative might be due to the presence of chlorine atom which make more rigid the system enhancing the emission quantum yield. Notably the quantum yields of these species resulted to be three times more than that observed for borazatruxenes. Theoretically borazatruxene framework is more rigid and flat than these species, consequently the vibrational relaxation pathway causing a quenching of fluorescence should be more favourable for the latter. This unexpected observation can be rationalized considering the formation of aggregates in the case of borazatruxene species leading to a nonradiative deactivation of the singlet excited state through a possible combination of intersystem crossing (ISC). Inclusion of a CH_2 group between the benzylic position and nitrogen as in borazines **18** and **64**, instead destabilize the formation of aggregates by steric hindrance thus disfavouring the non-radiative deactivation of the singlet excited state.

3.8 VT-NMR isodesmic model[40] for the aggregation studies of borazine 18

The self-assembly processes of borazine **18** was studied by using temperature-dependent spectroscopic measurements. First investigation of the aggregation process of borazine **18** was carried out in 1,1,2,2-tetrachloroethane-d_2 as described by Dr. Hemmett. Temperature dependent ^{1}H NMR analysis was performed using a Bruker Advance 400 (^{1}H 400 MHz), on a 0.5 mL solution in a dry NMR tube of 5.5 mM concentration of **18**. Investigation of temperatures ranging from -20 to 110 °C led to collect a series of ^{1}H NMR spectra shown in Figure 3.29.

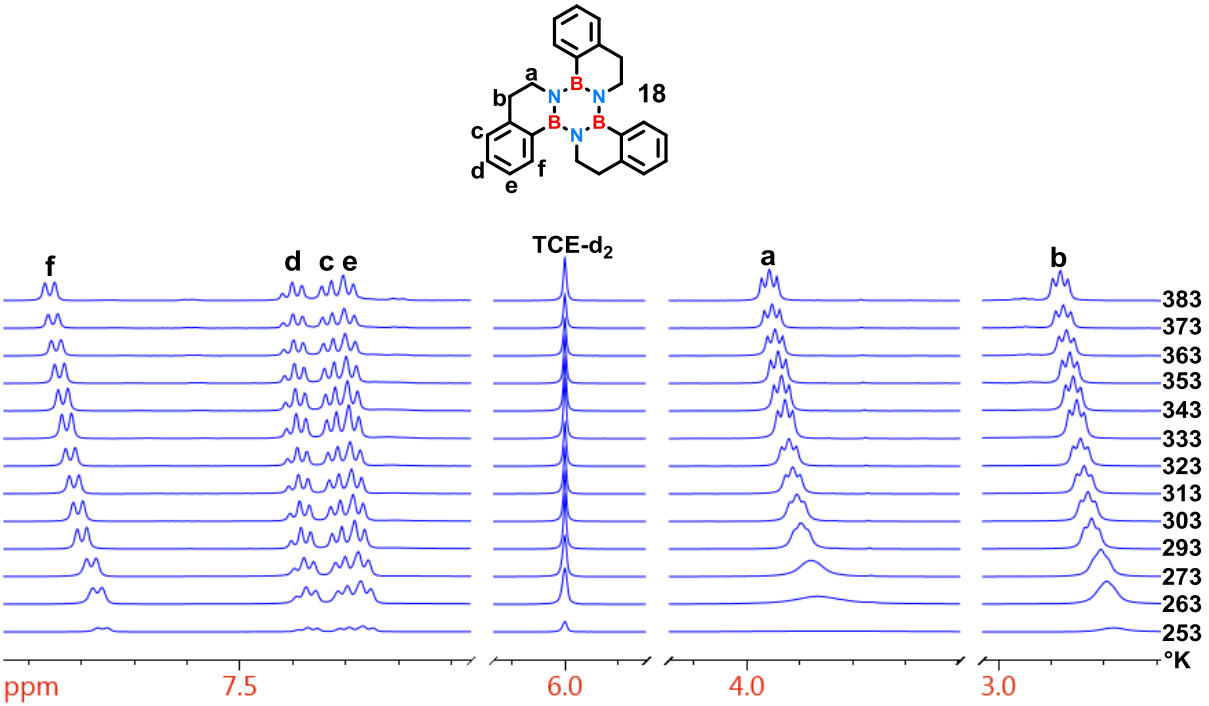

Figure 3.29 Variable temperature ^{1}H NMR spectra of **18**.

The chemical shift of protons **f**, **a** and **b** become more deshielded upon temperature increases. However, the full of both dissociation and aggregation of the polymeric species was not observed since no plateau was reached either at high or low temperatures. A more defined deshielding behaviour upon temperature increasing has been shown by proton **f**, which clearly is the more affected from the aggregation process characterizing borazine **18**. The temperature-dependant data calculated considering the chemical shift of **Hf**, was fitted to the isodesmic model using the Boltzmann equation.[41]

$$y = A_2 + \frac{A_2 - A_1}{1 + \exp\left[\frac{x - x_0}{dx}\right]}$$

Where:

A_1 = minimum value of the physical parameter monitored

A_2 = maximum value of the physical parameter monitored

x_0 = melting temperature (T_m when $\emptyset_{agg}$ = 0.5)

dx = characteristic temperature that is related to the slope of the function at the melting temperature (T^*).

This slope is related to ΔH via:

$$T^* = \frac{-RT_m^2}{0.908\Delta H}$$

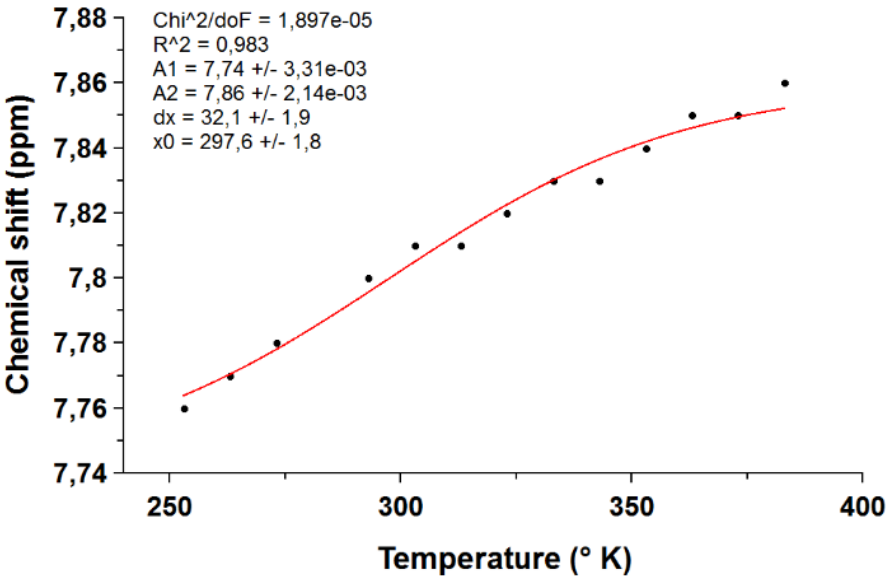

Figure 3.30 Plot of Hf chemical shift vs temperature of **18**.

The degree of aggregation, $\emptyset$, as a function of temperature, *T* is given by:

$$\emptyset(T) \approx \frac{1}{1 + exp\left[-0.0908\Delta H \frac{T - T_m}{RT_m^2}\right]}$$

From the degree of aggregation, the number-averaged degree of polymerisation DP_N can be calculated directly, via:

$$DP_n(T) = \frac{1}{\sqrt{1 - \emptyset(T)}}$$

The DP_N can then be related to the total concentration of molecules C_T, and the association constant *K*, via[42]:

$$DP_n(T) = \frac{1}{2} + \frac{1}{2}\sqrt{4KC_T + 1}$$

From this equation the distribution of material was calculated using the following equations.

$$C_1 = \frac{2KC_T + 1 - \sqrt{4KC_T + 1}}{2K^2C_T}$$

and $C_n = K^{n-1}C_1^n$

The number average aggregate size or the mean number of monomers per π-stack (*N*mers) can be calculated, via[41,43–46]:

$$N = \frac{C_T}{C_N} = \frac{C_1 + 2C_2 + 3C_3 + \ldots + nC_n}{C_1 + C_2 + C_3 + \ldots + C_n}$$

The association constant *K* can be calculated, via:

$$K = \frac{x}{2(C - 2x)}$$

Where:

C = initial concentration

x = *C*[ppm Hf (T)-ppm Hf (final)]/2[ppm Hf (initial)-ppm Hf (final)]

Finally using the Van't Hoff equation is possible to extrapolate the thermodynamic data.

$$lnK = \left(\frac{-\Delta H}{R}\right)\left(\frac{1}{T}\right) + \frac{\Delta S}{R}$$

The graph of ln*K* vs 1/*T* showed a linear relationship as consistent with Van't Hoff fitting, the slope of the graph is related to the *ΔH* while the intercept to the *ΔS* (Figure 2.31).

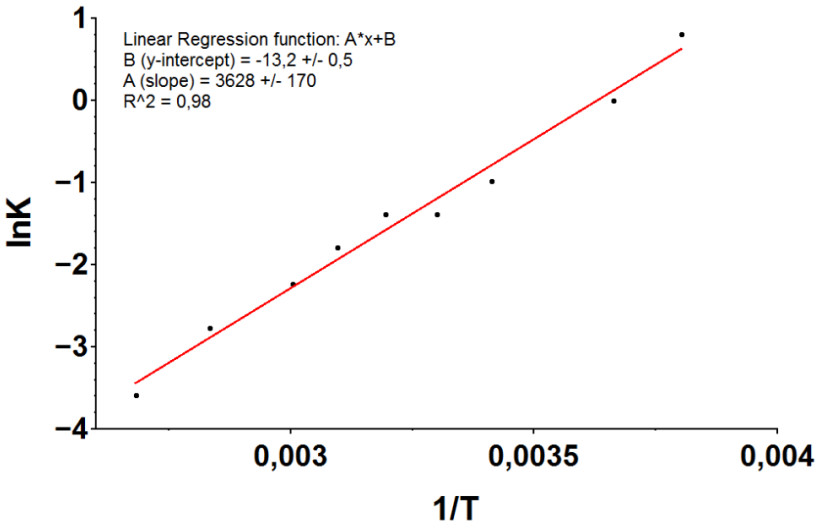

Figure 3.31 Plot of ln*K* vs 1/*T* of **18**.

The data collected were then fitted with the isodesmic polymerisation model described before with equations 1-10 and the graph shown in Figure 3.32 was obtained.

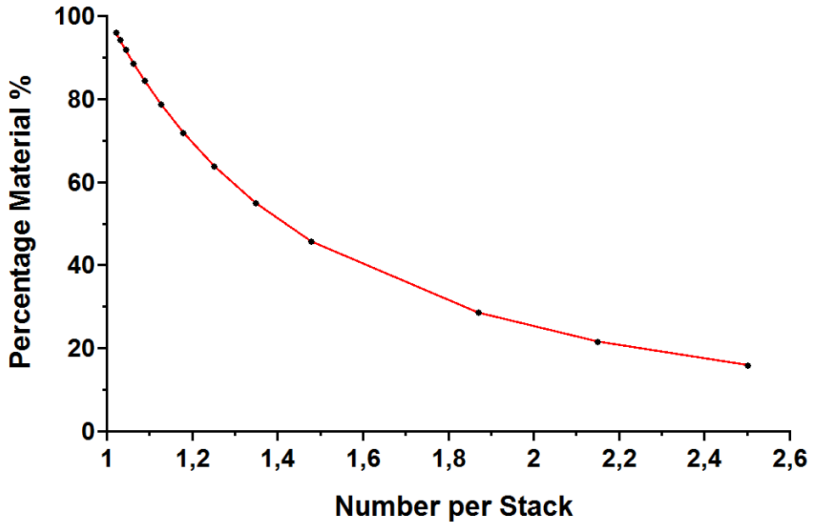

Figure 3.32 Distribution of species of **18**.

The graph obtained showed that at room temperature the majority of borazine **18** (≈96%) exists as a monomer along with the concentration analysed (5.5 mM) with 20% of dimers. These results suggested that the dimerization process of borazine **18** in 1,1,2,2-tetrachloroethane-d_2 is not dominant as we expected since most of the material is in the monomeric form.

REFERENCES

1 V. M. Tsefrikas and L. T. Scott, *Chem. Rev.*, 2006, **106**, 4868.
2 H. W. Kroto, J. R. Heath, S. C. O'Brien, R. E. Smalley and R. F. Curl, *Nature*, 1985, **318**, 162.
3 R. F. C. Brown, *Pyrolytic Methods in Organic Chemistry: Application of Flow and Flash Vacuum Pyrolytic Techniques*, Academic Press, New York, 1980.
4 R. F. C. Brown, *Pure Appl. Chem.*, 1990, **62**, 1981.
5 H. McNab, *Aldrichimica Acta*, 2004, **37**, 19.
6 X. Li, F. Kang and M. Inagaki, *Small*, 2016, **12**, 3206.
7 A. H. Abdourazak, Z. Marcinow, A. Sygula, R. Sygula and P. W. Rabideau, *J. Am. Chem. Soc.*, 1995, **117**, 6410.
8 M. Jurícek, N. L. Strutt, J. C. Barnes, A. M. Butterfield, E. J. Dale, K. K. Baldridge, J. F. Stoddart and J. S. Siegel, *Nat. Chem.*, 2014, **6**, 222.
9 A. J. Olson, Y. H. E. Hu and E. Keinan, *Proc. Nat. Acad. Sci. USA*, 2007, **104**, 20731.
10 B. L. Feringa, *Acc. Chem. Res.*, 2001, **34**, 504.
11 B. L. Feringa, *J. Org. Chem.*, 2007, **72**, 6635.
12 R. Shenhar, I. Willner, D. V. Preda, L. T. Scott and M. Rabinovitz, *J. Phys. Chem. A*, 2000, **104**, 10631.
13 J. Plater, H. S. Rzepa, F. Stoppa and S. Stossel, *J. Chem. Soc., Perkin Trans.*, 1994, **2**, 399.
14 A. Sygula and P. W. Rabideau, *J. Chem. Soc., Chem. Commun.*, 1994, 2271.
15 S. Hagen, M. S. Bratcher, M. S. Erickson, G. Zimmermann and L. T. Scott, *Angew. Chem., Int. Ed.*, 1997, **36**, 406.
16 K. Lammertsma' and B. V. Prasad, 9.
17 R. A. Clark and D. C. Parker, *J. Am. Chem. Soc.,* 1971, **93**, 7257.
18 G. A. Molander and S. R. Wisniewski, *J. Org. Chem.*, 2014, **79**, 6663.
19 G. A. Molander, S. R. Wisniewski and K. M. Traister, *Org. Lett.*, 2014, **16**, 3692.
20 G. A. Molander and M. R. Rivero, *Org. Lett.*, 2002, **4**, 107.
21 Steven R. Wisniewski, Courtney L. Guenther, O. Andreea Argintaru and Gary A. Molander, *J. Org. Chem.*, 2014, **79**, 365.
22 M. J. D. Bosdet, W. E. Piers, T. S. Sorensen and M. Parvez, *Angew. Chem., Int. Ed.*, 2007, **46**, 4940.
23 M. J. D. Bosdet, C. A. Jaska, W. E. Piers, T. S. Sorensen and M. Parvez, *Org. Lett.*, 2007, **9**, 1395.
24 C. A. Jaska, D. J. H. Emslie, M. J. D. Bosdet, W. E. Piers, T. S. Sorensen and M. Parvez, *J. Am. Chem. Soc.*, 2006, **128**, 10885.
25 X.-Y. Wang, J.-Y. Wang and J. Pei, *Chem. -Eur. J.*, 2015, **21**, 3528.
26 P. G. Campbell, A. J. V. Marwitz and S.-Y. Liu, *Angew. Chem. Int. Ed.*, 2012, **51**, 6074.
27 J. S. A. Ishibashi, J. L. Marshall, A. Mazière, G. J. Lovinger, B. Li, L. N. Zakharov, A. Dargelos, A. Graciaa, A. Chrostowska and S.-Y. Liu, *J. Am. Chem. Soc.*, 2014, **136**, 15414.
28 Y. Gabr, *Acta chimica slovenica*, 2007, **54**, 818.
29 X.-S. Ning, X. Liang, K.-F. Hu, C.-Z. Yao, J.-P. Qu and Y.-B. Kang, *Adv. Syn. Cat.*, 2018, **360**, 1590.
30 M. J. S. Dewar and R. Dietz, *J. Chem. Soc.*, 1959, 2728.
31 S. R. Wisniewski, C. L. Guenther, O. A. Argintaru and G. A. Molander, *J. Org. Chem.*, 2014, **79**, 365.
32 E. V. van Loef, J. Marshall, L. N. Zakharov, S.-Y. Liu and K. S. Shah, *IEEE Trans. Nuc. Sci.*, 2013, **60**, 952.
33 W. Luo, P. G. Campbell, L. N. Zakharov and S.-Y. Liu, *J. Am. Chem. Soc.*, 2011, **133**, 19326.
34 M. Lysén, H. M. Hansen, M. Begtrup and J. L. Kristensen, *J. Org. Chem.,* 2006, **71**, 2518.
35 W. C. Ripka and D. E. Applequist, *J. Am. Chem. Soc.*, 1967, **89**, 4035.
36 C. Rochais, R. Yougnia, T. Cailly, J. Sopková-de Oliveira Santos, S. Rault and P. Dallemagne, *Tetrahedron*, 2011, **67**, 5806.
37 J.-C. Hsieh, A.-Y. Cheng, J.-H. Fu and T.-W. Kang, *Org. Biomol. Chem.*, 2012, **10**, 6404.
38 K. Fuchibe, Y. Ohshima, K. Mitomi and T. Akiyama, *Org. Lett.*, 2007, **9**, 1497.
39 *International Tables for Crystallography*, Springer, 1965.
40 N. Ponnuswamy, G. D. Pantoş, M. M. J. Smulders and J. K. M. Sanders, *J. Am. Chem. Soc.*, 2012, **134**, 566.
41 M. M. J. Smulders, M. M. L. Nieuwenhuizen, T. F. A. De Greef, P. van der Schoot, A. P. H. J. Schenning and E. W. Meijer, *Chem. -Eur. J.*, 2010, **16**, 362.
42 Z. Chen, A. Lohr, C. R. Saha-Möller and F. Würthner, *Chem. Soc. Rev.*, 2009, **38**, 564.
43 N. J. Baxter, M. P. Williamson, T. H. Lilley and E. Haslam, *J. Chem. Soc. Faraday Trans.*, 1996, **92**, 231.
44 A. Ciferri, *Supramolecular Polymers*, CRC Press, Boca Raton, Florida, 2nd edn., 2005.
45 J. R. Henderson, *J. Chem. Phys.*, 2000, **113**, 5965.
46 D. Zhao and J. S. Moore, *Org. Biomol. Chem.*, 2003, **1**, 3471.

CHAPTER 4

Attempted synthesis of Hybrid Boron, Nitrogen and Carbon C_3-Hemifullerene

4.1 Introduction

With the success achieved in the synthesis of functionalized BN-doped truxene and octahydrobenzo(c)naphtho(2,1-p) chrysene derivatives, we believed that with our methodologies we could synthesise larger BN-doped polycyclic aromatic hydrocarbons (PAHs). In this regard, as anticipated in Chapter 3, one of our greatest dreams was the synthesis of hemifullerene molecule BN doped by substitution of the central aromatic core with the borazine ring. During this project we have always been looking for suitable building blocks to use as precursors for the synthesis of **1** following different strategies. The pioneering works on the synthesis of extended PAHs and bowl-shaped fullerene fragments obtained by Flash Vacuum Pyrolysis (FVP) reported by Scott and co-workers[1,2] always attracted us. To this end we decide to use this technique to promote the ring closure by the formation of new C-C bonds needed for the synthesis of BN-doped hemifullerene **1**. From the retrosynthetic perspective detailed in Chapter 3 (Scheme 4.1), we envisioned that the BN-doped hemifullerene **1** could be achieved following two different synthetic pathways.

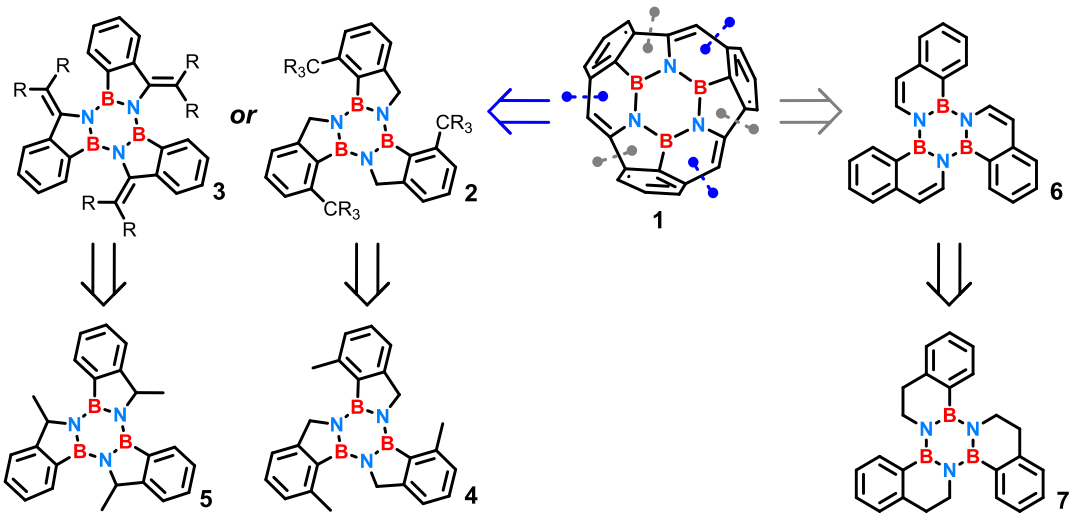

Scheme 4.1 Retrosynthetic analysis of BN-doped hemifullerene **1**.

In the first approach considered (blue), either vinyl functionalized borazatruxenes **3** in the benzylic position or borazatruxenes ortho substituted respect to the boron atom **2** seemed to be valid precursors for the synthesis of **1**. Therefore, the borazatruxenes **4** and **5** synthesised in Chapter 2 were chosen as building blocks for the synthesis of **1**. Despite the substituent in the benzylic position of borazine **5** was an sp^3 methyl group we considered to achieve the vinyl functional group by dehydrogenation in presence of Pd/C and then with the real precursor **8** in hand to proceed with the synthesis of **1**.

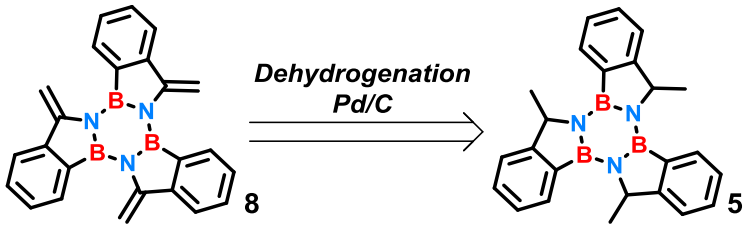

Scheme 4.2 Retrosynthetic analysis of compound **8**.

Regarding borazine **4**, we believed that under the drastic reaction conditions used in the flash vacuum pyrolysis (FVP) procedure, both benzylic positions might be susceptible to the radical formation, which in turn could react internally, closing the ring as shown in Scheme 4.3.

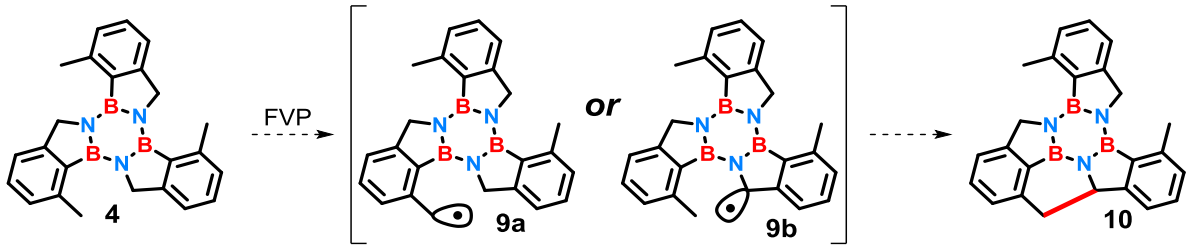

Scheme 4.3 Mechanism proposed for the ring closure of **4** by FVP.

The alternative strategy was starting from benzo(c)naphtho(2,1-p)borazachrysene **6**, which could be prepared by dehydrogenation of the corresponding hydrogenate analogue **7** synthesised in Chapter 3 (Scheme 4.4).

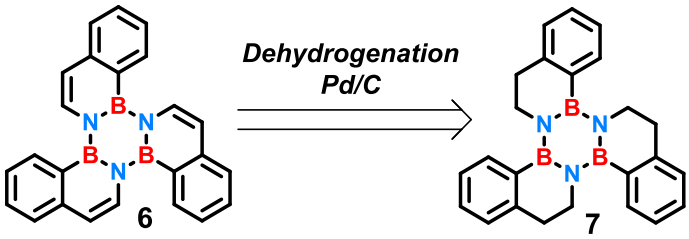

Scheme 4.4 Alternative approach for the synthesis of **1**.

4.2 Dehydrogenation of borazines 5 and 7

Initially we attempted at the dehydrogenation of borazines **5** and **7** to prepare the desired building blocks **8** and **6** to use in the FVP procedure. The most versatile methods for the dehydrogenation of saturated organic molecule requires the use of metal-based catalysts such as Pd/C, which is the most commonly used in the dehydrogenation procedures.[3] To begin our study, we investigated the reactivity of borazine **7** for

dehydrogenation, in presence of 21 mol% (7 mol% per bond) of Pd/C in anhydrous ethyl acetate. The reaction was performed under inert atmosphere (Argon) and irradiated by microwave dielectric heating at 100 °C. The reaction was followed by TLC chromatography analysis where a sample of reaction beforehand diluted with CH_2Cl_2 was eluted with *n*-hexane/CH_2Cl_2 (50:50). However, after 7 hours of stirring at this temperature the reaction was stopped since TLC analysis revealed the presence of the only starting material unreacted. Indeed the ^{1}H NMR spectrum of the crude mixture showed the -CH_2- groups in α and β positions to the nitrogen atom untouched. Probably the reaction conditions used were not thermodynamically favourable to overcome the energy barrier for reactant-to-product transformation. In a second attempt at the synthesis of **6** we followed a literature procedure introduced by Z. P. Liu and co-workers[4] for the dehydrogenation of sterols in DMF. Considering that our system was different from that reported in literature, application of this protocol required some changes to be adapted to our substrate: the percentage of Pd/C was increase to 21% and the use of $NaCO_3$ as additive was excluded to avoid side nucleophilic reactions at the boron atoms.

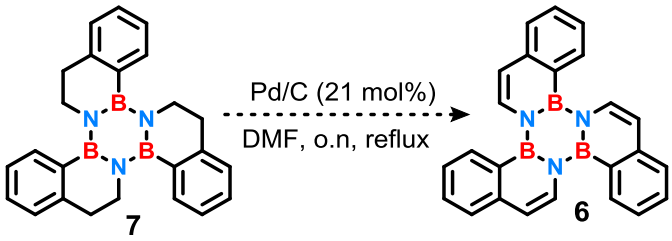

Scheme 4.5 Reaction conditions attempted for the dehydrogenation of **7**.

TLC analysis after overnight reaction (eluent, *n*-hexane/CH_2Cl_2 (50:50)) displayed a new product, therefore the crude mixture was cooled to room temperature and then filtered over a plug of celite to remove the catalyst. The organic solution was diluted with ethyl acetate and washed with brine several times to remove DMF. After solvent removal the solid was analysed by NMR. The ^{1}H-NMR spectrum in $CDCl_3$ displayed two distinct sets of symmetric signals possibly related to two different products, however when deuterated methanol was added, and the NMR analysis was repeated, the spectrum collected shown half of the signals previously seen. Instead the ^{11}B-NMR spectrum of the crude mixture showed only one signal resonating at 29.6 ppm, diagnostic of boronic acid/ester species.

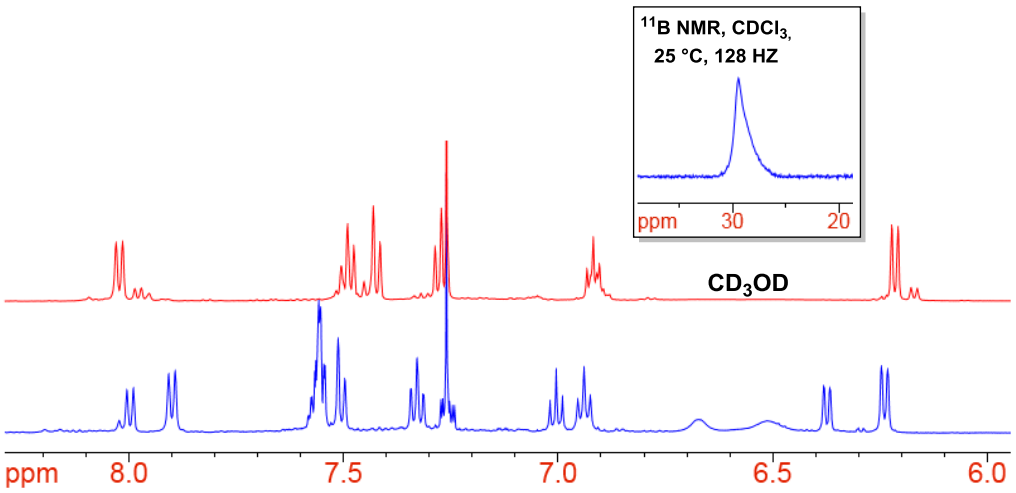

Figure 4.1 Comparison between ^{1}H-NMR spectra in $CDCl_3$ of the crude mixture of the dehydrogenation of **7** before (blue) and after(red) addition of deuterated methanol.

In this case a boronic ester species was formed since the broad peaks at 6.67 and 6.51 ppm disappeared upon addition of deuterated methanol. The absence of signals associated to the -CH_2- groups in α and β positions to the nitrogen atom suggested that dehydrogenation in that position occurred, confirmed also by the presence of two new doublets at 8.02 and 6.21 ppm with a *J* coupling of 7.5 Hz. After further 2D NMR analysis we tentatively assigned to the unknown compound molecular structure of **11**.

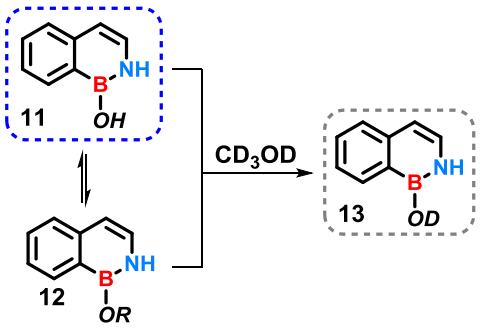

Scheme 4.6 Equilibrium proposed between species **11** and **12**, which led to **13** upon addition of deuterated methanol.

Considering that boronic acids are always involved in equilibrium reactions such as dimerization, NMR results obtained in absence of deuterated methanol can reflect a similar situation in which **11** is in equilibrium with an its derivative. Upon addition of a large amount of deuterated methanol this equilibrium is shifted towards species **13**, which is the only product detected by NMR. Borazine decomposition into the α, β unsaturated aminoborane **23** can be rationalized in terms of dehydrogenation of **7** followed by a re-hydrogenation (reduction) of the borazine ring of **7** into **21**.

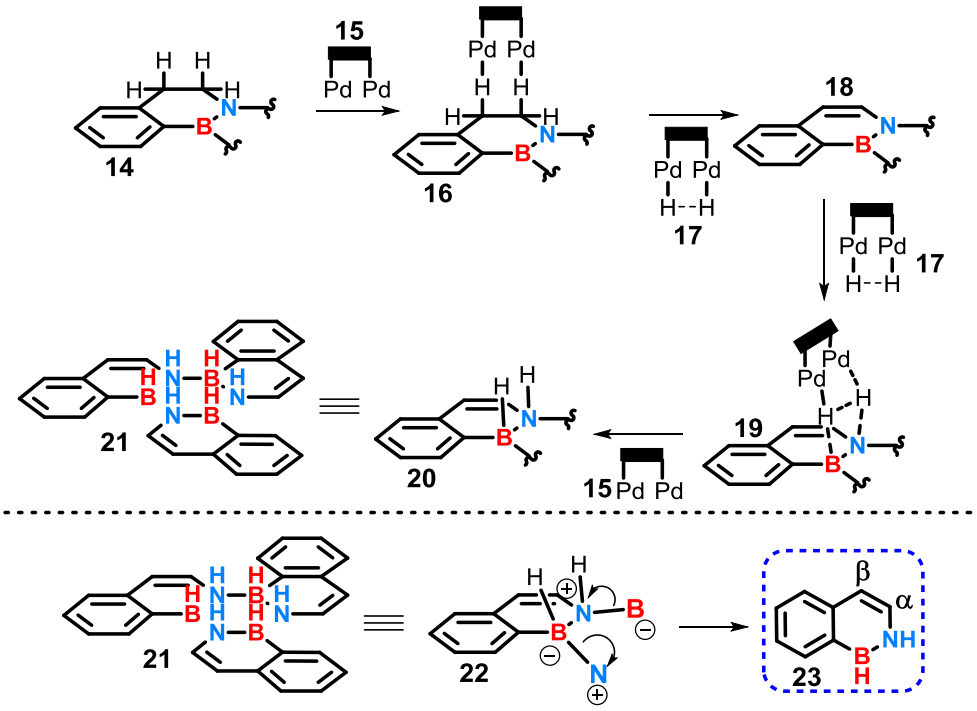

Scheme 4.7 Proposed mechanism for the formation of **23**.

Palladium catalyst interact with hydrogens in α, β position to the nitrogen atom in in a syn fashion **16** promote the cis dehydrogenation with the double bond formation. Hydrogen molecule absorbed on the catalyst surface **17** subsequently interact with polarized BN units **19** in a catalytic hydrogenation reaction where a molecule of hydrogen is in turn transferred in a syn fashion. At this point the hydrogenate borazine species **21** rearrange to monomer **23**. This result suggested that the dehydrogenated borazine species **6** formed, subsequently reacted as hydrogen acceptor. Therefore, we believed that to avoid this collateral reaction an oxidant or a hydrogen acceptor to react with the generated hydrogen instead of the borazine molecule, was required. Styrene is widely used as hydrogen acceptor in the common dehydrogenation reactions providing an external driving force to make thermodynamically favourable this reaction.[5] To this end we repeated this reaction, in the same conditions, in presence of styrene. After work up, four fractions were isolated and by NMR analysis the first two revealed to be starting material **7** and ethyl benzene. While attempts to identify products of the last two fractions proved to be inconclusive because of the presence of a complex mixture of by-products, which made the ^{1}H NMR spectra difficult to interpret. The effect of the solvent was also studied; however, when the reaction was repeated under the same reaction conditions in toluene, unfortunately, only starting material was recovered. While replacing DMF, which undergo to partial decomposition to high temperatures, with the more stable analogue DMA the outcome was identical to that previously described. In an attempt to understand the behave of our borazine system towards the dehydrogenation reaction, we decided to make a screening of different catalysts to use. Along with this idea we had a careful review of the literature and we came across with an interesting report by Grimme and Paradies.[6] This group developed an acceptorless dehydrogenation method catalysed by the

strong Lewis acid $B(C_6F_5)_3$. Unfortunately, application of this protocol to our system led only to the recovery of starting material. We finally attempted at the dehydrogenation of **7** using the strong oxidizing agent DDQ, which is widely reported in literature to be very effective to catalyse the formation of new C-C bonds by loss of H_2. The reaction was thus performed in DMF at reflux under inert atmosphere (Argon). TLC analysis after overnight reaction (eluent, *n*-hexane/CH_2Cl_2 (50:50)) displayed a series of new products formed suggesting that a decomposition pathway occurred. Indeed, after work up, NMR analysis of the crude mixture proved to be inconclusive in determining the presence of **8** because of difficult interpretation due to the presence of a complex mixture of by-products. Table 4.1 summarise all the conditions described for the dehydrogenation of borazine **7**.

Table 4.1 Selected conditions for the dehydrogenation of **7.**

N°	catalyst	solvent	T°	t	Outcome
1	Pd/C (21 mol%)	EtOAc	100	7 h	Starting material
2	Pd/C (21 mol%)	DMF	150	o.n.	Product **11**
3	Pd/C (21 mol%)	DMF/Styrene	150	o.n.	Starting material Mix of by-products
4	Pd/C (21 mol%)	Toluene/Styrene	180	7 h, μW	Starting material
5	$B(C_6F_5)_3$ (30 mol%)	Toluene	110	o.n.	Starting material
6	DDQ (3.0 equiv.)	DMF	150	o.n.	Mix of by-products

Given the fact that the synthesis of **7** was a failure we next explored the possibility of synthesising borazine **8** following the method introduced by Z. P. Liu[4] using Pd/C in DMF as reported in Scheme 4.8.

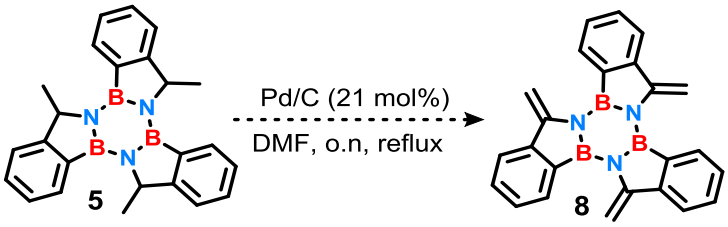

Scheme 4.8 Reaction conditions attempted for the dehydrogenation of **5**.

Exposure of **5** to the same reaction conditions detailed for the attempted synthesis of **6** led to a mixture of products. After separation of the major product by flash chromatography (eluent, *n*-hexane/CH_2Cl_2 (50:50)), ^1H and ^{11}B NMR spectra were collected to identify product **8**. However, ^1H NMR spectrum showed an unexpected pattern, different from that predicted for compound **8** and from that of starting material **5**. While from ^{11}B NMR we could not obtain any useful information because no signal was detected. Therefore, all our efforts to assign a molecular structure to the unknown compound, unfortunately, resulted to be inconclusive.

4.3 Flash vacuum pyrolysis (FVP) of borazines 7 and 27

At this juncture, we became convinced that dehydrogenation of borazine **5** and **7** would not prove viable. We therefore decided to proceed with the flash vacuum pyrolysis (FVP) experiment employing directly borazine **5**, **4** and **7**. Our plan was therefore to follow the same procedure reported by Scott and co-workers for the syntheses of geodesic polyarenes.[1] The flash vacuum pyrolysis (FVP) system was set up was as reported in literature. A boat containing the sample is placed into a quartz tube, which in turn is horizontally inserted into the electric oven. The hot zone typically reaches temperatures in the range of 500-1100 °C (Figure 4.2).

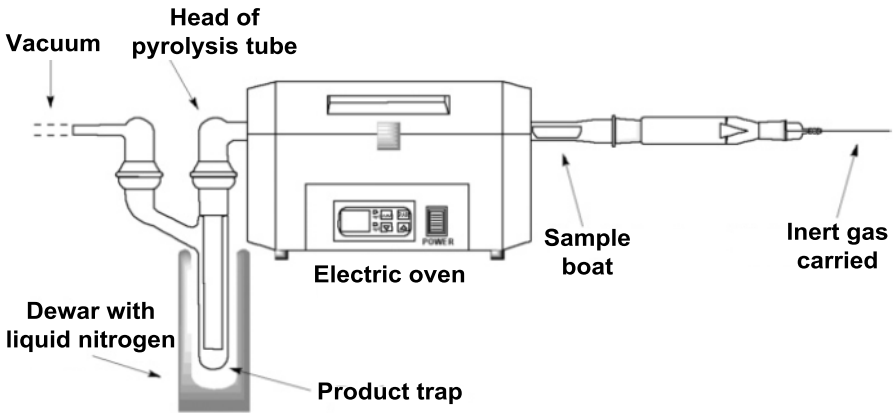

Figure 4.2 Schematic view of the FVP apparatus.[1]

The principle of this method is to heat molecules in the gas phase to very high temperatures for a very short time. Therefore, under vacuum the sample is sublimed and a gentle stream of inert gas carrier (nitrogen/argon) is commonly used to facilitate the flight of molecules in the vapour phase through the hot zone. Finally, products are collected in a cold trap and then analysed. Borazine **7** was chosen as test compound in our initial evaluation. The reaction was performed under a vacuum pressure of (4.5-4.7) 10^{-1} mBar, while the electric furnace was heated to 1100 °C. The temperature rate was set to 50 °C/min, once the furnace reached the temperature of 1100 °C the sample was reacted for 30 min. After cooled the system to room temperature the boat, quartz tube and trap were washed with CH_2Cl_2 and EtOAc, and the washes were separately collected in order to be analysed by NMR. Unfortunately, by analysis of the ^{1}H-NMR spectra in $CDCl_3$ of the three fractions collected, starting material **7** was the only species observed. Considering that Scott and co-workers reported the synthesis of **24** by FVP of differently brominated benzo(c)naphtho(2,1-p) chrysene precursors **25** and **26**,[7,8] we later decided to follow this rout by using borazine **27**.

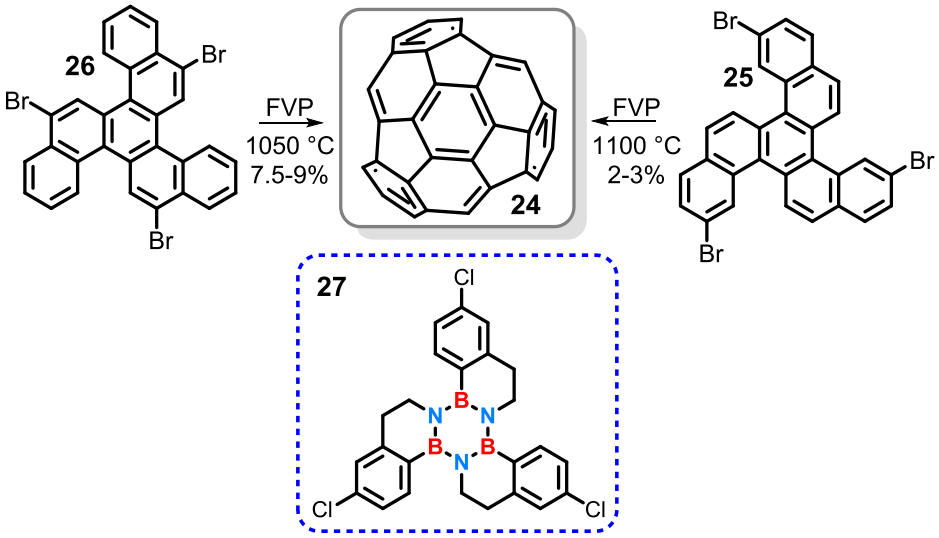

Scheme 4.9 Alternative starting material for the synthesis of **1** by FVP.

The choice of using borazine **27** previously synthesised in Chapter 3, was made along with the idea that the presence of halogen atoms on the peripheral aromatic ring enhance the probability to generate radicals by homolysis of C-X (X = halogens) bond. To this end borazine **27** was subjected to the same FVP conditions previously described for **7**. Unfortunately, also in this case, starting material was recovered. A possible explanation of the failure in the synthesis of **1** by FVP of both precursors **7** and **27** could be associated to the dwell time of the letter into the oven. Probably the high vacuum set made the sublimation process too fast and the flowing rate of the gas carrier set was too high, thereby leading to a quick fly of molecules in the vapour phase through the hot zone of the oven. Also, another important aspect that we need to take in consideration is that Scott and co-workers reported examples of new C-C bond formed by a radical pathway of two sp^2 hybridized carbon atoms. In our case instead, because of the failure of the dehydrogenation of **7,** we relied on the C-C bond formation by stitching of an sp^2 and an sp^3 carbon atoms, which obviously have different reactivity. Attempts at the synthesis of **1** employing borazines **4** and **5** have been postponed to a near future since before a better knowledge of these systems by theoretical models is needed.

REFERENCES

1 V. M. Tsefrikas and L. T. Scott, *Chem. Rev.*, 2006, **106**, 4868.
2 L. T. Scott, *J. Org. Chem.*, 2016, **81**, 11535.
3 X. Liu and D. Astruc, *Adv. Synth. Catal.*, 2018, **360**, 3426.
4 Y.-Z. Yin, C. Liu, L.-Q. Tang and Z.-P. Liu, *Steroids*, 2012, **77**, 1419.
5 J. Zhang, Q. Jiang, D. Yang, X. Zhao, Y. Dong and R. Liu, *Chem. Sci.*, 2015, **6**, 4674.
6 A. F. G. Maier, S. Tussing, T. Schneider, U. Flörke, Z.-W. Qu, S. Grimme and J. Paradies, *Angew. Chem., Int. Ed.*, 2016, **55**, 12219.
7 S. Hagen, M. S. Bratcher, M. S. Erickson, G. Zimmermann and L. T. Scott, *Angew. Chem., Int. Ed.*, 1997, **36**, 406.
8 G. Mehta, G. Panda and P. V. V. Srirama Sarma, *Tetrahedron Lett.*, 1998, **39**, 5835.

CHAPTER 5

Synthesis and Characterization of Hybrid Boron, Nitrogen and Carbon Oligomers and 2D Polymeric Materials

5.1 Introduction

In the last stage of our project we became attracted to the possibility of synthesising hybrid boron, nitrogen and carbon 2D materials following a bottom-up synthetic strategy. At the moment one of the most feasible methods to introduce BN units into the graphene lattice is the chemical vapor deposition (CVD). This physical method, introduced by Ajayan in 2010 for the synthesis of the first BN-doped graphene hybrid semiconductor,[1] is widely used for the preparation of thin films of BN-embedded graphene semiconductors. With the CVD technique the graphene doping is achieved by thermal decomposition of different precursors of carbon, boron and nitrogen atoms such as methane and ammonia borane ($NH_3{\cdot}BH_3$). The electronic properties of these material can be finely tuned by controlling the experimental parameters such as the carbon concentration to pass from insulating to highly conducting materials.[2]

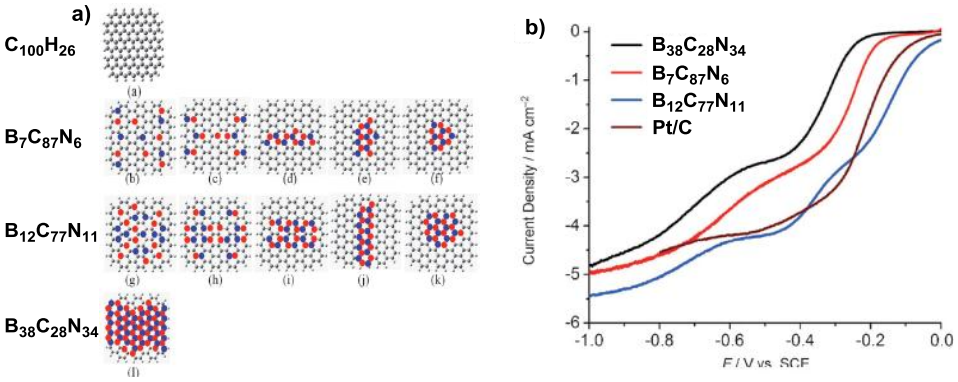

Figure 5.1 a) BCN graphene models and b) current density of BCN graphene calculated at different compositions of BN dopants.[2]

However, one of the key challenges in advancing the graphene doping technologies is the differences between batches in terms of atomically structure composition. This problem is mainly due to the thermodynamically favoured phase separation of h-BN and graphene domains within the hybrid material.

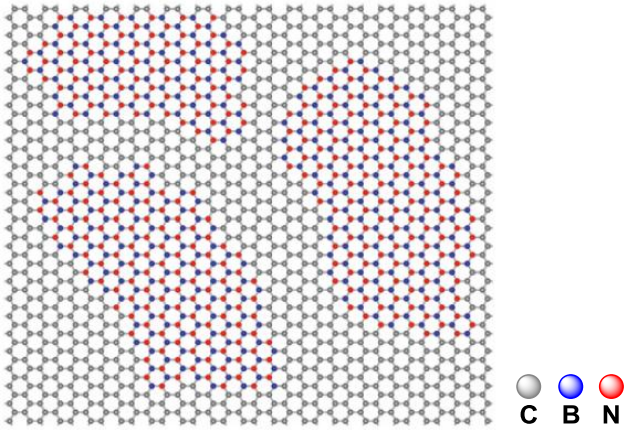

Figure 5.2 Atomic model of the h-BNC film showing hybridised h-BN and graphene domains based upon elemental analysis of the material.[1]

Therefore, to have a better control on the distribution of the BN units dispersed in the graphene framework and achieve more homogeneously doped semiconducting materials a bottom-up organic synthesis needs to be explored. In this regard, considering the successful synthetic strategies developed for the synthesis of borazatruxenes and 7,8,15,16,23,24-hexahydroborazabenzonaphtho(2,1-p) chrysenes, we envisaged to synthesise 2D-CBN hybrid materials by polymerization of aromatic building blocks containing two amine-borane functional groups.

5.2 Synthesis of bis BN [2,1,8,7] 1,2,3,5,6,7-hexahydro-s-indacene

5.2.1 Synthesis of 2,5-bis(diboron-neopentyl) terephthalonitrile

The synthesis of 2D hybrid materials was designed based on the borazatruxene framework because this molecule is the simplest borazine synthesised, and well characterized in our group. We believed that the key step to achieve 2D heterostructures **1** was the thermolysis of a diamino-diborane species **2,** which in turn could be obtained by one-step reduction of 2,5-di(boronic ester)terephthalonitrile **3**.

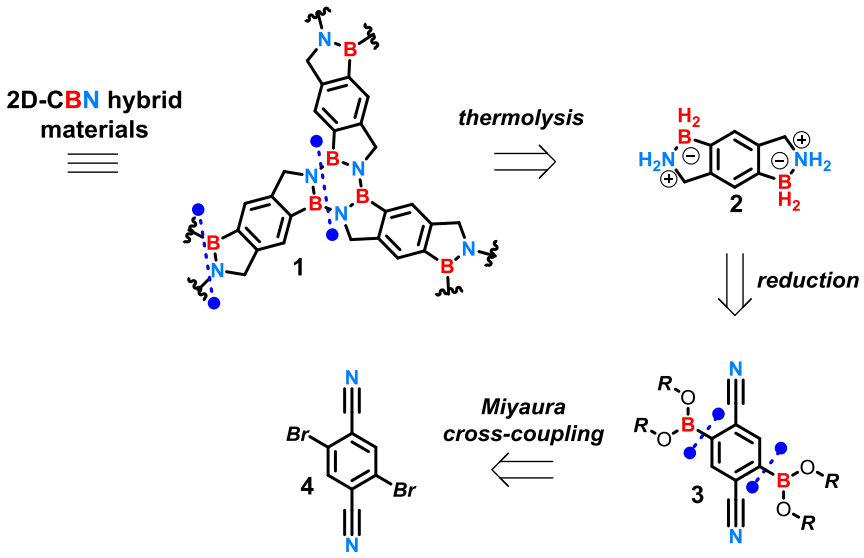

Scheme 5.1 Retrosynthetic analysis of CBN-2D networks **1**.

The regioselective borylation in positions 2 and 5 of terephthalonitrile **5** could be conceived by Miyaura cross-coupling reaction of the 2,5-di-bromo derivative **4**. The lithiation-borylation of terephthalonitrile was exclude because lithiation could occur either in positions 2 and 5 leading to the desired product **3** or in positions 2 and 6 leading to the undesired by-product **7** thus lowering the yield of **3**.

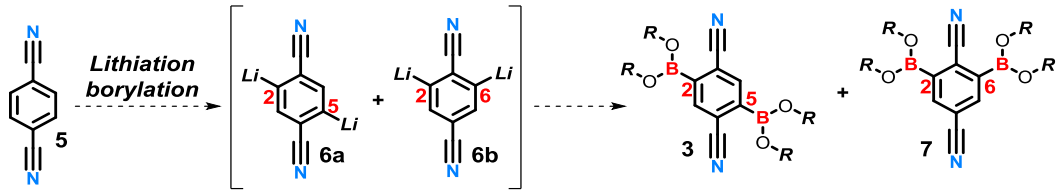

Scheme 5.2 Plane envisioned for the lithiation-borylation of **5**.

Unfortunately starting material **4** was affordable only in low quantities to a conspicuous price (1g ≈ $ 400) therefore we decide to synthesise the latter via *ortho* bromination of terephthalonitrile **4** following the same method[3] described in Chapter 2. Exposure of **5** to the standard reaction conditions used for the *ortho* bromination led to a 3:2 mixture of the two regioisomers **4** and **8**, after chromatography purification (eluent, *n*-hexane:CH_2Cl_2 90:10).

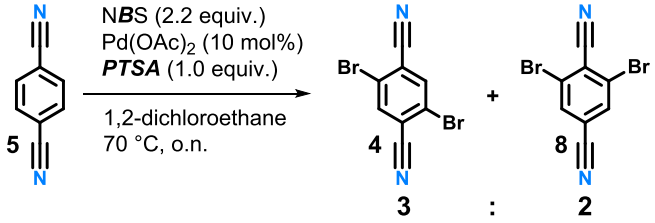

Scheme 5.3 *Ortho* bromination of **5**.

Unable to install bromine atoms regioselectively in positions 2 and 5 onto terephthalonitrile **5** we decided to consider an alternative tactic for the synthesis of **4**. Pondering to the fact that there are more synthetic procedures to have access to the nitriles group by manipulation of a wider range of functional groups, we decided to start from a substrate already containing bromine atoms in positions 2 and 5 with masked nitrile groups in positions 1 and 4. By a careful review of the literature we found an interesting report[4] by Yu detailing the synthesis of **4** starting from the corresponding di-aldehyde precursor **10** that could be obtained by reduction, under controlled conditions, of the corresponding 2,5-dibromoterephthalate diester **11**.

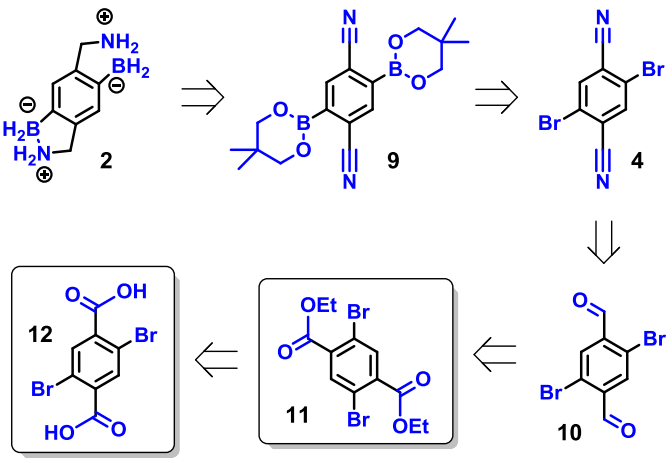

Scheme 5.4 Retrosynthetic analysis of **2**.

Considering that the difference in price between commercially available 2,5-dibromoterephthalic acid **12** and the corresponding diethyl ester **11** was almost the double we decide to start from the cheaper starting material **12** at the expense to add one step more to the synthetic pathway. Esterification of **12** was carried out in anhydrous ethanol, refluxing the resulting mix in presence of a catalytic amount of H_2SO_4 conc.

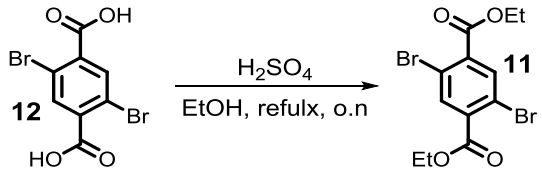

Scheme 5.5 Synthesis of compound **11**.

After purification the desired **11** was delivered in 66% yield and direct comparison of ^{1}H-NMR with that reported in literature[5] confirmed molecular structure of **11**. For the selective reduction of the ester groups into the aldehyde functional groups it was followed a method introduced by Keun An.[6] This efficient one-pot synthetic procedure relies upon the formation of a more reactive morpholine amides intermediate **17** which is easily reduced to the corresponding aldehyde under mild reaction conditions when exposed to reducing agents such as DIBAL-H or LDBMA. Morpholine amides **17** is obtained by aminolysis of esters **16** with diisobutyl(morpholino)aluminium adduct **15** which in turn is prepared in situ by deprotonation of morpholine **13** when threated with DIBAL-H **14**.

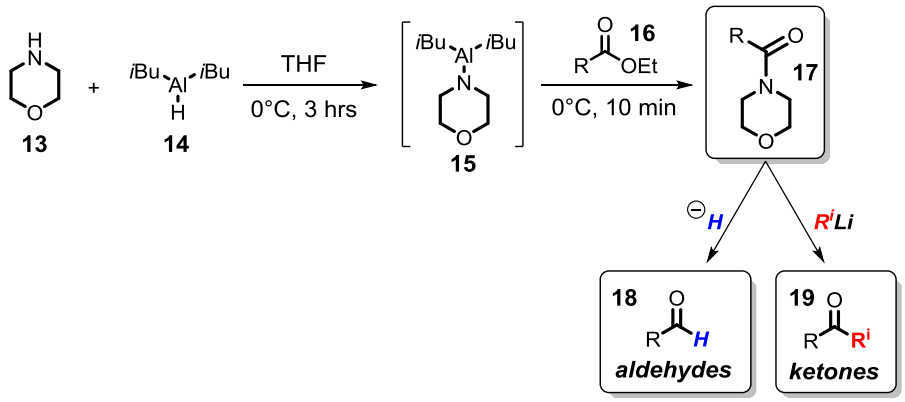

Scheme 5.6 One-pot synthesis of ketones and aldehydes from esters bymorpholine amide intermediates.

The reaction was performed under inert atmosphere (argon) and DIBAL-H was slowly added dropwise to a solution of morpholine **13** in anhydrous THF at 0 °C. Parallelly 2,5-dibromoterephthalate **11** was dissolved under argon atmosphere in anhydrous THF and then added dropwise to the solution containing the diisobutyl(morpholino)aluminium adduct **15** at 0 °C. The morpholine amide intermediate formed was subsequently reduce to the corresponding di-aldehyde specie **10** upon slow addition of DIBAL-H. At this stage a changing in colour of the reaction mixture from transparent to light yellow was observed. The

reaction was finally quenched with 1 M solution of HCl and extracted with EtOAc. Pure **10** was obtained in very good yield (90%) after column chromatography purification (*n*-hexane:CH_2Cl_2 60:40).

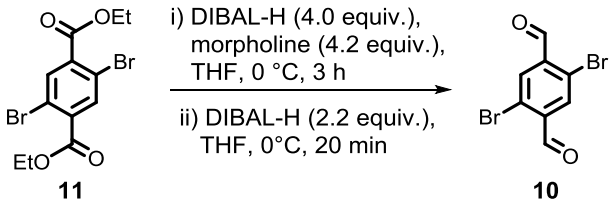

11 **10**

Scheme 5.7 Synthesis of compound **10**.

However, we noticed that this reaction was highly moisture sensitive indeed when the reaction was repeated with either solvent or reactants less anhydrous the percentage of yield of **10** drastically dropped. Likewise, when we attempted at the scaling-up to gram scale the yield of **10** dropped to 50-60%. This was basically due to the difficulties concerning the anhydrification of solvents and reactants when used for large scale reactions. Comparison of ^{1}H and ^{13}C-NMR spectra of **10** in DMSO-d_6 with that reported in literature[6] confirmed molecular structure of **10**. The 2,5-dibromoterephthalaldehyde **10** was converted into 2,5-dibromoterephthalonitrile **4** following the procedure introduce by Yu. Exposure of **10** to hydroxylamine hydrochloride and sodium acetate dissolved in concentrated formic acid under refluxing conditions led directly to the desired **4** in 96% yield.

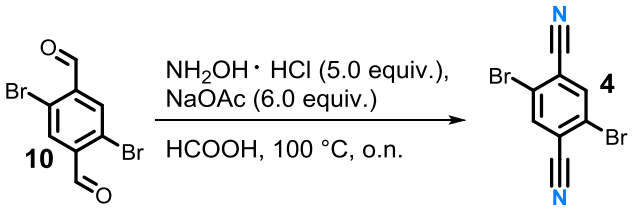

Scheme 5.8 Synthesis of compound **4**.

Analysis of the NMR data collected on the crude after the work up procedure revealed **4** to be highly pure. However, we decide to wash quickly the solid with a mix of *n*-hexane:CH_2Cl_2 (80:20) as the literature procedure suggested. This purification procedure was very efficient in removing by-products formed without dissolving the desired **4**. With pure building block **4** in hand, we proceeded with the Miyaura cross-coupling reaction following the same protocol[7] described in Chapter 2. The reaction was followed by TLC analysis, and after 2 hours of refluxing all the starting material was converted. Proceeding with the work up we noticed that the desired **9**, and eventually side products formed, were much less soluble compared with the boronic esters previously synthesised. Indeed, a conspicuous amount of EtOAc was required to dissolve the crude, to be purified by washing with water. However, we subsequently found that the desired **9** could be easily isolated by precipitation from a statured solution in CH_2Cl_2 by adding *n*-hexane. Surprisingly, **9** was obtained in only 43% yield after purification. This unexpected outcome was readily

rationalized by considering the possibility of **9** to react with the corresponding starting material **4** delivering a complex mixture of oligomers and polymers. Indeed, during the course of the reaction the presence of both species **4** and **9** at the same time can led to the formation of polymers following the Suzuki-Miyaura cross-coupling pathway at the expense of the Miyaura cross-coupling reaction.

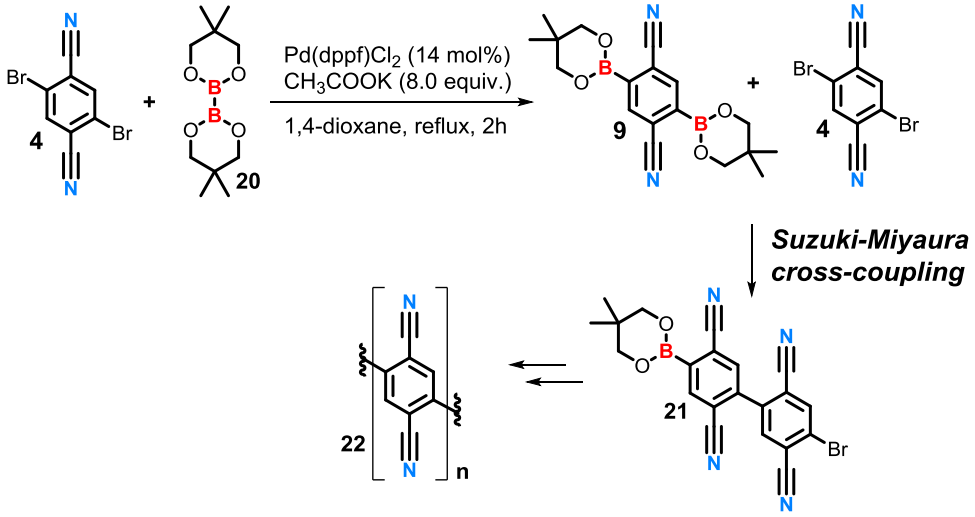

Scheme 5.9 Suzuki-Miyaura cross-coupling pathway between compounds **9** and **4**, explaining the formation of oligomers and polymers.

This plausible hypothesis was later confirmed by the presence of an insoluble dark red solid, and the ^{1}H-NMR spectrum in DMSO-d_6 displayed broad peaks in the aromatic region suggesting the solid to be a complex mixture of polymeric species. In an attempt to minimize the amount of side products formed we repeated the synthesis using different reaction conditions. We initially explored the procedure reported by B. Wang[7] using DMSO as described in Chapter 2. Unfortunately, these conditions revealed to be less effective since the desired **9** was obtained in only 26% yield (half than before). Other attempts using different solvents revealed to be less successful, indeed when the reaction was carried out in a mix of THF:toluene 2:1, the desired **9** was isolated in 30% yield while, when refluxed in toluene led only to recovery of starting material. Subsequently we decided to evaluate the effect of the catalyst switching $Pd(dppf)Cl_2$ with $Pd(PPh_3)_4$. Therefore, the reaction was repeated in 1,4-dioxane and toluene in presence of $Pd(PPh_3)_4$ but, unfortunately, only starting material was recovered. Also increasing the equivalents of bis(neopentyl glycolato)diboron proved unsuccessful since **9** was delivered in 33% yield. In an effort to reduce the side polymerization process we later envisioned to overcome the problem working in diluted conditions in order to minimise interactions between starting material **4** and product **9**. Guided by this hypothesis we repeated the synthesis with an initial concentration of **4** in 1,4-dioxane four orders of magnitude lower than the beginning (from 0.06 to 0.017 M). Surprisingly, a notable improvement in yield was observed since **9** was provided in 78% yield confirming our theory. Table 5.1 summarise all the reaction conditions attempted for the synthesis of **9**.

Table 5.1 Reaction conditions used for the synthesis of **9.**

Concentration of 4 [M]	*solvent*	*T (°C)*	*t (h)*	*catalyst*	*% yield*
0.06	1,4-dioxane	reflux	2	$Pd(dppf)Cl_2$	43
0.06	DMSO	90	2	$Pd(dppf)Cl_2$	26
0.03	1,4-dioxane	reflux	2	$Pd(dppf)Cl_2$	33
0.06	THF : Toluene 2:1	90	3	$Pd(dppf)Cl_2$	30
0.06	1,4-dioxane	reflux	3	$Pd(PPh_3)_4$	s.m. recovered
0.06	Toluene	reflux	3	$Pd(PPh_3)_4$	s.m. recovered
0.017	1,4-dioxane	reflux	2	$Pd(dppf)Cl_2$	**9**

Pleasingly, we finally discovered that this reaction was entirely concentration dependent moreover, when repeated at this concentration revealed to be reproducible delivering **9** in the same percentage yield.

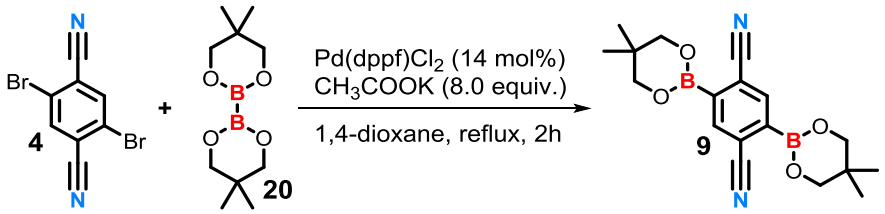

Scheme 5.10 Synthesis of compound **9**.

Purification of **9** was easily achieved by evaporation of the solvent and volatile side products. The remained impurities were subsequently removed by repeated washing of the solid with acetone in the reaction flask. Exploiting the poor solubility of **9** in this solvent, it could be isolated by centrifugation as insoluble powder. The NMR data collected for **9** were compared with that reported in literature[8] for a similar substrate containing the pinacol rather than the neopentyl glycol protecting group onto the boron atom resulting to be very similar. The ^{11}B NMR spectrum in $CDCl_3$ displayed a signal resonating at 25.4 ppm confirming the boronic ester functional groups. The mass spectroscopy analysis displayed a good match between the predicted isotope pattern distribution and the observed data, confirming molecular structure of **9**.

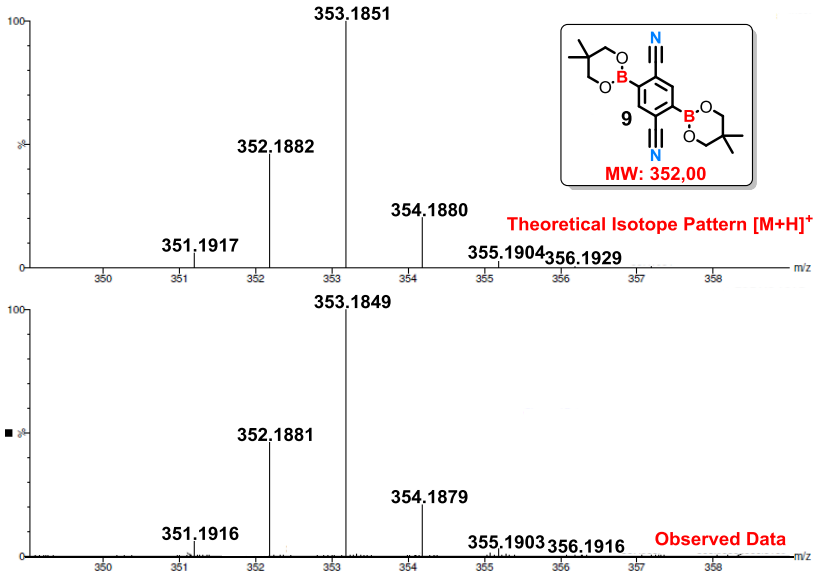

Figure 5.3 Mass Spectrum of compound **9** from Swansea University.

Surprisingly, in a later stage of our studies we discovered that building block **4** could be easily synthesised by one-pot reaction starting from commercially available 2,5-dibromobenzoquinone **26**. Indeed, recently Glöcklhofer and co-workers reported a straightforward synthetic procedure[9] to readily have access to cyanoarenes **25** starting from the corresponding quinone precursors **23** by one-pot reaction. Application of this protocol to our synthetic pathway to produce 2D hybrid materials, allowed us to make quicker the total synthesis involving less work up and purification procedures. This low-cost, one-pot synthesis relay on the formation of a silylated cyanohydrin intermediate **24** as shown in Scheme 5.11.

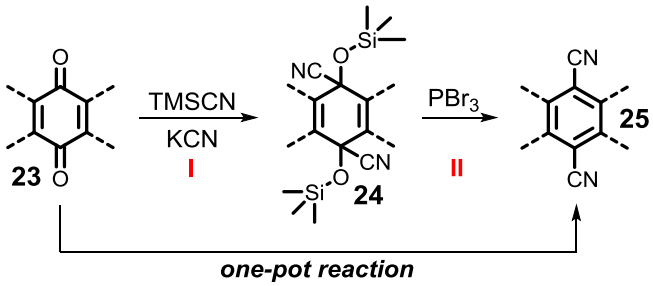

Scheme 5.11 One-pot synthesis of cyanated acenes **25** from quinones **23** in two steps via silylated cyanohydrin intermediates **24**.

In the first step the carbonyl groups of starting material **23** are converted into silylated cyanohydrin **24** using a stoichiometric amount of trimethylsilyl cyanide (TMSCN) in presence of a catalytic amount of a cyanide salt such as KCN. The subsequent exposure of intermediate **24** to PBr_3 undergo to the reductive aromatization providing the corresponding cyanoarene **25**. Following the reported procedure using 2,5-dibromobenzoquinone **26** as starting material we obtained the desired **4** in 76% yield after chromatography purification (*n*-hexane:EtOAc 70:30).

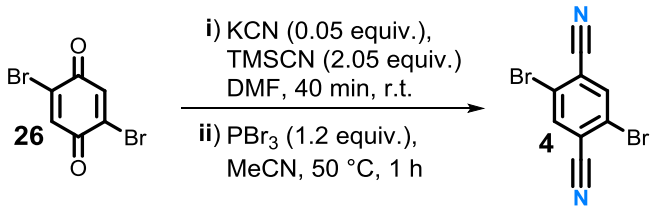

Scheme 5.12 One-pot synthesis of **4** from quinone **26.**

Comparison of the NMR data collected for **4** with that reported in literature[9] proved molecular structure of **4**. Pleased of these results obtained following this procedure, we moved towards the next step of the reduction of **9**.

5.2.2 Reduction of 2,5-bis(diboron-neopentyl) terephthalonitrile

With building block **9** in hand, we next explored the possibility of reducing in one-pot reaction the double cyano and boronic esters functional groups to achieve the corresponding di-amine-di-borane specie **2**. Application of the same protocol described in Chapter 2, based on the use of microwave assisted conditions, to this system necessitated the use of double quantities of $LiAlH_4$. This made the setting of the reaction more challenging. Indeed, a higher $LiAlH_4$ loading (11.0 equivalents instead of 5.0 equivalents) required to review part of the synthetic procedure in order to keep the main parameters such as pressure, temperature, total volume and stirring within the standard limits. For instance, the more $LiAlH_4$ used the more H_2 is released during the progress of the reaction. As pressure limitations of a microwave tube is always a concern, this parameter needs to be constantly monitored to avoid undesired explosions. Another important parameter that we had to take account was the total reaction volume which is set to ensure both a good stirring and a good heating distribution. Therefore, the increased in volume of $LiAlH_4$ employed, necessitated the use of less THF to dissolve **9** which in turn displayed poor solubility in this solvent. To by-pass all these problems, we decide to proceed with the synthesis of **2** halving the amount of starting material **9** employed. The reaction was therefore performed on 65 mg of starting **9** so that the amount of $LiAlH_4$ resulted to be similar to that usually used and, hence the amount of H_2 evolved did not result in overpressure and explosions. After microwave irradiation for one hour at 90 °C, the reaction was quenched by careful addition of water and then filtered over a plug of anhydrous magnesium sulfate. Following solvent removal, the crude was subjected to the same work up procedure detailed in Chapter 2 providing pure **2** in 47% yield. However, under these reaction conditions, reduction of **9** resulted to be incomplete producing a significant amount of side products. Specifically, by analysis of the NMR data we identified one of the main by-product to be the partially reduced form **27**.

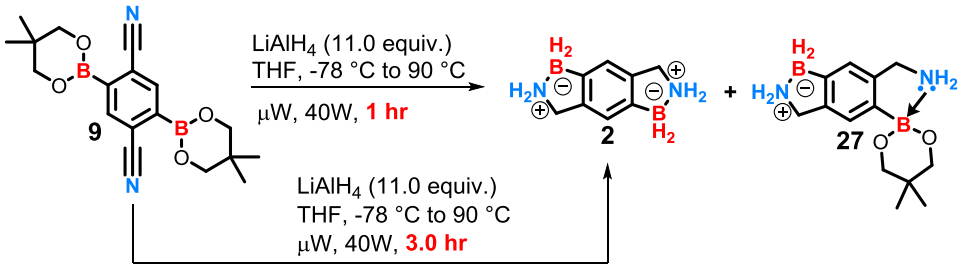

Scheme 5.13 Reduction of boronic ester **9** by microwave assisted conditions.

The observed outcome can be rationalized by considering, as mentioned before, the poor solubility of starting material **9** in THF. This suggest that **9** was partially involved in supramolecular aggregates thus making molecules less available to take part to the reaction. Along this idea we decided to repeat the synthesis on 50 mg of **9** and stirring the resulting mix at 90 °C for three hours. With these parameters modified a notable improvement in product conversion was observed, indeed **2** was provided in 67% yield after purification. A series of NMR spectra (^{1}H, ^{11}B and ^{13}C) were collected to proof molecular structure of **2** which was also confirmed by mass spectroscopy analysis that displayed a good match between the predicted isotope pattern distribution and the observed data.

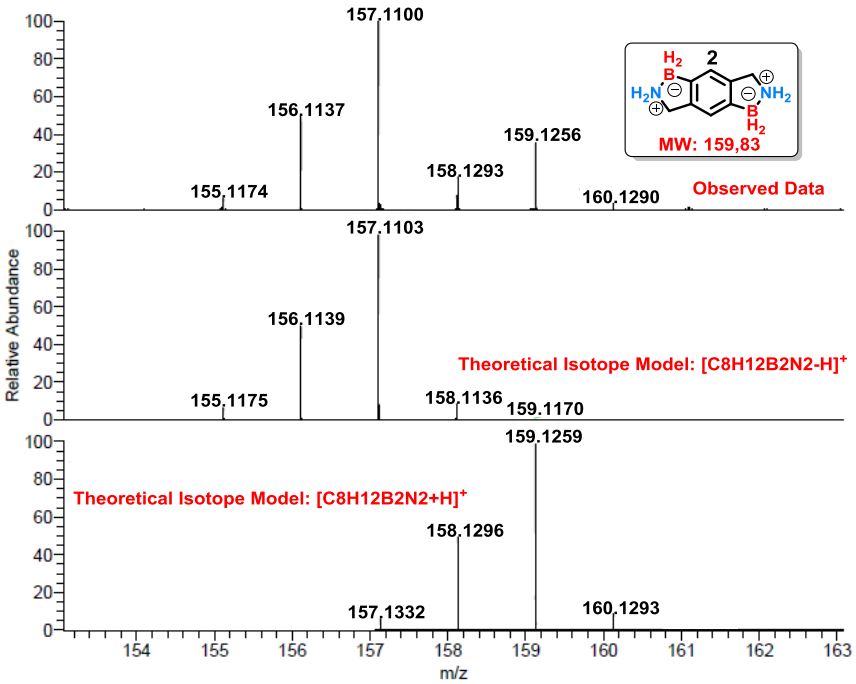

Figure 5.4 Mass Spectrum of compound **2** from Swansea University.

5.3 Synthesis of2D-CBN hybrid materials by thermolysis of diamine-diborane 2

5.3.1 Overview to the past synthesis of 2D-CBN hybrid materials

In the early stage of this project, Dr. Emmett already experienced the synthesis of 2D-CBN hybrid materials following a bottom-up synthetic method.[10] Initially the synthetic pathway developed for the preparation of arene borazines followed a different approach than that described in this manuscript. Specifically, the synthesis was designed starting from 2-aminophenols **35** following a procedure introduced by Ortiz-Marciales and co-workers.[11] The mechanism suggested for the formation of the borazine ring is shown in Scheme 5.14.

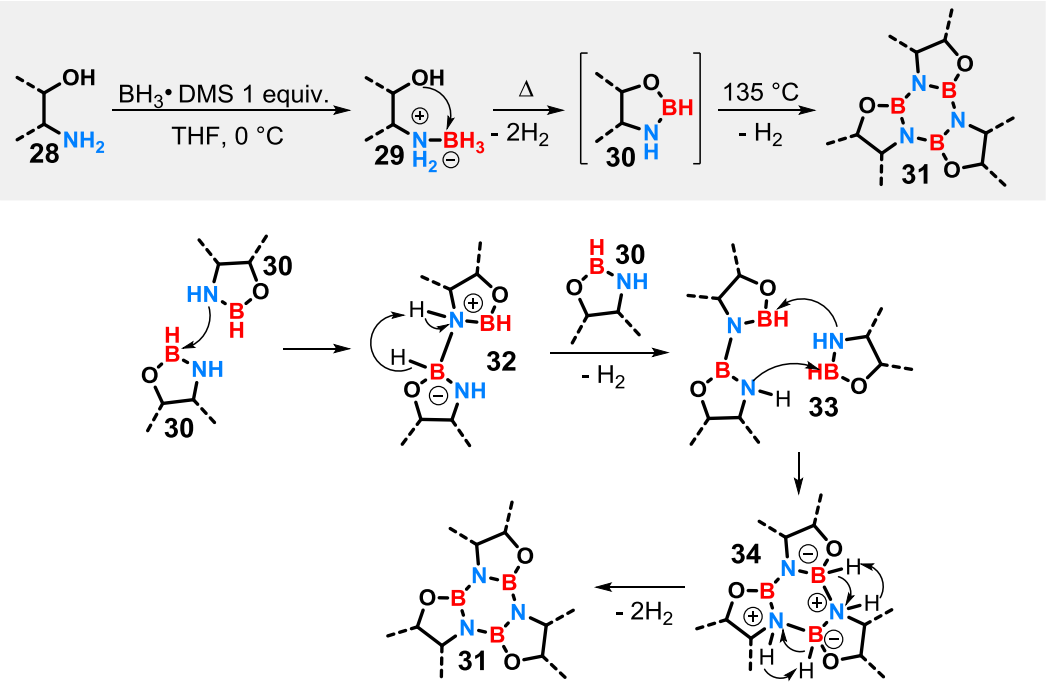

Scheme 5.14 Proposed mechanism for the synthesis of borazines **31**.

In the first step exposure of starting materials **28** to $BH_3 \cdot DMS$ results in the nucleophilic attack of both amine and alcohol functionalities to the electron deficient boron centre leading to the 5-membered heterocycle oxazaborolidine **30**. Subsequently trimerization of **30** take places *via* an intermolecular dehydrogenation process providing to the formation of the borazine ring followed by the elimination of H_2. In modification of this procedure $BH_3 \cdot DMS$ was replaced with the more reactive BX_3 Lewis acid specie, also the synthesis was performed in one-pot reaction taking advance of the microwave assisted conditions. Following this innovative method phenoxylene borazines **37** were successfully achieved starting from differently substituted 2-aminophenols **35** (Scheme 5.15).

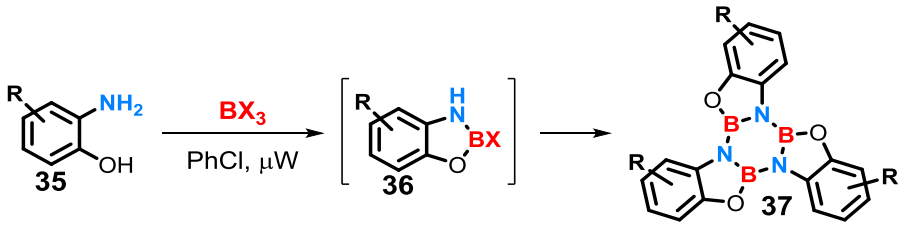

Scheme 5.15 Synthesis of phenoxylene borazines **37**.

In perspective of the synthesis of 2D-CBN hybrid materials, this method was later tested on starting materials functionalized on both sides of the benzene ring in order to propagate the monomeric borazine formation into a 2D polymer. It was envisaged that replacing 2-aminophenol with 2,5-diaminohydroquinone **38**, in presence of BX_3, the polymerisation should occur since, in both sides amine and alcohol groups react with BX_3 to form the desired borazine moieties.

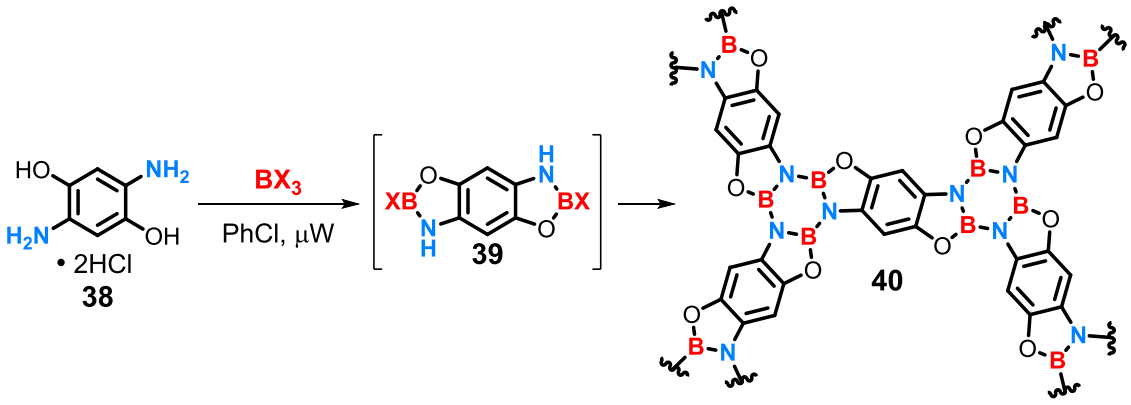

Scheme 5.16 Proposed synthesis of 2D networks from 2,5-diaminohydroquinone **38**.

The first attempt at the synthesis of 2D networks **40** was performed reacting starting material 2,5-diaminohydroquinone **38** with BBr_3 in chlorobenzene at 180 °C for 24 hours. Unfortunately, as expected, this reaction led to an insoluble precipitate difficult to characterize by using the most common analytic techniques such as NMR, UV etc. Therefore, to confirm and establish the successful formation of a 2D polymer the use of solid state analysis techniques such as solid-state NMR, Raman and XPS spectroscopy and EELS was required. Preliminary analysis obtained for the new material were comparable to that observed for the unsubstituted phenoxylene borazine **37**. Indeed, solid-state ^{11}B NMR spectrum displayed peaks assigned to a tricoordinate and tetra-coordinate boron environments, while Raman spectroscopy showed the distinct bands at 1357 cm^{-1} and 1604 cm^{-1} corresponding to BN and CC regions respectively. Moreover, XPS analysis displayed three deconvoluted peaks at 190.0, 192.1 and 193.5 eV attributable to B-N and B-O bonds confirming the presence of borazine regions within the material.

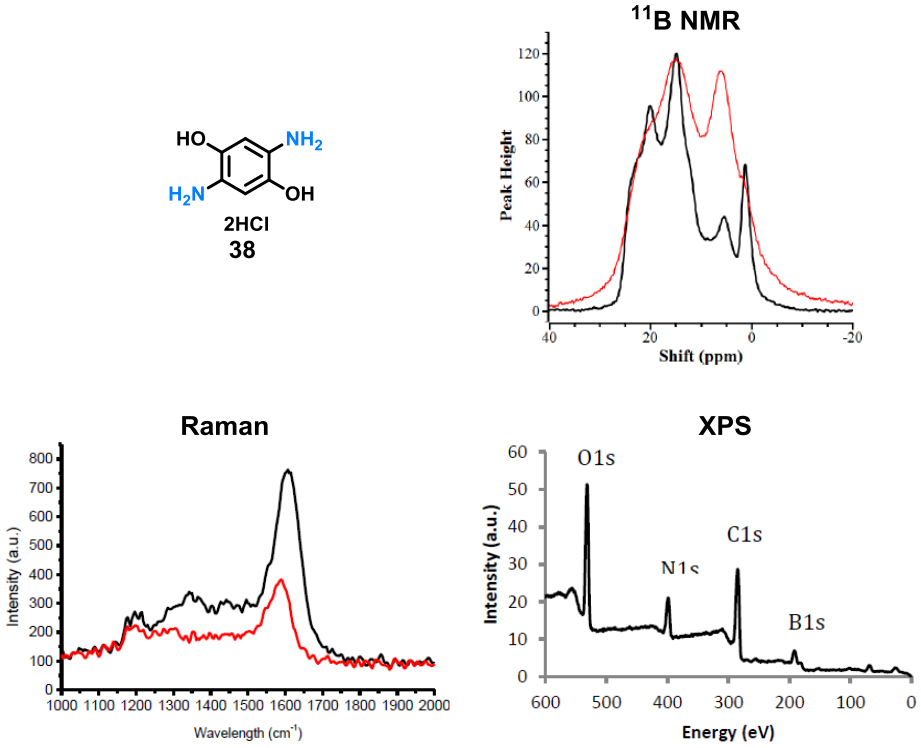

Figure 5.5 Solid-state analysis for 2D polymer created from 2,5-diaminohydroquinone. Unsubstituted phenoxylene borazine shown in red.[10]

However, despite these promising results obtained, a full characterization is required to define the molecular structure of this hybrid CBN polymeric specie. This is fundamental for future applications in the organic electronic field. Also, another very important aspect to consider is the ability of producing thin films to perform conductivity measurements to proof its applicability as semiconducting material.

5.3.2 Synthesis of CBN hybrid Oligomers

To by-pass limitations in the characterization and processability of these materials affected by poor solubility, we decide, in this project, to create more soluble species. To this end we adopted a different strategy exploring the possibility of synthesising more soluble oligomers composed by few monomeric units. This would have given us the chance to gain insight the polymerization process and the molecular structure of the hybrid material obtained. Unfortunately, unable to control the rate of the propagation (as in the living polymerization) to stop the reaction to short chains formed, we decided to react diamine-diborane **2** in presence of an excess of an amine-borane specie **41** to create short oligomers **42**.

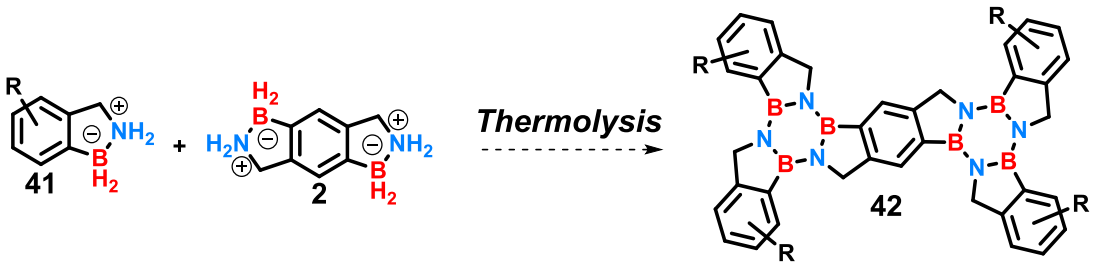

Scheme 5.17 Proposed synthesis of oligomers by thermolysis of building blocks **41** and **2**.

Guided by this idea, we decided to test the synthesis reacting diamine-diborane **2** with the fluorine amine-borane derivative **43** in ratio 1:4 in the thermolysis process to produce the hypothesized di-borazine specie **44**. Amine-borane **43** was chosen as compound test to employ in this synthetic process because the corresponding borazine displayed a good solubility in the most common organic solvents. Also, another important advantage of using substituted amine-boranes was that to reduce the number of aromatic protons to make easier the interpretation of the ^{1}H NMR spectrum. As first attempt at the synthesis of **44** we employed the same reaction condition established for each successful borazine synthesised. However preliminary results obtained by NMR analysis of the crude revealed the main product to be borazine **45**, obtained by self-trimerization of amine-borane **43**, and unreacted **2**.

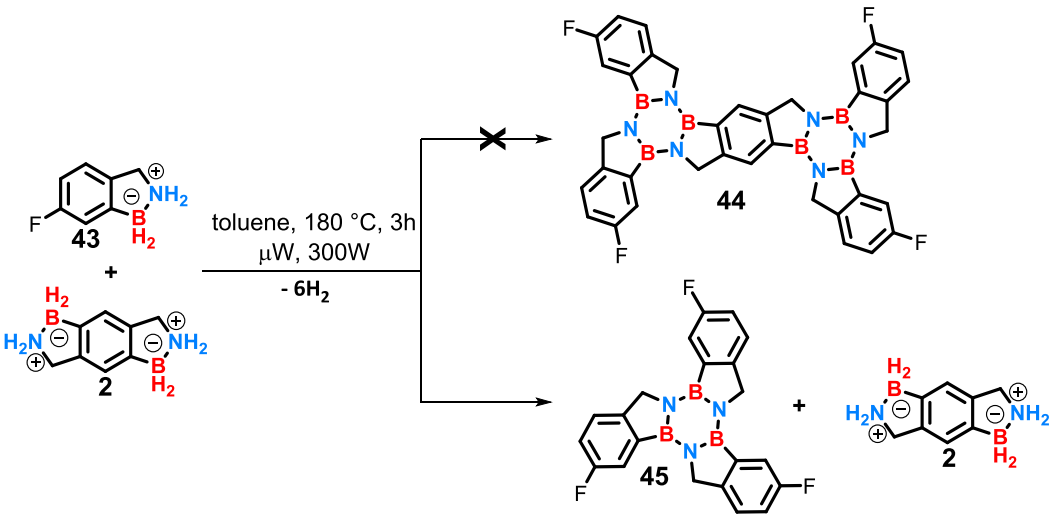

Scheme 5.18 Synthesis of fluorinated oligomer **44** by thermolysis of building blocks **43** and **2**.

This unexpected outcome can be anyway rationalized considering the difference in solubility of the two monomers in toluene. Indeed, **43** displayed a better solubility in toluene than **2** which in turn was a suspension even after sonication. This made more favourable the self-trimerization of **43** rather than the formation of the hetero oligomer being **44** partially in solution thus less available to take part at the reaction. Building block **2** was then subjected to a solubility test displaying a good affinity for chlorobenzene. The latter was already used during the solvent screening for the borazatruxene synthesis and it revealed to be a good solvent for this reaction. Therefore, in a second attempt at the synthesis of

44, toluene was replaced by chlorobenzene and the reaction was carried out following the standard protocol. After solvent removal analysis of the ^{1}H NMR spectrum of the crude revealed the major product to be again borazine **45**, however the presence of a complex pattern at lower ppm suggested the presence of another product. In an effort to identify the unknown compound we decided to send a sample of the crude to the National Mass Spectrometry Facility in Swansea, avoiding long purification procedures which might led to the product decomposition. Pleasingly, after several analyses using different mass spectroscopy techniques molecular structure of **44** was confirmed by the Electron Ionization (Air-sensitive, MAT95) method.

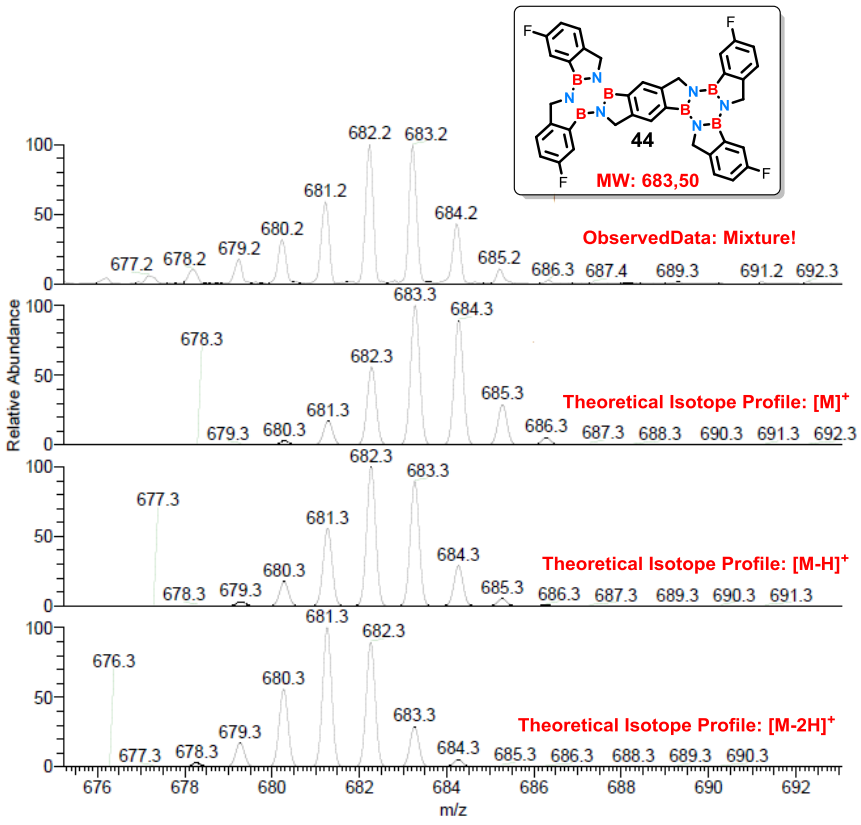

Figure 5.6 Mass Spectrum of compound **44** from Swansea University.

Specifically, compound **44** was identified as a mixture of different molecular ions as showed in Figure 5.6. The theoretical isotope profile of the mix composed by molecular ions $[M]^{+}$, $[M\text{-}H]^{+}$ and $[M\text{-}2H]^{+}$ was in perfect agreement with the observed data.

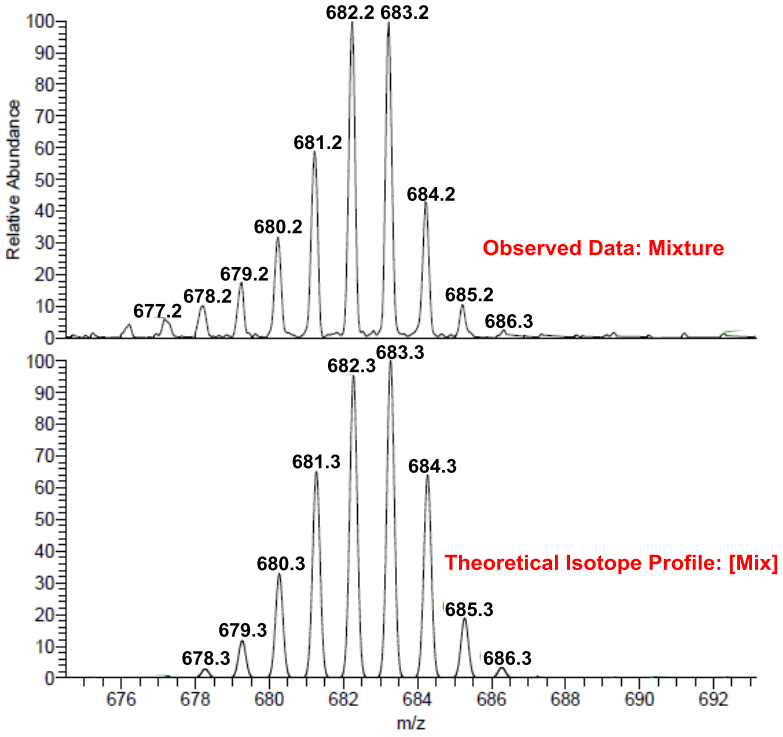

Figure 5.7 Enlargements of the mass Spectrum of compound **18**.

For a full characterization purposes of **44**, NMR analysis (^{1}H, ^{11}B and ^{13}C) would have been required. Unfortunately, attempts to isolate the desired **44** by washing the crude with a different ratio of *n*-hexane:CH_2Cl_2, resulted in inseparable mixtures of the two specie. Instead purification by flash silica gel chromatography resulted in loss of the product, probably due to decomposition. The difficulties surrounding the large-scale availability of amine-borane specie are often associated with their synthetic procedures which are highly moisture sensitive and concentration dependent. This limit the possibility of using larger quantities of amine-boranes in the thermolysis process thus making, as in this case, more difficult the isolation and identification of minor products obtained by this reaction. The limited availably of **2** led us to review our strategy for the synthesis of the hybrid oligomer. To improve product conversion and isolation, we decided to create a more soluble oligomer in order to make easier both purification and characterization. Guided by this idea we evaluated the possibility of using amine-borane **47** bearing peripheral dodecyl alkyl chains for the synthesis of the new oligomer. As described in Chapter 2 this compound displayed remarkable solubility features proving to be a good candidate to employ. Also, the doubly functionalized aromatic ring of **46** would have made the interpretation of the ^{1}H NMR spectrum of the theorized product easier. Indeed, considering the symmetry of the molecule being on the benzene ring bridging the two dimers, we expected to see three different distinct signals for each internal -**CH_2**- bridge between 5.0 and 6.0 ppm. Also, we supposed to observe five more signals in the aromatic region: two for each aromatic ring bearing the alkyl chain groups B and C, and one more for the benzene ring bridging the two dimers A.

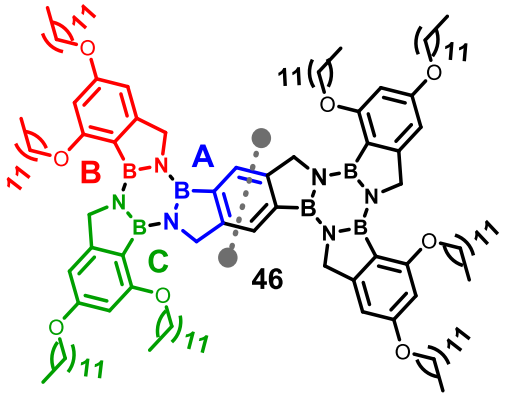

Figure 5.8 Strategy envisioned for the synthesis and characterization of **46**.

Confident with these analytical considerations we carried on with the synthesis of **46**. The synthesis was performed in anhydrous chlorobenzene using the same conditions and the same ratio between **2** and **47** (1:4) previously described.

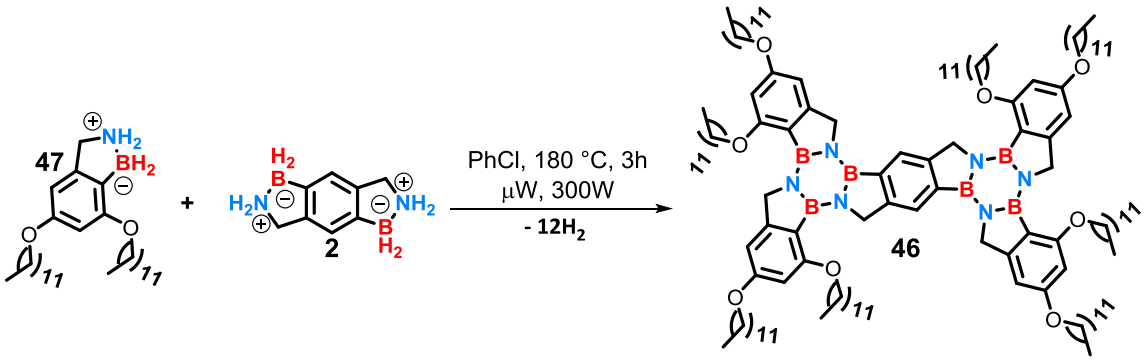

Scheme 5.19 Synthesis of compound **46**.

After three hours, the reaction was cooled to room temperature and the solvent removed to yield a glassy white material. As first attempt to remove impurities we proceed in the same manner we did with for the borazatruxenes purification, washing the solid with a mix of *n*-hexane:CH_2Cl_2 80:20. The suspension was centrifuged, and the supernatant was separated from the solid in order to be analyzed separately. Direct comparison of ^{1}H NMR spectra in $CDCl_3$ of both fractions isolated is showed in Figure 5.9.

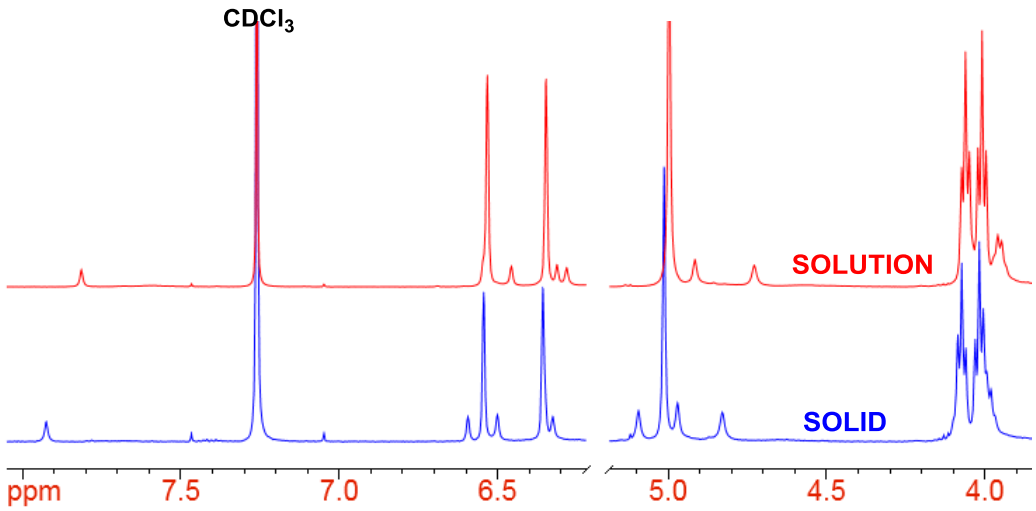

Figure 5.9 Comparison between ^{1}H-NMR spectra in $CDCl_3$ of the solid and the solution isolated after work-up of the synthesis of **46.**

Despite the major product formed was again the self-trimerization of **47**, is interesting to note the presence of a minor product showing a similar pattern to that predicted. We thus became attracted to the possibility of isolating the minor compound for full characterization purposes in order to proof molecular structure theorized for **46**. Considering that the reaction was performed in small scale on a total of 100 mg of **2** and **47**, we decided to avoid silica gel chromatography purification which might have led to the product decomposition. To this end we proceeded with the purification of both fractions by repeated washing with *n*-hexane:CH_2Cl_2 90:10. Finally, after several washes, the ^{1}H NMR spectrum in $CDCl_3$ of the last fraction collected revealed the presence of the only desired minor product.

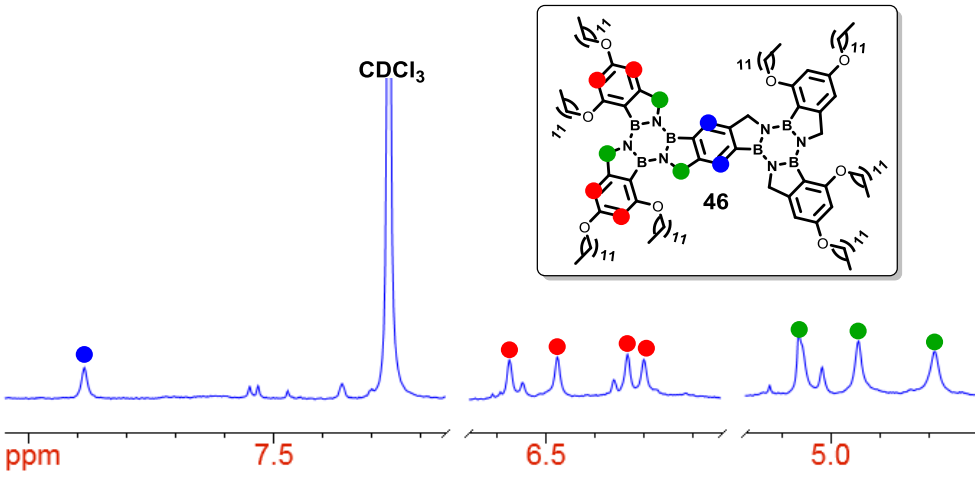

Figure 5.10 Interpretation of the ^{1}H NMR spectrum in $CDCl_3$ possibly associated to the desired product **46**.

The ^{1}H NMR spectrum in $CDCl_3$ showed distinct aromatic protons for the benzene ring bridging the two dimers at 7.88 ppm and for the two dimers at 6.57, 6.47, 6.33 and 6.29 ppm as expected. Also, at lower ppm (around 5.0 ppm) three distinct singlets assigned to the three chemically non-equivalents internal -

CH_2- bridges were observed. Therefore, preliminary result obtained led us to believe to have synthetized the desired molecule **46**, however further analyses are required to proof structure of **46**. Unfortunately, we could isolate only few milligrams of **46** after washes, therefore our efforts to full characterize **46** by ^{11}B and ^{13}C NMR analysis failed. Unable to repeat the synthesis on larger scale because of the lack of both starting materials, whose total synthesis was very time demanding, we decided to send a sample of **46** to the National Mass Spectrometry Facility in Swansea. Preliminary attempts to identify the molecular ion using the standard techniques failed, therefore at the moment further analysis using different techniques such as MALDI or DCTB matrix are ongoing.

5.3.3 Attempted synthesis of 2D CBN hybrid materials

In parallel to these experiments we attempted also at the polymerization of **2** employing the same reaction conditions used for the oligomers formation.

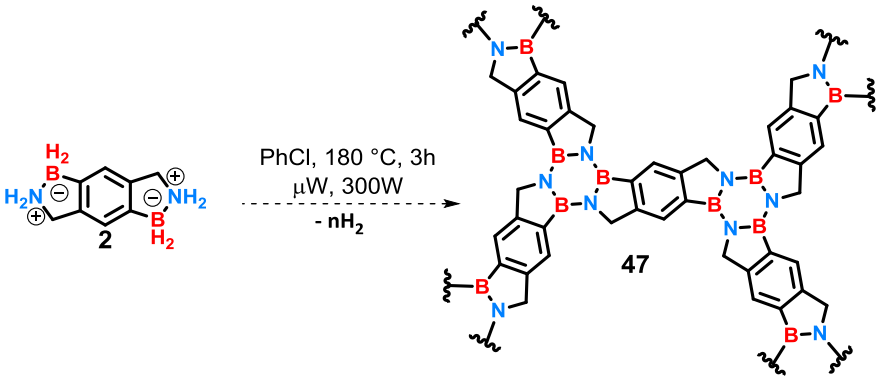

Scheme 5.20 Attempted synthesis of CBN-2D networks **47**.

As expected, after solvent removal and purification by washing the crude with chlorobenzene and CH_2Cl_2, we obtained an insoluble yellow powder. Attempt at the characterization of the unknown compound by NMR analysis failed since the product displayed poor solubility even in wormed both TCl-d_2 and DMSO-d_6 to 100 °C. Therefore, to confirm the formation of a 2D polymer we proceeded with the solid-state analysis techniques. Initially to characterize the CBN 2D-hybrid structure, Fourier transform infrared (FTIR) analyses was conducted. The FTIR spectrum displayed in Figure 5.11 was compared with FTIR spectra of similar materials reported in literature.

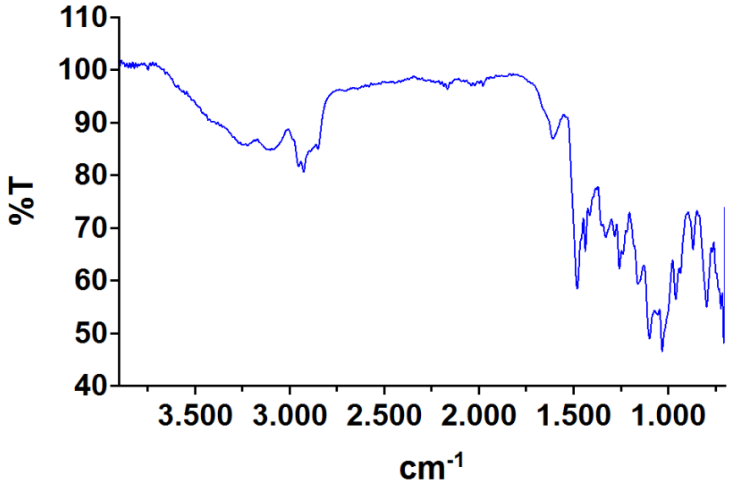

Figure 5.11 Interpretation of the ^{1}H NMR spectrum in $CDCl_3$ possibly associated to the desired product

The peak at approximately 800 cm^{-1} can be associated to the out-of-plane bending vibration mode of the B-N bond while the sharp peak at about 1500 cm^{-1} can be ascribed to the B–N in-plane stretching vibration, although the latter, usually, is centred around 1370-1400 cm^{-1}.[12,13] The presence of peaks in the region between 1200-900 cm^{-1} associated to the B–N–O, C–O and B–O–H vibrational mode,[12] suggested that the material was partially oxidized. A further evidence of the presence of oxygen atom bearing functional groups is due to the peak at 1600 cm^{-1} associated to the carbonyl functional group and the broad band centred around 3000 cm^{-1} was assigned to B-OH/B-NH_2 functional groups in line with that reported in literature.[13] X-ray Powder Diffraction (XRD) analysis shown in Figure 5.12 also confirmed the presence of oxygen in the final material.

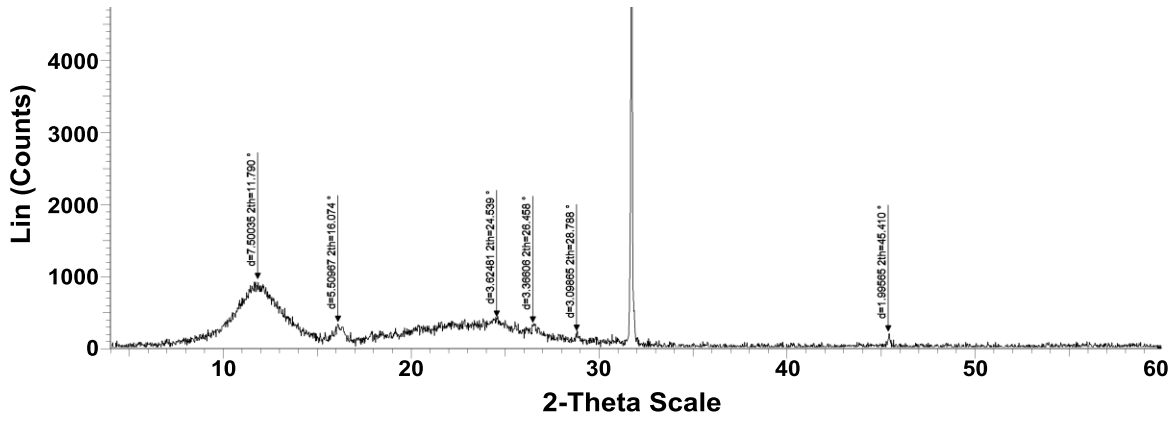

Figure 5.12 Interpretation of the ^{1}H NMR spectrum in $CDCl_3$ possibly associated to the desired product

The XRD pattern at 2θ = 11.79° and 45.41° is the characteristic diffraction peak of graphene oxide (GO).[14] The broad band centred around 25° instead can be attributed to the presence of BCN functionality as reported in literature,[15] while the sharp peak at 2θ = 31.70° has been observed for compounds containing both nitrogen and oxygen atoms. Therefore, these preliminary results obtained by combining FTIR and

XRD analysis indicated, as outlined before, that oxygen-containing functional groups are present in the final hybrid material. Also, a sample of **47** was sent to the National Mass Spectrometry Facility in Swansea. Unfortunately, preliminary results obtained by S-F MALDI analysis were in disagreement with the proposed molecular structure since there was no evidence for the incorporation of boron atoms into the molecular ions observed. Further analysis using the APCI(ASAP) (atmospheric pressure chemical ionization, solids analysis probe) method, suggested the possible presence of boron from the isotope pattern observed but no correlation between the monomer and any obvious polymeric combination was detected. At the moment further analysis using different mass spectrometry techniques are ongoing. Overall, further analysis would need to be made to have a better confirmation of the synthesis of 2D CBN hybrid material. Specifically, the combination of Raman and XPS spectroscopy and solid-state NMR analysis would have been beneficial to give more information on the nature of this material. It would have been very interesting also to explore the possibility of producing thin films to perform conductivity measurements so that electronic applications can be realised. Unfortunately, we could not proceed with further analysis, tests and experiments on this material because of the short time left.

REFERENCES

1L. Ci, L. Song, C. Jin, D. Jariwala, D. Wu, Y. Li, A. Srivastava, Z. F. Wang, K. Storr, L. Balicas, F. Liu and P. M. Ajayan, *Nat. Chem.*, 2010, **9**, 430.
2 S. Wang, L. Zhang, Z. Xia, A. Roy, D. W. Chang, J.-B. Baek and L. Dai, *Angew. Chem. Int. Ed.*, 2012, **51**, 4209.
3 B. Du, X. Jiang and P. Sun, *J. Org. Chem.*, 2013, **78**, 2786.
4 W. You, L. Wang, Q. Wang and L. Yu, *Macromol.*, 2002, **35**, 4636.
5 H. H. Nguyen, X. Li, N. Wang, Z. Y. Wang, J. Ma, W. J. Bock and D. Ma, *Macromol.*, 2009, **42**, 921.
6 A. R. Jeon, M. E. Kim, J. K. Park, W. K. Shin and D. K. An, *Tetrahedron*, 2014, **70**, 4420.
7 H. Fang, G. Kaur, J. Yan and B. Wang, *Tetrahedron Lett.*, 2005, **46**, 1671.
8 G. A. Chotana, M. A. Rak and M. R. Smith III, *J. Am. Chem. Soc.*, 2005, **127**, 10539.
9 F. Glöcklhofer, M. Lunzer, B. Stöger and J. Fröhlich, *Chem. - Eur. J*, 2016, **22**, 5173.
10 Liam Emmett, Doctoral dissertation, University of Bath, 2015.
11 V. Stepanenko, M. Ortiz-Marciales, C. E. Barnes and C. Garcia, *Tetrahedron Lett.*, 2006, **47**, 7603.
12 P. M. Sudeep, S. Vinod, S. Ozden, R. Sruthi, A. Kukovecz, Z. Konya, R. Vajtai, M. R. Anantharaman, P. M. Ajayan and T. N. Narayanan, *RSC Adv.*, 2015, **5**, 93964.
13 J. Li, X. Xiao, X. Xu, J. Lin, Y. Huang, Y. Xue, P. Jin, J. Zou and C. Tang, *Sci. Rep.*, DOI:10.1038/srep03208.
14 P. Chen, H. Li, S. Song, X. Weng, D. He and Y. Zhao, *Res. Phys.*, 2017, **7**, 2281.
15 H. Li, S. Zhu, M. Zhang, P. Wu, J. Pang, W. Zhu, W. Jiang and H. Li, *ACS Omega*, 2017, **2**, 5385.

6 CONCLUSIONS

In this work we have demonstrated the use of borazine as a versatile modular building block to prepare hybrid CBN polyphenylenes. Truxene has been chosen as PAH model to introduce boron and nitrogen doping by replacing the central aromatic core with the borazine ring. The novel BN-doped derivative called borazatruxene has been achieved by trimerization of cyclic aromatic amine-borane precursors using microwave dielectric heating technology. In turn amine-borane building blocks can be synthesised following three different synthetic procedures developed in our group. The initial synthetic protocol establishes the synthesis of amine-boranes by lithiation-borylation of aryl-substituted benzonitrile molecules followed by reduction of the corresponding boronic ester derivatives. The poor solubility in the most common organic solvents characterizing borazatruxene derivatives synthesised with this method necessitated the design of more soluble materials. Installation of long alkyl chains on the peripheral aromatic rings to increase the solubility of these materials led us to review the synthetic protocol. In this regard Miyaura cross-coupling reaction was utilized to introduce boron atom to ensure the cyclization to amine-borane functionality by reduction. Recognizing the possibility of functionalizing borazatruxene in the -CH_2- bridge (benzylic position) commercially available 2-acetylphenylboronic acid was used in a 3-step procedure for the synthesis a chiral borazatruxene derivative. The letter was obtained in very high yield and we have successfully reported the first example of chiral separation of enantiomeric species of borazine based materials. All the borazatruxenes have been fully characterized by using the most common analytical techniques, and these materials showed a high thermal stability. The electronic properties of these materials have been investigated by UV-Visible absorption and emission spectroscopy analysis and compared with the all carbon analogue truxene. Temperature-dependent ^{1}H NMR studies in TCE-d_2 to determine the thermodynamics of formation for a one-dimensional columnar aggregate of borazatruxenes. Fitting an isodesmic model to data obtained from monitoring the change in ^{1}H NMR chemical shift, allowed us to deduce the thermodynamic functions characterising these supramolecular polymers. The knowledge in synthesising aryl borazine based materials has been subsequently utilized for the synthesis of hydrogenated benzo(c)naphtho(2,1-p)borazachrysene derivatives starting from commercially available aryl-substituted *o*-bromophenyl acetonitriles. Formation of the borazine core was achieved through trimerization of the amine-borane precursors utilising microwave dielectric heating as established with borazatruxenes. These novel materials shown a good solubility in the most organic solvents and a high thermal stability. they have been fully characterized by using the most common analytical techniques and the electronic properties have been investigated by UV-Visible absorption and emission spectroscopy analysis. Temperature-dependent ^{1}H NMR studies in TCE-d_2 has been used to determine the thermodynamics parameters characterizing the aggregation process of these materials as

described for borazatruxenes. Attempts at the dehydrogenation to achieve the corresponding benzo(c)naphtho(2,1-p)borazachrysene derivatives, unfortunately resulted either in product decomposition or recovering of starting material. Therefore the unsubstituted and chlorinated hydrogenated benzo(c)naphtho(2,1-p)borazachrysene derivative were subjected to the Flash Vacuum Pyrolysis (FVP) process to attempt at the synthesis of borazine doped C_3-hemifullerene. However preliminary results obtained suggested that the reaction conditions used were not effective to promote the radical formation needed to achieve the intramolecular ring closing. Indeed, in both cases starting materials was recovered after this process. Finally, we have attempted the synthesis of 2D-CBN hybrid materials using the same protocol developed for the synthesis of borazatruxenes. We designed a diamine-diborane species as building block to use in the thermolysis process to use in this polymerization process. Initially we explored the possibility of synthesising arene-borazine oligomers by reaction of the diamine-diborane species with differently substituted amine-boranes. Depside we observe a preference for the amine-borane species to react with them-self leading to the formation of the corresponding C_3-simmetric borazine materials, we observed also the formation of oligomers. However, problems associated to the small-scale synthesis and the low yield of the oligomers obtained, made difficult the isolation of these products. Therefore, they have been observed by NMR analysis as mixture with borazatruxenes derivatives and then confirmed by Mass Spectrometry analysis. Polymerization of the diamine-diborane species following the thermolysis protocol lead to an insoluble powder which required the solid-state analysis techniques to be identified. Preliminary results obtained by combining the Fourier transform infrared (FTIR) and X-ray Powder Diffraction (XRD) analysis revealed the presence of oxygen-containing functional groups present in the final hybrid material suggesting that it was partially oxidized. However, we also observed the presence of CBN-containing functional groups suggesting the presence of arene and borazine regions. This protocol has laid some excellent ground-work for the development of 2D BNC materials. However, to be taken forward would require further analysis to be fully characterized and also to explore the possibility of whether producing thin films to perform conductivity measurements so that electronic applications can be realised.

6 FUTURE WORK

The microwave technology is a versatile method for the synthesis of a considerable number of borazine derivatives. However, one of the key challenges in advancing the arene-borazine based technologies remains the scale-up of these synthetic protocols. Most of the procedures requires the use of anhydrous conditions and inert atmosphere plus some reactions are also concentration dependent. Another important aspect to consider is the great difference in yield of arene-borazine production dependent on the nature and the position of substituents of these materials. We observed that the yield drastically decreased for those borazine species more soluble in organic solvents. Therefore, the elaboration of empirical models combined with mechanistic studies to gain insight the mechanism characterizing the formation of the borazine ring is highly desired to improve the production of these materials. To elucidate better the electrochemical properties of arene-borazine species, experiments such as cyclic voltammetry (CV) can be combined with the UV-Visible spectroscopy data to determine the HOMO and LUMO energy levels. Attempts at the synthesis of borazine doped C_3-hemifullerene have opened a fantastic opportunity to study the reactivity of arene-borazine species towards the dehydrogenation and Flash Vacuum Pyrolysis (FVP) process. However, C-H activation for the formation of radicals to achieve the intramolecular ring closing is allowed only for two sp^2 carbon atoms. To this end the design of different substrates to use in the FVP process remains one of the main challenges in advancing the BN-doped hemifullerene synthesis. An area that has yet to be probed is the possibility of creating oligomers by thermolysis of diamine-diborane in presence of amine-borane species and 2D-CBN hybrid materials by polymerization of the diamine-diborane species. Development of a more appropriate thermolysis procedure, which drives the synthesis towards the formation of oligomers is required to increase in yield and fully characterise these new species. Also, functionalized oligomers can be used as active materials for the fabrication of electronic disposals or opportunely reacted in a polymerization process to have a more controlled distribution of the arene and borazine regions. Limitations encountered in the characterization of the 2D-CBN hybrid material synthesised could be overcome with the inclusion of peripheral alkyl substituents on the benzene ring of the diamine-diborane building block. This would decrease the p-p staking interactions enhancing the solubility of the 2D-hybrid materials in the organic solvents thus opening the possibility of producing thin films to perform conductivity measurements so that electronic applications can be realised. To realise our goal and use these materials for organic electronics, fabrication of such systems needs to be achieved. Achievement as such will not only allow the molecular structure to be better analysed, it will also allow us to probe the materials electronic properties. Whether this is obtained by depositing already formed materials or by modification of the reaction pathway, this needs to be realised as it will to transform these

materials from a theoretical marvel to a state-of-the-art component, satisfying our target for an arene-borazine hybrid material.

7 EXPERIMENTAL SECTION

All reactions were carried out using anhydrous solvents and kept under an inert atmosphere of argon as specified. Solvents were obtained by passing through anhydrous alumina columns using Innovative Technology Inc. PS-400-7 solvent purification system. All reagents were purchased from commercial suppliers: Across Organics, Alfa Aesar, Sigma Aldrich, TCI Europe, Gross, Fluorochem or Apollo Scientific and used without further purifications. All reactions were monitored using thin layer chromatography (TLC) using pre-coated MN Alugram Sil G/UV254 silica gel 60 aluminium backed plates. Plates were developed using standard techniques, UV light followed by a chemical dip, either $KMnO_4$, bromocresol green and cerium-ammonium-molybdate staining solution (mainly sensitive for amines and amides). Flash Chromatography was performed on chromatography grade, silica 60 Å particle size 35-70 micron from Sigma Aldrich using the solvent system as stated. ^{1}H, ^{11}B and ^{13}C were performed on Bruker Advance 300 (^{1}H 300 MHz, ^{11}B 96 MHz ^{13}C 75 MHz), Bruker Advance 400 (^{1}H 400 MHz, ^{11}B 128 MHz and ^{13}C 100 MHz) and Bruker Advance 500 (^{1}H 500 MHz, ^{11}B 160 MHz and ^{13}C 125 MHz) as stated. Chemical shifts are reported in parts per million (ppm) relative to tetramethyl silane ($\delta = 0.00$) and $BF_3 \cdot Et_2O$ ($\delta = 0.00$) for ^{1}H NMR and ^{11}B NMR respectively. Coupling constants are reported in Hertz (Hz) and signal multiplicity is denoted as singlet (s), doublet (d), triplet (t), apparent triplet (app t), multiplet (m) and broad (br). All spectra were acquired at 25 °C if not otherwise specified. All spectra were referenced to the residual solvent peaks. Mass spectrometry (MS) was performed using either a Finnigan MAT 95 XP high resolution double focusing (BE) mass spectrometer in EI mode performed by the EPSRC National Mass Spectrometry Facility at Swansea, UK. The microwave reactions were carried out in either CEM Discovery, CEM Explorer 12, or Biotage Initiator dedicated microwave reactors.

PROCEDURE A: Lithiation-borylation of benzonitrile derivatives.

In a flame-dried 50 mL two necked flask under argon atmosphere 2,2,6,6-tetramethylpiperidine (1.5 equiv.) was dissolved in anhydrous THF and the mixture was cooled to -10 °C. Freshly titrated *n*-BuLi (≈2.5 M in *n*-hexane) (1.5 equiv.) was added dropwise. The mixture was stirred for 10 min and then cooled to -78 °C. At -78 °C, $B(O\text{-}i\text{-}Pr)_3$ (2.0 equiv.) was added and stirred for 10 min. In parallel benzonitrile derivative was dissolved in anhydrous THF under argon atmosphere and the resulting solution was cannulated dropwise to the lithiate at -78 °C. A changing in color was observed. The resulting mixture was allowed to react overnight, slowly warming to room temperature. The reaction was quenched with glacial acetic acid (2.2 equiv.) and stirred for 30 min, then 1,3-propanediol) (6.0 equiv.) was added. The mixture was stirred for 3 h at room temperature and then transferred to a separating funnel with CH_2Cl_2 (30 mL) and washed with aqueous KH_2PO_4 (10 w/w %) (4 x 10 mL). The combined water phase was back-extracted once with CH_2Cl_2 (15 mL) while the combined organic phase was dried over $MgSO_4$, filtered and the solvent removed under reduced pressure. The resulting crude material was re-dissolved in CH_2Cl_2 (5 mL) and THF (2 mL) and 1,3-propanediol (4.0 equiv.) was added and the solution was stirred for 3 h. Then the mixture was transferred to a separating funnel with CH_2Cl_2 (20 mL) and washed with aqueous KH_2PO_4 (10 w/w %) (4 x 10 mL). The combined water phase was back-extracted once with CH_2Cl_2 (15 mL) while the combined organic phase was dried over $MgSO_4$, filtered and the solvent removed under reduced pressure.

PROCEDURE B: Reduction of benzonitrile boronic ester derivatives to amine-boranes.

In a flame-dried 50 mL two necked flask equipped with condenser, under argon atmosphere, benzonitrile boronic ester derivative was dissolved in anhydrous THF and the mixture was cooled to -78 °C. Freshly titrated $LiAlH_4$ (≈1.0 M in THF) (3.0 equiv.) was added dropwise, and the resulting mix was stirred for 15 min at -78 °C and then it was allowed to warm to room temperature and finally refluxed for 3 h. After cooling to room temperature and then to -5 °C, the reaction was quenched dropwise with water under vigorous stirring yielding a white precipitate. The formed suspension was filtered on a plug of $MgSO_4$ and the solid was washed with THF (3 x 10 mL) and EtOAc (3 x 10 mL). After the organic solvents were removed under reduced pressure, the residue was re-dissolved in EtOAc (30 mL), transferred to a separating funnel and washed with distilled water (6 x 10 mL) and brine (1 x 10 mL). The combined water phase was back-extracted once with EtOAc (15 mL) while the combined organic phase was dried over $MgSO_4$, filtered and the solvent removed under reduced pressure to afford the purified desired.

PROCEDURE C: Reduction of benzonitrile boronic ester and phenylacetonitrile boronic ester derivatives to amine-boranes by μW assisted conditions.

A 10 mL μW tube equipped with a stirring bar and sealed with a perforated plastic cap was flame-dried under reduced pressure though a needle. After back filling with argon, a solution of either benzonitrile

boronic ester or phenylacetonitrile boronic ester derivative in anhydrous THF under argon atmosphere was cannulated and the system was cooled to -78°C. After 15 min, freshly titrated $LiAlH_4$ (≈1.0 M in THF) (5.0 equiv.) was added dropwise under vigorous stirring, and then the resulting mix was slowly allowed to warm to room temperature. The needle was removed to seal, and the μW tube was placed into the μW machine and the mixture was stirred and irradiated by microwave dielectric heating at 90 °C (power 40W). After 1.5 h, the reaction mixture was cooled to room temperature, diluted with anhydrous THF and transferred in a 100 mL conical flask. After cooling to -5 °C, the reaction was quenched dropwise with water under vigorous stirring yielding a white precipitate. The formed suspension was filtered on a plug of $MgSO_4$ and the solid was washed with THF (3 x 10 mL) and EtOAc (3 x 10 mL). After the organic solvents were removed under reduced pressure, the residue was re-dissolved in EtOAc (20 mL), transferred to a separating funnel and washed with distilled water (6 x 10 mL) and brine (1 x 10 mL). The combined water phase was back-extracted once with EtOAc (15 mL) while the combined organic phase was dried over $MgSO_4$, filtered and the solvent removed under reduced pressure to afford the purified desired.

PROCEDURE D: Synthesis of borazine derivatives.

A 10 mL μW tube equipped with a stirring bar and sealed with a perforated plastic cap was flame-dried under reduced pressure though a needle. After back filling with argon, a solution of amine-borane derivative in anhydrous toluene was cannulated and the suspension was stirred and irradiated by microwave dielectric heating at 180 °C (power 300W). After 2 h, the reaction mixture was cooled to room temperature, diluted with EtOAc and transferred in a 100 mL flask. After the organic solvents were removed under reduced pressure, the crude was washed with hexane (3 x 5 mL) and hexane:CH_2Cl_2 (50:50) (3 x 5 mL) and then dried under reduced pressure to afford the purified desired.

CHAPTER 2

Synthesis of 4-(dec-1-yn-1-yl)benzonitrile

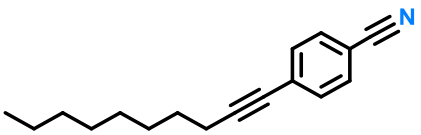

15

In a flame-dried 50 mL two necked flask, under argon atmosphere, 4-Bromobenzonitrile (1000 mg, 5.5 mmol), $Pd(PPh_3)_4$ (127 mg, 0.11 mmol, 2 mmol%) and CuI (31 mg, 0.17 mmol, 3 mmol%), were vacuumed for 1 h and back filled with argon, then 1-decyno (1.2 mL, 6.6 mmol, 1.2 equiv.) and triethylamine (20 mL) were added and the mixture was stirred at 75 °C. After 50 min the reaction was cooled to room temperature and the organic solvent was removed under reduced pressure. The crude product was purified by silica gel flash chromatography (*n*-hexane/CH_2Cl_2 80:20) to afford the desired **15** as a light-yellow oil (1207 mg, 92%). ***^{1}H NMR***: (500 MHz, $CDCl_3$) δ (ppm) 7.57-7.55 (m, 2H), 7.46-7.44 (m, 2H), 2.42 (t, *J*=7.5 Hz, 2H), 1.63-1.58 (m, 2H), 1.46-1.41 (m, 2H), 1.35-1.24 (m, 8H), 0.88 (t, *J*=6.5 Hz, 3H).

Synthesis of 3,5-bis(dodecyloxy)benzonitrile

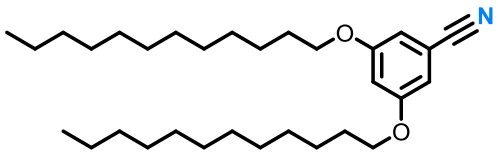

16

In a flame-dried 25 mL two necked flask, under argon atmosphere, 3,5-dihydoxybenzonitrile (519 mg, 3.84 mmol), 1-bromododecane (2.31 mL, 9.6 mmol, 2.5 equiv.) and K_2CO_3 (2650 mg, 19.2 mmol, 5.0 equiv.) were dissolved in anhydrous DMF (7 mL) and the mixture was stirred at 80 °C. After 12 h the reaction was cooled to room temperature and the organic solvent was removed under reduced pressure, the residue was re-dissolved in EtOAc (30 mL), transferred to a separating funnel and washed with distilled water (2 x 10 mL) and brine (6 x 10 mL). The combined water phase was back-extracted once with EtOAc (15 mL) while the combined organic phase was dried over $MgSO_4$, filtered and the solvent removed under reduced pressure. The crude product was purified by silica gel flash chromatography (*n*-hexane/CH_2Cl_2 70:30) to afford the desired **16** as a white powder (1811 mg, >99%). ***^{1}H NMR***: (500 MHz, $CDCl_3$) δ (ppm) 6.73 (d, *J*=3.0 Hz, 2H), 6.63 (t, *J*=3.0 Hz, 1H), 3.93 (t, *J*=8.0 Hz, 4H), 1.80-1.73 (m, 4H), 1.47-1.41 (m, 4H), 1.36-1.23 (m, 32H), 0.88 (t, *J*=8.5 Hz, 6H).

Synthesis of 2-(1,3,2-dioxaborinan-2-yl)benzonitrile

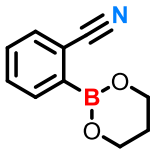

20

Compound **20** was synthesized according to the general **PROCEDURE A** reacting in a flame-dried 100 mL two necked flask under argon atmosphere, 2,2,6,6- tetramethylpiperidine (3.7 mL, 21.8 mmol, 1.5 equiv.) and *n*-BuLi (8.7 mL, 21.8 mmol, 1.5 equiv.) in anhydrous THF (20 mL). After the reaction mixture was cooled to -78 °C, B(O-*i*-Pr)$_3$ (6.7 mL, 29.1 mmol, 2.0 equiv.) and a solution of benzonitrile (1500 mg, 14.5 mmol) in anhydrous THF (20 mL) were added and the resulting mixture was allowed to react overnight, slowly warming to room temperature. The reaction was quenched with glacial acetic acid (2.0 mL, 32.0 mmol, 2.2 equiv.) and stirred for 2 h, then 1,3-propanediol (6.3 mL, 87.3 mmol, 6.0 equiv.) was added. The mixture was diluted with anhydrous THF (15 mL) and stirred for 4 h at room temperature. The crude product was purified as described in the general **PROCEDURE A** (CH_2Cl_2 (20 mL), THF (5 mL) and 1,3-propanediol (4.2 mL, 58.2 mmol, 4.0 equiv.) to afford the desired **20** as a brown solid (2027 mg, 75%). ***^{1}H NMR***: (400 MHz, $CDCl_3$) δ (ppm) 7.86 (d, *J*=7.0 Hz, 1H), 7.67 (d, *J*=7.5 Hz, 1H), 7.53 (app t, *J*=7.5 Hz, 1H), 7.47 (app t, *J*=7.0 Hz, 1H), 4.22 (t, *J*=5.5 Hz, 4H), 2.10 (q, *J*=5.5 Hz, 2H). ***^{11}B NMR***: (160 MHz, $CDCl_3$) δ (ppm) 26.2.

Synthesis of 4-chloro-2-(1,3,2-dioxaborinan-2-yl)benzonitrile

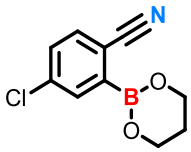

21

Compound **21** was synthesized according to the general **PROCEDURE A** reacting in a flame-dried 50 mL two necked flask under argon atmosphere, 2,2,6,6- tetramethylpiperidine (1.5 mL, 8.7 mmol, 1.2 equiv.) and *n*-BuLi (3.5 mL, 8.7 mmol, 1.2 equiv.) in anhydrous THF (10 mL). After the reaction mixture was cooled to -78 °C, B(O-*i*-Pr)$_3$ (2.4 mL, 10.2 mmol, 1.4 equiv.) and a solution of 4-chlorobenzonitrile (1000 mg, 7.3 mmol) in anhydrous THF (10 mL) were added and the resulting mixture was allowed to react overnight, slowly warming to room temperature. The reaction was quenched with glacial acetic acid (0.8 mL, 14.5 mmol, 2.0 equiv.) and stirred for 2 h, then 1,3-propanediol (3.1 mL, 43.6 mmol, 6.0 equiv.) was added. The mixture was diluted with anhydrous THF (10 mL) and stirred for 4 h at room temperature. The crude product was purified as described in the general **PROCEDURE A** (CH_2Cl_2 (20 mL), THF (5 mL) and 1,3-propanediol (2.1 mL, 29.1 mmol, 4.0 equiv.) to afford the desired **21** as a brown solid (1643 mg, 85%). ***^{1}H***

NMR: (500 MHz, $CDCl_3$) δ (ppm) 7.81 (d, *J*=2.5 Hz, 1H), 7.58 (d, *J*=8.5 Hz, 1H), 7.43 (dd, *J*=8.5, ^1J=2.5 Hz, 1H), 4.21 (t, *J*=5.5 Hz, 4H), 2.09 (q, *J*=5.5 Hz, 2H). ***^{13}C NMR***: (125 MHz, $CDCl_3$) δ (ppm) 138.6, 135.4, 135.0, 130.8, 119.0, 114.7, 62.6, 27.3. ***^{11}B NMR***: (160 MHz, $CDCl_3$) δ (ppm) 26.0.

Synthesis of 4-bromo-2-(1,3,2-dioxaborinan-2-yl)benzonitrile

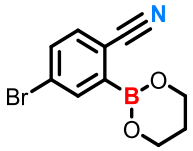

22

Compound **22** was synthesized according to the general **PROCEDURE A** reacting in a flame-dried 25 mL two necked flask under argon atmosphere, 2,2,6,6- tetramethylpiperidine (0.14 mL, 0.8 mmol, 1.5 equiv.) and *n*-BuLi (0.33 mL, 0.8 mmol, 1.5 equiv.) in anhydrous THF (2 mL). After the reaction mixture was cooled to -78 °C, B(O-*i*-Pr)$_3$ (0.25 mL, 1.1 mmol, 2.0 equiv.) and a solution of 4-bromobenzonitrile (100 mg, 0.5 mmol) in anhydrous THF (3 mL) were added and the resulting mixture was allowed to react overnight, slowly warming to room temperature. The reaction was quenched with glacial acetic acid (0.07 mL, 1.2 mmol, 2.0 equiv.) and stirred for 2 h, then 1,3-propanediol (0.24 mL, 3.3 mmol, 6.0 equiv.) was added. The mixture was diluted with anhydrous THF (5 mL) and stirred for 4 h at room temperature. The crude product was purified as described in the general **PROCEDURE A** (CH_2Cl_2 (5 mL), THF (2 mL) and 1,3-propanediol (0.13 mL, 2.2 mmol, 4.0 equiv.) to afford the desired **22** as a brown solid (126 mg, 86%). ***^{1}H NMR***: (400 MHz, $CDCl_3$) δ (ppm) 7.97 (d, *J*=2.0 Hz, 1H), 7.59 (dd, *J*=8.0, ^1J=2.0 Hz, 1H), 7.50 (d, *J*=8.0 Hz, 1H), 4.20 (t, *J*=5.5 Hz, 4H), 2.09 (q, *J*=5.5 Hz, 2H). ***^{13}C NMR***: (125 MHz, $CDCl_3$) δ (ppm) 138.3, 135.0, 133.8, 127.3, 119.1, 115.2, 62.5, 27.2. ***^{11}B NMR***: (128 MHz, $CDCl_3$) δ (ppm) 26.0.

Synthesis of 10-(1,3,2-dioxaborinan-2-yl)phenanthrene-9-carbonitrile

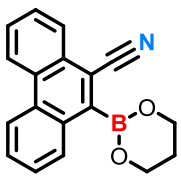

24

Compound **24** was synthesized according to the general **PROCEDURE A** reacting in a flame-dried 25 mL two necked flask under argon atmosphere, 2,2,6,6- tetramethylpiperidine (0.73 mL, 4.3 mmol, 2.2 equiv.) and *n*-BuLi (1.73 mL, 4.3 mmol, 2.2 equiv.) in anhydrous THF (3 mL). After the reaction mixture was cooled to -78 °C, B(O-*i*-Pr)$_3$ (0.9 mL, 4.0 mmol, 2.0 equiv.) and a solution of 9-Cyanophenanthrene (400 mg, 2.0

mmol) in anhydrous THF (5 mL) were added and the resulting mixture was allowed to react overnight, slowly warming to room temperature. The reaction was quenched with glacial acetic acid (0.25 mL, 4.3 mmol, 2.2 equiv.) and stirred for 2 h, then 1,3-propanediol (0.85 mL, 11.8 mmol, 6.0 equiv.) was added. The mixture was diluted with anhydrous THF (5 mL) and stirred for 4 h at room temperature. The crude product was purified as described in the general **PROCEDURE A** (CH_2Cl_2 (5 mL), THF (2 mL) and 1,3-propanediol (0.57 mL, 7.9 mmol, 4.0 equiv.) to afford the desired **24** as a dark green solid (534 mg, 95%). ***^{1}H NMR***: (400 MHz, $CDCl_3$) δ (ppm) 8.71-8.68 (m, 2H), 8.38-8.35 (m, 1H), 8.18 (d, *J*=8.0 Hz, 1H), 7.76-7.72 (m, 3H), 7.68-7.64 (m, 1H), 4.37 (t, *J*=5.0 Hz, 4H), 2.34-2.28 (q, *J*=5.0 Hz, 2H). ***^{13}C NMR***: (125 MHz, $CDCl_3$) δ (ppm) 135.8, 130.5, 130.4, 130.3, 129.3, 129.0, 128.8, 128.3, 128.0, 127.4, 126.4, 123.1, 123.0, 63.0, 25.8. ***^{11}B NMR***: (128 MHz, $CDCl_3$) δ (ppm) 28.9.

Synthesis of 4-(dec-1-yn-1-yl)-2-(1,3,2-dioxaborinan-2-yl)benzonitrile

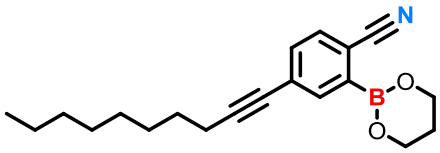

25

Compound **25** was synthesized according to the general **PROCEDURE A** reacting in a flame-dried 50 mL two necked flask under argon atmosphere, 2,2,6,6- tetramethylpiperidine (1.3 mL, 7.56 mmol, 1.5 equiv.) and *n*-BuLi (3.0 mL, 7.56 mmol, 1.5 equiv.) in anhydrous THF (5 mL). After the reaction mixture was cooled to -78 °C, B(O-*i*-Pr)$_3$ (2.3 mL, 10.1 mmol, 2.0 equiv.) and a solution of 4-(dec-1-yn-1-yl)benzonitrile (1207 mg, 5.0 mmol) in anhydrous THF (10 mL) were added and the resulting mixture was allowed to react overnight, slowly warming to room temperature. The reaction was quenched with glacial acetic acid (0.64 mL, 11.1 mmol, 2.2 equiv.) and stirred for 1 h, then 1,3-propanediol (2.2 mL, 30.3 mmol, 6.0 equiv.) was added. The mixture was diluted with anhydrous THF (10 mL) and stirred for 4 h at room temperature. The crude product was purified as described in the general **PROCEDURE A** (CH_2Cl_2 (20 mL), THF (5 mL) and 1,3-propanediol (1.5 mL, 20.2 mmol, 4.0 equiv.) to afford the desired **25** as a dark brown oil (1460 mg, 90%). ***^{1}H NMR***: (500 MHz, $CDCl_3$) δ (ppm) 7.87 (s, 1H), 7.57 (d, *J*=8.0 Hz, 1H), 7.45 (d, *J*=8.0 Hz, 1H), 4.21 (t, *J*=5.5 Hz, 4H), 2.41 (t, *J*=7.5 Hz, 2H), 2.11-2.07 (m, 2H), 1.62-1.56 (m, 2H), 1.46-1.40 (m, 2H), 1.34-1.25 (m, 8H), 0.88 (t, *J*=7.0 Hz, 3H). ***^{13}C NMR***: (125 MHz, $CDCl_3$) δ (ppm) 138.3, 133.5, 133.2, 119.7, 114.8, 62.4, 31.9, 29.3, 29.2, 29.1, 28.6, 27.3, 22.8, 19.6, 14.3, 14.2. ***^{11}B NMR***: (160 MHz, $CDCl_3$) δ (ppm) 26.2.

Synthesis of 2-bromo-4-methylbenzonitrile

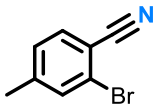

37

In a flame-dried 25 mL two necked flask, under argon atmosphere, 4-methylbenzonitrile 3,5-bis(dodecyloxy)benzonitrile (468 mg, 4.0 mmol), *N*-bromosuccinimide (783 mg, 4.4 mmol, 1.1 equiv.), $Pd(OAc)_2$ (45 mg, 0.2 mmol, 5 mmol%) and *p*-Toluenesulfonic acid (380 mg, 2.0 mmol, 0.5 equiv.) were dissolved in anhydrous 1,2-dichloroethene (5 mL) and the mixture was stirred at 70 °C. After 12 h the reaction was cooled to room temperature and the organic solvent was removed under reduced pressure. The crude product was purified by silica gel flash chromatography (*n*-hexane/CH_2Cl_2 80:20) to afford the desired **37** as a white powder (705 mg, 90%). ***^{1}H NMR***: (500 MHz, $CDCl_3$) δ (ppm) 7.53 (d, *J*=7.5 Hz, 1H), 7.51 (s, 1H), 7.21 (d, *J*=8.0 Hz, 1H), 2.41 (m, 3H).

Synthesis of 2-bromo-3,5-bis(dodecyloxy)benzonitrile

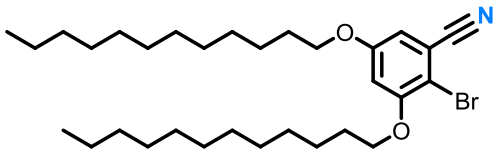

38

In a flame-dried 25 mL two necked flask, under argon atmosphere, 3,5-bis(dodecyloxy)benzonitrile (1000 mg, 2.1 mmol), *N*-bromosuccinimide (415 mg, 2.3 mmol, 1.1 equiv.), $Pd(OAc)_2$ (24 mg, 0.1 mmol, 5 mmol%) and *p*-toluenesulfonic acid (202 mg, 1.1 mmol, 0.5 equiv.) were dissolved in anhydrous 1,2-dichloroethene (10 mL) and the mixture was stirred at 70 °C. After 12 h the reaction was cooled to room temperature and the organic solvent was removed under reduced pressure. The crude product was purified by silica gel flash chromatography (*n*-hexane/CH_2Cl_2 80:20) to afford the desired **38** as a white powder (900 mg, 78%). ***^{1}H NMR***: (500 MHz, $CDCl_3$) δ (ppm) 6.73 (d, *J*=3.0 Hz, 1H), 6.63 (d, *J*=3.0 Hz, 1H), 3.99 (t, *J*=6.5 Hz, 2H), 3.93 (t, *J*=6.5 Hz, 2H), 1.86-1.81 (m, 2H), 1.80-1.75 (m, 2H), 1.51-1.41 (m, 4H), 1.37-1.27 (m, 32H), 0.88 (t, *J*=6.5 Hz, 6H). ***^{13}C NMR***: (125 MHz, $CDCl_3$) δ (ppm) 159.5, 157.2, 123.5, 117.6, 109.9, 105.7, 70.3, 69.8, 69.0, 32.1, 29.8, 29.7, 29.6, 29.5, 29.4, 29.2, 29.1, 29.0, 26.1, 22.8, 14.3. ***HRMS*** calc. for C31H52BrNO2 $[M+H]^+$ ($^m/_z$): 550.3260, 552.3245, found: 550.3271, 552.3254.

Synthesis of 2-(5,5-dimethyl-1,3,2-dioxaborinan-2-yl)-3-methylbenzonitrile

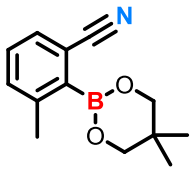

48

In a flame-dried 50 mL two necked flask equipped with condenser, under argon atmosphere, 2-bromo-3-methylbenzonitrile (800 mg, 4.1 mmol), bis(neopentyl glycolato)diboron (1383 mg, 6.1 mmol, 1.5 equiv.), Pd(dppf)Cl_2 (233 mg, 0.3 mmol, 7 mmol%) and CH_3COOK (1602 mg, 16.3 mmol, 4.0 equiv.) were vacuumed for 1 h and back filled with argon, then dissolved in anhydrous 1,4-dioxane (20 mL) and heated up under reflux. After 1 h, the reaction mixture was cooled to room temperature and the organic solvent was removed under reduced pressure. The residue was re-dissolved in EtOAc (30 mL), transferred to a separating funnel and washed with distilled water (2 x 20 mL) and brine (1 x 20 mL). The combined water phase was back-extracted once with EtOAc (20 mL) while the combined organic phase was dried over $MgSO_4$, filtered and the solvent removed under reduced pressure. The crude product was purified by silica gel flash chromatography (*n*-hexane/CH_2Cl_2 70:30 to CH_2Cl_2 100) to afford the desired **48** as a white solid (830 mg, 89%). ***^{1}H NMR***: (500 MHz, $CDCl_3$) δ (ppm) 7.47 (d, *J*=7.5 Hz, 1H), 7.34-7.28 (m, 2H), 3.84 (s, 4H), 2.46 (s, 3H), 1.11 (s, 6H). ***^{13}C NMR***: (125 MHz, $CDCl_3$) δ (ppm) 142.8, 133.6, 130.2, 129.3, 120.1, 116.0, 72.7, 31.9, 22.2, 22.1. ***^{11}B NMR***: (160 MHz, $CDCl_3$) δ (ppm) 27.4. ***HRMS*** calc. for C13H16BNO2 $[M+H]^+$ ($^m/_z$): 230.1347, found: 230.1350.

Synthesis of 2-(5,5-dimethyl-1,3,2-dioxaborinan-2-yl)-4-methylbenzonitrile

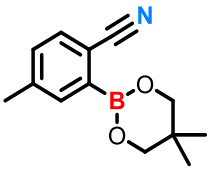

49

In a flame-dried 25 mL two necked flask equipped with condenser, under argon atmosphere, 2-bromo-4-methylbenzonitrile (230 mg, 1.2 mmol), bis(neopentyl glycolato)diboron (394 mg, 1.7 mmol, 1.5 equiv.), Pd(dppf)Cl_2 (66 mg, 0.1 mmol, 7 mmol%) and CH_3COOK (457 mg, 4.7 mmol, 4.0 equiv.) were vacuumed for 1 h and back filled with argon, then dissolved in anhydrous 1,4-dioxane (5 mL) and heated up under reflux. After 1 h, the reaction mixture was cooled to room temperature and the organic solvent was removed under reduced pressure. The residue was re-dissolved in EtOAc (20 mL), transferred to a separating funnel and washed with distilled water (2 x 10 mL) and brine (1 x 10 mL). The combined water phase was back-

extracted once with EtOAc (20 mL) while the combined organic phase was dried over $MgSO_4$, filtered and the solvent removed under reduced pressure. The crude product was purified by silica gel flash chromatography (*n*-hexane/CH_2Cl_2 70:30 to CH_2Cl_2 100) to afford the desired **49** as a white solid (830 mg, 90%). ***^{1}H NMR***: (500 MHz, $CDCl_3$) δ (ppm) 7.69 (s, 1H), 7.57 (d, *J*=7.5 Hz, 1H), 7.28 (d, *J*=7.5 Hz, 1H), 3.83 (s, 4H), 2.40 (s, 3H), 1.05 (s, 6H). ***^{11}B NMR***: (160 MHz, $CDCl_3$) δ (ppm) 26.1.

Synthesis of 2-(5,5-dimethyl-1,3,2-dioxaborinan-2-yl)-3,5-bis(dodecyloxy)benzonitrile

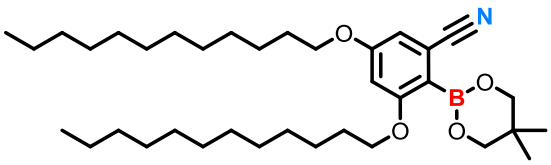

50

In a flame-dried 10 mL two necked flask equipped with condenser, under argon atmosphere, 2-bromo-3,5-bis(dodecyloxy)benzonitrile (200 mg, 0.4 mmol), bis(neopentyl glycolato)diboron (123 mg, 0.5 mmol, 1.5 equiv.), Pd(dppf)Cl_2 (21 mg, 0.03 mmol, 7 mmol%) and CH_3COOK (143 mg, 1.5 mmol, 4.0 equiv.) were vacuumed for 1 h and back filled with argon, then dissolved in anhydrous 1,4-dioxane (4 mL) and heated up under reflux. After 12 h, the reaction mixture was cooled to room temperature and the organic solvent was removed under reduced pressure. The residue was re-dissolved in EtOAc (30 mL), transferred to a separating funnel and washed with distilled water (2 x 10 mL) and brine (1 x 10 mL). The combined water phase was back-extracted once with EtOAc (15 mL) while the combined organic phase was dried over $MgSO_4$, filtered and the solvent removed under reduced pressure. The crude product was purified by silica gel flash chromatography (*n*-hexane/CH_2Cl_2 60:40) to afford the desired **50** as a light yellow powder (126 mg, 60%). **Alternative procedure**, in a flame-dried 10 mL two necked flask, under argon atmosphere, 2-bromo-3,5-bis(dodecyloxy)benzonitrile (200 mg, 0.4 mmol), bis(neopentyl glycolato)diboron (99 mg, 0.4 mmol, 1.2 equiv.), Pd(dppf)Cl_2 (10 mg, 0.01 mmol, 3 mmol%) and CH_3COOK (107 mg, 1.1 mmol, 3.0 equiv.) were vacuumed for 1 h and back filled with argon, then dissolved in anhydrous DMSO (4 mL) and the mixture was stirred at 80 °C. After 12 h the reaction mixture was cooled to room temperature, diluted with EtOAc (30 mL), transferred to a separating funnel and washed with distilled water (2 x 10 mL) and brine (1 x 10 mL). The combined water phase was back-extracted once with EtOAc (15 mL) while the combined organic phase was dried over $MgSO_4$, filtered and the solvent removed under reduced pressure. The crude product was re-dissolved, under argon atmosphere, in a mix of anhydrous CH_2Cl_2/THF (2:1, 3 mL) then CH_3COOH (0.02 mL, 0.4 mmol, 2.5 equiv.) and neopentylglycol (122 mg, 1.2 mmol, 6.0 equiv.) were added and the system was stirred at room temperature. After 12 h, the reaction mixture was diluted with CH_2Cl_2 (20 mL), transferred to a separating funnel and washed with distilled water (3 x 10 mL) and brine (1 x 10 mL). The combined organic phase was dried over $MgSO_4$, filtered and the solvent removed under reduced

pressure. The crude product was purified by silica gel flash chromatography (*n*-hexane/CH_2Cl_2 60:40) to afford the desired **50** as a light yellow powder (133 mg, 63%). ***^{1}H NMR***: (500 MHz, $CDCl_3$) δ (ppm) 6.68 (d, *J*=2.0 Hz, 1H), 6.55 (d, *J*=2.0 Hz, 1H), 3.94-3.89 (m, 4H), 3.80 (s, 4H), 1.79-1.73 (m, 4H), 1.48-1.40 (m, 4H), 1.36-1.23 (m, 32H), 1.09 (s, 6H), 0.88 (t, *J*=7.0 Hz, 6H). ***^{13}C NMR***: (125 MHz, $CDCl_3$) δ (ppm) 163.5, 161.3, 119.7, 116.9, 110.4, 109.2, 103.9, 72.8, 68.7, 68.6, 32.1, 32.0, 29.8, 29.7, 29.6, 29.5, 29.4, 29.3, 29.2, 26.1, 26.0, 22.8, 22.1, 14.3. ***^{11}B NMR***: (160 MHz, $CDCl_3$) δ (ppm) 27.3. ***HRMS*** calc. for C36H62BNO4 $[M+H]^+$ ($^m/_z$): 584.4857, found: 584.4869.

Synthesis of (2-((methoxyamino)methyl)benzene boronic acid

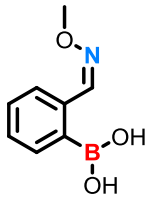

63

In a 25 mL two necked flask 2-formylbenzeneboronic acid (200 mg, 1.33 mmol) was stirred for 30 min at 45 °C in deionised water (5 mL) to hydrolyse any boroxine impurities. The system was cooled to room temperature and methoxylamine hydrochloride (151 mg, 1.81 mmol) was added portion-wise, resulting in the formation of a distinct white precipitate. The suspension was neutralised (pH 7) by addition of NaOH solution (10% v/v) and then refluxed for 30 min. During cooling, the stir bar was removed, and the flask replaced on the warm heating mantle and cooled slowly, allowing for slow crystallisation of the product. At RT the flask was placed in a fridge to further crystallise overnight. After filtration and removal of residual water under vacuum, the desired **63** was isolated as glassy crystals (83% yield). ***^{1}H NMR*** (300 MHz, $CDCl_3$) 11.01 (br, 2H), 8.21-8.17 (m, 2H), 7.51-7.36 (m, 3H), 4.02 (s, 3H). ***^{11}B NMR*** (96 MHz, $CDCl_3$); 32.2.

Synthesis of 2,3-dihydro-1H-benzo[c][1,2]azaborole

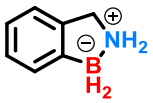

80

Compound **80** was synthesized according to the general **PROCEDURE B** reacting in a flame-dried 25 mL two necked flask under argon atmosphere, 2-(1,3,2-dioxaborinan-2-yl)benzonitrile (100 mg, 0.5 mmol) and $LiAlH_4$ (≈1.0 M in THF) (1.9 mL, 1.9 mmol, 3.5 equiv.) in anhydrous THF (5.0 mL). The desired product was obtained as a white powder (34 mg, 53%). ***^{1}H NMR***: (500 MHz, $CDCl_3$) δ (ppm) 7.45 (d, *J*=7.0 Hz, 1H), 7.21 (app t, *J*=7.0 Hz, 1H), 7.12-7.08 (m, 2H), 4.07 (t, *J*=6.0 Hz, 2H), 3.96 (br, 1H), 3.83 (t, *J*=4.5 Hz, 1H). ***^{13}C NMR***:

(125 MHz, $CDCl_3$) δ (ppm) 139.4, 129.4, 127.3, 125.2, 121.6, 51.0. ***^{11}B NMR***: (160 MHz, $CDCl_3$) δ (ppm) -10.1 (t, *J*=96 Hz). Following the general **PROCEDURE C** the desired **80** was obtained after 1.5 h in 67% yield.

Synthesis of 6-chloro-2,3-dihydro-1H-benzo[c][1,2]azaborole

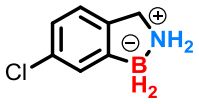

81

Compound **81** was synthesized according to the general **PROCEDURE B** reacting 4-chloro-2-(1,3,2-dioxaborinan-2-yl)benzonitrile (500 mg, 2.2 mmol) and $LiAlH_4$ (≈1.0 M in THF) (6.8 mL, 6.8 mmol, 3.0 equiv.) in anhydrous THF (10.0 mL) under argon atmosphere for 3 h. The desired product was obtained as a white powder (191 mg, 56%). ***^{1}H NMR***: (300 MHz, $CDCl_3$) δ (ppm) 7.38 (s, 1H), 7.05 (dd, *J*=8.0, ^{1}*J*=2.0 Hz, 1H), 6.99 (d, *J*=8.0 Hz, 1H), 4.28 (br, 2H), 4.14 (t, *J*=5.5 Hz, 2H). ***^{13}C NMR***: (125 MHz, DMSO-d_6) δ (ppm) 140.1, 131.1, 128.0, 123.8, 122.9, 48.9. ***^{11}B NMR***: (96 MHz, $CDCl_3$) δ (ppm) -7.1 (t, *J*=94 Hz). Following the general **PROCEDURE C** the desired **81** was obtained after 1.5 h in 70% yield.

Synthesis of 6-bromo-2,3-dihydro-1H-benzo[c][1,2]azaborole

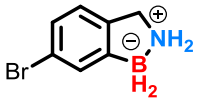

82

Compound **82** was synthesized according to the general **PROCEDURE B** reacting 4-bromo-2-(1,3,2-dioxaborinan-2-yl)benzonitrile (126 mg, 0.5 mmol) and $LiAlH_4$ (≈1.0 M in THF) (1.4 mL, 1.4 mmol, 3.0 equiv.) in anhydrous THF (5.0 mL) under argon atmosphere for 3 h. The desired product was obtained as a white powder (50 mg, 53%). ***^{1}H NMR***: (400 MHz, $CDCl_3$) δ (ppm) 7.54 (s, 1H), 7.20 (d, *J*=8.0 Hz, 1H), 6.93 (d, *J*=8.0 Hz, 1H), 4.28 (br, 2H), 4.10 (t, *J*=6.0 Hz, 2H). ***^{13}C NMR***: (125 MHz, DMSO-d_6) δ (ppm) 140.5, 130.9, 126.6, 123.4, 120.2, 48.9. ***^{11}B NMR***: (128 MHz, $CDCl_3$) δ (ppm) -10.3 (t, *J*=90 Hz). Following the general **PROCEDURE C** the desired **82** was obtained after 1.5 h in 70% yield.

Synthesis of 2,3-dihydro-1H-phenanthro[9,10-c][1,2]azaborole

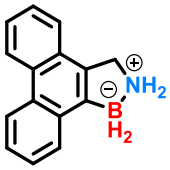

83

Compound **83** was synthesized according to the general **PROCEDURE B** reacting 10-(1,3,2-dioxaborinan-2-yl)phenanthrene-9-carbonitrile (250 mg, 0.9 mmol) and $LiAlH_4$ (≈1.0 M in THF) (5.7 mL, 5.7 mmol, 6.5 equiv.) in anhydrous THF (5.0 mL) under argon atmosphere for 16 h. The desired product was obtained as a white powder (110 mg, 57%). ***^{1}H NMR***: (400 MHz, $CDCl_3$) δ (ppm) 8.54-8.49 (m, 2H), 7.90-7.88 (m, 1H), 7.55-7.53 (m, 2H), 7.42 (app t, *J*=7.5 Hz, 1H), 7.32-7.28 (m, 2H), 4.38 (br, 2H), 3.90 (t, *J*=5.0 Hz, 2H). ***^{13}C NMR***: (125 MHz, $CDCl_3$) δ (ppm) 139.8, 132.4, 131.3, 131.1, 130.1, 128.6, 127.3, 126.7, 126.6, 125.2, 121.6, 51.0 . ***^{11}B NMR***: (128 MHz, $CDCl_3$) δ (ppm) -10.1.

Synthesis of 6-(dec-1-yn-1-yl)-2,3-dihydro-1H-benzo[c][1,2]azaborole

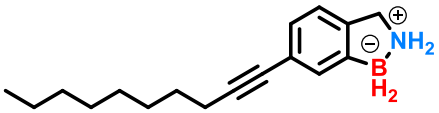

84

In a flame-dried 25 mL two necked flask equipped with condenser, under argon atmosphere, 4-(dec-1-yn-1-yl)-2-(1,3,2-dioxaborinan-2-yl)benzonitrile (107 mg, 0.33 mmol) was vacuumed for 1 h and back filled with argon, then dissolved in anhydrous 1,4-dioxane (6 mL) and cooled to 10 °C. Freshly titrated $LiAlH_4$ (≈1.0 M in THF) (2.3 mL, 2.3 mmol, 7.0 equiv.) was added dropwise, and the resulting mix was stirred for 15 min at 10 °C and then it was allowed to warm to room temperature and finally refluxed for 5 h. After cooling to room temperature and then to 10 °C, the reaction was quenched dropwise with water under vigorous stirring yielding a white precipitate. The formed suspension was filtered on a plug of $MgSO_4$ and the solid was washed with THF (3 x 10 mL) and EtOAc (3 x 10 mL). After the organic solvents were removed under reduced pressure, the residue was re-dissolved in EtOAc (20 mL), transferred to a separating funnel and washed with distilled water (6 x 10 mL) and brine (1 x 10 mL). The combined water phase was back-extracted once with EtOAc (15 mL) while the combined organic phase was dried over $MgSO_4$, filtered and the solvent removed under reduced pressure. The desired product was obtained as a white powder (28 mg, 34%). ***^{1}H NMR***: (400 MHz, $CDCl_3$) δ (ppm) 7.49 (s, 1H), 7.14 (d, *J*=8.0 Hz, 1H), 7.00 (d, *J*=8.0 Hz, 1H), 4.17 (br, 2H), 3.86 (t, *J*=5.5 Hz, 2H), 2.39 (t, *J*=7.0 Hz, 2H), 1.63-1.55 (m, 2H), 1.48-1.41 (m, 2H), 1.33-1.24

(m, 8H), 0.88 (t, *J*=6.5 Hz, 3H). ***^{13}C NMR***: (125 MHz, $CDCl_3$) *δ* (ppm) 136.8, 136.2, 130.3, 126.1, 121.3, 119.7, 114.8, 50.9, 31.9, 29.1, 28.6, 27.3, 22.8, 19.6, 14.3, 14.2. ***^{11}B NMR***: (128 MHz, $CDCl_3$) *δ* (ppm) -10.0.

Synthesis of 7-methyl-2,3-dihydro-1H-benzo[c][1,2]azaborole

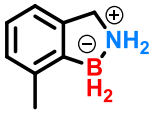

90

Compound **90** was synthesized according to the general **PROCEDURE C** reacting 2-(5,5-dimethyl-1,3,2-dioxaborinan-2-yl)-3-methylbenzonitrile (103 mg, 0.2 mmol) and $LiAlH_4$ (≈1.0 M in THF) (2.2 mL, 2.2 mmol, 5.0 equiv.) in anhydrous THF (2.0 mL) under argon atmosphere. The desired product was obtained as a white powder (56 mg, 95%). ***^{1}H NMR***: (500 MHz, $CDCl_3$) *δ* (ppm) 7.06-7.01 (m, 2H), 6.94 (d, *J*=7.0 Hz, 1H), 4.15 (t, *J*=6.5 Hz, 2H), 3.96 (br, 2H), 2.32 (s, 3H). ***^{13}C NMR***: (125 MHz, $CDCl_3$) *δ* (ppm) 139.7, 138.4, 127.7, 125.7, 118.6, 51.5, 22.1. ***^{11}B NMR***: (160 MHz, $CDCl_3$) *δ* (ppm) -10.4 (t, *J*=85 Hz). ***HRMS*** calc. for C8H12BN $[M-H]^+$ ($^m/_z$): 132.0979, found: 132.0975.

Synthesis of 6-methyl-2,3-dihydro-1H-benzo[c][1,2]azaborole

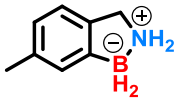

91

Compound **91** was synthesized according to the general **PROCEDURE C** reacting 2-(5,5-dimethyl-1,3,2-dioxaborinan-2-yl)-4-methylbenzonitrile (116 mg, 0.5 mmol) and $LiAlH_4$ (≈1.0 M in THF) (2.5 mL, 2.5 mmol, 5.0 equiv.) in anhydrous THF (2.0 mL) under argon atmosphere. The desired product was obtained as a white powder (56 mg, 75%). ***^{1}H NMR***: (500 MHz, $CDCl_3$) *δ* (ppm) 7.29 (s, 1H), 7.03 (d, *J*=8.0 Hz, 1H), 6.92 (d, *J*=8.0 Hz, 1H), 4.25 (t, *J*=6.5 Hz, 2H), 4.11 (br, 2H), 2.32 (s, 3H). ***^{13}C NMR***: (125 MHz, $CDCl_3$) *δ* (ppm) 136.8, 136.2, 130.3, 126.1, 121.3, 50.9, 21.5. ***^{11}B NMR***: (160 MHz, $CDCl_3$) *δ* (ppm) -9.4 (t, *J*=85 Hz). ***HRMS*** calc. for C8H12BN $[M-H]^+$ ($^m/_z$): 132.0979, found: 132.0975.

Synthesis of 5,7-bis(dodecyloxy)-2,3-dihydro-1H-benzo[c][1,2]azaborole

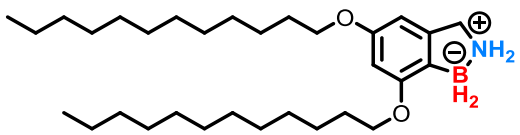

92

Compound **92** was synthesized according to the general **PROCEDURE C** reacting 2-(5,5-dimethyl-1,3,2-dioxaborinan-2-yl)-3,5-bis(dodecyloxy)benzonitrile (118 mg, 0.2 mmol) and $LiAlH_4$ (≈1.0 M in THF) (1.0 mL, 1.0 mmol, 5.0 equiv.) in anhydrous THF (2 mL) under argon atmosphere. The desired product was obtained as a white powder (30 mg, 30%). ***^{1}H NMR***: (500 MHz, $CDCl_3$) δ (ppm) 6.33 (s, 2H), 4.17 (t, *J*=6.0 Hz, 2H), 4.07 (br, 2H), 4.01 (t, *J*=6.5 Hz, 2H), 3.90 (t, *J*=6.5 Hz, 2H), 1.78-1.72 (m, 4H), 1.46-1.41 (m, 4H), 1.36-1.26 (m, 32 H), 0.88 (t, *J*=7.0 Hz, 6H). ***^{13}C NMR***: (125 MHz, $CDCl_3$) δ (ppm) 160.1, 159.5, 141.7, 100.6, 100.3, 70.3, 69.8, 69.0, 32.1, 29.8, 29.7, 29.6, 29.5, 29.4, 29.2, 29.1, 29.0, 26.1, 22.8, 14.3. ***^{11}B NMR***: (160 MHz, $CDCl_3$) δ (ppm) -10.6. ***HRMS*** calc. for C31H58BNO2 $[M-H]^+$ ($^m/_z$): 486.4597, found: 486.4586.

Synthesis of 2,3-dihydro-1H-benzo[c][1,2]azaborole

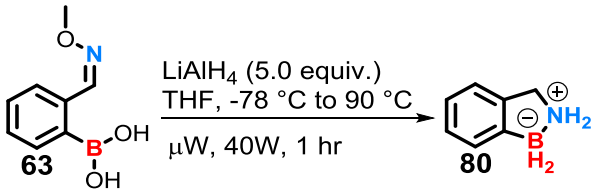

63 **80**

Compound **80** was synthesized according to the general **PROCEDURE B** reacting in a flame-dried 50 mL two necked flask under argon atmosphere, (2-((methoxyamino)methyl)benzene boronic acid (100 mg, 0.5 mmol) and $LiAlH_4$ (≈1.0 M in THF) (2.8 mL, 2.8 mmol, 5.0 equiv.) in anhydrous THF (2.0 mL). The desired product was obtained as a white powder (53 mg, 80%). ***^{1}H NMR***: (500 MHz, $CDCl_3$) δ (ppm) 7.45 (d, *J*=7.0 Hz, 1H), 7.21 (app t, *J*=7.0 Hz, 1H), 7.12-7.08 (m, 2H), 4.07 (t, *J*=6.0 Hz, 2H), 3.96 (br, 1H), 3.83 (t, *J*=4.5 Hz, 1H). ***^{13}C NMR***: (125 MHz, $CDCl_3$) δ (ppm) 139.4, 129.4, 127.3, 125.2, 121.6, 51.0. ***^{11}B NMR***: (160 MHz, $CDCl_3$) δ (ppm) -10.1 (t, *J*=96 Hz).

Synthesis of 3-methyl-2,3-dihydro-1H-benzo[c][1,2]azaborole

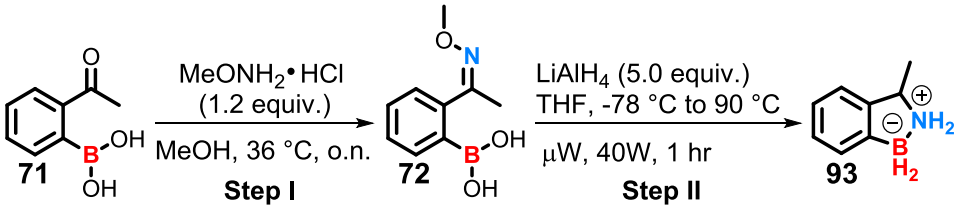

In a flame-dried 10 mL two necked flask, under argon atmosphere, (2-acetylphenyl)boronic acid (100 mg, 0.6 mmol) and methoxyamine hydrochloride (60 mg, 0.7 mmol, 1.2 equiv.) were was dissolved in anhydrous methanol (4 mL) and the mixture was stirred at 36 °C overnight. After cooling to room temperature, the organic solvent was removed under reduced pressure, the residue was re-dissolved in anhydrous THF (3 mL) and transferred via cannula in a beforehand flame-dried 10 mL μW tube equipped with a stirring bar and sealed with a perforated plastic cap under argon atmosphere. The system was cooled to -78°C and after 15 min, freshly titrated $LiAlH_4$ (≈1.0 M in THF) (3.0 mL, 3.0 mmol, 5.0 equiv.) was added dropwise under vigorous stirring, and then the resulting mix was slowly allowed to warm to room temperature. The needle was removed to seal, and the μW tube was placed into the μW machine and the mixture was stirred and irradiated by microwave dielectric heating at 90 °C (power 40W). After 1 h, the reaction mixture was cooled to room temperature, diluted with anhydrous THF and transferred in a 100 mL conical flask. After cooling to -5 °C, the reaction was quenched dropwise with water under vigorous stirring yielding a white precipitate. The formed suspension was filtered on a plug of $MgSO_4$ and the solid was washed with THF (3 x 10 mL) and EtOAc (3 x 10 mL). After the organic solvents were removed under reduced pressure, the residue was re-dissolved in EtOAc (20 mL), transferred to a separating funnel and washed with distilled water (6 x 10 mL) and brine (1 x 10 mL). The combined water phase was back-extracted once with EtOAc (15 mL) while the combined organic phase was dried over $MgSO_4$, filtered and the solvent removed under reduced pressure to afford the desired **93** as a white solid (56 mg, 70% over 2 steps). ***^{1}H NMR***: (500 MHz, $CDCl_3$) δ (ppm) 7.46 (d, *J*=7.5 Hz, 1H), 7.22 (t, *J*=7.5 Hz, 1H), 7.14 (t, *J*=7.0 Hz, 1H), 7.07 (d, *J*=7.5 Hz, 1H), 4.57-4.50 (m, 1H), 4.39 (br, 2H), 1.61 (d, *J*=6.5 Hz, 3H). ***^{13}C NMR***: (125 MHz, $CDCl_3$) δ (ppm) 144.0, 129.6, 127.4, 125.4, 121.1, 59.0, 20.6. ***^{11}B NMR***: (160 MHz, $CDCl_3$) δ (ppm) -11.0 (t, *J*=96 Hz). ***HRMS*** calc. for C8H12BN $[M+H]^+$ ($^m/_z$): 132.0979, found: 132.0975.

Synthesis of 7H,14H,21H-benzo[3,4][1,2]azaborolo[1,2-a]benzo[3,4][1,2]azaborolo[1,2-c]benzo[3,4][1,2]azaborolo[1,2-e][1,3,5,2,4,6]triazatriborinine

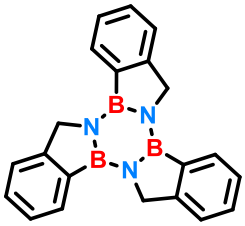

96

Compound **96** was synthesized according to the general **PROCEDURE D** reacting 2,3-dihydro-1H-benzo[c][1,2]azaborole (113 mg, 0.9 mmol) in anhydrous toluene (3 mL) under argon atmosphere. After 2 h, the reaction mixture was cooled to room temperature, diluted with EtOAc (20 mL) and transferred in a 100 mL flask. After the organic solvents were removed under reduced pressure, the crude product was purified by washing the solid with (*n*-hexane/CH_2Cl_2 80:20) (4 x 5 mL) to afford the desired **96** as a white solid (70 mg, 64%). ***^{1}H NMR***: (500 MHz, $CDCl_3$) δ (ppm) 8.01 (d, *J*=7.0 Hz, 3H), 7.65 (d, *J*=7.5 Hz, 3H), 7.51 (t, *J*=7.0 Hz, 3H), 7.44 (t, *J*=7.0 Hz, 3H), 4.95 (s, 6H). ***^{13}C NMR***: (125 MHz, $CDCl_3$) δ (ppm) 154.2, 131.0, 129.8, 126.5, 123.2, 52.4. ***^{11}B NMR***: (160 MHz, $CDCl_3$) δ (ppm) 34.6.

Synthesis of 3,10,17-trichloro-7H,14H,21H-benzo[3,4][1,2]azaborolo[1,2-a]benzo[3,4][1,2]azaborolo[1,2-c]benzo[3,4][1,2]azaborolo[1,2-e][1,3,5,2,4,6]triazatriborinine

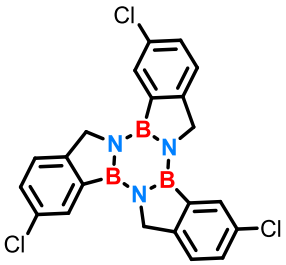

97

Compound **97** was synthesized according to the general **PROCEDURE D** reacting 6-chloro-2,3-dihydro-1H-benzo[c][1,2]azaborole (100 mg, 0.66 mmol) in anhydrous toluene (3 mL) under argon atmosphere. After 2 h, the reaction mixture was cooled to room temperature, diluted with EtOAc (20 mL) and transferred in a 100 mL flask. After the organic solvents were removed under reduced pressure, the crude product was purified by washing the solid with (*n*-hexane/CH_2Cl_2 80:20) (4 x 5 mL) to afford the desired **97** as a white solid (44 mg, 45%). ***^{1}H NMR***: (500 MHz, DMSO-d_6, 358 °K) δ (ppm) 8.04 (s, 3H), 7.67 (d, *J*=8.0 Hz, 3H), 7.58 (d, *J*=8.0 Hz, 3H), 5.05 (s, 6H). ***^{11}B NMR***: (160 MHz, $CDCl_3$) δ (ppm) 31.3.

Synthesis of 3,10,17-tribromo-7H,14H,21H-benzo[3,4][1,2]azaborolo[1,2-a]benzo[3,4][1,2]azaborolo[1,2-c]benzo[3,4][1,2]azaborolo[1,2-e][1,3,5,2,4,6]triazatriborinine

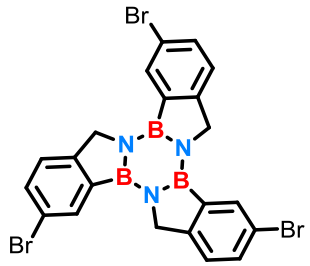

98

Compound **98** was synthesized according to the general **PROCEDURE D** reacting 6-bromo-2,3-dihydro-1H-benzo[c][1,2]azaborole (100 mg, 0.50 mmol) in anhydrous toluene (3 mL) under argon atmosphere. After 2 h, the reaction mixture was cooled to room temperature, diluted with EtOAc (20 mL) and transferred in a 100 mL flask. After the organic solvents were removed under reduced pressure, the crude product was purified by washing the solid with (*n*-hexane/CH_2Cl_2 80:20) (4 x 5 mL) to afford the desired **98** as a white solid (44 mg, 45%). ***^{1}H NMR***: (500 MHz, DMSO-d_6, 373 °K) δ (ppm) 8.18 (s, 3H), 7.71 (d, *J*=8.0 Hz, 3H), 7.61 (d, *J*=8.0 Hz, 3H), 5.02 (s, 6H). ***^{11}B NMR***: (160 MHz, DMSO-d_6, 373 °K) δ (ppm) 31.4.

Synthesis of 4,11,18-trimethyl-7H,14H,21H-benzo[3,4][1,2]azaborolo[1,2-a]benzo[3,4][1,2]azaborolo[1,2-c]benzo[3,4][1,2]azaborolo[1,2-e][1,3,5,2,4,6]triazatriborinine

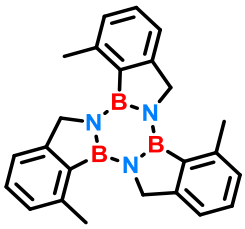

101

Compound **101** was synthesized according to the general **PROCEDURE D** reacting 7-methyl-2,3-dihydro-1H-benzo[c][1,2]azaborole (100 mg, 0.75 mmol) in anhydrous toluene (3 mL) under argon atmosphere. After 2 h, the reaction mixture was cooled to room temperature, diluted with EtOAc (20 mL) and transferred in a 100 mL flask. After the organic solvents were removed under reduced pressure, the crude product was purified by washing the solid with (*n*-hexane/CH_2Cl_2 80:20) (4 x 5 mL) to afford the desired **101** as a white solid (70 mg, 72%). ***^{1}H NMR***: (400 MHz, TCE-d_2, 348 °K) δ (ppm) 7.42 (d, *J*=5.0 Hz, 6H), 7.25 (t, *J*=5.0 Hz, 3H), 5.18 (s, 6H), 2.97 (s, 9H). ***^{13}C NMR***: (126 MHz, TCE-d_2, 353 °K) δ (ppm) 154.7, 140.7, 129.8, 128.8, 120.2, 56.2, 25.6. ***^{11}B NMR***: (128 MHz, TCE-d_2, 348 °K) δ (ppm) 36.7. ***HRMS*** calc. for C24H25B3N3 $[M+H]^+$ ($^m/_z$): 388.2322, found: 388.2326.

Synthesis of 3,10,17-trimethyl-7H,14H,21H-benzo[3,4][1,2]azaborolo[1,2-a]benzo[3,4][1,2]azaborolo[1,2-c]benzo[3,4][1,2]azaborolo[1,2-e][1,3,5,2,4,6]triazatriborinine

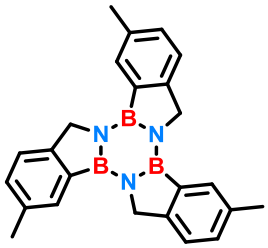

102

Compound **102** was synthesized according to the general **PROCEDURE D** reacting 6-methyl-2,3-dihydro-1H-benzo[c][1,2]azaborole (100 mg, 0.75 mmol) in anhydrous toluene (3 mL) under argon atmosphere. After 2 h, the reaction mixture was cooled to room temperature, diluted with EtOAc (20 mL) and transferred in a 100 mL flask. After the organic solvents were removed under reduced pressure, the crude product was purified by washing the solid with (*n*-hexane/CH_2Cl_2 80:20) (4 x 5 mL) to afford the desired **102** as a white solid (68 mg, 70%). ***^{1}H NMR***: (500 MHz, TCE-d_2, 323 °K) δ (ppm) 7.87 (s, 3H), 7.52 (d, *J*=7.5 Hz, 3H), 7.38 (d, *J*=7.5 Hz, 3H), 5.01 (s, 6H), 2.54 (s, 9H). ***^{13}C NMR***: (126 MHz, TCE-d_2, 323 °K) δ (ppm) 151.5, 136.1, 131.5, 313.1, 123.0, 52.3, 21.5. ***^{11}B NMR***: (128 MHz, TCE-d_2, 348 °K) δ (ppm) 36.7. ***HRMS*** calc. for C24H25B3N3 $[M+H]^+$ ($^m/_z$): 388.2322, found: 388.2327.

Synthesis of 2,4,9,11,16,18-hexakis(dodecyloxy)-7H,14H,21H-benzo[3,4][1,2]azaborolo[1,2-a]benzo[3,4][1,2]azaborolo[1,2-c]benzo[3,4][1,2]azaborolo[1,2-e][1,3,5,2,4,6]triazatriborinine

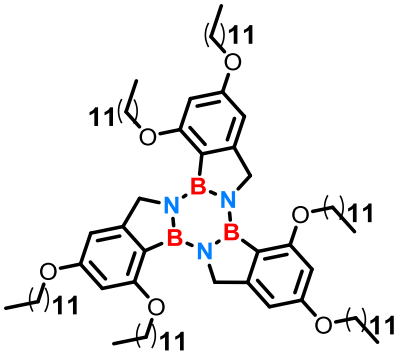

103

Compound **103** was synthesized according to the general **PROCEDURE D** reacting 5,7-bis(dodecyloxy)-2,3-dihydro-1H-benzo[c][1,2]azaborole (75 mg, 0.15 mmol) in anhydrous toluene (2 mL) under argon atmosphere. After 3 h, the reaction mixture was cooled to room temperature, diluted with EtOAc and transferred in a 100 mL flask. After the organic solvents were removed under reduced pressure, the crude product was purified by silica gel flash chromatography (*n*-hexane/CH_2Cl_2 70:30) to afford the desired **103**

as a white powder (10 mg, 13%). ***^{1}H NMR***: (500 MHz, $CDCl_3$) δ (ppm) 6.55 (s, 3H), 6.36 (s, 3H), 5.02 (s, 6H), 4.08 (t, *J*=6.5 Hz, 6H), 4.02 (t, *J*=6.5 Hz, 6H), 2.01-1.95 (m, 6H), 1.84-1.79 (m, 6H), 1.64-1.58 (m, 6H), 1.51-1.45 (m, 6H), 1.37-1.26 (m, 96H), 0.90-0.86 (m, 18H). ***^{13}C NMR***: (125 MHz, $CDCl_3$) δ (ppm) 163.0, 162.4, 159.2, 99.6, 97.2, 68.2, 68.1, 55.9, 32.1, 31.7, 30.0, 29.9, 29.8, 29.7, 29.6, 29.5, 26.9, 26.3, 22.8, 14.3, 1.2. ***HRMS*** calc. for C93H162B3N3O6 $[M+H]^+$ ($^m/_z$): 1451.2858, found: 1451.2847.

Synthesis of 7,14,21-trimethyl-7H,14H,21H-benzo[3,4][1,2]azaborolo[1,2-a]benzo[3,4][1,2]azaborolo[1,2-c]benzo[3,4][1,2]azaborolo[1,2-e][1,3,5,2,4,6]triazatriborinine

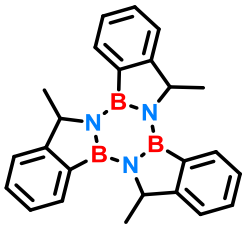

104

Compound **104** was synthesized according to the general **PROCEDURE D** reacting 3-methyl-2,3-dihydro-1H-benzo[c][1,2]azaborole (100 mg, 0.75 mmol) in anhydrous toluene (3 mL) under argon atmosphere. After 2 h, the reaction mixture was cooled to room temperature, diluted with EtOAc (20 mL) and transferred in a 100 mL flask. The organic solvents were removed under reduced pressure to afford the desired **104** as a white solid (90 mg, 93%). By washing the solid with a mix of (*n*-hexane/CH_2Cl_2 80:20) (3 x 2 mL) was possible to isolate the *syn* diastereoisomers from the *anti*, showing more affinity for the mix utilized.

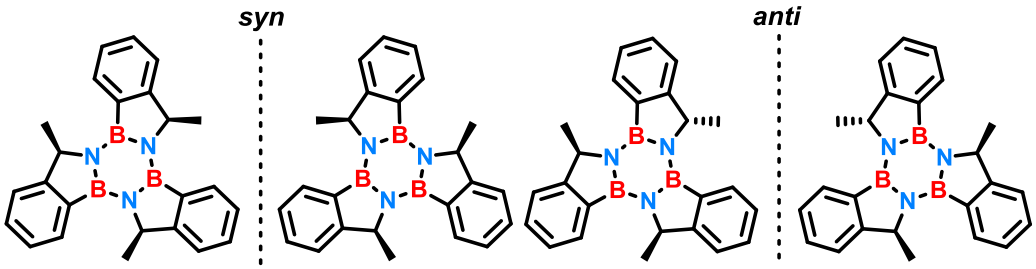

104a (7*R*,14*R*,21*R*) ***RRR*** | **104b** (7*S*,14*S*,21*S*) ***SSS*** | **104c** (7*R*,14*R*,21*S*) ***RRS*** | **104d** (7*R*,14*S*,21*S*) ***RSS***

Syn: ***^{1}H NMR***: (500 MHz, $CDCl_3$) δ (ppm) 8.03 (d, *J*=7.5 Hz, 3H), 7.54-7.49 (m, 6H), 7.44 (t, *J*=7.0 Hz, 3H), 5.27-5.23 (q, *J*=7.0 Hz, 3H), 1.78 (d, *J*=7.0 Hz, 9H). ***Anti***: ***^{1}H NMR***: (500 MHz, $CDCl_3$) δ (ppm) 8.04 (d, *J*=7.5 Hz, 3H), 7.54-7.50 (m, 6H), 7.44 (t, *J*=7.0 Hz, 3H), 5.36-5.32 (q, *J*=7.0 Hz, 3H), 1.75 (d, *J*=6.5 Hz, 3H), 1.70 (d, *J*=6.5 Hz, 3H), 1.65 (d, *J*=6.5 Hz, 3H). ***^{13}C NMR***: (125 MHz, $CDCl_3$) δ (ppm) 160.0, 131.7, 129.9, 126.8, 122.9,

58.9, 24.7. ***^{11}B NMR***: (160 MHz, $CDCl_3$) δ (ppm) 34.4. ***HRMS*** calc. for C24H24B3N3 $[M+H]^+$ ($^m/_z$): 388.2322, found: 388.2322.

Synthesis of 3,5-bis(3-hydroxypropoxy)benzonitrile

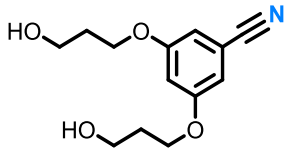

111

In a flame-dried 25 mL two necked flask equipped with condenser, under argon atmosphere, 3,5-dihydoxybenzonitrile (200 mg, 1.5 mmol), 3-bromo-1-propanol (0.35 mL, 3.7 mmol, 2.5 equiv.) and K_2CO_3 (1024 mg, 7.4 mmol, 5.0 equiv.) were dissolved in anhydrous DMF (12 mL) and the mixture was heated up under reflux. After 12 h, the reaction mixture was cooled to room temperature and the organic solvent was partially removed under reduced pressure. The residue was re-dissolved in CH_2Cl_2 (20 mL), transferred to a separating funnel and washed with brine (7 x 10 mL). The combined water phase was back-extracted once with CH_2Cl_2 (10 mL) while the combined organic phase was dried over $MgSO_4$, filtered and the solvent removed under reduced pressure. The crude product was purified by silica gel flash chromatography (*n*-hexane/CH_2Cl_2 60:40) to afford the desired **111** as a light yellow powder (300 mg, 81%). ***^{1}H NMR***: (500 MHz, $CDCl_3$) δ (ppm) 6.77 (d, *J*=2.5 Hz, 2H), 6.68 (app t, *J*=2.5 Hz, 1H), 4.10 (t, *J*=6.0 Hz, 4H), 3.85 (t, *J*=5.5 Hz, 4H), 2.04 (q, *J*=6.0 Hz, 4H), 1.61 (br, 2H). ***^{13}C NMR***: (125 MHz, $CDCl_3$) δ (ppm) 160.3, 118.6, 114.4, 110.3, 106.7, 70.4, 67.2, 29.4. ***HRMS*** calc. for C13H17NO4 $[M+H]^+$ ($^m/_z$): 252.1236, found: 252.1237.

Synthesis of 3,5-bis(3-(dodecyloxy)propoxy)benzonitrile

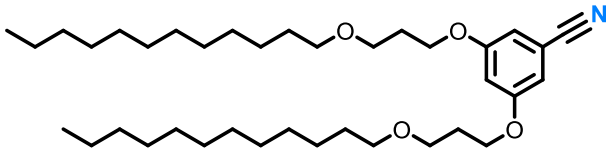

112

In a flame-dried 10 mL two necked flask, under argon atmosphere, NaH (60% dispersion in mineral oil, 48 mg, 1.2 mmol, 3.0 equiv.) was suspended in anhydrous DMF (1 mL) and sonicated for 10 min. In parallel 3,5-bis(3-hydroxypropoxy)benzonitrile (100 mg, 0.4 mmol) was dissolved in anhydrous DMF (2 mL), under argon atmosphere, and the resulting solution was cannulated dropwise to the suspension. The resulting mixture was stirred at room temperature for 1 h, then 1-bromododecane (0.3 mL, 1.2 mmol, 3.0 equiv.) was added dropwise. After being stirred at room temperature for 12h, the reaction mixture was diluted with EtOAc (20 mL), transferred to a separating funnel and washed with distilled water (1 x 10 mL) and

brine (6 x 10 mL). The combined water phase was back-extracted once with EtOAc (10 mL) while the combined organic phase was dried over $MgSO_4$, filtered and the solvent removed under reduced pressure. The crude product was purified by silica gel flash chromatography (*n*-hexane 100%, then *n*-hexane/EtOAc 98:2) to afford the desired **112** as a white powder (211 mg, 90%). ***^{1}H NMR***: (400 MHz, $CDCl_3$) δ (ppm) 6.74 (d, *J*=2.0 Hz, 2H), 6.66 (app t, *J*=2.0 Hz, 1H), 4.04 (t, *J*=6.0 Hz, 4H), 3.56 (t, *J*=6.0 Hz, 4H), 3.41 (t, *J*=6.5 Hz, 4H), 2.03 (q, *J*=6.0 Hz, 4H), 1.56 (q, *J*=6.0 Hz, 4H), 1.33-1.25 (m, 36H), 0.87 (t, *J*=6.5 Hz, 6H). ***^{13}C NMR***: (125 MHz, $CDCl_3$) δ (ppm) 160.5, 118.9, 113.4, 110.5, 106.6, 71.4, 67.0, 65.6, 32.0, 29.8, 29.7, 29.6, 29.5, 26.3, 22.8, 14.2. ***HRMS*** calc. for C37H65NO4 $[M+H]^+$ ($^m/_z$): 588.4992, found: 588.4997.

Synthesis of 2-bromo-3,5-bis(3-(dodecyloxy)propoxy)benzonitrile

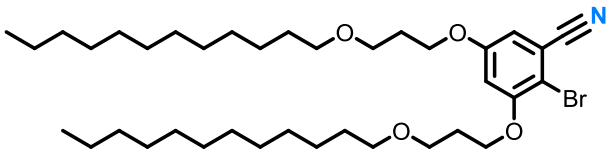

113

In a flame-dried 50 mL two necked flask, under argon atmosphere, 3,5-bis(3-(dodecyloxy)propoxy)benzonitrile (1000 mg, 1.7 mmol), *N*-bromosuccinimide (300 mg, 1.7 mmol, 1.0 equiv.), $Pd(OAc)_2$ (20 mg, 0.1 mmol, 5 mmol%) and *p*-Toluenesulfonic acid (160 mg, 0.9 mmol, 0.5 equiv.) were dissolved in anhydrous 1,2-dichloroethene (20 mL) and the mixture was stirred at 70 °C. After 12 h the reaction was cooled to room temperature and the organic solvent was removed under reduced pressure. The crude product was purified by silica gel flash chromatography (*n*-hexane/EtOAc 98:2) to afford the desired **113** as a white powder (580 mg, 70%). ***^{1}H NMR***: (500 MHz, $CDCl_3$) δ (ppm) 6.76 (d, *J*=2.5 Hz, 1H), 6.67 (d, *J*=2.5 Hz, 1H), 4.11 (t, *J*=6.0 Hz, 2H), 4.05 (t, *J*=6.5 Hz, 2H), 3.62 (t, *J*=6.0 Hz, 2H), 3.56 (t, *J*=6.0 Hz, 2H), 3.43-3.40 (m, 4H), 2.11-2.01 (m, 4H), 1.59-1.52 (m, 4H), 1.33-1.21 (m, 36H), 0.88 (t, *J*=6.5 Hz, 6H). ***^{13}C NMR***: (125 MHz, $CDCl_3$) δ (ppm) 159.4, 157.1, 117.5, 116.8, 110.3, 106.7, 105.6, 71.4, 66.8, 66.7, 66.6, 66.0, 32.1, 29.8, 29.7, 29.6, 29.5, 29.3, 22.8, 14.3. ***HRMS*** calc. for C37H64BrNO4 $[M+H]^+$ ($^m/_z$): 666.4097, 668.4064, found: 666.4087, 668.4075.

Synthesis of 2-(5,5-dimethyl-1,3,2-dioxaborinan-2-yl)-3,5-bis(3-(dodecyloxy)propoxy)benzonitrile

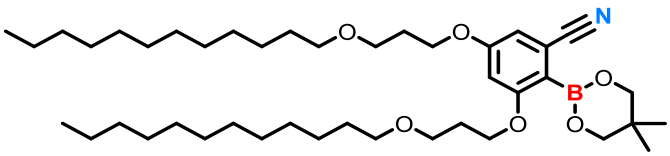

115

In a flame-dried 10 mL two necked flask equipped with condenser, under argon atmosphere, 2-bromo-3,5-bis(3-(dodecyloxy)propoxy)benzonitrile (200 mg, 0.3 mmol), bis(neopentyl glycolato)diboron (102 mg, 0.5 mmol, 1.5 equiv.), Pd(dppf)Cl_2 (17 mg, 0.02 mmol, 7 mmol%) and CH_3COOK (118 mg, 1.2 mmol, 4.0 equiv.) were vacuumed for 1 h and back filled with argon, then dissolved in anhydrous 1,4-dioxane (4 mL) and heated up under reflux. After 12 h, the reaction mixture was cooled to room temperature and the organic solvent was removed under reduced pressure. The residue was re-dissolved in EtOAc (30 mL), transferred to a separating funnel and washed with distilled water (2 x 10 mL) and brine (1 x 10 mL). The combined water phase was back-extracted once with EtOAc (15 mL) while the combined organic phase was dried over $MgSO_4$, filtered and the solvent removed under reduced pressure. The crude product was purified by silica gel flash chromatography (*n*-hexane/EtOAc 85:15) to afford the desired **115** as a light brown viscous liquid (130 mg, 62%). ***^{1}H NMR***: (500 MHz, $CDCl_3$) δ (ppm) 6.72 (d, *J*=2.0 Hz, 1H), 6.58 (d, *J*=2.0 Hz, 1H), 4.06-4.01 (m, 4H), 3.80 (s, 4H), 3.59-3.54 (m, 4H), 3.43-3.39 (m, 4H), 2.06-2.00 (m, 4H), 1.58-1.52 (m, 8H), 1.33-1.21 (m, 32H), 1.09 (s, 6H), 0.88 (t, *J*=6.5 Hz, 6H). ***^{13}C NMR***: (125 MHz, $CDCl_3$) δ (ppm) 163.4, 161.2, 119.6, 117.0, 109.6, 103.8, 72.8, 71.4, 71.3, 67.1, 67.0, 65.7, 65.6, 32.1, 29.9, 29.8, 29.7, 29.6, 29.5, 26.3, 22.8, 22.0, 14.2. ***^{11}B NMR***: (160 MHz, $CDCl_3$) δ (ppm) 27.0. ***HRMS*** calc. for C42H74BNO6 $[M+H]^+$ ($^m/_z$): 700.5695, found: 700.5735.

Synthesis of 5,7-bis(3-(dodecyloxy)propoxy)-2,3-dihydro-1H-benzo[c][1,2]azaborole

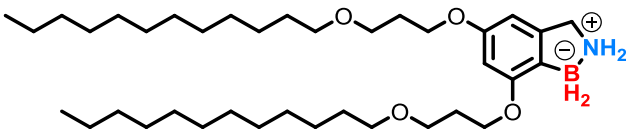

116

Compound **116** was synthesized according to the general **PROCEDURE C** reacting 2-(5,5-dimethyl-1,3,2-dioxaborinan-2-yl)-3,5-bis(3-(dodecyloxy)propoxy)benzonitrile (120 mg, 0.2 mmol) and $LiAlH_4$ (≈1.0 M in THF) (0.9 mL, 0.9 mmol, 5.0 equiv.) in anhydrous THF (2.5 mL) under argon atmosphere. The desired product was obtained as a white powder (66 mg, 64%). ***^{1}H NMR***: (500 MHz, $CDCl_3$) δ (ppm) 6.34 (s, 1H), 6.32 (s, 1H), 4.22 (br, 2H), 4.11-4.07 (m, 4H), 3.99 (t, *J*=6.5 Hz, 2H), 3.60-3.55 (m, 4H), 3.42-3.39 (m, 4H), 2.03-1.99 (m, 4H), 1.59-1.52 (m, 8H), 1.33-1.25 (m, 34H), 0.88 (t, *J*=6.5 Hz, 6H). ***^{13}C NMR***: (125 MHz, $CDCl_3$)

δ (ppm) 160.1, 159.5, 141.7, 100.6, 100.3, 71.3, 71.2, 67.8, 67.6, 65.5, 65.3, 51.1, 32.1, 30.1, 30.0, 29.9, 29.8, 29.7, 29.6, 29.5, 26.3, 22.8, 14.3. ***^{11}B NMR***: (160 MHz, $CDCl_3$) δ (ppm) -11.2. ***HRMS*** calc. for C37H70BNO4 $[M-2H]^{\cdot -}$ ($^m/_z$): 602.5326, found: 602.5328.

Synthesis of 2,4,9,11,16,18-hexakis(3-(dodecyloxy)propoxy)-7H,14H,21H-benzo[3,4][1,2]azaborolo[1,2-a]benzo[3,4][1,2]azaborolo[1,2-c]benzo[3,4][1,2]azaborolo[1,2-e][1,3,5,2,4,6]triazatriborinine

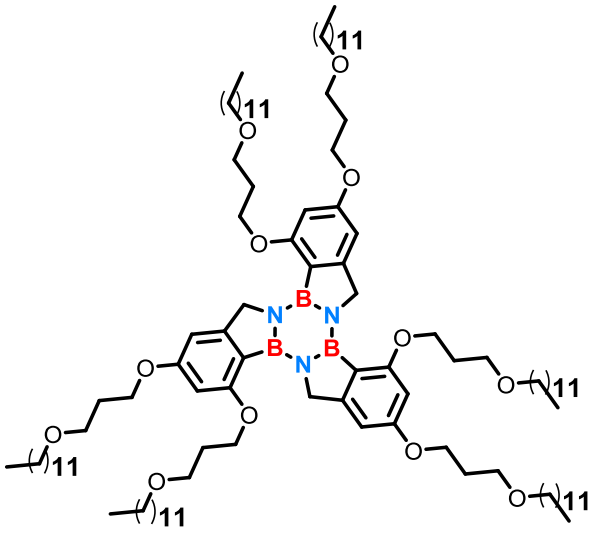

117

Compound **117** was synthesized according to the general **PROCEDURE D** reacting 5,7-bis(3-(dodecyloxy)propoxy)-2,3-dihydro-1H-benzo[c][1,2]azaborole (100 mg, 0.17 mmol) in anhydrous toluene (2 mL) under argon atmosphere. After 3 h, the reaction mixture was cooled to room temperature, diluted with EtOAc and transferred in a 100 mL flask. After the organic solvents were removed under reduced pressure, the crude product was washed with a solution of *n*-hexane/CH_2Cl_2 (80:20), (5 x 5 mL) to afford the desired **117** as a white powder (26 mg, 26%). ***^{1}H NMR***: (500 MHz, TCE-d_2) 6.60 (s, 3H), 6.42 (s, 3H), 5.00 (s, 6H), 4.20 (t, *J*=6.0 Hz, 6H), 4.15 (t, *J*=6.0 Hz, 6H), 3.72 (t, *J*=6.5 Hz, 6H), 3.62 (t, *J*=6.0 Hz, 6H), 3.48-3.43 (m, 12H), 2.28-2.23 (m, 6H), 2.11-2.06 (m, 6H), 1.63-1.55 (m, 12H), 1.34-1.25 (m, 108H), 0.90-0.86 (m, 18H). ***^{13}C NMR***: (125 MHz, TCE-d_2) δ (ppm) 162.7, 161.8, 158.6, 116.8, 100.0, 96.8, 71.2, 70.9, 67.5, 67.0, 65.0, 64.9, 55.6, 31.8, 29.7, 29.6, 29.5, 29.4, 29.3, 26.1, 26.0, 22.6, 14.1. ***^{11}B NMR***: (128 MHz, TCE-d_2, 348 °K) δ (ppm) 31.0.

Synthesis of 3-((R)-3-hydroxy-2-methylpropoxy)-5-((S)-3-hydroxy-2-methylpropoxy)benzonitrile

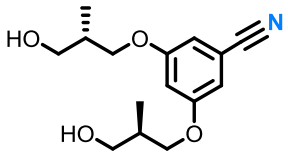

118

In a flame-dried 10 mL two necked flask equipped with condenser, under argon atmosphere, 3,5-dihydoxybenzonitrile (100 mg, 0.7 mmol) and K_2CO_3 (409 mg, 3.0 mmol, 4.0 equiv.) were vacuumed for 1 h and back filled with argon, then dissolved in anhydrous DMF (3 mL). Finally (S)-(+)-3-bromo-2-methyl-1-propanol (0.2 mL, 1.9 mmol, 2.6 equiv.) was syringed and the resulting mixture was stirred at 120 °C. After 17 h, the reaction mixture was cooled to room temperature, diluted with EtOAc (30 mL), transferred to a separating funnel and washed with distilled water (2 x 10 mL) and brine (6 x 10 mL). The combined water phase was back-extracted once with EtOAc (15 mL) while the combined organic phase was dried over $MgSO_4$, filtered and the solvent removed under reduced pressure. The crude product was purified by silica gel flash chromatography (*n*-hexane/EtOAc 70:30, and then EtOAc 100) to afford the desired **118** as a light yellow solid (140 mg, 70%). ***^{1}H NMR***: (500 MHz, $CDCl_3$) δ (ppm) 6.76 (d, *J*=2.5 Hz, 2H), 6.68 (app t, *J*=2.5 Hz, 1H), 3.97-3.89 (dd, *J*=9.0, ^1J=6.5 Hz, 4H), 3.71-3.64 (m, 4H), 2.21-2.13 (m, 2H), 1.75 (br, 2H), 1.04 (d, *J*=6.5 Hz, 6H). ***^{13}C NMR***: (125 MHz, $CDCl_3$) δ (ppm) 160.6, 160.3, 118.7, 113.6, 110.6, 110.4, 107.6, 72.3, 71.4, 71.3, 70.7, 35.7, 34.0, 14.3, 14.2. ***HRMS*** calc. for C15H21NO4 $[M-H]^-$ ($^m/_z$): 278.1398, found: 278.1399.

Synthesis of 3-((R)-3-(dodecyloxy)-2-methylpropoxy)-5-((S)-3-(dodecyloxy)-2-methylpropoxy)benzonitrile

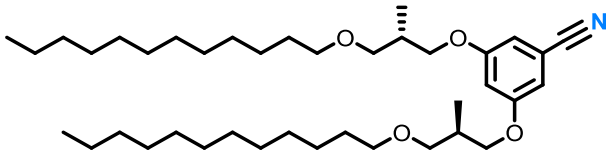

119

In a flame-dried 10 mL two necked flask, under argon atmosphere, NaH (60% dispersion in mineral oil, 62 mg, 1.6 mmol, 3.0 equiv.) was suspended in anhydrous DMF (1 mL) and sonicated for 10 min. In parallel 3-((R)-3-hydroxy-2-methylpropoxy)-5-((S)-3-hydroxy-2-methylpropoxy)benzonitrile (145 mg, 0.5 mmol) was dissolved in anhydrous DMF (3 mL), under argon atmosphere, and the resulting solution was cannulated dropwise to the suspension. The resulting mixture was stirred at room temperature for 1 h, then 1-bromododecane (0.37 mL, 1.6 mmol, 3.0 equiv.) was added dropwise. After being stirred at room temperature for 12h, the reaction mixture was diluted with EtOAc (20 mL), transferred to a separating funnel and washed with distilled water (1 x 10 mL) and brine (6 x 10 mL). The combined water phase was

back-extracted once with EtOAc (10 mL) while the combined organic phase was dried over $MgSO_4$, filtered and the solvent removed under reduced pressure. The crude product was purified by silica gel flash chromatography (*n*-hexane 100%, then *n*-hexane/EtOAc 95:5) to afford the desired **119** as a white powder (222 mg, 70%). ***^{1}H NMR***: (500 MHz, $CDCl_3$) δ (ppm) 6.75 (d, *J*=2.0 Hz, 2H), 6.67 (app t, *J*=2.5 Hz, 1H), 3.96-3.93 (dd, *J*=9.0, ^1J=5.5 Hz, 2H), 3.84-3.81 (dd, *J*=9.0, ^1J=6.0 Hz, 2H), 3.42-3.38 (m, 8H), 2.24-2.18 (m, 2H), 1.58-1.52 (m, 4H), 1.34-1.25 (m, 36H), 1.04 (d, *J*=7.0 Hz, 6H), 0.90-0.86 (m, 6H). ***^{13}C NMR***: (125 MHz, $CDCl_3$) δ (ppm) 160.8, 160.4, 118.9, 113.4, 110.8, 110.4, 106.6, 72.5, 71.5, 71.1, 70.8, 65.3, 35.7, 34.0, 32.1, 29.8, 29.7, 29.6, 29.5, 26.3, 22.8, 14.3, 14.2, 13.7. ***HRMS*** calc. for C39H69NO4 $[M+H]^+$ ($^m/_z$): 616.5305, found: 616.5309.

Synthesis of 2-bromo-3-((R)-3-(dodecyloxy)-2-methylpropoxy)-5-((S)-3-(dodecyloxy)-2-methylpropoxy)benzonitrile

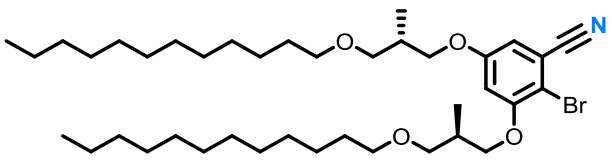

120

In a flame-dried 10 mL two necked flask, under argon atmosphere, 3-((R)-3-(dodecyloxy)-2-methylpropoxy)-5-((S)-3-(dodecyloxy)-2-methylpropoxy)benzonitrile (213 mg, 0.4 mmol), *N*-bromosuccinimide (61 mg, 0.4 mmol, 1.0 equiv.), $Pd(OAc)_2$ (20 mg, 0.01 mmol, 3 mmol%) and *p*-Toluenesulfonic acid (33 mg, 0.2 mmol, 0.5 equiv.) were dissolved in anhydrous 1,2-dichloroethene (3 mL) and the mixture was stirred at 70 °C. After 12 h the reaction was cooled to room temperature and the organic solvent was removed under reduced pressure. The crude product was purified by silica gel flash chromatography (*n*-hexane/EtOAc 98:2) to afford the desired **120** as a white powder (140 mg, 61%). ***^{1}H NMR***: (400 MHz, $CDCl_3$) δ (ppm) 6.76 (d, *J*=3.0 Hz, 1H), 6.67 (d, *J*=3.0 Hz, 1H), 4.01-3.91 (m, 3H), 3.84-3.80 (dd, *J*=9.0, ^1J=6.5 Hz, 1H), 3.49-3.36 (m, 8H), 2.31-2.17 (m, 2H), 1.58-1.51 (m, 6H), 1.33-1.25 (m, 34H), 1.09 (d, *J*=7.0 Hz, 3H), 1.04 (d, *J*=7.0 Hz, 3H), 0.89-0.86 (m, 6H). ***^{13}C NMR***: (125 MHz, $CDCl_3$) δ (ppm) 158.4, 156.4, 119.6, 116.2, 106.8, 102.7, 72.1, 71.9, 71.5, 34.1, 32.1, 29.8, 29.7, 29.6, 29.5, 26.3, 22.8, 14.3. ***HRMS*** calc. for C39H68BrNO4 $[M+H]^+$ ($^m/_z$): 694.4410, 696.4398 found: 694.4412, 696.4400.

Synthesis of 2-(5,5-dimethyl-1,3,2-dioxaborinan-2-yl)-3-((R)-3-(dodecyloxy)-2-methylpropoxy)-5-((S)-3-(dodecyloxy)-2-methylpropoxy)benzonitrile

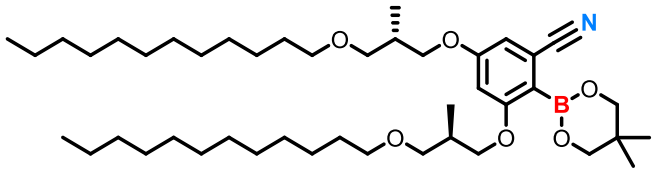

121

In a flame-dried 10 mL two necked flask equipped with condenser, under argon atmosphere, 2-bromo-3-((R)-3-(dodecyloxy)-2-methylpropoxy)-5-((S)-3-(dodecyloxy)-2-methylpropoxy)benzonitrile (100 mg, 0.1 mmol), bis(neopentyl glycolato)diboron (50 mg, 0.2 mmol, 1.5 equiv.), Pd(dppf)Cl_2 (8 mg, 0.01 mmol, 7 mmol%) and CH_3COOK (56 mg, 0.6 mmol, 4.0 equiv.) were vacuumed for 1 h and back filled with argon, then dissolved in anhydrous 1,4-dioxane (2.5 mL) and heated up under reflux. After 12 h, the reaction mixture was cooled to room temperature and the organic solvent was removed under reduced pressure. The crude product was purified by silica gel flash chromatography (*n*-hexane/EtOAc 85:15) to afford the desired **121** as a light brown viscous liquid (130 mg, 63%). ***^{1}H NMR***: (500 MHz, $CDCl_3$) δ (ppm) 6.71 (d, *J*=2.0 Hz, 1H), 6.57 (d, *J*=2.0 Hz, 1H), 4.03-3.99 (m, 1H), 3.96-3.90 (m, 2H), 3.83-3.81 (m, 1H), 3.80 (s, 4H), 3.43-3.35 (m, 8H), 2.25-2.17 (m, 2H), 1.57-1.52 (m, 4H), 1.32-1.25 (m, 36H), 1.09 (s, 6H), 1.06-1.03 (m, 6H), 0.89-0.86 (m, 6H). ***^{13}C NMR***: (125 MHz, $CDCl_3$) δ (ppm) 160.7, 119.0, 113.4, 110.5, 106.6, 72.6, 71.5, 70.8, 34.1, 32.1, 29.8, 29.7, 29.6, 29.5, 26.3, 22.8, 14.4, 14.3. ***^{11}B NMR***: (160 MHz, $CDCl_3$) δ (ppm) 27.7. ***HRMS*** calc. for C44H78BNO6 $[M+H]^+$ ($^m/_z$): 728.6008, found: 728.6009.

Synthesis of 7-((R)-3-(dodecyloxy)-2-methylpropoxy)-5-((S)-3-(dodecyloxy)-2-methylpropoxy)-2,3-dihydro-1H-benzo[c][1,2]azaborole

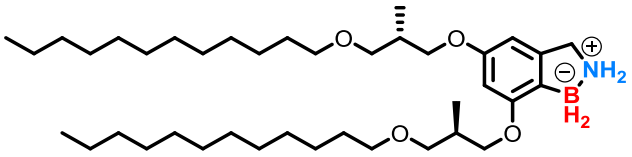

122

Compound **122** was synthesized according to the general **PROCEDURE C** reacting 2-(5,5-dimethyl-1,3,2-dioxaborinan-2-yl)-3-((R)-3-(dodecyloxy)-2-methylpropoxy)-5-((S)-3-(dodecyloxy)-2methylpropoxy) benzonitrile (100 mg, 0.1 mmol) and $LiAlH_4$ (≈1.0 M in THF) (0.7 mL, 0.7 mmol, 5.0 equiv.) in anhydrous THF (2.5 mL) under argon atmosphere. The desired product was obtained as a white powder (50 mg, 60%). ***^{1}H NMR***: (500 MHz, $CDCl_3$) δ (ppm) 6.33 (d, *J*=1.5 Hz, 1H), 6.28 (d, *J*=1.5 Hz, 1H), 4.30 (s, 2H), 4.02 (t, *J*=6.0 Hz, 2H), 3.98-3.95 (dd, *J*=9.0, ^{1}*J*=6.0 Hz, 1H), 3.90-3.86 (m, 2H), 3.77-3.74 (dd, *J*=9.0, ^{1}*J*=6.0 Hz, 1H), 3.43-3.34 (m, 8H), 2.24-2.16 (m, 2H), 1.58-1.52 (m, 4H), 1.33-1.26 (m, 36H), 1.04 (d, *J*=7.0 Hz, 3H), 1.03 (d, *J*=7.0

Hz, 3H), 0.88 (t, *J*=7.0 Hz, 6H). ***^{13}C NMR***: (125 MHz, $CDCl_3$) δ (ppm) 161.0, 159.7, 141.6, 100.6, 100.1, 98.4, 73.3, 73.1, 71.5, 71.4, 70.8, 70.6, 32.1, 29.9, 29.8, 29.7, 29.6, 29.5, 26.3, 22.8, 14.3. ***^{11}B NMR***: (160 MHz, $CDCl_3$, 314 °K) δ (ppm) -10.4.

CHAPTER 3

Synthesis of 2-vinylaniline

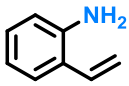

27

In a flame-dried 50 mL two necked flask equipped with condenser, under argon atmosphere, 2-iodoaniline (200 mg, 0.9 mmol), potassium vinyltrifluoroborate (147 mg, 1.1 mmol, 1.2 equiv.) and $Pd(dppf)Cl_2$ (33 mg, 0.05 mmol, 5 mmol%), were vacuumed for 1 h and back filled with argon, then dissolved in anhydrous toluene (12 mL) and n-propyl alcohol (10 mL) beforehand degassed by three freeze-pump-thaw cycles. Then triethylamine (0.15 mL, 1.1 mmol, 1.2 equiv.) was syringed and the resulting mixture was heated up under reflux. After 1 h, the reaction was cooled to room temperature, diluted with ether (20 mL), transferred to a separating funnel and washed with distilled water (2 x 20 mL) and brine (1 x 20 mL). The combined water phase was back-extracted once with ether (15 mL) while the combined organic phase was dried over $MgSO_4$, filtered and the solvent removed under reduced pressure. The crude product was purified by silica gel flash chromatography (*n*-hexane/EtOAc 80:20) to afford the desired **27** as a colorless oil (95 mg, 87%). ***^{1}H NMR***: (300 MHz, $CDCl_3$) δ (ppm) 7.29 (dd, *J*=7.5 Hz, *J'*=1.5 Hz, 1H), 7.10 (d app t, *J*=8.0 Hz, *J'*=1.5 Hz, 1H), 6.83-6.68 (m, 2H), 5.64 (dd, *J*=17.5 Hz, *J'*=1.5 Hz, 1H), 5.32 (dd, *J*=11.0 Hz, *J'*=1.5 Hz, 1H), 3.76 (s, 2H).

Synthesis of 5-chloro-2-vinylaniline

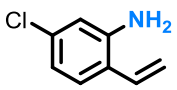

28

In a flame-dried 50 mL two necked flask equipped with condenser, under argon atmosphere, 5-chloro-2-iodoaniline (200 mg, 0.9 mmol), potassium vinyltrifluoroborate (180 mg, 1.3 mmol, 1.7 equiv.) and $Pd(dppf)Cl_2$ (30 mg, 0.05 mmol, 5 mmol%), were vacuumed for 1 h and back filled with argon, then dissolved in anhydrous toluene (12 mL) and n-propyl alcohol (10 mL) beforehand degassed by three freeze-

pump-thaw cycles. Then triethylamine (0.2 mL, 1.3 mmol, 1.7 equiv.) was syringed and the resulting mixture was heated up under reflux. After 3 h, the reaction was cooled to room temperature, diluted with ether (20 mL), transferred to a separating funnel and washed with distilled water (2 x 20 mL) and brine (1 x 20 mL). The combined water phase was back-extracted once with ether (15 mL) while the combined organic phase was dried over $MgSO_4$, filtered and the solvent removed under reduced pressure. The crude product was purified by silica gel flash chromatography (*n*-hexane/EtOAc 80:20) to afford the desired **28** as a red oil (86 mg, 70%). ***^{1}H NMR***: (500 MHz, $CDCl_3$) δ (ppm) 7.18 (d, *J*=8.0 Hz, 1H), 6.72 (d, *J*=8.5 Hz, 1H), 6.67 (s, 1H), 6.67 (d, *J*=17 Hz, 1H), 5.61 (d, *J*=17.5 Hz, 1H), 5.33 (d, *J*=11.0 Hz, 1H).

Synthesis of 1,2-dihydrobenzo[e][1,2]azaborinine

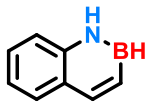

23

In a flame-dried 25 mL two necked flask equipped with condenser, under argon atmosphere, 2-vinylaniline (240 mg, 2.0 mmol) was dissolved in anhydrous toluene (10 mL) and the mixture was cooled to -30 °C. Cold boron trichloride solution (≈1.0 M in n-hexanes) (5.0 mL, 5.0 mmol, 2.5 equiv.) was added dropwise and the resulting suspension was stirred at the same temperature for 15 min, then slowly wormed to room temperature and finally refluxed. After 18 h, the reaction was cooled to room temperature and the solvent was removed under reduced pressure. The residue was re-dissolved in anhydrous THF (10 mL) and the mixture was cooled to -78 °C. After 15 min, freshly titrated $LiAlH_4$ (≈1.0 M in THF) (4.4 mL, 4.4 mmol, 3.0 equiv.) was added dropwise under vigorous stirring, and then the resulting mix was slowly allowed to warm to room temperature and finally refluxed for 12 h. After cooling to room temperature and then to -5 °C, the reaction was quenched dropwise with HCl 1 M under vigorous stirring, transferred to a separating funnel, diluted with water (10 mL) and extracted with CH_2Cl_2 (3 x 20 mL). The combined organic phase was dried over $MgSO_4$, filtered and the solvent removed under reduced pressure. The crude product was purified by silica gel flash chromatography (*n*-hexane/EtOAc 80:20) to afford the desired **23** as a sublimating white solid (110 mg, 43% over 2 steps). ***^{1}H NMR***: (500 MHz, $CDCl_3$) δ (ppm) 8.21 (br, 1H), 8.09 (d, *J*=11.5 Hz, 1H), 7.66 (d, *J*=8.0 Hz, 1H), 7.44 (app t, *J*=7.5 Hz, 1H), 7.30 (d, *J*=8.0 Hz, 1H), 7.21 (t, *J*=7.5 Hz, 1H), 7.01 (d, *J*=13.0 Hz, 1H). ***^{11}B NMR***: (160 MHz, $CDCl_3$) δ (ppm) 32.0 (d, *J*=112 Hz).

Synthesis of 7-chloro-1,2-dihydrobenzo[e][1,2]azaborinine

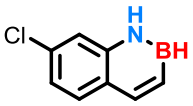

35

In a flame-dried 25 mL two necked flask equipped with condenser, under argon atmosphere, 5-chloro-2-vinylaniline (130 mg, 0.8 mmol) was dissolved in anhydrous toluene (10 mL) and the mixture was cooled to -30 °C. Cold boron trichloride solution (≈1.0 M in n-hexanes) (2.1 mL, 2.1 mmol, 2.5 equiv.) was added dropwise and the resulting suspension was stirred at the same temperature for 15 min, then slowly wormed to room temperature and finally refluxed. After 18 h, the reaction was cooled to room temperature and the solvent was removed under reduced pressure. The residue was re-dissolved in anhydrous THF (10 mL) and the mixture was cooled to -78 °C. After 15 min, freshly titrated $LiAlH_4$ (≈1.0 M in THF) (4.0 mL, 4.0 mmol, 3.0 equiv.) was added dropwise under vigorous stirring, and then the resulting mix was slowly allowed to warm to room temperature and finally refluxed for 12 h. After cooling to room temperature and then to -5 °C, the reaction was quenched dropwise with HCl 1 M under vigorous stirring, transferred to a separating funnel, diluted with water (10 mL) and extracted with CH_2Cl_2 (3 x 20 mL). The combined organic phase was dried over $MgSO_4$, filtered and the solvent removed under reduced pressure. The crude product was purified by silica gel flash chromatography (*n*-hexane/EtOAc 80:20) to afford the desired **35** as a white solid (58 mg, 43% over 2 steps). ***^{1}H NMR***: (500 MHz, $CDCl_3$) δ (ppm) 8.03 (m, 2H), 7.56 (d, *J*=8.5 Hz, 1H), 7.31 (s, 1H), 7.16 (dd, *J*=8.0 Hz, *J'*=2.0 Hz, 1H), 6.99 (dt, *J*=11 Hz, *J'*=2.0 Hz, 1H). ***^{11}B NMR***: (160 MHz, $CDCl_3$) δ (ppm) 32.5 (d, *J*=131 Hz).

Synthesis of 2-(2-(5,5-dimethyl-1,3,2-dioxaborinan-2-yl)phenyl)acetonitrile

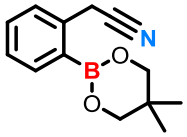

50

In a flame-dried 50 mL two necked flask equipped with condenser, under argon atmosphere, 2-bromophenylacetonitrile (0.45 mL, 3.5 mmol), bis(neopentyl glycolato)diboron (1175 mg, 5.2 mmol, 1.5 equiv.), $Pd(dppf)Cl_2$ (200 mg, 0.24 mmol, 7 mmol%) and CH_3COOK (1464 mg, 15 mmol, 4.3 equiv.) were vacuumed for 1 h and back filled with argon, then dissolved in anhydrous 1,4-dioxane (20 mL) and heated up under reflux. After 3 h, the reaction mixture was cooled to room temperature and the organic solvent was removed under reduced pressure. The residue was re-dissolved in EtOAc (50 mL), transferred to a separating funnel and washed with distilled water (2 x 10 mL) and brine (1 x 10 mL). The combined water

phase was back-extracted once with EtOAc (15 mL) while the combined organic phase was dried over $MgSO_4$, filtered and the solvent removed under reduced pressure. The crude product was purified by silica gel flash chromatography (*n*-hexane/CH_2Cl_2 60:40) to afford the desired **50** as a light brown viscous liquid (830 mg, 98%). ***^{1}H NMR***: (500 MHz, $CDCl_3$) δ (ppm) 7.87 (d, *J*=7.5 Hz, 1H), 7.44-7.38 (m, 2H), 7.31 (app t, *J*=7.5 Hz, 1H), 4.07 (s, 2H), 3.80 (s, 4H), 1.04 (s, 6H). ***^{13}C NMR***: (125 MHz, $CDCl_3$) δ (ppm) 136.1, 131.2, 128.9, 127.3, 119.4, 72.5, 31.8, 23.9, 22.0. ***^{11}B NMR***: (160 MHz, $CDCl_3$) δ (ppm) 26.8. ***HRMS*** calc. for C13H16BNO2 $[M+H]^+$ ($^m/_z$): 230.1355, found: 230.1361.

Synthesis of 2-(2-bromo-5-chlorophenyl)acetonitrile

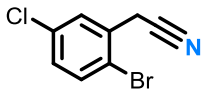

52

In a 25 mL two necked flask equipped with condenser 1-bromo-2-(bromomethyl)-4-chlorobenzene (250 mg, 0.9 mmol) and KCN (115 mg, 1.8 mmol, 2.0 equiv.) were dissolved in EtOH / H_2O (7 : 1) (8 mL). The condenser was topped by a septum linked with a plastic tube to an aqueous solution of NaOH (20 w/w %) and the resulting mixture was heated up under reflux. After 8 h, the reaction mixture was cooled to room temperature and the organic solvent was partially removed under reduced pressure. The residue was diluted with EtOAc (20 mL), transferred to a separating funnel and washed with aqueous $NaHCO_3$ (5 w/w %) (2 x 10 mL) and brine (1 x 10 mL), dried over $MgSO_4$, filtered and the solvent removed under reduced pressure to afford the desired **52** as a light brown solid (193 mg, 95%). ***^{1}H NMR***: (500 MHz, $CDCl_3$) δ (ppm) 7.54 (d, *J*=8.5 Hz, 1H), 7.53 (d, *J*=2.5 Hz, 1H), 7.22 (dd, *J*=8.5, ^{1}*J*=2.5 Hz, 1H), 3.82 (s, 2H).

Synthesis of 2-(5-chloro-2-(5,5-dimethyl-1,3,2-dioxaborinan-2-yl)phenyl)acetonitrile

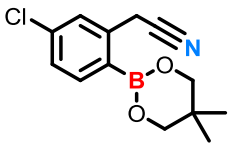

53

In a flame-dried 50 mL two necked flask equipped with condenser, under argon atmosphere, 2-(2-bromo-5-chlorophenyl)acetonitrile (400 mg, 1.7 mmol), bis(neopentyl glycolato)diboron (588 mg, 2.6 mmol, 1.5 equiv.), $Pd(dppf)Cl_2$ (100 mg, 0.12 mmol, 7 mmol%) and CH_3COOK (732 mg, 7.5 mmol, 4.3 equiv.) were vacuumed for 1 h and back filled with argon, then dissolved in anhydrous 1,4-dioxane (14 mL) and heated up under reflux. After 1 h, bis(neopentyl glycolato)diboron (80 mg, 0.3 mmol, 0.2 equiv.) was added and the reaction mixture was stirred at the same temperature. After 30 min the reaction mixture was cooled

to room temperature and the organic solvent was removed under reduced pressure. The residue was re-dissolved in EtOAc (30 mL), transferred to a separating funnel and washed with distilled water (2 x 10 mL) and brine (1 x 10 mL). The combined water phase was back-extracted once with EtOAc (15 mL) while the combined organic phase was dried over $MgSO_4$, filtered and the solvent removed under reduced pressure. The crude product was purified by silica gel flash chromatography (*n*-hexane/CH_2Cl_2 70:30 to CH_2Cl_2 100) to afford the desired **53** as a light brown solid (330 mg, 71%). ***^{1}H NMR***: (500 MHz, $CDCl_3$) δ (ppm) 7.81 (d, *J*=8.0 Hz, 1H), 7.39 (d, *J*=2.0 Hz, 1H), 7.29 (dd, *J*=8.0, ^1J=2.0 Hz, 1H), 4.05 (s, 2H), 3.79 (s, 4H), 1.02 (s, 6H). ***^{13}C NMR***: (125 MHz, $CDCl_3$) δ (ppm) 138.0, 137.6, 137.3, 129.0, 127.6, 118.7, 72.5, 31.9, 23.6, 22.0. ***^{11}B NMR***: (160 MHz, $CDCl_3$) δ (ppm) 26.9. ***HRMS*** calc. for C13H15BClNO2 $[M+H]^+$ ($^m/_z$): 264.0965, found: 264.0961.

Synthesis of 2-(2-(5,5-dimethyl-1,3,2-dioxaborinan-2-yl)-4-(trifluoromethyl)phenyl)acetonitrile

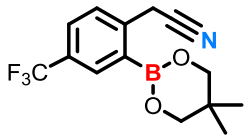

56

In a flame-dried 100 mL two necked flask equipped with condenser, under argon atmosphere, 2-bromo-4-(trifluoromethyl)phenylacetonitrile (0.6 mL, 3.8 mmol), bis(neopentyl glycolato)diboron (1283 mg, 5.7 mmol, 1.5 equiv.), $Pd(dppf)Cl_2$ (216 mg, 0.27 mmol, 7 mmol%) and CH_3COOK (1600 mg, 16.3 mmol, 4.3 equiv.) were vacuumed for 1 h and back filled with argon, then dissolved in anhydrous 1,4-dioxane (40 mL) and heated up under reflux. After 1 h, the reaction mixture was cooled to room temperature and the organic solvent was removed under reduced pressure. The residue was re-dissolved in EtOAc (50 mL), transferred to a separating funnel and washed with distilled water (2 x 20 mL) and brine (1 x 20 mL). The combined water phase was back-extracted once with EtOAc (15 mL) while the combined organic phase was dried over $MgSO_4$, filtered and the solvent removed under reduced pressure. The crude product was purified by silica gel flash chromatography (*n*-hexane/CH_2Cl_2 70:30 to CH_2Cl_2 100) to afford the desired **56** as a light brown solid (960 mg, 87%). ***^{1}H NMR***: (500 MHz, $CDCl_3$) δ (ppm) 8.14 (s, 1H), 7.67 (d, *J*=8.0 Hz, 1H), 7.53 (d, *J*=8.0 Hz, 1H), 4.13 (s, 2H), 3.82 (s, 4H), 1.05 (s, 6H). ***^{13}C NMR***: (125 MHz, $CDCl_3$) δ (ppm) 140.0, 132.9, 129.8, 129.2, 127.9, 125.3, 123.1, 118.6, 72.7, 31.9, 23.9, 22.0. ***^{11}B NMR***: (160 MHz, $CDCl_3$) δ (ppm) 26.4. ***HRMS*** calc. for C14H15BF3NO2 $[M+H]^+$ ($^m/_z$): 298.1221, found: 298.1221.

Synthesis of 2-(2-(5,5-dimethyl-1,3,2-dioxaborinan-2-yl)-4,5-dimethoxyphenyl)acetonitrile

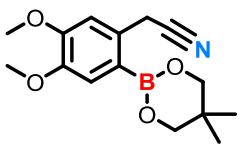

57

In a flame-dried 100 mL two necked flask equipped with condenser, under argon atmosphere, 2-(2-bromo-4,5-dimethoxyphenyl)acetonitrile (200 mg, 0.8 mmol), bis(neopentyl glycolato)diboron (265 mg, 1.2 mmol, 1.5 equiv.), Pd(dppf)Cl_2 (45 mg, 0.06 mmol, 7 mmol%) and CH_3COOK (330 mg, 3.4 mmol, 4.3 equiv.) were vacuumed for 1 h and back filled with argon, then dissolved in anhydrous 1,4-dioxane (7 mL) and heated up under reflux. After 3 h, the reaction mixture was cooled to room temperature and the organic solvent was removed under reduced pressure. The residue was re-dissolved in EtOAc (20 mL), transferred to a separating funnel and washed with distilled water (2 x 10 mL) and brine (1 x 10 mL). The combined water phase was back-extracted once with EtOAc (15 mL) while the combined organic phase was dried over $MgSO_4$, filtered and the solvent removed under reduced pressure. The crude product was purified by silica gel flash chromatography (*n*-hexane/CH_2Cl_2 50:50 to CH_2Cl_2 100) to afford the desired **57** as a white solid (204 mg, 90%). ***^{1}H NMR***: (500 MHz, $CDCl_3$) δ (ppm) 7.36 (s, 1H), 6.88 (s, 1H), 4.05 (s, 2H), 3.92 (s, 3H), 3.91 (s, 3H), 3.78 (s, 4H), 1.03 (s, 6H). ***^{13}C NMR***: (125 MHz, $CDCl_3$) δ (ppm) 151.1, 147.9, 129.7, 119.7, 118.2, 112.3, 110.2, 72.5, 71.7, 56.1, 56.0, 31.9, 23.3, 22.3, 22.0. ***^{11}B NMR***: (160 MHz, $CDCl_3$) δ (ppm) 26.6. ***HRMS*** calc. for C15H20BNO4 $[M]^+$ ($^m/_z$): 289.1488, found: 289.1617.

Synthesis of 1,2,3,4-tetrahydrobenzo[c][1,2]azaborinine

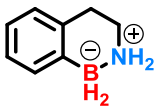

19

Compound **19** was synthesized according to the general **PROCEDURE C** reacting 2-(2-(5,5-dimethyl-1,3,2-dioxaborinan-2-yl)phenyl)acetonitrile (100 mg, 0.4 mmol) and $LiAlH_4$ (≈1.0 M in THF) (2.2 mL, 2.2 mmol, 5.0 equiv.) in anhydrous THF (2.0 mL) under argon atmosphere for 1.5 h. The desired product was obtained as a white powder (33 mg, 56%). ***^{1}H NMR***: (500 MHz, $CDCl_3$) δ (ppm) 7.28 (d, *J*=7.0 Hz, 1H), 7.12 (app t, *J*=7.0 Hz, 1H), 7.04 (app t, *J*=8.0 Hz, 1H), 6.99 (d, *J*=6.0 Hz, 1H), 3.80 (br, 2H), 3.28-3.23 (m, 2H), 2.97 (t, *J*=6.0 Hz, 2H). ***^{13}C NMR***: (100 MHz, $CDCl_3$) δ (ppm) 151.6, 137.0, 132.7, 127.5, 124.7, 42.3, 30.5. ***^{11}B NMR***: (160 MHz, $CDCl_3$) δ (ppm) -13.4 (t, *J*=96 Hz). ***HRMS*** calc. for C8H12BN $[M-H]^-$ ($^m/_z$): 132.0990, found: 132.0993.

Synthesis of 6-chloro-1,2,3,4-tetrahydrobenzo[c][1,2]azaborinine

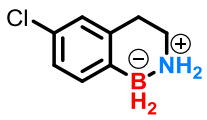

58

Compound **58** was synthesized according to the general **PROCEDURE C** reacting 2-(5-chloro-2-(5,5-dimethyl-1,3,2-dioxaborinan-2-yl)phenyl)acetonitrile (100 mg, 0.4 mmol) and $LiAlH_4$ (≈1.0 M in THF) (2.0 mL, 2.0 mmol, 5.0 equiv.) in anhydrous THF (2.0 mL) under argon atmosphere for 1.5 h. The desired product was obtained as a white powder (30 mg, 47%). ***^{1}H NMR***: (500 MHz, $CDCl_3$) δ (ppm) 7.18 (d, *J*=8.0 Hz, 1H), 7.08 (d, *J*=8.0 Hz, 1H), 6.97 (s, 1H), 3.88 (br, 2H), 3.21-3.17 (m, 2H), 2.89 (t, *J*=6.0 Hz, 2H). ***^{13}C NMR***: (125 MHz, $CDCl_3$) δ (ppm) 138.4, 134.1, 130.2, 127.1, 125.9, 42.2, 30.3. ***^{11}B NMR***: (160 MHz, $CDCl_3$) δ (ppm) -13.6 (t, *J*=96 Hz). ***HRMS*** calc. for C8H11BClN $[M-H]^-$ ($^m/_z$): 166.0596, found: 166.0598.

Synthesis of 7-(trifluoromethyl)-1,2,3,4-tetrahydrobenzo[c][1,2]azaborinine

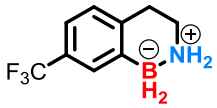

59

Compound **59** was synthesized according to the general **PROCEDURE C** reacting 2-(2-(5,5-dimethyl-1,3,2-dioxaborinan-2-yl)-4-(trifluoromethyl)phenyl)acetonitrile (118 mg, 0.4 mmol) and $LiAlH_4$ (≈1.0 M in THF) (2.0 mL, 2.0 mmol, 5.0 equiv.) in anhydrous THF (2.0 mL) under argon atmosphere for 2 h. The desired product was obtained as a white powder (31 mg, 40%). ***^{1}H NMR***: (500 MHz, $CDCl_3$) δ (ppm) 7.52 (s, 1H), 7.25 (d, *J*=7.0 Hz, 1H), 7.05 (d, *J*=8.0 Hz, 1H), 3.92 (br, 2H), 3.26-3.21 (m, 2H), 2.97 (t, *J*=6.0 Hz, 2H). ***^{13}C NMR***: (125 MHz, $CDCl_3$) δ (ppm) 140.4, 129.3, 127.4, 126.2, 125.6, 121.3, 42.2, 30.5. ***^{11}B NMR***: (160 MHz, $CDCl_3$) δ (ppm) -13.6 (t, *J*=96 Hz). ***HRMS*** calc. for C9H13BN $[M+H]^+$ ($^m/_z$): 146.1136, found: 146.1132.

Synthesis of 6,7-dimethoxy-1,2,3,4-tetrahydrobenzo[c][1,2]azaborinine

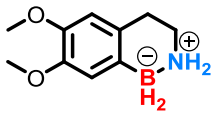

60

Compound **60** was synthesized according to the general **PROCEDURE C** reacting 2-(2-(5,5-dimethyl-1,3,2-dioxaborinan-2-yl)-4,5-dimethoxyphenyl)acetonitrile (100 mg, 0.3 mmol) and $LiAlH_4$ (≈1.0 M in THF) (1.7 mL, 1.7 mmol, 5.0 equiv.) in anhydrous THF (2.0 mL) under argon atmosphere for 1 h. The desired product

was obtained as a white powder (32 mg, 50%). ***^{1}H NMR***: (500 MHz, $CDCl_3$) δ (ppm) 6.78 (s, 1H), 6.54 (s, 1H), 3.92 (s, 2H), 3.86 (s, 3H), 3.82 (s, 3H), 3,28-3.24 (m, 2H), 2.92 (t, *J*=6.0 Hz, 2H). ***^{13}C NMR***: (125 MHz, $CDCl_3$) δ (ppm) 151.7, 147.7, 146.7, 125.7, 114.9, 111.3, 56.1, 55.9, 42.8, 30.1. ***^{11}B NMR***: (160 MHz, $CDCl_3$) δ (ppm) -13.5 (t, *J*=96 Hz).

Synthesis of 7,8,15,16,23,24-hexahydrobenzo[3,4][1,2]azaborinino[1,2-a]benzo[3,4][1,2]azaborinino[1,2-c]benzo[3,4][1,2]azaborinino[1,2-e][1,3,5,2,4,6]triazatriborinine

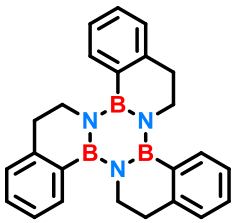

18

Compound **18** was synthesized according to the general **PROCEDURE D** reacting 1,2,3,4-tetrahydrobenzo[c][1,2]azaborinine (75 mg, 0.56 mmol) in anhydrous toluene (2 mL) under argon atmosphere. After 3 h, the reaction mixture was cooled to room temperature, diluted with EtOAc and transferred in a 100 mL flask. After the organic solvents were removed under reduced pressure, the crude product was purified by silica gel flash chromatography (*n*-hexane/CH_2Cl_2 80:20) to afford the desired **18** as a white powder (17 mg, 20%). ***^{1}H NMR***: (500 MHz, $CDCl_3$) δ (ppm) 7.79 (d, *J*=7.5 Hz, 3H), 7.37 (t, *J*=7.5 Hz, 3H), 7.29 (t, *J*=7.5 Hz, 3H), 7.26 (d, *J*=7.5 Hz, 3H), 3.89 (t, *J*=6.0 Hz, 6H), 2.82 (t, *J*=6.0 Hz, 6H). ***^{13}C NMR***: (125 MHz, $CDCl_3$) δ (ppm) 147.3, 133.9, 129.6, 126.8, 125.4, 46.6, 35.4. ***^{11}B NMR***: (128 MHz, $CDCl_3$) δ (ppm) 33.5. ***HRMS*** calc. for C24H24B3N3 $[M+H]^+$ ($^m/_z$): 388.2340, found: 388.2331.

Synthesis of 2,10,18-trichloro-7,8,15,16,23,24-hexahydrobenzo[3,4][1,2]azaborinino[1,2-a]benzo[3,4][1,2]azaborinino[1,2-c]benzo[3,4][1,2]azaborinino[1,2-e][1,3,5,2,4,6]triazatriborinine

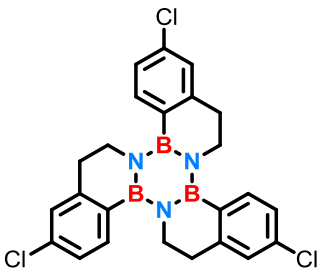

64

Compound **64** was synthesized according to the general **PROCEDURE D** reacting 6-chloro-1,2,3,4-tetrahydrobenzo[c][1,2]azaborinine (270 mg, 1.6 mmol) in anhydrous toluene (3 mL) under argon

atmosphere. After 3 h, the reaction mixture was cooled to room temperature, diluted with EtOAc and transferred in a 100 mL flask. After the organic solvents were removed under reduced pressure, the crude product was purified by silica gel flash chromatography (*n*-hexane/CH_2Cl_2 80:20) to afford the desired **64** as a white powder (40 mg, 15%). ***^{1}H NMR***: (500 MHz, $CDCl_3$) δ (ppm) 7.67 (d, *J*=8.0 Hz, 3H), 7.28-7.25 (m, 6H), 3.81 (t, *J*=6.0 Hz, 6H), 2.78 (t, *J*=6.0 Hz, 6H). ***^{13}C NMR***: (125 MHz, $CDCl_3$) δ (ppm) 149.1, 135.6, 135.2, 127.0, 125.7, 46.3, 35.1. ***^{11}B NMR***: (160 MHz, $CDCl_3$) δ (ppm) 32.0. ***HRMS*** calc. for C24H21B3Cl3N3 $[M+H]^+$ ($^m/_z$): 490.1175, found: 490.1163.

Synthesis of 2,3,10,11,18,19-hexamethoxy-7,8,15,16,23,24-hexahydrobenzo[3,4][1,2]azaborinino[1,2-a]benzo[3,4][1,2]azaborinino[1,2-c]benzo[3,4][1,2]azaborinino[1,2-e][1,3,5,2,4,6]triazatriborinine

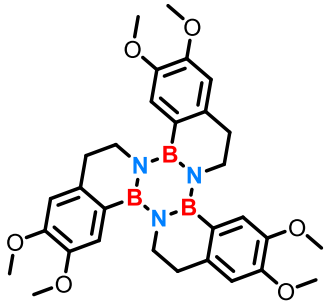

65

Compound **65** was synthesized according to the general **PROCEDURE D** reacting 6,7-dimethoxy-1,2,3,4-tetrahydrobenzo[c][1,2]azaborinine (100 mg, 1.6 mmol) in anhydrous toluene (3 mL) under argon atmosphere. After 3 h, the reaction mixture was cooled to room temperature, diluted with EtOAc and transferred in a 100 mL flask. After the organic solvents were removed under reduced pressure, the crude product was purified by silica gel flash chromatography (*n*-hexane/CH_2Cl_2 80:20) to afford the desired **65** as a white powder (25 mg, 26%). ***^{1}H NMR***: (400 MHz, $CDCl_3$) δ (ppm) 7.13 (s, 3H), 6.43 (s, 3H), 3.89 (s, 9H), 3.80 (s, 9H), 3.14 (t, *J*=6.0 Hz, 6H), 2.71 (t, *J*=6.0 Hz, 6H). ***^{13}C NMR***: (125 MHz, $CDCl_3$) δ (ppm) 148.6, 147.7, 132.9, 115.2, 111.2, 72.0, 56.0, 40.5, 32.6. ***^{11}B NMR***: (160 MHz, $CDCl_3$) δ (ppm) 32.0. ***HRMS*** calc. for C30H36B3N3O6 $[M+H]^+$ ($^m/_z$): 568.2971, found: 568.2944.

CHAPTER 5

Synthesis of diethyl 2,5-dibromoterephthalate

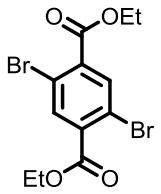

11

In a 150 mL two necked flask equipped with condenser, 2,5-dibromoterephthalic acid (5000 mg, 15.4 mmol) was dissolved in ethanol (70 mL) then H_2SO_4 conc. (0.7 mL) was added dropwise to the solution under stirring and the resulting mixture was heated up under reflux. After 8 h, the reaction mixture was cooled to room temperature and the organic solvent was partially removed under reduced pressure. The residue was diluted with EtOAc (50 mL), transferred to a separating funnel and washed with aqueous $NaHCO_3$ (5 w/w %) (4 x 20 mL) and brine (1 x 20 mL). The combined water phase was back-extracted once with EtOAc (20 mL) while the combined organic phase was dried over $MgSO_4$, filtered and the solvent removed under reduced pressure to afford the desired **11** as a white powder (3852 mg, 66%). ***^{1}H NMR***: (400 MHz, DMSO-d_6) δ (ppm) 8.07 (s, 2H), 4.38-4.32 (q, *J*=7.0, 2H), 1.33 (t, *J*=7.0, 3H).

Synthesis of 2,5-dibromoterephthalaldehyde

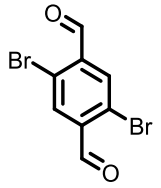

10

In a flame-dried 25 mL two necked flask, under argon atmosphere, morpholine (0.22 mL, 2.6 mmol, 4.2 equiv.), was dissolved in anhydrous THF (4 mL). After cooling to 0 °C, DIBALH (1.0 M in *n*-hexane) (2.5 mL, 2.5 mmol, 4.0 equiv.), was added dropwise and the mixture was stirred for 3 h at the same temperature. In parallel diethyl 2,5-dibromoterephthalate (235 mg, 0.6 mmol) was dissolved in anhydrous THF (6 mL) under argon atmosphere and the resulting solution was cannulated dropwise to the reaction mixture at 0 °C. After 10 min DIBALH (1.0 M in n-hexane) (1.4 mL, 1.4 mmol, 2.2 equiv.), was added dropwise and the reaction mixture was stirred at the same temperature. After 10 min the reaction was quenched with aqueous HCl (1 N) and extracted with EtOAc (3 x 10 mL). The combined organic phase was dried over $MgSO_4$, filtered and the solvent removed under reduced pressure. The crude product was purified by silica

gel flash chromatography (*n*-hexane/CH_2Cl_2 60:40) to afford the desired **10** as a light yellow solid (160 mg, 90%). ***^{1}H NMR***: (500 MHz, DMSO-d_6) δ (ppm) 10.17 (s, 2H), 8.10 (s, 2H).

Synthesis of 2,5-dibromoterephthalonitrile

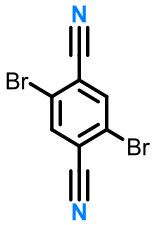

4

In a 25 mL two necked flask equipped with condenser, 2,5-dibromoterephthalaldehyde (340 mg, 1.2 mmol), hydroxyamine hydrochloride (405 mg, 5.8 mmol, 5.0 equiv.) and sodium acetate (573 mg, 7.0 mmol, 6.0 equiv.) were dissolved in formic acid conc. (10 mL) and heated up under reflux. After 12 h, the reaction mixture was cooled to room temperature, diluted with water (20 mL), transferred to a separating funnel and extracted with chloroform (3 x 10 mL). The combined organic phase was washed with aqueous NH_4OH (10 w/w %) (4 x 10 mL) and brine (1 x 10 mL), dried over $MgSO_4$, filtered and the solvent removed under reduced pressure. The crude product was purified by washing the solid with *n*-hexane/CH_2Cl_2 (80:20) (3 x 5 mL) to afford the desired **4** as a white solid (266 mg, 96%). ***^{1}H NMR***: (500 MHz, $CDCl_3$) δ (ppm) 7.96 (s, 2H).

Synthesis of 2,5-dibromoterephthalonitrile

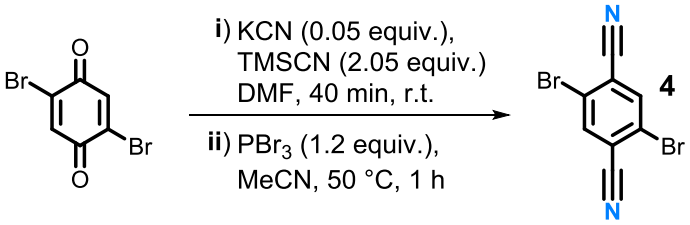

In a flame-dried 10 mL two necked flask, under argon atmosphere, 2,5-Dibromo-1,4-benzoquinone (266 mg, 1.0 mmol) and KCN (3.3 mg, 0.05 mmol, 0.05 equiv.) were dissolved/suspended in anhydrous DMF (0.5 mL, 2.0 M). TMSCN (0.26 mL, 2.05 mmol, 2.05 equiv.) was added dropwise and the resulting mixture was stirred at room temperature. After 40 min anhydrous MeCN (3 mL) and PBr_3 (0.11 mL, 1.2 mmol, 1.2 equiv.) were added and the reaction mixture was stirred at 50 °C. After 1 h, the reaction mixture was cooled to room temperature, diluted with CH_2Cl_2 (10 mL) and absorbed on celite. The solvent was removed under reduced pressure and the crude product was purified by silica gel flash chromatography (*n*-hexane/CH_2Cl_2 70:30) to afford the desired **4** as a white solid (217 mg, 76%). ***^{1}H NMR***: (500 MHz, $CDCl_3$) δ (ppm) 7.96 (s, 2H)

Synthesis of 2,5-bis(5,5-dimethyl-1,3,2-dioxaborinan-2-yl)terephthalonitrile

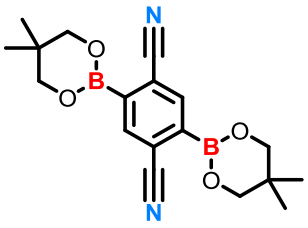

9

In a flame-dried 50 mL two necked flask equipped with condenser, under argon atmosphere, 2,5-dibromoterephthalonitrile (100 mg, 0.3 mmol), bis(neopentyl glycolato)diboron (237 mg, 1.1 mmol, 3.0 equiv.), $Pd(dppf)Cl_2$ (40 mg, 0.05 mmol, 14 mmol%) and CH_3COOK (274 mg, 2.8 mmol, 8.0 equiv.) were vacuumed for 1 h and back filled with argon, then dissolved in anhydrous 1,4-dioxane (20 mL) sonicated for 5 min and heated up under reflux. After 2 h, the reaction mixture was cooled to room temperature and the organic solvent was removed under reduced pressure. The residue was re-dissolved in EtOAc (50 mL), transferred to a separating funnel and washed with distilled water (2 x 10 mL) and brine (1 x 10 mL). The combined water phase was back-extracted once with EtOAc (15 mL) while the combined organic phase was dried over $MgSO_4$, filtered and the solvent removed under reduced pressure. The crude product was purified by washing the solid with acetone (6 x 5 mL) and CH_2Cl_2 (2 x 5 mL) to afford the desired **9** as a low soluble white solid (100 mg, 80%). ***^{1}H NMR***: (500 MHz, $CDCl_3$) δ (ppm) 8.19 (s, 2H), 3.84 (s, 4H), 1.05 (s, 6H). ***^{13}C NMR***: (125 MHz, $CDCl_3$) δ (ppm) 140.3, 136.4, 120.6, 116.0, 72.7, 22.7, 22.1. ***^{11}B NMR***: (160 MHz, $CDCl_3$) δ (ppm) 25.4. ***HRMS*** calc. for C18H22B2N2O4 $[M+H]^+$ ($^m/_z$): 353.1851, found: 353.1849.

Synthesis of 1,2,3,5,6,7-hexahydrobenzo[1,2-c:4,5-c']bis([1,2]azaborole)

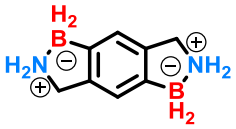

2

Compound **2** was synthesized according to the general **PROCEDURE C** reacting 2,5-bis(5,5-dimethyl-1,3,2-dioxaborinan-2-yl)terephthalonitrile (50 mg, 0.14 mmol) and $LiAlH_4$ (≈1.0 M in THF) (1.5 mL, 1.5 mmol, 11.0 equiv.) in anhydrous THF (3.0 mL) under argon atmosphere. After 3 h, the reaction mixture was cooled to room temperature, diluted with anhydrous THF (60 mL) and transferred in a 100 mL conical flask. After cooling to -5 °C, the reaction was quenched dropwise with water under vigorous stirring yielding a white precipitate. The formed suspension was filtered on a plug of $MgSO_4$ and the solid was washed with THF (3 x 10 mL) and EtOAc (3 x 10 mL). After the organic solvents were removed under reduced pressure, the residue was re-dissolved in EtOAc (50 mL), transferred to a separating funnel and washed with distilled

water (3 x 10 mL) and brine (1 x 10 mL). The combined water phase was back-extracted once with EtOAc (20 mL) while the combined organic phase was dried over $MgSO_4$, filtered and the solvent removed under reduced pressure to afford the desired **2** as a low soluble white solid (15 mg, 67%). ***^{1}H NMR***: (500 MHz, DMSO-d_6) δ (ppm) 6.89 (s, 2H), 5.78 (br, 4H), 3.86 (t, J=6.0 Hz, 4H). ***^{13}C NMR***: (125 MHz, DMSO-d_6) δ (ppm) 139.1, 121.5, 49.3. ***^{11}B NMR***: (160 MHz, DMSO-d_6) δ (ppm) -11.2. ***HRMS*** calc. for C8H14B2N2 $[M-2H]^{-}$ ($^m/_z$): 157.1103, found: 157.1100.